

Factor Graphs for Quantum Information Processing

CAO, Michael Xuan

A Thesis Submitted in Partial Fulfillment
of the Requirements for the Degree of
Doctor of Philosophy
in
Information Engineering

The Chinese University of Hong Kong
April 2021

This work is licensed under a Creative Commons
“Attribution 4.0 International” license.



Abstract of thesis entitled:

Factor Graphs for Quantum Information Processing

Submitted by CAO, Michael Xuan

For the degree of Doctor of Philosophy

At the Chinese University of Hong Kong in April 2021

Statistical graphical models are frameworks that use graphs to represent dependencies among a large number of random variables. Such frameworks have been proven useful for developing analytical/algorithmic methods in characterizing the behavior of systems involving a large number of variables. Among these frameworks, the factor graphs are a popular variant. A factor graph represents a factorization of a multivariate function, and in many practical examples, a factorization of some probability function. It is a recurring problem in physics and engineering to compute the marginals (or partition sums) of a given multivariate function. With the factor graph representation, such marginals (or partition sums) can be computed/estimated via a class of algorithms known as belief-propagation algorithms.

In recent years, quantum computing and quantum communications have received increasing attention. In these applications, information is represented and processed by suitable quantum systems. Quantum theory, which is a generalization of probability theory, describes the uncertainty of quantum systems. Classical graphical models, which are based on probability theory, can no longer efficiently describe the dependencies among such systems.

In this thesis, we are interested in generalizing factor graphs and the relevant methods toward describing quantum systems. Two generalizations of classical graphical models are investigated, namely double-edge factor graphs (DeFGs) and quantum factor graphs (QFGs). Conventionally, a factor in a factor graph represents a nonnegative real-valued local functions. Two different approaches to generalize factors in classical factor graphs yield DeFGs and QFGs, respectively. We proposed/re-proposed and analyzed generalized versions of belief-propagation algorithms for DeFGs/QFGs. As a particular application of the DeFGs, we investigate the information rate and their upper/lower bounds of classical communications over quantum channels with memory. In this study, we also propose a data-driven method for optimizing the upper/lower bounds on information rate.

標題如下之論文之摘要

用於量子信息處理的因子圖方法的探討

提交者 曹 軒

所申請之學位 哲學博士

二零二零年十一月 於香港中文大學

統計圖形模型是使用圖形表示大量隨機變量之間的依存關係的框架。在研究涉及大量變量的系統的行為時，此類框架有助開發相關的分析手段和計算方法。在這類框架中，因子圖（factor graph）是一種流行的方法。因子圖用圖表示因式分解。而在許多實例中，它往往用於表示某些概率函數的分解。計算給定因式分解的邊際（marginal）或配分和（partition sum）是物理學和工程學中常見的問題。利用因子圖，這樣的邊際或配分和可用置信傳播算法（belief-propagation algorithm）（估）算出。

近年來，量子計算和量子通信領域所受關注愈增。在這些應用中，訊息由量子系統（的狀態）表示。量子論（quantum theory）是描述量子系統不確定性的理論，它是概率論的延伸。由於前述圖模型上的方法均基於概率論，它們難以高效地描述此類系統之間的依賴性。

在本文中，我們關注因子圖和相關方法的拓展，以期用於描述量子系統。本研究涉及了兩個拓展模型：雙邊因子圖（DeFGs）和量子因子圖（QFGs）。傳統上，因子圖中的因子表示的是非負實值局部函數。而DeFG和QFG分別對應了兩種對經典因子圖中的因子的拓展。本文分別提出/重新提出並分析了針對DeFG/QFG而拓展的置信傳播算法。我們還研究了量子記憶信道（quantum channel with memory）的經典通信率及其上下界。該研究使用了DeFG來表示量子系統。在本研究中，我們提出了一種基於數據來優化信息速率的上下界的方法。

Preface

Factor graphs [KFL01; Loe04; WJ08, Section 2.1] are a type of graphical models that uses bipartite graphs (or some equivalence) to describe *factorizations* of multivariate functions, where a factorization of a function is a decomposition of itself into the *product of a several sub-functions* (see (1.1)). Though the method itself does not impose any constraints on the functions to be factorized, it is often used to represent the factorizations of probability functions and thus can be used to illustrate the dependencies among the involved random variables. Many interesting computer science and physics problems can be modeled as computing the *marginals* of certain functions with some knowledge of its factorization structure. Examples include problems in coding theory (*e.g.*, decoding of low-density parity-check (LDPC) codes [Gal62]) and problems in statistical mechanics (*e.g.*, the Ising models (see, *e.g.*, [ML13])). Besides visualizing such factorizations, factor graphs also provide an efficient approach to compute or estimate the aforementioned marginals using a class of algorithms known as *belief-propagation* (BA) algorithms.

In recent years, quantum computing and quantum communications have received increasing attention. Though technically speaking, such systems *can* be described by probability theory, it is hugely inefficient to do so since a discrete quantum system's state space is continuous. For example, in a quantum system of n -qubits, the states of the system can be $\sum_{\mathbf{x}_1^n \in \mathbb{F}_2^n} \alpha_{\mathbf{x}_1^n} |\mathbf{x}_1^n\rangle$ for any complex numbers $\{\alpha_{\mathbf{x}_1^n}\}_{\mathbf{x}_1^n \in \mathbb{F}_2^n}$ such that $\sum_{\mathbf{x}_1^n \in \mathbb{F}_2^n} |\alpha_{\mathbf{x}_1^n}|^2 = 1$. In this case, describing the system using probability theory would require a $(2^{n+1} - 1)$ -dimensional (real) continuous random variable. On the other hand, due to the physical nature of observations (as we understand them so far), it is equivalent to describe the same system using a 2^n -by- 2^n density matrix (operator). The latter description is the key to quantum theory, a generalization of probability theory (see Section 1.2). Thus, solving the interference problem on a system involving quantum

components using the traditional method of factor graphs and probability theory would be extremely inefficient. This has motivated us to consider generalizations of the model and the methods of factor graphs for quantum theory.

Problems and Contributions

As introduced below, we consider three particular topics/problems in this thesis. The first two topics are two different generalizations of the method of factor graphs with quantum theory in mind. The last topic solves a specific problem in quantum information theory and demonstrates how factor graphs could be helpful in these problems.

Double-Edge Factor Graphs

In Chapter 2, we focus on a generalized class of factor graphs called double-edge factor graphs (DeFGs). A DeFG represents a factorization of the form $g(\mathbf{s}, \tilde{\mathbf{s}}; \mathbf{x}) = \prod_{a \in \mathcal{F}} f_a(\mathbf{s}_{\partial a}, \tilde{\mathbf{s}}_{\partial a}; \mathbf{x}_{\delta a})$, where f_a is complex-valued for each a and where the matrix associated with f_a , *i.e.*, $[f_a(\mathbf{x}_{\delta a})]_{\mathbf{s}_{\partial a}, \tilde{\mathbf{s}}_{\partial a}} \triangleq f_a(\mathbf{s}_{\partial a}, \tilde{\mathbf{s}}_{\partial a}; \mathbf{x}_{\delta a})$, is PSD for each $\mathbf{x}_{\delta a}$. This class of graphical models is closely related to the factor graphs for quantum probabilities introduced in [LV12; LV17] and is helpful in representing quantum systems. In particular, the results of quantum dynamics can be expressed as marginals of some global functions represented by suitable DeFGs.

In our work, we are interested in the problem of computing the marginals and partition sums of DeFGs. We generalize the “closing-the-box” operations to DeFGs, and show that the marginals/partition sum of an acyclic DeFG can be computed using a sequence of “closing-the-box” operations. We also generalize the belief-propagation (BP) algorithm to DeFGs. In particular, we define the holographic transformation of DeFGs, and derive a loop calculus expansion for DeFGs. We study multiple numerical examples in which BP algorithms for DeFGs show promising results.

Parts of the contents of Chapter 2 have been published in [CV17a].

Quantum Factor Graphs

In Chapter 3, we focus on a graphical model called *quantum factor graphs* (QFGs) [LP08]. The graphical model is a direct generalization of the *bifactor networks* proposed

in the same paper, in which the authors considered a “factorization” in the form of $\rho \triangleq \star_{a \in \mathcal{F}} \rho_a$ where \star is a commutative and associative binary operator of linear operators (matrices). The target is to compute the (partial) trace of ρ . The major results in [LP08] are based on additional commutativity assumptions.

In our work, we consider a different setup without commutativity assumptions, but with the local operators being “close” to identity operators. We establish an approximated distributivity of \star over (partial) trace functions under such a setup and generalize the “closing-the-box” operations to QFGs. We also show that the trace of an acyclic QFG can always be approximated via a sequence of “closing-the-box” operations. The belief-propagation algorithm for QFGs, which coincides with the quantum belief-propagation algorithm in [LP08], is then a natural and heuristic generalization of the “closing-the-box” based method to QFGs with cycles. We generalize the Bethe approximation to QFGs and define Helmholtz, Gibbs, and the Bethe free energies for this new setup. We show that, provided that all local operators are close to I , the fixed points of the belief-propagation algorithm for QFGs approximately correspond to the stationary points of the Bethe free energy. A numerical demonstration is also included at the end of that chapter.

Parts of the contents of Chapter 3 have been published in [CV16].

Bounding and Estimating the Classical Information Rate of Quantum Channels with Memory

In Chapter 4, we focus on the information rate of classical communications over a finite-dimensional quantum channel with memory. A quantum channel with memory is a CPTP map (see Definition 1.41) from $\mathcal{H}_A \otimes \mathcal{H}_S$ to $\mathcal{H}_B \otimes \mathcal{H}_{S'}$, where A and B are, respectively, the input and output systems and where S and S' are, respectively, the memory systems before and after the channel use (see Definition 4.2). In particular, we are interested in computing and bounding the information rate of classical communications over a quantum channel with memory using only separable-state ensemble and local measurements. This restriction is equivalent to the scenario where no quantum computing device is present at the sending or receiving end or where our manipulation of the channel is limited to a single-channel use. The difficulty of the problem lies with the presence of quantum memory. In the most straightforward situation, where

the memory system exhibits classical properties under certain ensembles and measurements, the classical communication setup is equivalent to a finite-state-machine channel (FSMC) [Gal68]. Though the evaluation of the information rate of an FSMC is nontrivial in general, efficient stochastic methods for estimating and bounding this quantity have been developed [ALV+06; SVS09].

Our work is inspired by [ALV+06], where the authors proposed an efficient stochastic method in estimating the information rate of indecomposable FSMCs, and [SVS09], where the authors proposed upper and lower bounds of the information rate of FSMCs based on auxiliary FSMCs and efficient methods for optimizing the bounds. We propose algorithms for estimating the information rate of such communication setups, along with algorithms for bounding the information rate based on so-called auxiliary channels. Some of the algorithms are generalized versions of the methods in [ALV+06; SVS09]. We also discuss suitable graphical models for doing the relevant computations. We emphasize that the auxiliary channels are learned in a data-driven approach, *i.e.*, only input/output sequences of the actual channel are needed, but not the channel model of the actual channel.

Chapter 4 is adapted from [CV20], with the majority of its contents published in [CV17b; CV19; CV20].

Structure of this Thesis

The rest of this thesis consists of the four main chapters, followed by a summary, appendices, bibliography, and an index of terms. Chapter 1 provides an introduction to some preliminary knowledge regarding factor graphs and basic quantum information theory. Readers may skip this chapter if they are already familiar with these topics. Chapters 2 and 3 discuss double-edge factor graphs and quantum factor graphs, respectively. Chapter 4 studies classical information rate of quantum channels with memory. These three chapters are relatively independent of each other, and readers may read them in any desired order.

Acknowledgment

I want to thank my supervisor Prof. Pascal VONTOBEL for his patient guidance in the past few years, and my co-supervisor, Prof. Chandra NAIR, for his suggestions and help. I also want to thank Dr. Joseph RENES for hosting my internship during the winter of 2019 and enlightening discussions.

I also want to thank the thesis committee members, Prof. Chandra NAIR, Prof. Angela ZHANG, Prof. Changhong ZHAO, Prof. Cheuk-Ting LI, and Prof. Henry PFISTER, for their time in reading this thesis and for their helpful comments.

Finally, I want to thank my wife, July, for providing continuous joy and support to my life.

The work in this thesis was supported in part by the Research Grants Council of the Hong Kong Special Administrative Region, China, under Project CUHK 14209317 and Project CUHK 14207518.

Notations

Sets

\mathcal{X}	a set
$\mathcal{A} \sqcup \mathcal{B}$	union of disjoint sets \mathcal{A} and \mathcal{B}
$\mathcal{B} \setminus \mathcal{A}$	the relative complement of \mathcal{A} with respect to \mathcal{B}
$\mathcal{B} \setminus a$	equivalent to $\mathcal{B} \setminus \{a\}$
$\mathbb{Z}, \mathbb{Z}_{>0}, \mathbb{Z}_{<0}, \mathbb{Z}_{\geq 0}$	the sets of integers, positive integers, negative integers, non-negative integers, respectively
$\mathbb{Q}, \mathbb{Q}_{>0}, \mathbb{Q}_{<0}, \mathbb{Q}_{\geq 0}$	the sets of rationals, positive rationals, negative rationals, non-negative rationals, respectively
$\mathbb{R}, \mathbb{R}_{>0}, \mathbb{R}_{<0}, \mathbb{R}_{\geq 0}$	the sets of real numbers, positive real numbers, negative real numbers, non-negative real numbers, respectively
\mathbb{C}	the sets of complex numbers

Probability and Quantum Theory

X	a random variable
P_X	probability mass function (PMF) or probability density function (PDF) w.r.t. X
$\langle X \rangle$	expectation of the random variable X
$\langle f(X) \rangle_b$	expectation of $f(X)$, where the PMF of X is b
X_1^n	a list of random variables, <i>i.e.</i> , (X_1, \dots, X_n)
$\mathfrak{P}(\mathcal{X})$	the set of all PMFs or PDFs over the set \mathcal{X}
S	a quantum system
\mathcal{H}_S	state space associated with system S , which is a Hilbert space ¹
ρ_S	a density operator associated with system S

\mathcal{S}_0^n	a list of quantum systems, <i>i.e.</i> , $(\mathcal{S}_1, \dots, \mathcal{S}_n)$
$\mathfrak{L}(\mathcal{H})$	the set of all linear operators (<i>i.e.</i> , linear transformations) on \mathcal{H}
$\mathfrak{L}_+(\mathcal{H})$	the set of all positive operators on \mathcal{H}
$\mathfrak{L}_{++}(\mathcal{H})$	the set of all strictly positive operators on \mathcal{H}
$\mathfrak{D}(\mathcal{H})$	the set of all density operators on \mathcal{H}

Linear Algebra and Matrices

\mathbf{x}	a vector
\mathbf{x}_1^n	a vector of length n , <i>i.e.</i> , $\mathbf{x}_1^n = (x_1, x_2, \dots, x_n)$
x_i	i -th entry of the vector \mathbf{x}
$\ \mathbf{v}\ _p$	ℓ_p -norm of the real vector \mathbf{x} , <i>i.e.</i> , $\ \mathbf{v}\ _p \triangleq (\sum_{i=1}^n \mathbf{v}_i ^p)^{\frac{1}{p}}$
A	a matrix
$A \geq 0$	a PD matrix, <i>i.e.</i> , $A \in \mathbb{C}^{n \times n}$ for some positive integer n and $\mathbf{v}^\dagger A \mathbf{v} \geq 0$ for all $\mathbf{v} \in \mathbb{C}^n$
$A > 0$	a PSD matrix, <i>i.e.</i> , $A \in \mathbb{C}^{n \times n}$ for some positive integer n and $\mathbf{v}^\dagger A \mathbf{v} > 0$ for all $\mathbf{v} \in \mathbb{C}^n$
$[T]$	a matrix representation of the linear transformation T
$A_{i,j}$	(i, j) -th entry of the matrix A
$\text{vec}(A)$	vectorization of an $n \times m$ matrix A , <i>i.e.</i> , $A_{i,j} = \text{vec}(A)_{i+n \cdot (j-1)}$
$\text{tr}(A), \text{tr}(T), \text{tr}(\rho)$	trace of the matrix A , of the transformation T , of the operator ρ , respectively
$ \phi\rangle$	a column vector
$\langle\phi $	a row vector adjoint to $ \phi\rangle$, equivalently $\langle\phi $ is the linear transformation $ \psi\rangle \mapsto \langle\phi \psi\rangle$
$\langle\phi \psi\rangle$	inner product between the vectors $ \phi\rangle$ and $ \psi\rangle$
$\langle\phi_A \psi_{AB}\rangle$	equivalent to $(\langle\phi_A \otimes I_B)(\psi_{AB}\rangle)$
$\exp A$	matrix exponential of the matrix A
$\log A$	matrix logarithm of the matrix A
\otimes	tensor product between two vector spaces or two operators

¹All Hilbert spaces involved in this thesis are finite-dimensional, unless stated otherwise.

\odot	Hadamard product between two matrices or vectors
\perp	perpendicular ($\mathbf{v} \perp \mathbf{u} \iff \langle \mathbf{v} \mathbf{u} \rangle = 0$)

Classical and Quantum Information Theory

$\mathbf{H}(\mathbf{X}), \mathbf{H}(p)$	Shannon entropy of the random variable \mathbf{X} and the PMF p , respectively
$\mathbf{H}(\mathbf{A}), \mathbf{H}(\rho)$	von Neumann entropy of the quantum system \mathbf{A} and the density operator ρ , respectively
$\mathbf{I}(\mathbf{X} : \mathbf{Y})$	mutual information between the random variables \mathbf{X} and \mathbf{Y}
$\mathbf{I}(\mathbf{A} : \mathbf{B})$	quantum mutual information between the systems \mathbf{A} and \mathbf{B}
$\mathbf{D}(p \ q)$	relative entropy between the PMFs p and q
$\mathbf{D}(\rho \ \sigma)$	quantum relative entropy between the density operators ρ and σ

Graph Theory

$\mathcal{G} = (\mathcal{V}, \mathcal{E}, R)$	a graph: \mathcal{V} is called the vertex set, \mathcal{E} is called the edge set, and $R : \mathcal{E} \rightarrow \mathcal{V} \times \mathcal{V}$ is called the relationship function ² of \mathcal{G}
$\mathcal{G} = (\mathcal{V}_1, \mathcal{V}_2, \mathcal{E})$	a bipartite graph, <i>i.e.</i> , $\mathcal{G} = (\mathcal{V}_1 \sqcup \mathcal{V}_2, \mathcal{E} \subseteq \mathcal{V}_1 \times \mathcal{V}_2, R : e \mapsto e)$
$\deg(v)$	the degree of the vertex v
∂v	the set of neighbors of v
$(v_1 - \dots - v_n)$	a backtrackless walk in a graph: requiring $v_i \neq v_{i+1}$ and v_i connected to v_{i+1}

Others

\star	star product between two Hermitian operators (see Eqs. (3.3) and (3.4))
---------	---

²All graphs involved in this thesis are simple, finite, and undirectional.

Acronyms

CC-QSC	classical-input classical-output quantum-state channel
CPTP	completely positive trace-preserving
CtB	closing-the-box
DeFG	double-edge factor graph
FG	(classical) factor graph
FSMC	finite-state-machine channel
i.i.d.	independent and identically distributed
NFG	normal factor graph
PD	(strictly) positive definite
PDF	probability density function
PMF	probability mass function
PSD	positive semi-definite
QFG	quantum factor graph

Note that, unless stated otherwise (only in a few numerical examples), all appearances of logarithm in this thesis should be treated as natural logarithm.

List of Figures and Tables

1.1	Some factor graphs.	2
1.2	Examples of applications of factor graphs.	5
1.3	A chain NFG, and the process to compute the marginal w.r.t. x_0 as described by (1.8).	6
1.4	Product-state setup for classical communications over a quantum channel.	29
2.1	FG describing a simple quantum system.	33
2.2	Quantum NFG for an elementary quantum system.	34
2.3	Conversions between factor graphs and DeFGs	36
2.4	n steps of unitary evolution followed by a projective measurement w.r.t. the computation basis.	38
2.5	A factor graph describing a two-measurement quantum system.	38
2.6	A factor graph describing a two-measurement quantum system with projective measure onto 1-dimension eigenspace.	39
2.7	A quantum system with two partial measurements.	39
2.8	Representing quantum systems using factor graphs and DeFGs.	40
2.9	Computing the partition sum of a normal <i>acyclic</i> DeFG.	41
2.10	Plots for Example 2.22.	50
2.11	Plots for Example 2.23.	51
2.12	Plots for Example 2.24.	52
3.1	QFG in Example 3.3.	56
3.2	QFG in Example 3.5.	57
3.3	A chain QFG. ($n \geq 3$).	61
3.4	Distribution of η for random positive operators ρ_a and ρ_b under different randomization schemes.	62

3.5	QFG in Section 3.4.	77
3.6	The partition sum Z and the induced partition sum Z_{induced} produced by Algorithm 3.2. The plot consists of 10,000 instances based on the QFG in Figure 3.5, where each local factors $\{\rho_i\}_{i=1}^6$ are generated independently as $\rho_i \leftarrow U \cdot \text{diag}(\lambda_1^{16}) \cdot U$, and where (for each ρ_i) U is some 16-by-16 unitary matrix (independently) randomly generated according to Haar measure, and where each $\{\lambda_k\}_{k=1}^{16}$ are independently uniformly distributed on $[0, 1]$	77
3.7	The partition sum Z and the induced partition sum Z_{induced} produced by Algorithm 3.2. The plot consists of 10,000 instances based on the QFG in Figure 3.5, where each local factors $\{\rho_i\}_{i=1}^6$ are generated independently as $\rho_i \leftarrow U \cdot \text{diag}(\lambda_1^{16}) \cdot U$, and where (for each ρ_i) U is some 16-by-16 unitary matrix (independently) randomly generated according to Haar measure, and where each $\{\lambda_k\}_{k=1}^{16}$ are independently distributed according to $ \mathcal{N}(1, 1) $. ($\mathcal{N}(\mu, \sigma)$ denotes the Gaussian distribution with mean μ and standard variation σ .)	78
4.1	Interpretations of quantum channels with memory.	81
4.2	Classical communications over quantum channels.	82
4.3	Classical communication over a quantum channel with memory using a separable ensemble and local measurements.	83
4.4	Channel with a classical state: closing the top box yields the input process $Q^{(n)}$, closing the bottom box yields the joint channel law $W(\mathbf{y}_1^n \mathbf{x}_1^n)$	86
4.5	Representation of $\{W^{y x}\}_{x,y}$ using an NFG.	97
4.6	The joint channel law (4.48) and (4.52) can be visualized as the result of the “closing of the outermost box” above, which can in turn be carried out by a sequence of “closing-the-box” operations as indicated.	97
4.7	Computation of the marginal PMF $P_{\mathbf{X}_\ell \mathbf{Y}_1^n; \mathbf{S}_0}$ using a sequence of “closing-the-box” operations.	98
4.8	NFG representation of the channel-ensemble-measurement configuration $(\mathcal{N}, \{\rho_A^{(x)}\}_{x \in \mathcal{X}}, \{\Lambda_B^{(y)}\}_{y \in \mathcal{Y}})$	100

4.9	A quantum Gilbert–Elliott channel (LHS), and a variant where the memory system consists of multiple qubits with only one of them controlling $U^{[s]}$ (RHS).	114
4.10	Quantum Gilbert–Elliott channel: $p_g = 0.05$ is fixed; p_b varies from 0 to 1; $V_S = \exp(-j\alpha H)$, where H is some fixed 2-by-2 Hermitian matrix and where $\alpha = 1$ is fixed; $n = 10^5$	116
4.11	Variant of the quantum Gilbert–Elliott channel described in the RHS of Figure 4.9. Parameters: $p_g = 0.05$; $p_b \in [0, 1]$; $\tilde{V}_S = \exp(-j\alpha H)$, where H is some fixed 4-by-4 Hermitian matrix and where $\alpha = 1$ is fixed; $n = 10^5$	116
4.12	Quantum Gilbert–Elliott channel: $p_g = 0.05$ is fixed; $p_b = 0.95$ is fixed; $V_S = \exp(-j\alpha H)$, where H is the same 2-by-2 Hermitian matrix as in Figure 4.10 and where α varies from 0.1 to +1.5; $n = 10^5$	117
4.13	Same variant of the quantum Gilbert–Elliott channel as in Figure 4.11 with different parameters: $p_g = 0.05$; $p_b = 0.95$; $V_S = \exp(-j\alpha H)$, where H is the same 4-by-4 Hermitian matrix as in Figure 4.11 and where α varies from 0.1 to +1.5; $n = 10^5$	117
4.14	Minimizing the difference function $\Delta_W^{(n)}$ using different methods. The markers appear after every 400 updates.	118
D.1	Verification of (4.6). Note that every “closing-the-box” operation yields a function node representing the constant function 1.	127
D.2	Counterpart of Figure D.1 for QSCs. Note that every “closing-the-box” operation yields a function node representing a Kronecker-delta function node, <i>i.e.</i> , a degree-two equality function node.	127
D.3	Efficient simulation of the channel output at step ℓ given the channel input $\tilde{\mathbf{x}}_1^n$ and the channel output $\tilde{\mathbf{y}}_1^{\ell-1}$ for an FSMC.	128
D.4	Efficient simulation of the channel output at step ℓ given the channel input $\tilde{\mathbf{x}}_1^n$ and the channel output $\tilde{\mathbf{y}}_1^{\ell-1}$ for a QSC.	128
D.5	The iterative computation of μ_ℓ^Y as in (4.20) can be understood as a sequence of “closing-the-box” operations as shown above.	129
D.6	The iterative computation of σ_ℓ^Y as in (4.71) can be understood as a sequence of “closing-the-box” operations as shown above.	129

D.7	The iterative computation of μ_ℓ^{XY} can be understood as a sequence of “closing-the-box” operations as shown above.	130
D.8	The iterative computation of σ_ℓ^{XY} as in (4.72) can be understood as a sequence of “closing-the-box” operations as shown above.	130

List of Algorithms

1.1	Belief-Propagation Algorithm (Flooding Schedule with Timeout)	9
2.1	Belief-Propagation Algorithm for Acyclic DeFGs	42
2.2	Belief-Propagation Algorithm for DeFGs (Flooding Schedule with Time- out)	44
3.1	Belief-Propagation Algorithm for Acyclic QFGs	65
3.2	Belief-Propagation Algorithm for QFGs (Flooding Schedule with Timeout)	67
4.1	Estimating the Information Rate of an FSMC	90
4.2	Estimating the Information Rate of a CC-QSC	108
4.3	Optimizing the Difference Function $\Delta_W^{(n)}(\hat{W})$	113

List of Publications

- M. X. Cao and P. O. Vontobel, “Quantum factor graphs: closing-the-box operation and variational approaches,” in *Proceedings International Symposium on Information Theory and Its Applications (ISITA)*, Monterey, CA, USA, 2016, pp. 651–655.
- M. X. Cao and P. O. Vontobel, “Estimating the information rate of a channel with classical input and output and a quantum state,” in *Proceedings IEEE International Symposium on Information Theory (ISIT)*, Aachen, Germany, 2017, pp. 3205–3209.
- M. X. Cao and P. O. Vontobel, “Double-edge factor graphs: Definition, properties, and examples,” in *Proceedings IEEE Information Theory Workshop (ITW)*, Kaohsiung, Taiwan, 2017, pp. 136–140.
- M. X. Cao and P. O. Vontobel, “Optimizing bounds on the classical information rate of quantum channels with memory,” in *Proceedings IEEE International Symposium on Information Theory (ISIT)*, Paris, France, 2019, pp. 265–269.
- M. X. Cao and P. O. Vontobel, “Bounding and estimating the classical information rate of quantum channels with memory,” *IEEE Transactions on Information Theory*, vol. 66, no. 9, pp. 5601–5619, 2020.

Contents

Preface	iii
Acknowledgment	vii
List of Figures and Tables	xv
List of Algorithms	xvi
List of Publications	xvii
1 Preliminaries	1
1.1 Factor Graphs and Belief-Propagation Algorithms	1
1.2 Basic quantum information theory	20
2 Double-Edge Factor Graphs	32
2.1 From FGs for Quantum Probabilities to DeFGs	33
2.2 DeFGs and Quantum Systems: Examples	37
2.3 Belief-Propagation Algorithms for DeFGs	39
2.4 Numerical Examples	49
3 Quantum Factor Graphs	54
3.1 The \star -Product and Quantum Factor Graphs (QFGs)	55
3.2 Quantum Belief-Propagation Algorithms	63
3.3 Generalization of Bethe's approximation for QFGs	69
3.4 Numerical Example	76
4 IRs of Quantum Channels with Memory	80
4.1 Review of FSMCs	85

4.2	QCwM & their Graphical Representation	92
4.3	Information Rate and its Estimation	100
4.4	IRUB/IRLB and their Optimization	107
4.5	Example: Quantum Gilbert–Elliott Channels	114
	Summary and Outlook	119
	Appendix A Alternative Distributivity	121
	Appendix B Quantum Exponential Family	123
	Appendix C Differentiability of $-\text{tr}(\sigma \cdot \log \rho(\boldsymbol{\eta}))$	125
	Appendix D Additional Figures for Chapter 4	127
	Bibliography	130
	Index	139

Chapter 1

Preliminaries

The preliminaries of this thesis, as introduced in this chapter, include basic results regarding *classical* factor graphs (FGs) and basic quantum information theory, each comprising one section of the chapter. Readers may skip the corresponding section(s) provided familiarity with the topic(s). We emphasize the reviewing nature of this chapter; namely, the results are either known contributions, or derived rather straightforwardly.

1.1 Factor Graphs and Belief-Propagation Algorithms

This section reviews factor graphs, belief-propagation (BP) algorithms, and several interpretations of BP algorithms' outputs.

1.1.1 Factor Graphs and Normal Factor Graphs

Given a real-valued function g of multiple variables, a factorization of g is an expression in the form

$$g((x_i)_{i \in \mathcal{V}}) = \prod_{a \in \mathcal{F}} f_a(\mathbf{x}_{\partial a}), \quad (1.1)$$

where \mathcal{V} , \mathcal{F} are some finite sets and where, for each $a \in \mathcal{F}$, $\partial a \subseteq \mathcal{V}$ denotes the indices of the arguments of f_a . A factorization as in (1.1) can be represented by a *bipartite* graph between \mathcal{V} and \mathcal{F} , with $i \in \mathcal{V}$ being a neighbor of $a \in \mathcal{F}$ if and only if $i \in \partial a$ (see Figure 1.1a); conversely, such a graph is called a *factor graph* (FG) *representing* (1.1).

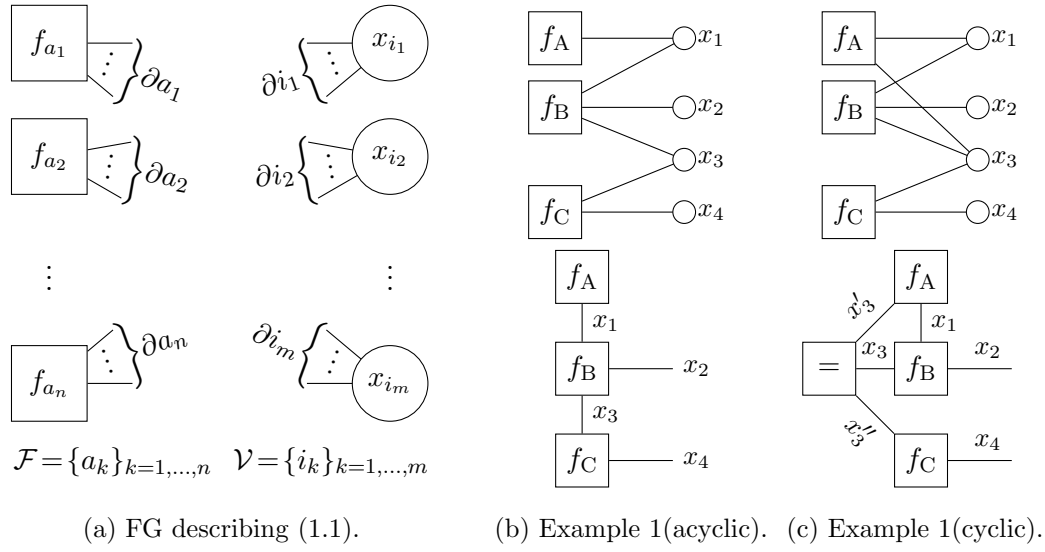


Figure 1.1: Some factor graphs.

Example 1.1 (Two simple examples). The factor graph in Figure 1.1b depicts the factorization

$$g(x_1, x_2, x_3, x_4) = f_A(x_1) \cdot f_B(x_1, x_2, x_3) \cdot f_C(x_3, x_4). \quad (1.2)$$

Note that in this factor graph, $\deg(i) \leq 2$ for each $i \in \mathcal{V}$. In this case, one can simplify the graph by drawing all the vertices in \mathcal{V} as edges, as shown in the bottom part of the figure. Note that vertices in \mathcal{V} with degree 1 result in so-called half-edges. The bottom graph is often known as a *normal* factor graph (NFG) [For01; AMV11].

The factor graph in Figure 1.1c depicts the factorization

$$g(x_1, x_2, x_3, x_4) = f_A(x_1, x_3) \cdot f_B(x_1, x_2, x_3) \cdot f_C(x_3, x_4). \quad (1.3)$$

In comparison with the previous example, this factor graph is cyclic. Despite the fact that $\deg(x_3) > 2$, we can still redraw this graph as an NFG by introducing an *equality* node, as depicted in the bottom part of Figure 1.1c. \square

We formalize the above discussion as follows.

Definition 1.2 (Factor Graph). A *factor graph* (FG) is a bipartite graph $\mathcal{G} = (\mathcal{V}, \mathcal{F}, \mathcal{E} \subseteq \mathcal{V} \times \mathcal{F})$ associated with a variable set \mathfrak{V} and a factor set \mathfrak{F} , where

- $\mathfrak{V} = \{\mathcal{X}_i\}_{i \in \mathcal{V}}$ is indexed by \mathcal{V} , and each element of \mathfrak{V} is a set (a.k.a. alphabets);
- $\mathfrak{F} = \{f_a\}_{a \in \mathcal{F}}$ is indexed by \mathcal{F} , and $f_a : \times_{i \in \partial a} \mathcal{X}_i \rightarrow \mathbb{R}$ for each $a \in \mathcal{F}$.

The function $g(\mathbf{x}) \triangleq \prod_{a \in \mathcal{F}} f_a(\mathbf{x}_{\partial a})$ is called the *global function* of \mathcal{G} , and in this case, \mathcal{G} is said to be representing the factorization $g(\mathbf{x}) = \prod_{a \in \mathcal{F}} f_a(\mathbf{x}_{\partial a})$.¹ A factor graph is *normal* if the degree of any vertex in \mathcal{V} is at most 2. \square

Remark 1.3. We often redraw the vertices in \mathcal{V} in an NFG as edges, as in Figure 1.1b.

Remark 1.4. Any factor graph can be converted into an NFG by properly introducing equality node(s), as in the bottom part of Figure 1.1c.

1.1.2 Marginals and Partition Sums

The *marginals* (or *partition sum*) of a multivariable function are the results of the summation over some (or all) of its arguments. Computing marginals and partition sums of factorizations is a recurring problem in physics and computer science, as demonstrated in the following two examples.

Example 1.5 (A 2-D Ising Model [ML13]). Figure 1.2a depicts the factorization of the configuration probability of a 2-D $n \times n$ Ising model:

$$p^{(\beta)}(\mathbf{x}_{1,1}^{n,n}) \propto g^{(\beta)}(\mathbf{x}_{1,1}^{n,n}) \triangleq \prod_{i,j=1,\dots,n} h_{i,j}^{(\beta)}(x_{i,j}) \cdot \prod_{\substack{i,j,i',j' \in \{1,\dots,n\} \\ |i-i'|+|j-j'|=1}} f^{(\beta)}(x_{i,j}, x_{i',j'}), \quad (1.4)$$

where

- $x_{i,j} \in \{-1, 1\}$ describes the spin configuration of the particle at location (i, j) ;
- $\beta \in (0, +\infty)$ is the inverse temperature;
- $h_{i,j}^{(\beta)}(x_{i,j}) \triangleq \exp\left(-\beta \cdot \tilde{h}_{i,j} \cdot x_{i,j}\right)$, where $(\tilde{h}_{i,j} \cdot x_{i,j})$ is the energy contributed by the external magnetic field on the particle at (i, j) ;
- $f^{(\beta)}(x_{i,j}, x_{i',j'}) \triangleq \exp\left(-\beta \cdot x_{i,j} x_{i',j'}\right)$, where $(x_{i,j} x_{i',j'})$ is the energy contributed by the ferromagnetic interaction between the particles (i, j) and (i', j') .

In this case, the *partition function* (as a function of β) of the system is given by

$$Z(\beta) = \sum_{\mathbf{x}_{1,1}^{n,n}} \exp\left(-\beta \cdot \left(\sum_{i,j=1,\dots,n} \tilde{h}_{i,j} \cdot x_{i,j} + \sum_{\substack{i,j,i',j' \in \{1,\dots,n\} \\ |i-i'|+|j-j'|=1}} x_{i,j} x_{i',j'}\right)\right) = \sum_{\mathbf{x}_{1,1}^{n,n}} g^{(\beta)}(\mathbf{x}_{1,1}^{n,n}), \quad (1.5)$$

¹Here, $\mathbf{x} \triangleq (x_i)_{i \in \mathcal{V}}$. This also applies for later appearances of “ \mathbf{x} ” as an argument of global functions.

and the *Helmholtz free energy* of the system is

$$F = -\beta^{-1} \log Z(\beta), \quad (1.6)$$

which is the maximum useful work obtainable from the system.² \square

We borrow the terms *partition function* and *Helmholtz free energy* from statistical mechanics.

Definition 1.6 (Partition Sum, Free energy). Given a factor graph \mathcal{G} describing the factorization $g(\mathbf{x}) = \prod_{a \in \mathcal{F}} f_a(\mathbf{x}_{\partial a})$, the *partition sum* of \mathcal{G} is defined as

$$Z(\mathcal{G}) \triangleq \sum_{\mathbf{x}} g(\mathbf{x}) = \sum_{\mathbf{x}} \prod_{a \in \mathcal{F}} f_a(\mathbf{x}_{\partial a}). \quad (1.7)$$

Also, the (*Helmholtz*) *free energy* of \mathcal{G} is defined as $F_H(\mathcal{G}) \triangleq -\log Z(\mathcal{G})$. \square

Example 1.7 (Bit-wise Decoding of an LDPC Code [Gal62]). Figure 1.2b depicts the factorization of the conditional distribution of the inputs $(\mathbf{X}_1, \dots, \mathbf{X}_n)$ given the detected outputs (y_1, \dots, y_n) , using a regular LDPC code and i.i.d. copies of a memoryless channel. Namely,

$$P_{\mathbf{X}_1^n | \mathbf{Y}_1^n}(\mathbf{x}_1^n | \mathbf{y}_1^n) \propto g(\mathbf{x}_1^n, \mathbf{y}_1^n) \triangleq \prod_{\ell=1}^n P_{Y|X}(y_\ell | x_\ell) \cdot \prod_{a=1}^d f_+(\mathbf{x}_{\partial a}),$$

where

- the input/output alphabet are some finite sets;
- $P_{Y|X}$ is the conditional PMF characterizing the memoryless channel in use;
- d is a positive integer smaller than n and where, for each $a \in \{1, \dots, d\}$, $\partial a \subseteq \{1, \dots, n\}$ and $|\partial a| = k$ for some positive integer $k \ll n$;
- $f_+(\mathbf{v}) \triangleq \begin{cases} 1 & \sum_{i=1}^k v_i = 0_{\mathbb{F}} \\ 0 & \text{otherwise} \end{cases}, \forall \mathbf{v} \in \mathbb{F}^k.$

In this case, bit-wise decoding is equivalent to computing the marginals

$$P_{\mathbf{X}_i | \mathbf{Y}_1^n}(x_i | \mathbf{y}_1^n) \propto \sum_{\mathbf{x}_{\{1, \dots, n\} \setminus i}} g(\mathbf{x}_1^n, \mathbf{y}_1^n) = \sum_{\mathbf{x}_{\{1, \dots, n\} \setminus i}} \prod_{\ell=1}^n P_{Y|X}(y_\ell | x_\ell) \cdot \prod_{a=1}^d f_+(\mathbf{x}_{\partial a})$$

for each $i = 1, \dots, n$. \square

²Note that the term “partition function” and “Helmholtz free energy” are established terms in thermodynamics, and describe a physical system’s statistical properties. These two terms were later borrowed, and defined differently in the context of statistical models and graphical methods.

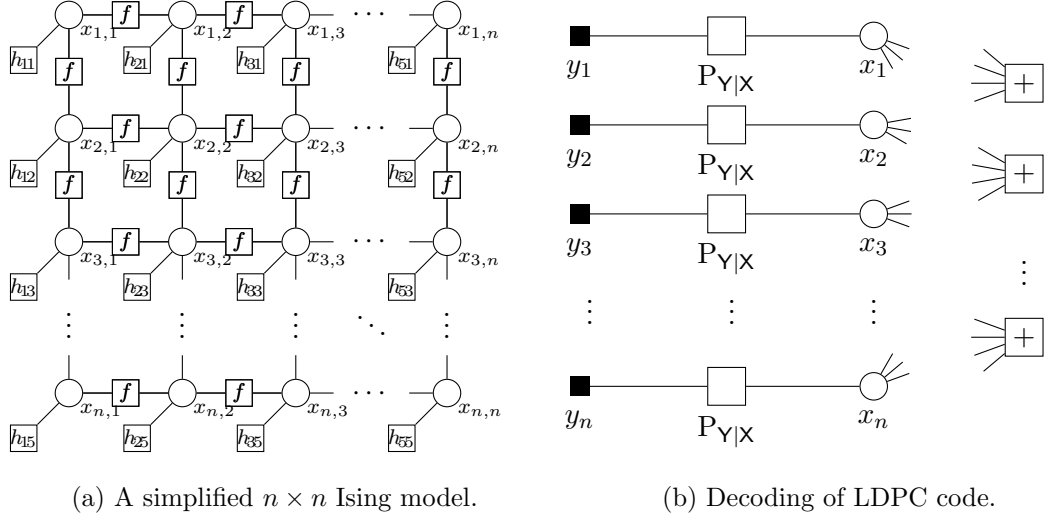


Figure 1.2: Examples of applications of factor graphs.

1.1.3 Computing the Marginals/Partition Sums of Acyclic Factor Graphs

In both examples in the last section, the quantities of interest are some marginals (or partition sum) of the factorization involved. However, direct computation of the marginals (or partition sum) is not scalable, as the number of configurations grows exponentially w.r.t. the number of variables. Utilizing the distributivity of \cdot over $+$, one can compute the marginals more efficiently in some, but not all, cases (*e.g.*, a complete bipartite factor graph). This is particularly the case for acyclic factor graphs, where marginals can be computed by summing over exactly *one* variable at each step. For example, the marginal w.r.t. x_0 of the NFG in Figure 1.3(0) can be computed in $n + 1$ steps as

$$\begin{aligned}
 p(x_0) &\triangleq \sum_{x_1, \dots, x_n} \mu(x_0) \cdot \prod_{\ell=1}^n p(x_\ell | x_{\ell-1}) \\
 &= \mu(x_0) \cdot \sum_{x_1} \left(p(x_1 | x_0) \sum_{x_2} \left(p(x_2 | x_1) \cdots \sum_{x_{n-1}} \left(p(x_{n-1} | x_{n-2}) \sum_{x_n} p(x_n | x_{n-1}) \right) \cdots \right) \right).
 \end{aligned} \tag{1.8}$$

Such computations (by exploiting distributivity) can be illustrated as a sequence of “closing-the-box” (CtB) operations, where at each step we replace the subgraph *in the box* with the result of the summation over the variables *inside* the box (as shown in Figure 1.3(1)–(n+1)).

Equivalently, the above process can also be described as a *message-passing algorithm*. Namely, for an acyclic factor graph $((\mathcal{V}, \mathcal{F}, \mathcal{E}), \{\mathcal{X}_i\}_{i \in \mathcal{V}}, \{f_a\}_{a \in \mathcal{F}})$, there exists a

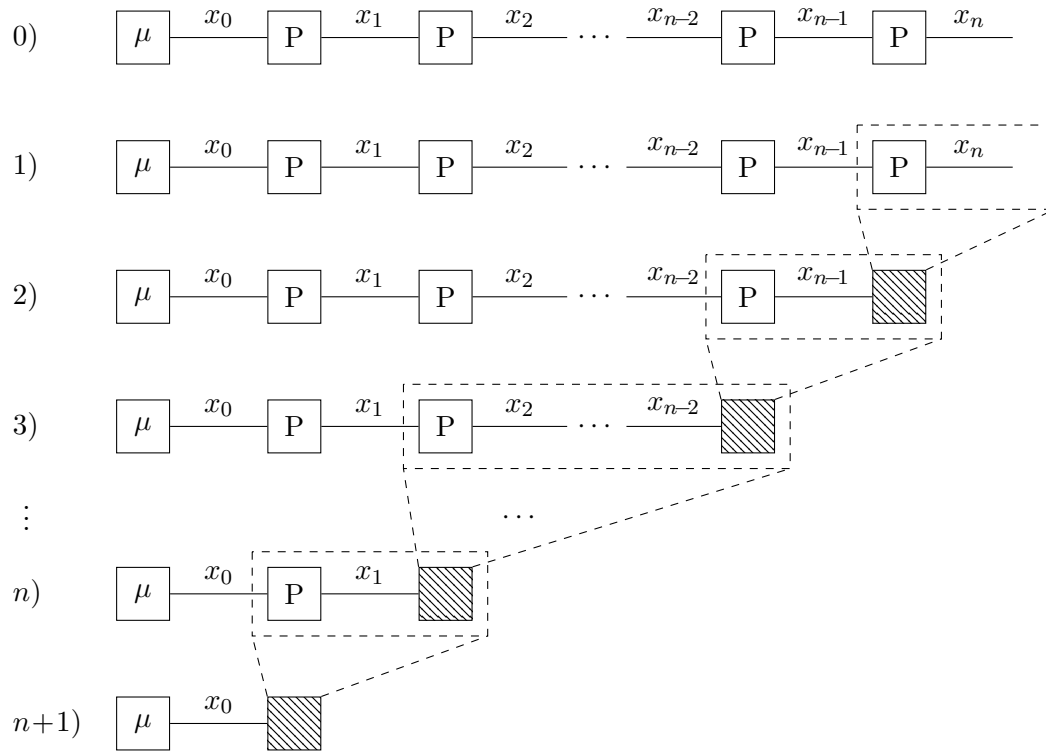


Figure 1.3: A chain NFG, and the process to compute the marginal w.r.t. x_0 as described by (1.8).

unique set of functions (a.k.a. *messages*) $\{m_{i \rightarrow a}, m_{a \rightarrow i} : \mathcal{X}_i \rightarrow \mathbb{R}\}_{(i,a) \in \mathcal{E}}$ such that

$$m_{i \rightarrow a}(x_i) = \prod_{c \in \partial i \setminus a} m_{c \rightarrow i}(x_i) \quad (1.9)$$

$$m_{a \rightarrow i}(x_i) = \sum_{\mathbf{x}_{\partial a \setminus i}} f_a(\mathbf{x}_{\partial a}) \cdot \prod_{j \in \partial a \setminus i} m_{j \rightarrow a}(x_j) \quad (1.10)$$

for all $(i, a) \in \mathcal{E}$, where we treat a vacuous product as constant 1. Intuitively speaking, since the factor graph is acyclic, one can always construct a set of messages satisfying (1.9) and (1.10) from the leaves up to the root. We state and prove this result as the following theorem.

Theorem 1.8. *Consider an acyclic factor graph $((\mathcal{V}, \mathcal{F}, \mathcal{E}), \{\mathcal{X}_i\}_{i \in \mathcal{V}}, \{f_a\}_{a \in \mathcal{F}})$. There exists a unique set of messages $\{m_{i \rightarrow a}, m_{a \rightarrow i} : \mathcal{X}_i \rightarrow \mathbb{R}\}_{(i,a) \in \mathcal{E}}$ satisfying (1.9) and (1.10), and*

$$\sum_{\mathbf{x}_{\mathcal{V} \setminus i}} \prod_{a \in \mathcal{F}} f_a(\mathbf{x}_{\partial a}) = \prod_{c \in \partial i} m_{c \rightarrow i}(x_i) \quad \forall x_i, \forall i \in \mathcal{V}, \quad (1.11)$$

$$\sum_{\mathbf{x}_{\mathcal{V} \setminus \partial a}} \prod_{c \in \mathcal{F}} f_c(\mathbf{x}_{\partial c}) = f_a(\mathbf{x}_{\partial a}) \cdot \prod_{i \in \partial a} m_{i \rightarrow a}(x_i) \quad \forall \mathbf{x}_{\partial a}, \forall a \in \mathcal{F}. \quad (1.12)$$

Proof. Without loss of generality, we assume the graph $(\mathcal{V}, \mathcal{F}, \mathcal{E})$ to be connected.

Existence: Since the bipartite graph $(\mathcal{V}, \mathcal{F}, \mathcal{E})$ is acyclic, by removing any edge $(i, a) \in \mathcal{E}$, the graph is split into two disjoint bipartite graphs $(\mathcal{V}_i^a, \mathcal{F}_i^a, \mathcal{E}_i^a)$ and $(\mathcal{V}_a^i, \mathcal{F}_a^i, \mathcal{E}_a^i)$ where $i \in \mathcal{V}_i^a$, $a \in \mathcal{F}_a^i$, and $(\mathcal{V}, \mathcal{F}, \mathcal{E}) = (\mathcal{V}_i^a \sqcup \mathcal{V}_a^i, \mathcal{F}_i^a \sqcup \mathcal{F}_a^i, \mathcal{E}_i^a \sqcup \{(i, a)\} \sqcup \mathcal{E}_a^i)$. For each $(i, a) \in \mathcal{E}$, we define

$$m_{i \rightarrow a}(x_i) \triangleq \sum_{x_j: j \in \mathcal{V}_i^a \setminus i} \prod_{c \in \mathcal{F}_i^a} f_c(\mathbf{x}_{\partial c}),$$

$$m_{a \rightarrow i}(x_i) \triangleq \sum_{x_j: j \in \mathcal{V}_a^i} \prod_{c \in \mathcal{F}_a^i} f_c(\mathbf{x}_{\partial c}).$$

Because the bipartite graph $(\mathcal{V}, \mathcal{F}, \mathcal{E})$ is acyclic, we observe:

1. For each $(i, a) \in \mathcal{E}$, $(\mathcal{V}_i^a, \mathcal{F}_i^a, \mathcal{E}_i^a) = (\{i\} \cup \bigsqcup_{c \in \partial i \setminus a} \mathcal{V}_c^i, \bigsqcup_{c \in \partial i \setminus a} \mathcal{F}_c^i, \bigsqcup_{c \in \partial i \setminus a} \mathcal{E}_c^i)$,
2. For each $(i, a) \in \mathcal{E}$, $(\mathcal{V}_a^i, \mathcal{F}_a^i, \mathcal{E}_a^i) = (\bigsqcup_{j \in \partial a \setminus i} \mathcal{V}_j^a, \{a\} \cup \bigsqcup_{j \in \partial a \setminus i} \mathcal{F}_j^a, \bigsqcup_{j \in \partial a \setminus i} \mathcal{E}_j^a)$,
3. For each $i \in \mathcal{V}$, $(\mathcal{V}, \mathcal{F}, \mathcal{E}) = (\{i\} \cup \bigsqcup_{a \in \partial i} \mathcal{V}_a^i, \bigsqcup_{a \in \partial i} \mathcal{F}_a^i, \{(i, a) | a \in \partial i\} \cup \bigsqcup_{a \in \partial i} \mathcal{E}_a^i)$,
4. For each $a \in \mathcal{F}$, $(\mathcal{V}, \mathcal{F}, \mathcal{E}) = (\bigsqcup_{i \in \partial a} \mathcal{V}_i^a, \{a\} \cup \bigsqcup_{i \in \partial a} \mathcal{F}_i^a, \{(i, a) | i \in \partial a\} \cup \bigsqcup_{i \in \partial a} \mathcal{E}_i^a)$,

which implies (1.9), (1.10), (1.11), and (1.12), respectively.

Uniqueness: Assume there exist two different sets of messages $\{m_{i \rightarrow a}, m_{a \rightarrow i}\}_{(i,a) \in \mathcal{E}}$ and $\{m'_{i \rightarrow a}, m'_{a \rightarrow i}\}_{(i,a) \in \mathcal{E}}$, both satisfying (1.9), (1.10), (1.11), and (1.12). Without loss of generality, let $m_{i_0 \rightarrow a_0} \neq m'_{i_0 \rightarrow a_0}$. By invoking (1.9) and (1.10) alternatively, one can construct a path (as long as possible) $(a_0 - i_0 - a_i - i_1 - \dots)$ such that $m_{a_k \rightarrow i_{k-1}} \neq m'_{a_k \rightarrow i_{k-1}}$ and $m_{i_k \rightarrow a_k} \neq m'_{i_k \rightarrow a_k}$ for each k . Since $(\mathcal{V}, \mathcal{F}, \mathcal{E})$ is finite and acyclic, such a path must be of finite length, with the last vertex being a leaf of the graph. If the last vertex is from \mathcal{V} , say i_{last} , we have $m_{i_{\text{last}} \rightarrow a_{\text{last}}} = \mathbf{1} = m_{i_{\text{last}} \rightarrow a_{\text{last}}}$. Otherwise, if it is from \mathcal{F} , say a_{last} , we have $m_{a_{\text{last}} \rightarrow i_{\text{last}-1}} = f_{a_{\text{last}}} = m'_{a_{\text{last}} \rightarrow i_{\text{last}-1}}$. In both cases, we have a contradiction. Therefore, the set of messages satisfying (1.9), (1.10), (1.11), and (1.12) must be unique. \square

1.1.4 Belief-Propagation Algorithms & BP Fixed Points

For generic factor graphs, the belief-propagation (BP) algorithms are *heuristic* generalizations of the message-passing algorithm described by (1.9) and (1.10). Such generalizations are made by initializing all the messages as constant functions and updating them according to (1.9) and (1.10). Namely,

$$m_{i \rightarrow a}^{(t)}(x_i) \propto \prod_{c \in \partial i \setminus a} m_{c \rightarrow i}^{(t)}(x_i) \quad \forall (i, a) \in \mathcal{E}, \quad (1.13)$$

$$m_{a \rightarrow i}^{(t)}(x_i) \propto \sum_{\mathbf{x}_{\partial a \setminus i}} f_a(\mathbf{x}_{\partial a}) \cdot \prod_{j \in \partial a \setminus i} m_{j \rightarrow a}^{(t-1)}(x_j) \quad \forall (i, a) \in \mathcal{E}, \quad (1.14)$$

where $t \in \{1, 2, \dots\}$ and where the initial message $m_{i \rightarrow a}^{(0)}$ is some constant function for each $(i, a) \in \mathcal{E}$. Notice that, in the above updating rules, all new messages are computed using the old messages from the last “batch”. Such a *sequence* of updates is known as the synchronous *schedule* (a.k.a. flooding schedule). Though asynchronous schedules do exist,³ and can be helpful in many specific situations (see, *e.g.*, [SLG07; FYZ17]), they are beyond our scope of discussion. Algorithm 1.1 lists the belief-propagation algorithm with the flooding schedule.

We consider an instance of BP algorithms to be “completed”, if the messages $\{m_{i \rightarrow a}^{(t)}, m_{a \rightarrow i}^{(t)}\}_{(i,a)}$ “converge” under the updating rules (1.13) and (1.14), namely when the changes of messages are *negligible* after applying the updates. In this sense, the result

³Thus, the belief-propagation algorithms are a class of algorithms instead of a single algorithm.

Algorithm 1.1 Belief-Propagation Algorithm (Flooding Schedule with Timeout)

Input: A factor graph $(\mathcal{G} = (\mathcal{V}, \mathcal{F}, \mathcal{E} \subseteq \mathcal{V} \times \mathcal{F}), \mathfrak{V} = \{\mathcal{X}\}_{i \in \mathcal{V}}, \mathfrak{F} = \{f_a\}_{a \in \mathcal{F}})$, $\varepsilon \geq 0$;**Output:** Messages $\{m_{i \rightarrow a}, m_{a \rightarrow i} : \mathcal{X}_i \rightarrow \mathbb{R}_+\}_{(i,a) \in \mathcal{E}}$, FLAG $\in \{\text{completed}, \text{timeout}\}$.

```

1: for all  $(i, a) \in \mathcal{E}$  do
2:    $m_{i \rightarrow a}^{(0)}(x_i) \leftarrow |\mathcal{X}_i|^{-1}$  for each  $x_i \in \mathcal{X}_i$ ;
3: end for
4:  $t \leftarrow 0$ ;
5: do
6:    $t \leftarrow t + 1$ ;
7:   for all  $(i, a) \in \mathcal{E}$  do
8:      $m_{a \rightarrow i}^{(t)}(x_i) \propto \sum_{\mathbf{x}_{\partial a \setminus i}} f(\mathbf{x}_{\partial a}) \cdot \prod_{j \in \partial a \setminus i} m_{j \rightarrow a}^{(t-1)}(x_j)$  for each  $x_i \in \mathcal{X}_i$ ;
9:   end for
10:  for all  $(i, a) \in \mathcal{E}$  do
11:     $m_{i \rightarrow a}^{(t)}(x_i) \propto \prod_{c \in \partial i \setminus a} m_{c \rightarrow i}^{(t)}(x_i)$  for each  $x_i \in \mathcal{X}_i$ ;
12:  end for
13:  while  $(\neg \text{timeout}) \wedge (\exists (i, a) \in \mathcal{E} \text{ s.t. } \|m_{i \rightarrow a}^{(t)} - m_{i \rightarrow a}^{(t-1)}\|_2 > \varepsilon \text{ or } \|m_{a \rightarrow i}^{(t)} - m_{a \rightarrow i}^{(t-1)}\|_2 > \varepsilon)$ 
     $\triangleright \text{timeout} = \text{false unless the operating time exceeds a pre-selected waiting time.}$ 
14:  if timeout then
15:    FLAG  $\leftarrow$  timeout;
16:  else
17:    FLAG  $\leftarrow$  completed;
18:    for all  $(i, a) \in \mathcal{E}$  do
19:       $m_{i \rightarrow a} \leftarrow m_{i \rightarrow a}^{(t)}$ ;
20:       $m_{a \rightarrow i} \leftarrow m_{a \rightarrow i}^{(t)}$ ;
21:    end for
22:  end if

```

of a “completed” BP algorithm will always be (or at least be close to) a *fixed point* of the update, namely a set of messages that stay unchanged w.r.t. (1.13) and (1.14). We call such sets of messages BP fixed points (see definition below).

Definition 1.9 (BP Fixed point). A set of messages $\{m_{i \rightarrow a}, m_{a \rightarrow i}\}_{i,a}$ is said to be a BP fixed point if

$$m_{i \rightarrow a}(x_i) \propto \prod_{c \in \partial i \setminus a} m_{c \rightarrow i}(x_i) \quad \forall (i, a) \in \mathcal{E}, \quad (1.15)$$

$$m_{a \rightarrow i}(x_i) \propto \sum_{\mathbf{x}_{\partial a \setminus i}} f_a(\mathbf{x}_{\partial a}) \cdot \prod_{j \in \partial a \setminus i} m_{j \rightarrow a}(x_j) \quad \forall (i, a) \in \mathcal{E}. \quad (1.16)$$

In this case, the set $\{m_{i \rightarrow a}, m_{a \rightarrow i}\}_{i,a}$ is also called a set of fixed-point messages. \square

Corollary 1.10. *Consider Algorithm 1.1 with acyclic input factor graph and with no “timeout” constraint (i.e., the pre-selected waiting time infinity). For any $\varepsilon \geq 0$, the algorithm will always end with “FLAG = completed” within finite time.*

Proof. Let $\{m_{i \rightarrow a}, m_{a \rightarrow i}\}_{(i,a) \in \mathcal{E}}$ be defined as in the proof of Theorem 1.8, and let $\{m_{i \rightarrow a}^{(t)}, m_{a \rightarrow i}^{(t)}\}_{(i,a) \in \mathcal{E}}$ denote the messages in Algorithm 1.1 at timestamp t . For any i, a, t such that $m_{a \rightarrow i}^{(t)} \not\propto m_{a \rightarrow i}$, using the same construction in the “Uniqueness” part of the proof of Theorem 1.8, one can construct a path $i - a - i_1 - a_1 - \dots - a_{t-1} - i_t$ such that $m_{i_t \rightarrow a_{t-1}}^{(0)} \not\propto m_{i_t \rightarrow a_{t-1}}$. Since the factor graph is acyclic, the diameter of the factor graph must be at least $2t + 1$. Thus, for any $t \geq \lceil \frac{D}{2} \rceil$, $m_{a \rightarrow i}^{(t)} \propto m_{a \rightarrow i}$, where D denotes the diameter of the graph. Similarly, $m_{i \rightarrow a}^{(t)} \propto m_{i \rightarrow a}$ for all $t \geq \lceil \frac{D}{2} \rceil$. In other words, for any $\varepsilon \geq 0$

$$\left\| m_{i \rightarrow a}^{(t)} - m_{i \rightarrow a}^{(t-1)} \right\|_2 \leq \varepsilon \text{ and } \left\| m_{a \rightarrow i}^{(t)} - m_{a \rightarrow i}^{(t-1)} \right\|_2 \leq \varepsilon \quad \forall (i, a) \in \mathcal{E} \quad \forall t \geq \left\lceil \frac{D}{2} \right\rceil + 1,$$

namely, the algorithm will “complete” within finite time. \square

As a direct result of Corollary 1.10, for acyclic factor graphs, taking $\varepsilon = 0$, Algorithm 1.1 (with no “timeout” constraint) will always produce the BP-fixed point within finite time. For cyclic factor graphs in general, however, such results do not generalize. On the one hand, there exist instances of BP algorithms that fail to converge. (More interestingly, there are examples of Gaussian message passing algorithms⁴ (GMPAs)

⁴Gaussian message passing algorithms or GMPAs are a special class of BP algorithms on continuous-alphabet factor graphs with additional constraints on its factors.

in which the convergence depends on the update schedule [FYZ17].) On the other hand, there also exist factor graphs with multiple BP fixed points. Though the algorithm has been justified for some special classes of factor graphs, *e.g.*, walk-sumable Gaussian graphical models [MJW06], more generic works have been focusing on various interpretations of BP fixed points [YFW05; Von13a; CC06]. In the remainder of this section, we review two of these interpretations of BP fixed points for factor graphs with non-negative local functions.

1.1.5 Interpretations of BP fixed points: The Variational Approach and Bethe's Approximation

In this section, we review a method known as the variational approach together with Bethe's approximation (see, *e.g.*, [YFW05]). The idea behind such methods has a deep root in statistical mechanics. Note that computing the marginals is equivalent to computing the partition sums (of some slightly modified factor graphs) and thus is equivalent to computing the Helmholtz free energies. The idea of this method consists of two parts: The variational approach and the Bethe free energy.

The Variational Approach

The variational approach is a method adopted from variational mechanics, in which one considers the Helmholtz free energy as the minimal Gibbs free energy over all possible configurations. The Gibbs free energy of a factor graph is defined as follows.

Definition 1.11 (Gibbs free energy). Given a factor graph \mathcal{G} describing the factorization $g(\mathbf{x}) = \prod_{a \in \mathcal{F}} f_a(\mathbf{x}_{\partial a})$ with $f_a \geq 0$ for each a , the *Gibbs free energy* (a.k.a. the variational free energy) of \mathcal{G} is defined as

$$F_{\mathcal{G}}(b) \triangleq - \sum_{a \in \mathcal{F}} \sum_{\mathbf{x}} b(\mathbf{x}) \log f_a(\mathbf{x}_{\partial a}) + \sum_{\mathbf{x}} b(\mathbf{x}) \log b(\mathbf{x}) \quad (1.17)$$

for each PMF $b(\mathbf{x})$ on $\times_{i \in \mathcal{V}} \mathcal{X}_i$. Note that for the case where there exists some \mathbf{x} such that $b(\mathbf{x}) > 0$ and $f_a(\mathbf{x}_a) = 0$ for some a , we take the convention that $F_{\mathcal{G}}(b) \triangleq +\infty$. \square

Proposition 1.12. For any PMF b on $\times_{i \in \mathcal{V}} \mathcal{X}_i$, we have

$$F_{\mathcal{G}}(b) \geq F_{\mathcal{H}}, \quad (1.18)$$

with equality if and only if $b(\mathbf{x}_{\mathcal{V}}) \propto \prod_{a \in \mathcal{F}} f_a(\mathbf{x}_{\partial a})$.

Proof. The proof is done by showing $F_G(b) - F_H = D(b||p)$, where the PMF $p(\mathbf{x}) \triangleq Z^{-1} \cdot \prod_{a \in \mathcal{F}} f_a(\mathbf{x}_{\partial a})$. We omit the details. \square

As a result of Proposition 1.12, the Helmholtz free energy F_H can be obtained by minimizing $F_G(b)$. However, such a minimization problem is generally intractable since the problem's dimension grows exponentially w.r.t. the number of variables. This has motivated physicists (since the 1900s) to develop “good” yet tractable approximations to F_G . The Bethe free energy [Bet35] reviewed below is one of these approximations.

The Bethe free energy

Definition 1.13 (Bethe free energy). Given a factor graph \mathcal{G} describing the factorization $g(\mathbf{x}) = \prod_{a \in \mathcal{F}} f_a(\mathbf{x}_{\partial a})$, the *Bethe free energy* is the function

$$F_B(\{b_a\}_{a \in \mathcal{F}}, \{b_i\}_{i \in \mathcal{V}}) \triangleq - \sum_{a \in \mathcal{F}} \sum_{\mathbf{x}_{\partial a}} b_a(\mathbf{x}) \log f_a(\mathbf{x}_{\partial a}) + \sum_{a \in \mathcal{F}} b_a(\mathbf{x}_{\partial a}) \log b_a(\mathbf{x}_{\partial a}) - \sum_{i \in \mathcal{V}} (d_i - 1) \cdot \sum_{x_i} b_i(x_i) \log(b_i(x_i)), \quad (1.19)$$

where the domain of F_B is

$$\mathcal{L}(\mathcal{G}) \triangleq \left\{ (\{b_a\}_{a \in \mathcal{F}}, \{b_i\}_{i \in \mathcal{V}}) \left| \begin{array}{ll} b_a \in \mathfrak{P}(\times_{i \in \partial a} \mathcal{X}_i) & \forall a \in \mathcal{F} \\ b_i \in \mathfrak{P}(\mathcal{X}_i) & \forall i \in \mathcal{V} \\ \sum_{\mathbf{x}_{\partial a \setminus i}} b_a(\mathbf{x}_{\partial a}) = b_i(x_i) & \forall x_i \quad \forall (i, a) \in \mathcal{E} \end{array} \right. \right\}$$

and where $d_i \triangleq \deg(i)$ is the degree of the vertex i for each $i \in \mathcal{V}$. \square

The set $\mathcal{L}(\mathcal{G})$ is often known as the *local marginal polytope*. The marginals of a global PMF always compose an element in $\mathcal{L}(\mathcal{G})$. However, the converse is not necessarily true. Namely, if we define the set $\mathcal{M}(\mathcal{G})$ (often known as the *marginal polytope*) as

$$\mathcal{M}(\mathcal{G}) \triangleq \left\{ (\{b_a\}_{a \in \mathcal{F}}, \{b_i\}_{i \in \mathcal{V}}) \left| \begin{array}{l} \exists b \in \mathfrak{P}(\times_{i \in \mathcal{V}} \mathcal{X}_i) \text{ s.t.} \\ b_a(\mathbf{x}_{\partial a}) = \sum_{\mathbf{x}_{\mathcal{V} \setminus \partial a}} b(\mathbf{x}) \quad \forall \mathbf{x}_{\partial a} \quad \forall a \in \mathcal{F} \\ b_i(x_i) = \sum_{\mathbf{x}_{\mathcal{V} \setminus i}} b(\mathbf{x}) \quad \forall x_i \quad \forall i \in \mathcal{V} \end{array} \right. \right\},$$

then $\mathcal{M}(\mathcal{G}) \subseteq \mathcal{L}(\mathcal{G})$, but there do exist \mathcal{G} such that $\mathcal{M}(\mathcal{G}) \subsetneq \mathcal{L}(\mathcal{G})$. For acyclic factor graphs, however, these two sets are the same.

Lemma 1.14 (see, e.g., [WJ08, Proposition 4.1]). *Given an acyclic factor graph \mathcal{G} , for any set of PMFs $(\{b_a\}_{a \in \mathcal{F}}, \{b_i\}_{i \in \mathcal{V}}) \in \mathcal{L}(\mathcal{G})$, the function*

$$b(\mathbf{x}) \triangleq \frac{\prod_{a \in \mathcal{F}} b_a(\mathbf{x}_{\partial a})}{\prod_{i \in \mathcal{V}} (b_i(x_i))^{(d_i-1)}} \quad (1.20)$$

is a PMF over $\times_{i \in \mathcal{V}} \mathcal{X}_i$. Notably, in this case, it holds that $\mathcal{L}(\mathcal{G}) = \mathcal{M}(\mathcal{G})$.

Proof. Since it is obvious that $b(\mathbf{x}) \geq 0$ for all \mathbf{x} , it suffices to check that $\sum_{\mathbf{x}} b(\mathbf{x}) = 1$. This is proven by exploiting the acyclic structure of the factor graph. We omit the details. \square

For acyclic factor graphs, Lemma 1.14 enables us to write

$$F_{\mathcal{G}}(b) = F_{\mathcal{B}}(\{b_a\}_{a \in \mathcal{F}}, \{b_i\}_{i \in \mathcal{V}}) \quad \forall (\{b_a\}_{a \in \mathcal{F}}, \{b_i\}_{i \in \mathcal{V}}) \in \mathcal{L}(\mathcal{G}), \quad (1.21)$$

where the PMF b is defined *based on* $(\{b_a\}_{a \in \mathcal{F}}, \{b_i\}_{i \in \mathcal{V}})$ as in (1.20). By showing that the minimizer of $F_{\mathcal{G}}$ can always be expressed in a form as in (1.20), one can show that the Bethe free energy and the variational free energy share the same minimum. Therefore, for acyclic factor graphs, the Helmholtz free energy $F_{\mathcal{H}}$ can be obtained by minimizing the Bethe free energy (see Theorem 1.15).

Theorem 1.15. *For acyclic factor graphs, it holds that*

$$\min_{(\{b_a\}_{a \in \mathcal{F}}, \{b_i\}_{i \in \mathcal{V}}) \in \mathcal{L}(\mathcal{G})} F_{\mathcal{B}}(\{b_a\}_{a \in \mathcal{F}}, \{b_i\}_{i \in \mathcal{V}}) = \min_{b \in \mathfrak{P}(\times_{i \in \mathcal{V}} \mathcal{X}_i)} F_{\mathcal{G}}(b) = F_{\mathcal{H}}. \quad (1.22)$$

Proof. As mentioned before, it suffices to prove that $b^*(\mathbf{x}) \triangleq Z^{-1} \cdot \prod_{a \in \mathcal{F}} f_a(\mathbf{x}_{\partial a})$ can be expanded into $b^*(\mathbf{x}) = \prod_{a \in \mathcal{F}} b_a(\mathbf{x}_{\partial a}) \cdot \prod_{i \in \mathcal{V}} b_i^{(1-d_i)}(x_i)$. However, since the factor graph is acyclic, by Theorem 1.8, we have

$$\begin{aligned} \prod_{a \in \mathcal{F}} b_a(\mathbf{x}_{\partial a}) \cdot \prod_{i \in \mathcal{V}} b_i^{(1-d_i)}(x_i) &\stackrel{(a)}{\propto} \prod_{a \in \mathcal{F}} \left(f_a(\mathbf{x}_{\partial a}) \cdot \prod_{i \in \partial a} m_{i \rightarrow a}(x_i) \right) \cdot \prod_{i \in \mathcal{V}} \left(\prod_{c \in \partial i} m_{c \rightarrow i}(x_i) \right)^{(1-d_i)} \\ &\stackrel{(b)}{=} \prod_{a \in \mathcal{F}} f_a(\mathbf{x}_{\partial a}) \cdot \prod_{(i,a) \in \mathcal{E}} m_{i \rightarrow a}(x_i) \cdot \prod_{(i,a) \in \mathcal{E}} m_{a \rightarrow i}^{(1-d_i)}(x_i) \\ &\stackrel{(c)}{=} \prod_{a \in \mathcal{F}} f_a(\mathbf{x}_{\partial a}) \cdot \prod_{(i,a) \in \mathcal{E}} \prod_{c \in \partial i \setminus a} m_{c \rightarrow i}(x_i) \cdot \prod_{(i,a) \in \mathcal{E}} m_{a \rightarrow i}^{(1-d_i)}(x_i) \\ &\stackrel{(d)}{=} \prod_{a \in \mathcal{F}} f_a(\mathbf{x}_{\partial a}) \cdot \prod_{(i,a) \in \mathcal{E}} m_{a \rightarrow i}^{(d_i-1)}(x_i) \cdot \prod_{(i,a) \in \mathcal{E}} m_{a \rightarrow i}^{(1-d_i)}(x_i) \\ &= \prod_{a \in \mathcal{F}} f_a(\mathbf{x}_{\partial a}) \propto b^*(\mathbf{x}), \end{aligned}$$

where $\{m_{i \rightarrow a}, m_{a \rightarrow i} : \mathcal{X}_i \rightarrow \mathbb{R}\}_{(i,a) \in \mathcal{E}}$ is the unique BP fixed point for the acyclic factor graph. Notice that we have used Theorem 1.8 for (a) and (1.9) for (c), whereas (b) and (d) are results of counting. Finally, by Lemma 1.14, one can prove that $b^*(\mathbf{x}) = \prod_{a \in \mathcal{F}} b_a(\mathbf{x}_{\partial a}) \cdot \prod_{i \in \mathcal{V}} b_i^{(1-d_i)}(x_i)$. \square

Bethe's approximation

Motivated by the above discussion, Bethe's approximation is defined as follows.

Definition 1.16 (Bethe's approximation). Given a factor graph \mathcal{G} , Bethe's approximation (of the partition sum) is defined as

$$Z_B(\mathcal{G}) \triangleq \exp \left(- \min_{(\{b_a\}_{a \in \mathcal{F}}, \{b_i\}_{i \in \mathcal{V}}) \in \mathcal{L}(\mathcal{G})} F_B(\{b_a\}_{a \in \mathcal{F}}, \{b_i\}_{i \in \mathcal{V}}) \right). \quad (1.23)$$

Bethe's approximation at $(\{b_a\}_{a \in \mathcal{F}}, \{b_i\}_{i \in \mathcal{V}}) \in \mathcal{L}(\mathcal{G})$ is defined as

$$Z_B(\{b_a\}_{a \in \mathcal{F}}, \{b_i\}_{i \in \mathcal{V}}) \triangleq \exp(-F_B(\{b_a\}_{a \in \mathcal{F}}, \{b_i\}_{i \in \mathcal{V}})). \quad (1.24)$$

□

By Theorem 1.15, it is clear that $Z_B(\mathcal{G}) = Z(\mathcal{G})$ for acyclic \mathcal{G} 's. For cyclic factor graphs, such "exactness" breaks down. Though some connections between Z_B and Z have been established [Von13a], except for some families of factor graphs (*i.e.*, [Ruo12; Von13b]), there is little we can guarantee about how accurate such approximations are⁵. On the other hand, however, the study of the Bethe free energy minimization problem reveals a deeper connection between the minimization problem of F_B and the fixed points of BP algorithms (as stated in the famous theorem below).

Theorem 1.17 (see [YFW05, Theorem 2]). *Given a factor graph $((\mathcal{V}, \mathcal{F}, \mathcal{E}), \{\mathcal{X}_i\}_{i \in \mathcal{V}}, \{f_a\}_{a \in \mathcal{F}})$ with non-negative local functions, $(\{b_a\}_{a \in \mathcal{F}}, \{b_i\}_{i \in \mathcal{V}}) \in \mathcal{L}(\mathcal{G})$ is an interior stationary point of F_B if there exists a positive BP fixed point $\{m_{i \rightarrow a}, m_{a \rightarrow i} : \mathcal{X}_i \rightarrow \mathbb{R}_{>0}\}_{(i,a) \in \mathcal{E}}$ such that*

$$b_a(\mathbf{x}_{\partial a}) \propto f(\mathbf{x}_{\partial a}) \cdot \prod_{i \in \partial a} m_{i \rightarrow a}(x_i), \quad (1.25)$$

$$b_i(x_i) \propto \prod_{a \in \partial i} m_{a \rightarrow i}(x_i). \quad (1.26)$$

Conversely, a set of positive messages $\{m_{i \rightarrow a}, m_{a \rightarrow i}\}_{(i,a) \in \mathcal{E}}$ is a BP fixed point if $(\{b_a\}_{a \in \mathcal{F}}, \{b_i\}_{i \in \mathcal{V}})$ defined according to (1.25) and (1.26) form an interior stationary point of F_B .

Proof. The proof uses the Lagrange multiplier theory (see [YFW05] for details). □

For factor graphs with positive local functions, the above theorem allows us to interpret BP algorithms as a process to find the stationary points of the Bethe free

⁵One can construct a sequence of factor graphs $\{\mathcal{G}_k\}_k$ such that $Z(\mathcal{G}_k) \rightarrow 0$ but $Z_B(\mathcal{G}_k) \rightarrow +\infty$.

energy (see [YFW05, Section IV-C]). For BP fixed points with messages containing zero entries, it is unclear (but plausible) whether they still correspond to some stationary points of F_B (see [YFW05, Conjecture 1]).

1.1.6 Interpretations of BP fixed points: The Loop Calculus

The loop calculus [CC06; CC07; Mor15b] is another approach to characterize Bethe's approximation; and provides another interpretation for the BP fixed points. The major result of the method can be summarized as the following theorem.

Theorem 1.18 (Loop calculus). *Let $\mathcal{G} = ((\mathcal{V}, \mathcal{E}, \mathcal{F}), \{\mathcal{X}_i\}_{i \in \mathcal{V}}, \{f_a\}_{a \in \mathcal{F}})$ be a factor graph with non-negative local functions. For any interior stationary point $(\{b_a\}_{a \in \mathcal{F}}, \{b_i\}_{i \in \mathcal{V}})$ of F_B , it holds that*

$$Z(\mathcal{G}) = Z_B(\{b_a\}_{a \in \mathcal{F}}, \{b_i\}_{i \in \mathcal{V}}) \cdot \sum_{E \in \mathfrak{L}(\mathcal{E})} \mathcal{K}(E), \quad (1.27)$$

where the set of generalized loops $\mathfrak{L}(\mathcal{E})$ is defined as

$$\mathfrak{L}(\mathcal{E}) \triangleq \{E \subseteq \mathcal{E} : |\{(i, a)\}_{a \in \partial i} \cap E| \neq 1 \ \forall i \in \mathcal{V}, |\{(i, a)\}_{i \in \partial a} \cap E| \neq 1 \ \forall a \in \mathcal{F}\} \quad (1.28)$$

and where

$$\mathcal{K}(E) \triangleq \prod_{a \in \mathcal{F}} \left\langle \prod_{i \in \partial a, (i, a) \in E} \frac{X_i - \langle X_i \rangle_{b_i}}{\text{Var}(X_i)} \right\rangle_{b_a} \cdot \prod_{i \in \mathcal{V}} \left\langle \left(\frac{X_i - \langle X_i \rangle_{b_i}}{\text{Var}(X_i)} \right)^{d_i(E)} \right\rangle_{b_i} \quad (1.29)$$

for the case with all alphabets \mathcal{X}_i being binary [CC06] and where

$$\mathcal{K}(E) \triangleq \sum_{\substack{\mathbf{y}_E: y_{(i, a)} \neq 0 \\ \forall (i, a) \in E}} \prod_{a \in \mathcal{F}} \left\langle \prod_{\substack{i \in \partial a, \\ (i, a) \in E}} \frac{\partial \log b_i(X_i)}{\partial \theta_{y_i, a}^{i, a}} \right\rangle_{b_a} \cdot \prod_{i \in \mathcal{V}} \left\langle \prod_{\substack{a \in \partial i, \\ (i, a) \in E}} \frac{\partial \log b_i(X_i)}{\partial \eta_{y_i, a}^{i, a}} \right\rangle_{b_i} \quad (1.30)$$

for non-binary alphabets [Mor15b]. Here, $(\theta_y^{i, a})_{y=1, \dots, |\mathcal{X}_i|-1}$ and $(\eta_y^{i, a})_{y=1, \dots, |\mathcal{X}_i|-1}$ are some dual coordinate systems [AN00] for $\log(\mathfrak{P}(\mathcal{X}_i)) \triangleq \{\log p : p \in \mathfrak{P}(\mathcal{X}_i)\}$.

Remark 1.19. Note that $\emptyset \in \mathfrak{L}(\mathcal{E})$, and for acyclic factor graphs, $\mathfrak{L}(\mathcal{E}) = \{\emptyset\}$.

Remark 1.20. For any factor graph, $\mathcal{K}(\emptyset) = 1$; thus for acyclic factor graphs, $Z(\mathcal{G}) = Z_B(\{b_a\}_{a \in \mathcal{F}}, \{b_i\}_{i \in \mathcal{V}})$ at interior stationary points $(\{b_a\}_{a \in \mathcal{F}}, \{b_i\}_{i \in \mathcal{V}})$.

One method to prove the theorem is to express $Z(\mathcal{G})$ as (see [WJ08])

$$Z(\mathcal{G}) = Z_B(\{b_a\}_{a \in \mathcal{F}}, \{b_i\}_{i \in \mathcal{V}}) \cdot \frac{\prod_{a \in \mathcal{F}} b_a(\mathbf{x}_{\partial a})}{\prod_{i \in \mathcal{V}} b_i^{(d_i-1)}(x_i)} \quad (1.31)$$

and expanding the terms on the right-hand side (see [SW08]). Another method [CC06; Mor15b], reviewed below, involves the *Holant theorem* [AM11].

Theorem 1.21 (Holant theorem). *Consider a factor graph \mathcal{G} representing the factorization $g(\mathbf{x}) = \prod_{a \in \mathcal{F}} f_a(\mathbf{x}_{\partial a})$, where each alphabet \mathcal{X}_i is finite. Given any set of invertible matrices $\{\phi_{i,a} \in \mathbb{R}^{\mathcal{X}_i \times \mathcal{Y}_{i,a}}\}_{(i,a) \in \mathcal{E}}$ (where $|\mathcal{X}_i| = |\mathcal{Y}_{i,a}|$), one can express the partition sum $Z(\mathcal{G})$ as*

$$Z(\mathcal{G}) = \sum_{\mathbf{y}} \prod_{a \in \mathcal{F}} \hat{f}_a(\mathbf{y}_{\partial a, a}) \cdot \prod_{i \in \mathcal{V}} \hat{h}_i(\mathbf{y}_{i, \partial i}), \quad (1.32)$$

where

$$\hat{f}_a(\mathbf{y}_{\partial a, a}) \triangleq \sum_{\mathbf{x}_{\partial a}} f_a(\mathbf{x}_{\partial a}) \prod_{i \in \partial a} \hat{\phi}_{i,a}(y_{i,a}, x_i), \quad (1.33)$$

$$\hat{h}_i(\mathbf{y}_{i, \partial i}) \triangleq \sum_{x_i} \prod_{a \in \partial i} \phi_{i,a}(x_i, y_{i,a}). \quad (1.34)$$

Here, $\hat{\phi}_{i,a}$ is the inverse matrix of $\phi_{i,a}$; and $\phi_{i,a}(x, y)$ and $\hat{\phi}_{i,a}(y, x)$ denote the (x, y) -th and the (y, x) -th entry of $\phi_{i,a}$ and $\hat{\phi}_{i,a}$, respectively.

Proof. This is a direct result of elementary linear algebra. We omit the details. \square

Using the elements from the theorem above, we consider the factorization

$$\tilde{g}(\mathbf{y}_{\mathcal{E}}) \triangleq \prod_{a \in \mathcal{F}} \hat{f}_a(\mathbf{y}_{\partial a, a}) \cdot \prod_{i \in \mathcal{V}} \hat{h}_i(\mathbf{y}_{i, \partial i}). \quad (1.35)$$

The corresponding factor graph $\tilde{\mathcal{G}}$ describing (1.35) is known as a *holographic transform* of the original factor graph \mathcal{G} (w.r.t. $\{\phi_{i,a}, \hat{\phi}_{i,a}\}_{(i,a) \in \mathcal{E}}$). Theorem 1.21 can then be rephrased as “holographic transformations do not change the partition sum.” For the sake of proving Theorem 1.18, we consider a holographic transform such that

$$\hat{f}_a(\mathbf{y}_{\partial a, a}) = 0, \text{ if } \text{wt}(\mathbf{y}_{\partial a, a}) = 1 \quad \forall a \in \mathcal{F}, \quad (1.36)$$

$$\hat{h}_i(\mathbf{y}_{i, \partial i}) = 0, \text{ if } \text{wt}(\mathbf{y}_{i, \partial i}) = 1 \quad \forall i \in \mathcal{V}, \quad (1.37)$$

where we have assumed that each alphabet $\mathcal{Y}_{i,a}$ contains an elements labeled as 0. This limits the support of \tilde{g} to those $\mathbf{y}_{\mathcal{E}}$'s such that the indices of the non-zero entries of $\mathbf{y}_{\mathcal{E}}$ form a generalized loop, i.e., $\text{Supp}(\tilde{g}) \subseteq \{\mathbf{y}_{\mathcal{E}} | \exists E \in \mathcal{L}(\mathcal{E}) \text{ s.t. } y_{i,a} = 0 \forall (i,a) \notin E\}$. Substituting (1.33) and (1.34) into (1.36) and (1.37), respectively, one can rewrite the latter as

$$\left[\sum_{\mathbf{x}_{\partial a \setminus i}} f_a(\mathbf{x}_{\partial a}) \cdot \prod_{j \in \partial a \setminus i} \hat{\phi}_{i,a}(0, x_j) \right]_{x_i} \perp \hat{\phi}_{i,a}(y, \cdot) \quad \forall y \neq 0, \quad (1.38)$$

$$\left[\prod_{c \in \partial i \setminus a} \phi_{i,c}(x_i, 0) \right]_{x_i} \perp \phi_{i,a}(\cdot, y) \quad \forall y \neq 0, \quad (1.39)$$

respectively. Since $\phi_{i,a}$ and $\hat{\phi}_{i,a}$ are the inverse matrix of each other, (1.38) and (1.39) (and thus (1.36) and (1.37)) are equivalent to

$$\phi_{i,a}(\cdot, 0) \propto \left[\sum_{\mathbf{x}_{\partial a \setminus i}} f_a(\mathbf{x}_{\partial a}) \cdot \prod_{j \in \partial a \setminus i} \hat{\phi}_{i,a}(0, x_j) \right]_{x_i}, \quad (1.40)$$

$$\hat{\phi}_{i,a}(0, \cdot) \propto \left[\prod_{c \in \partial i \setminus a} \phi_{i,c}(x_i, 0) \right]_{x_i}, \quad (1.41)$$

respectively. Compare the above with (1.9) and (1.10). Eqs. (1.40) and (1.41) (and thus (1.36) and (1.37)) are equivalent to the existence of some fixed-point messages $\{m_{i \rightarrow a}, m_{a \rightarrow i}\}_{(i,a)}$ such that

$$\phi_{i,a}(x_i, 0) = c_{i,a} \cdot m_{a \rightarrow i}(x_i), \quad (1.42)$$

$$\hat{\phi}_{i,a}(0, x_i) = \hat{c}_{i,a} \cdot m_{i \rightarrow a}(x_i), \quad (1.43)$$

where the constants $c_{i,a}, \hat{c}_{i,a}$ satisfy $(c_{i,a} \cdot \hat{c}_{i,a})^{-1} = Z_{i,a}(m_{i \rightarrow a}, m_{a \rightarrow i}) \triangleq \sum_{x_i} m_{i \rightarrow a}(x_i) \cdot m_{a \rightarrow i}(x_i)$ for each $(i, a) \in \mathcal{E}$. Therefore, retracing the steps above, given any positive BP fixed point $\{m_{i \rightarrow a}, m_{a \rightarrow i}\}_{(i,a) \in \mathcal{E}}$, we can construct a holographic transform satisfying (1.42) and (1.43), and thus satisfying (1.36) and (1.37).

If all of the alphabets are binary (*i.e.*, $\mathcal{X}_i = \mathcal{Y}_{i,a} = \mathbb{F}_2$ for all $i \in \mathcal{V}$ and $(i, a) \in \mathcal{E}$), since $\phi_{i,a} \cdot \hat{\phi}_{i,a} = \hat{\phi}_{i,a} \cdot \phi_{i,a} = \begin{bmatrix} 1 & 0 \\ 0 & 1 \end{bmatrix}$ for each $(i, a) \in \mathcal{E}$, it must hold that

$$\phi_{i,a}(x_i, 1) = (-1)^{\bar{x}_i} c_{i,a} \cdot m_{i \rightarrow a}(\bar{x}_i), \quad (1.44)$$

$$\hat{\phi}_{i,a}(1, x_i) = (-1)^{\bar{x}_i} \hat{c}_{i,a} \cdot m_{a \rightarrow i}(\bar{x}_i), \quad (1.45)$$

where $\bar{0} \triangleq 1$ and $\bar{1} \triangleq 0$. The proof of (1.29) in Theorem 1.18 involves substituting (1.44) and (1.45) into (1.32) and applying the following corollary.

Corollary 1.22. *Consider a factor graph \mathcal{G} representing the factorization $g(\mathbf{x}) = \prod_{a \in \mathcal{F}} f_a(\mathbf{x}_{\partial a})$. For a collection of positive fixed-point messages $\{m_{i \rightarrow a}, m_{a \rightarrow i}\}_{i,a}$, we have*

$$Z_B(\{b_a\}_{a \in \mathcal{F}}, \{b_i\}_{i \in \mathcal{V}}) = \frac{\prod_{a \in \mathcal{F}} Z_a(\{m_{i \rightarrow a}\}_{i \in \partial a}) \cdot \prod_{i \in \mathcal{V}} Z_i(\{m_{a \rightarrow i}\}_{a \in \partial i})}{\prod_{(i,a) \in \mathcal{E}} Z_{i,a}(m_{i \rightarrow a}, m_{a \rightarrow i})}, \quad (1.46)$$

where the PMFs $\{b_a\}_{a \in \mathcal{F}}$ and $\{b_i\}_{i \in \mathcal{V}}$ are defined according to (1.25) and (1.26) and

where

$$\begin{aligned} Z_a(\{m_{i \rightarrow a}\}_{i \in \partial a}) &\triangleq \sum_{\mathbf{x}_{\partial a}} f(\mathbf{x}_{\partial a}) \cdot \prod_{i \in \partial a} m_{i \rightarrow a}(x_i) & \forall a \in \mathcal{F}, \\ Z_i(\{m_{a \rightarrow i}\}_{a \in \partial i}) &\triangleq \sum_{x_i} \prod_{a \in \partial i} m_{a \rightarrow i}(x_i) & \forall i \in \mathcal{V}, \\ Z_{i,a}(m_{i \rightarrow a}, m_{a \rightarrow i}) &\triangleq \sum_{x_i} m_{i \rightarrow a}(x_i) \cdot m_{a \rightarrow i}(x_i) & \forall (i, a) \in \mathcal{E}. \end{aligned}$$

Proof. This is a direct result of Theorem 1.17 by substituting (1.25) and (1.26) into (1.19).

We omit the details. \square

Proof of (1.29) [see Mor15b, Proof of Lemma 5]. Using the aforementioned holographic transform, and by Theorem 1.21, we have

$$\begin{aligned} Z(\mathcal{G}) &= \sum_{\mathbf{y}_{\mathcal{E}} \in \text{Supp}(\tilde{g})} \prod_{a \in \mathcal{F}} \hat{f}_a(\mathbf{y}_{\partial a, a}) \cdot \prod_{i \in \mathcal{V}} \hat{h}_i(\mathbf{y}_{i, \partial i}) \\ &= \sum_{\mathbf{y}_{\mathcal{E}} \in \text{Supp}(\tilde{g})} \prod_{a \in \mathcal{F}} \sum_{\mathbf{x}_{\partial a}} f_a(\mathbf{x}_{\partial a}) \prod_{i \in \partial a} \hat{\phi}_{i,a}(y_{i,a}, x_i) \cdot \prod_{i \in \mathcal{V}} \sum_{x_i} \prod_{a \in \partial i} \phi_{i,a}(x_i, y_{i,a}) \\ &= \left(\prod_{a \in \mathcal{F}} \sum_{\mathbf{x}_{\partial a}} f_a(\mathbf{x}_{\partial a}) \prod_{i \in \partial a} \hat{c}_{i,a} \cdot m_{i \rightarrow a}(x_i) \cdot \prod_{i \in \mathcal{V}} \sum_{x_i} \prod_{a \in \partial i} c_{i,a} \cdot m_{a \rightarrow i}(x_i) \right) \\ &\quad \sum_{\mathbf{y}_{\mathcal{E}} \in \text{Supp}(\tilde{g})} \prod_{a \in \mathcal{F}} \frac{\sum_{\mathbf{x}_{\partial a}} f_a(\mathbf{x}_{\partial a}) \prod_{i \in \partial a} \hat{\phi}_{i,a}(y_{i,a}, x_i)}{\sum_{\mathbf{x}_{\partial a}} f_a(\mathbf{x}_{\partial a}) \prod_{i \in \partial a} \hat{\phi}_{i,a}(0, x_i)} \prod_{i \in \mathcal{V}} \frac{\sum_{x_i} \prod_{a \in \partial i} \phi_{i,a}(x_i, y_{i,a})}{\sum_{x_i} \prod_{a \in \partial i} \phi_{i,a}(x_i, 0)} \\ &\stackrel{(a)}{=} Z_B(\{b_a\}_a, \{b_i\}_i) \cdot \sum_{\mathbf{y}_{\mathcal{E}} \in \text{Supp}(\tilde{g})} \prod_{a \in \mathcal{F}} \left\langle \prod_{i \in \partial a} \frac{\hat{\phi}_{i,a}(y_{i,a}, \mathbf{X}_i)}{\hat{\phi}_{i,a}(0, \mathbf{X}_i)} \right\rangle_{b_a} \prod_{i \in \mathcal{V}} \left\langle \prod_{a \in \partial i} \frac{\phi_{i,a}(\mathbf{X}_i, y_{i,a})}{\phi_{i,a}(\mathbf{X}_i, 0)} \right\rangle_{b_i} \\ &\stackrel{(b)}{=} Z_B(\{b_a\}_a, \{b_i\}_i) \cdot \sum_{E \in \mathcal{L}(\mathcal{E})} \prod_{a \in \mathcal{F}} \left\langle \prod_{\substack{i \in \partial a, \\ (i,a) \in E}} \frac{\hat{\phi}_{i,a}(1, \mathbf{X}_i)}{\hat{\phi}_{i,a}(0, \mathbf{X}_i)} \right\rangle_{b_a} \prod_{i \in \mathcal{V}} \left\langle \prod_{\substack{a \in \partial i, \\ (i,a) \in E}} \frac{\phi_{i,a}(\mathbf{X}_i, 1)}{\phi_{i,a}(\mathbf{X}_i, 0)} \right\rangle_{b_i} \\ &\stackrel{(c)}{=} Z_B(\{b_a\}_a, \{b_i\}_i) \cdot \sum_{E \in \mathcal{L}(\mathcal{E})} \prod_{a \in \mathcal{F}} \left\langle \prod_{\substack{i \in \partial a, \\ (i,a) \in E}} \frac{(-1)^{\overline{\mathbf{X}}_i} m_{a \rightarrow i}(\overline{\mathbf{X}}_i) \cdot m_{i \rightarrow a}(\overline{\mathbf{X}}_i)}{m_{i \rightarrow a}(\mathbf{X}_i) \cdot m_{i \rightarrow a}(\overline{\mathbf{X}}_i)} \right\rangle_{b_a} \\ &\quad \cdot \prod_{i \in \mathcal{V}} \left\langle \prod_{\substack{a \in \partial i, \\ (i,a) \in E}} \frac{(-1)^{\overline{\mathbf{X}}_i} m_{i \rightarrow a}(\overline{\mathbf{X}}_i) \cdot m_{a \rightarrow i}(\overline{\mathbf{X}}_i)}{m_{a \rightarrow i}(\mathbf{X}_i) \cdot m_{a \rightarrow i}(\overline{\mathbf{X}}_i)} \right\rangle_{b_i} \\ &\stackrel{(d)}{=} Z_B(\{b_a\}_a, \{b_i\}_i) \cdot \sum_{E \in \mathcal{L}(\mathcal{E})} \prod_{a \in \mathcal{F}} \left\langle \prod_{\substack{i \in \partial a, \\ (i,a) \in E}} \frac{(-1)^{\overline{\mathbf{X}}_i} b_i(\overline{\mathbf{X}}_i)}{\sqrt{b_i(0)b_i(1)}} \right\rangle_{b_a} \prod_{i \in \mathcal{V}} \left\langle \prod_{\substack{a \in \partial i, \\ (i,a) \in E}} \frac{(-1)^{\overline{\mathbf{X}}_i} b_i(\overline{\mathbf{X}}_i)}{\sqrt{b_i(0)b_i(1)}} \right\rangle_{b_i}. \end{aligned}$$

Step (a) is based on Corollary 1.22, together with the observation that

$$\begin{aligned} \frac{\sum_{\mathbf{x}_{\partial a}} f_a(\mathbf{x}_{\partial a}) \prod_{i \in \partial a} \hat{\phi}_{i,a}(y_{i,a}, x_i)}{\sum_{\mathbf{x}_{\partial a}} f_a(\mathbf{x}_{\partial a}) \prod_{i \in \partial a} \hat{\phi}_{i,a}(0, x_i)} &= \sum_{\mathbf{x}_{\partial a}} \frac{f_a(\mathbf{x}_{\partial a}) \prod_{i \in \partial a} \hat{\phi}_{i,a}(0, x_i)}{\sum_{\tilde{\mathbf{x}}_{\partial a}} f_a(\tilde{\mathbf{x}}_{\partial a}) \prod_{i \in \partial a} \hat{\phi}_{i,a}(0, \tilde{x}_i)} \cdot \prod_{i \in \partial a} \frac{\hat{\phi}_{i,a}(y_{i,a}, x_i)}{\hat{\phi}_{i,a}(0, x_i)}, \\ \frac{\sum_{x_i} \prod_{a \in \partial i} \phi_{i,a}(x_i, y_{i,a})}{\sum_{x_i} \prod_{a \in \partial i} \phi_{i,a}(x_i, 0)} &= \sum_{x_i} \frac{\prod_{a \in \partial i} \phi_{i,a}(x_i, 0)}{\sum_{\tilde{x}_i} \prod_{a \in \partial i} \phi_{i,a}(\tilde{x}_i, 0)} \cdot \prod_{a \in \partial i} \frac{\phi_{i,a}(x_i, y_{i,a})}{\phi_{i,a}(x_i, 0)}. \end{aligned}$$

Step (b) exploits the setup that $\text{Supp}(\tilde{g}) \subseteq \{\mathbf{y}_{\mathcal{E}} | \exists E \in \mathfrak{L}(\mathcal{E}) \text{ s.t. } y_{i,a} = 0 \forall (i,a) \notin E\}$ and the assumption that all of the alphabets are binary. Step (c) is the result of substituting (1.42), (1.43), (1.44), and (1.45). Step (d) is shown by observing (from (1.26) and (1.15)) that $Z_{i,a}^{-1} \cdot m_{a \rightarrow i}(\bar{x}_i) \cdot m_{i \rightarrow a}(\bar{x}_i) = b_i(\bar{x}_i)$ for each $(i,a) \in \mathcal{E}$, and the fact that $m_{i \rightarrow a}(\mathbf{X}_i) m_{i \rightarrow a}(\bar{\mathbf{X}}_i)$ and $m_{a \rightarrow i}(\mathbf{X}_i) m_{a \rightarrow i}(\bar{\mathbf{X}}_i)$ are independent of the value taken by \mathbf{X}_i . Namely,

$$\begin{aligned} &\prod_{a \in \mathcal{F}} \left\langle \prod_{\substack{i \in \partial a, \\ (i,a) \in E}} \frac{1}{m_{i \rightarrow a}(\mathbf{X}_i) \cdot m_{i \rightarrow a}(\bar{\mathbf{X}}_i)} \right\rangle \prod_{b_a} \left\langle \prod_{\substack{a \in \partial i, \\ (i,a) \in E}} \frac{1}{m_{a \rightarrow i}(\mathbf{X}_i) \cdot m_{a \rightarrow i}(\bar{\mathbf{X}}_i)} \right\rangle_{b_i} \\ &= \prod_{a \in \mathcal{F}} \left\langle \prod_{\substack{i \in \partial a, \\ (i,a) \in E}} \frac{1}{m_{i \rightarrow a}(0) \cdot m_{i \rightarrow a}(1)} \right\rangle \prod_{b_a} \left\langle \prod_{\substack{a \in \partial i, \\ (i,a) \in E}} \frac{1}{m_{a \rightarrow i}(0) \cdot m_{a \rightarrow i}(1)} \right\rangle_{b_i} \\ &= \prod_{(i,a) \in E} m_{i \rightarrow a}(0) \cdot m_{i \rightarrow a}(1) \cdot m_{a \rightarrow i}(0) \cdot m_{a \rightarrow i}(1) = \prod_{(i,a) \in E} Z_{i,a}^2 \cdot b_i(0) \cdot b_i(1) \\ &= \prod_{a \in \mathcal{F}} \left\langle \prod_{\substack{i \in \partial a, \\ (i,a) \in E}} \frac{1}{Z_{i,a} \cdot \sqrt{b_i(0)b_i(1)}} \right\rangle \prod_{b_a} \left\langle \prod_{\substack{a \in \partial i, \\ (i,a) \in E}} \frac{1}{Z_{i,a} \cdot \sqrt{b_i(0)b_i(1)}} \right\rangle_{b_i}. \end{aligned}$$

Finally, (1.29) can be shown by noticing that for any binary random variable \mathbf{X} with its PMF being $P_{\mathbf{X}}$, it holds that $(-1)^{\bar{\mathbf{X}}} P_{\mathbf{X}}(\bar{\mathbf{X}}) = \mathbf{X} - \langle \mathbf{X} \rangle$, and $P_{\mathbf{X}}(0) \cdot P_{\mathbf{X}}(1) = \text{Var } \mathbf{X}$. \square

To prove the general case of Theorem 1.21, *i.e.*, (1.30), observe that for satisfying $\phi_{i,a} \cdot \hat{\phi}_{i,a} = \hat{\phi}_{i,a} \cdot \phi_{i,a} = I$ given (1.42) and (1.43), it is equivalent to require

$$\left\langle \frac{\phi_{i,a}(\mathbf{X}_i, y)}{\phi_{i,a}(\mathbf{X}_i, 0)} \right\rangle_{b_i} = 0 \quad \forall y \neq 0, \quad (1.47)$$

$$\left\langle \frac{\hat{\phi}_{i,a}(y, \mathbf{X}_i)}{\hat{\phi}_{i,a}(0, \mathbf{X}_i)} \right\rangle_{b_i} = 0 \quad \forall y \neq 0, \quad (1.48)$$

$$\left\langle \frac{\phi_{i,a}(\mathbf{X}_i, y)}{\phi_{i,a}(\mathbf{X}_i, 0)} \cdot \frac{\hat{\phi}_{i,a}(y', \mathbf{X}_i)}{\hat{\phi}_{i,a}(0, \mathbf{X}_i)} \right\rangle_{b_i} = \delta_{y,y'} \quad \forall y, y' \neq 0, \quad (1.49)$$

which, in turn, is equivalent to

$$\phi_{i,a}(\mathbf{X}_i, y) = \theta_y^{i,a} \cdot \phi_{i,a}(\mathbf{X}_i, 0) \quad \text{for each } y \in \mathcal{Y}_{i,a} \setminus 0 \quad (1.50)$$

$$\hat{\phi}_{i,a}(y, \mathbf{X}_i) = \eta_y^{i,a} \cdot \hat{\phi}_{i,a}(0, \mathbf{X}_i) \quad \text{for each } y \in \mathcal{Y}_{i,a} \setminus 0 \quad (1.51)$$

for some pair of dual coordinate systems $\{\theta_y^{i,a}\}_{y \in \mathcal{Y}_{i,a} \setminus 0}$ and $\{\eta_y^{i,a}\}_{y \in \mathcal{Y}_{i,a} \setminus 0}$ for the $(|\mathcal{Y}_{i,a}| - 1) = (|\mathcal{X}_i| - 1)$ -dimensional manifold $\log(\mathfrak{P}(\mathcal{X}_i)) \triangleq \{\log p : p \in \mathfrak{P}(\mathcal{X}_i)\}$ (see, *e.g.*, [AN00, Chapter 2]). Eq (1.30) can be proven by substituting (1.42), (1.43), (1.50), and (1.51) into (1.32) and following the same logic as in the proof of (1.29) above. We refer to [Mor15b, Section IV-C] for details.

1.2 Basic quantum information theory

This section provides a brief introduction to basic quantum information theory, including quantum postulates, quantum information measures, and quantum channels. Much of the contents of this section are based on Nielsen and Chuang [NC11].

1.2.1 Quantum Postulates

The following four postulates are based on our current understanding of physics and provide the framework in which quantum information is considered.

Postulate 1 (State space). A quantum system is fully described by a unit vector (a.k.a. its state vector or its state) from a complex Hilbert space (a.k.a. its state space).

Postulate 2 (Evolution). The evolution of a closed system is described by a unitary transformation applied to its state vector.

Postulate 3 (Measurement). A quantum measurement is described by an indexed set of operators⁶ $\{M_y \in \mathfrak{L}(\mathcal{H}_A)\}_{y \in \mathcal{Y}}$ on its state space, where $\sum_y M_y^\dagger M_y = I$. If the state of the system is $|\psi\rangle$ immediately before the measurement, then:

- The probability of the measurement outcome being \tilde{y} is $p(\tilde{y}) = \langle \psi | M_{\tilde{y}}^\dagger M_{\tilde{y}} | \psi \rangle$;
- Provided the measurement outcome y , the state of the system immediately after the measurement is $\frac{M_y |\psi\rangle}{\sqrt{\langle \psi | M_y^\dagger M_y | \psi \rangle}}$.

Postulate 4 (Composition). The state space of a composite system is the tensor product of the state spaces of each component system.

Example 1.23. A *single-qubit system* is a quantum system with 2-dimensional state space and is often referred to as a (single) qubit. Suppose $|0\rangle$ and $|1\rangle$ form an orthonormal basis of the state space. Under this basis (a.k.a. *computational basis*),

⁶As already mentioned in “Notations”, an operator is a linear transformation in this context.

- Any state vectors can be expressed as $\begin{bmatrix} a \\ b \end{bmatrix} \triangleq a|0\rangle + b|1\rangle$ where $a, b \in \mathbb{C}$, and $|a|^2 + |b|^2 = 1$.
- (Closed) Evolution on this system can be represented by a 2-by-2 unitary matrix U , where the post-evolution state will be $U \cdot \begin{bmatrix} a \\ b \end{bmatrix}$ given initial state $\begin{bmatrix} a \\ b \end{bmatrix}$.
- A quantum measurement can be described by a set of 2-by-2 matrices $\{M_y\}_y$ such that $\sum_y M_y^\dagger M_y = \begin{bmatrix} 1 & 0 \\ 0 & 1 \end{bmatrix}$, where, given the pre-measurement state being $\begin{bmatrix} a \\ b \end{bmatrix}$,
 - the probability of the outcome being \tilde{y} can be expressed as $\begin{bmatrix} \bar{a} & \bar{b} \end{bmatrix} \cdot M_{\tilde{y}}^\dagger M_{\tilde{y}} \cdot \begin{bmatrix} a \\ b \end{bmatrix}$,
 - provided the outcome y , the post-measurement state is $p(y)^{-1} \cdot M_y \begin{bmatrix} a \\ b \end{bmatrix}$. \square

Example 1.24. A *two-qubit system* is the composition of two single-qubit systems. According to Postulate 4, a basis of its state space can be expressed as

$$\{|00\rangle, |01\rangle, |10\rangle, |11\rangle\} \triangleq \{|0\rangle \otimes |0\rangle, |0\rangle \otimes |1\rangle, |1\rangle \otimes |0\rangle, |1\rangle \otimes |1\rangle\}. \quad \square$$

Density Operators

Like classical systems, there are cases when the state of a quantum system is *not* entirely known but rather known to be in the state $|\psi\rangle_i$ with probability p_i (for some indices i)⁷. In this case, the PMF of the measurement outcome w.r.t. the measurement $\{M_y\}_y$ can be expressed as

$$p(y) = \sum_i p_i \cdot \langle \psi_i | M_y^\dagger M_y | \psi_i \rangle = \text{tr} \left(M_y \cdot \left(\sum_i p_i \cdot |\psi_i\rangle \langle \psi_i| \right) \cdot M_y^\dagger \right). \quad (1.52)$$

Observe that (1.52) is a function of $\sum_i p_i \cdot |\psi_i\rangle \langle \psi_i|$. Namely, given another ensemble $\{q_j, |\phi_j\rangle\}_j$, *i.e.*, a setup that the state vector is $|\phi\rangle_j$ with probability q_j , such where $\sum_i p_i \cdot |\psi_i\rangle \langle \psi_i| = \sum_j q_j \cdot |\phi_j\rangle \langle \phi_j|$, it is impossible to distinguish between these two ensembles using measurements. This motivated physicists to treat $\rho \triangleq \sum_i p_i \cdot |\psi_i\rangle \langle \psi_i|$, known as the density operator (see Definition 1.25), as a *complete* description of the original system.

Definition 1.25 (Density Operator). Given a quantum system A with its state space being \mathcal{H}_A , a density operator (of A) is a positive trace-1 linear operator on \mathcal{H}_A . The set of all density operators on \mathcal{H}_A is denoted by $\mathfrak{D}(\mathcal{H}_A)$. \square

⁷Notice that the state space of a quantum system is continuous. Thus, the distribution of the state vector should also be continuous in general, in which case PDFs should be considered.

Remark 1.26. $\mathfrak{D}(\mathcal{H}_A)$ is the set of all possible operators such that $\rho = \sum_i p_i \cdot |\psi_i\rangle\langle\psi_i|$ for some ensemble $\{p_i, |\psi_i\rangle\}_i$.

Using the notations of density operators, Postulates 1–3 can be rewritten as follows.

Postulate 1a. A quantum system is fully described by a density operator on a complex Hilbert space (known as its state space). Each density operator on the state space describes some valid configurations of the system.

Postulate 2a. The evolution of a closed system is described by some unitary transformation U . Given the density operator of the system being ρ , the density operator after the evolution is $U\rho U^\dagger$.

Postulate 3a. A quantum measurement is described by an indexed set of operators $\{M_y \in \mathfrak{L}(\mathcal{H}_A)\}_{y \in \mathcal{Y}}$ on its state space, where $\sum_y M_y^\dagger M_y = I$. If the density operator of the system is ρ immediately before the measurement, then:

- The probability of the measurement outcome being \check{y} is $p(\check{y}) = \text{tr}(M_{\check{y}}\rho M_{\check{y}}^\dagger)$;
- Provided the measurement outcome y , the density operator immediately after the measurement will be $\frac{M_y \rho M_y^\dagger}{\text{tr}(M_y \rho M_y^\dagger)}$.

By the cyclic property of the trace operation, it suffices to know $\{M_y^\dagger M_y\}_y$ for a measurement, if the post-measurement state/density operator is irrelevant to us. In this case, a quantum measurement can be specified by a POVM $\{E_y\}_y$ (see Definition 1.27), and the probability of measurement outcome being \check{y} , given the pre-measurement density operator ρ , can be expressed as $p(\check{y}) = \text{tr}(E_{\check{y}}\rho)$.

Definition 1.27 (Positive-Operator-Valued Measurement (POVM)). Given a quantum system A with its state space being \mathcal{H}_A , a positive-operator-valued measurement (POVM) is an indexed set of positive operators $\{E_y \in \mathfrak{L}_+(\mathcal{H}_A)\}_y$ such that $\sum_y E_y = I$. \square

Partial Measurement and Partial-trace

Let AB be a composite system. A measurement in the form of $\{M_y \otimes I_B\}_y$, where $\{M_y\}_y$ is some measurement on the subsystem A, is known as a *partial measurement*. In particular, $\{M_y \otimes I_B\}_y$ is the unique measurement having the same effect as $\{M_y\}_y$ on the system A while leaving the system B intact, namely

$$(M_y \otimes I_B) \cdot (|\psi_A\rangle \otimes |\phi_B\rangle) = (M_y |\psi_A\rangle) \otimes |\phi_B\rangle \quad \forall |\psi_A\rangle \in \mathcal{H}_A, |\phi_B\rangle \in \mathcal{H}_B.$$

On the other hand, let ρ_{AB} be a density operator for the composite system AB. We argue that the density operator $\rho_A \triangleq \text{tr}_B(\rho_{AB})$ (a.k.a. *reduced operator*) describes the subsystem A, where tr_B is a linear map defined as

$$\text{tr}_B : |i_A\rangle \langle j_A| \otimes |i'_B\rangle \langle j'_B| \mapsto |i_A\rangle \langle j_A| \cdot \text{tr}(|i'_B\rangle \langle j'_B|) \quad \forall i, j, i', j' \quad (1.53)$$

for *arbitrary*⁸ bases $\{|k_A\rangle\}_k$ and $\{|k_B\rangle\}_k$ for \mathcal{H}_A and \mathcal{H}_B , respectively. In particular, given ρ_{AB} , the reduced density operator $\rho_A \triangleq \text{tr}_B(\rho_{AB})$ is the *unique* density operator such that

$$\text{tr} \left(M_y \rho_A M_y^\dagger \right) = \text{tr} \left((M_y \otimes I_B) \rho_{AB} (M_y \otimes I_B)^\dagger \right) \quad (1.54)$$

for any measurement $\{M_y\}_y$ on A. We refer to [NC11, Box 2.6] for details.

Example 1.28. Let A, B each be a single qubit system. Suppose the state vector of their composite system AB is $|\psi_{AB}\rangle = \frac{|00\rangle + |11\rangle}{\sqrt{2}}$. In this case, the matrix representations⁹ of ρ_{AB} and ρ_A are

$$\rho_{AB} = |\psi_{AB}\rangle \langle \psi_{AB}| = \frac{1}{2} \begin{bmatrix} 1 & 0 & 0 & 1 \\ 0 & 0 & 0 & 0 \\ 0 & 0 & 0 & 0 \\ 1 & 0 & 0 & 1 \end{bmatrix}$$

and $\rho_A = \text{tr}_B(\rho_{AB}) = \frac{1}{2} \begin{bmatrix} 1 & 0 \\ 0 & 1 \end{bmatrix} = \frac{1}{2} |0\rangle \langle 0| + \frac{1}{2} |1\rangle \langle 1|$, respectively. \square

1.2.2 Quantum Information Measures and Some Inequalities

This section reviews some basic elements of quantum information theory, including some of the common quantum information measures and some famous inequalities.

Definition 1.29 (von Neumann Entropy). Given a quantum system A described by the density operator ρ_A , the von Neumann entropy of A or ρ_A is defined as

$$\mathbf{H}(A) = \mathbf{H}(\rho_A) \triangleq -\text{tr}(\rho_A \cdot \log \rho_A),$$

where \log stands for the matrix logarithm, *i.e.*, $\log \rho_A \triangleq \sum_{k=1}^{\infty} \frac{(-1)^{k+1}}{k} (\rho_A - I)^k$. \square

⁸To check the well-definedness, one can show that the partial trace tr_B is the unique linear map such that $\text{tr}_B(\sigma_A \otimes \sigma_B) = \sigma_A \cdot \text{tr}(\sigma_B)$ for all operators σ_A and σ_B on \mathcal{H}_A and \mathcal{H}_B , respectively.

⁹In the remainder of this thesis, we may refer to an operator/state vector and their matrix representations (w.r.t. certain computational basis) interchangeably.

Remark 1.30. For a d -by- d PD matrix $A = UDU^\dagger$, where U is unitary, and $D = \text{diag}(\lambda_1, \lambda_2, \dots, \lambda_n) > 0$ is diagonal, one can show that

$$\log A = U \cdot \log D \cdot U^\dagger = U \cdot \begin{bmatrix} \log \lambda_1 & & & \\ & \log \lambda_2 & & \\ & & \ddots & \\ & & & \log \lambda_n \end{bmatrix} \cdot U^\dagger, \quad (1.55)$$

$$A \cdot \log A = U \cdot D \log D \cdot U^\dagger = U \cdot \begin{bmatrix} \lambda_1 \log \lambda_1 & & & \\ & \lambda_2 \log \lambda_2 & & \\ & & \ddots & \\ & & & \lambda_n \log \lambda_n \end{bmatrix} \cdot U^\dagger. \quad (1.56)$$

By a continuity argument ($\lim_{\lambda \rightarrow 0} \lambda \log \lambda = 0$), (1.56) also holds for PSD matrices A .

Theorem 1.31. *Let ρ be a density operator, and suppose a spectral decomposition of ρ is $\rho = \sum_i p_i |\psi_i\rangle\langle\psi_i|$, where $\{p_i\}_i$ is some PMF and where $\{|\psi_i\rangle\}_i$ are orthonormal w.r.t. each other, then $\mathbf{H}(\rho) = \mathbf{H}(p) = -\sum_i p_i \log p_i$.*

Proof. This is a direct result of Remark 1.30. We omit the details. \square

Corollary 1.32. *Let ρ be a density operator on a d -dimensional Hilbert space. Then, it holds that $0 \leq \mathbf{H}(\rho) \leq \log d$, where $\mathbf{H}(\rho) = 0$ if and only if ρ is in a pure state¹⁰ and where $\mathbf{H}(\rho) = \log d$ if and only if $\rho = I/d$.*

Definition 1.33 (Quantum Information Divergence). Given density operators ρ and σ (on the same Hilbert space), the *quantum information divergence* between ρ and σ is defined to be

$$D(\rho\|\sigma) \triangleq \text{tr}(\rho \log \rho) - \text{tr}(\rho \log \sigma). \quad \square$$

Theorem 1.34 (Klein's Inequality [Kle31]). *For all $\rho, \sigma \in \mathfrak{D}(\mathcal{H})$, it holds that $D(\rho\|\sigma) \geq 0$, and equality holds if and only if $\rho = \sigma$.*

Proof. Omitted. (See, e.g., [NC11, Theorem 11.7] for details.) \square

The von Neumann entropy is a continuous function, as shown by the following inequality.

Theorem 1.35 (Fannes' Inequality [Fan73]). *Let $\rho, \sigma \in \mathfrak{D}(\mathcal{H})$ be density operators on some d -dimensional Hilbert space \mathcal{H} . Then,*

$$|\mathbf{H}(\rho) - \mathbf{H}(\sigma)| \leq \|\rho - \sigma\|_1 \cdot \log d - \|\rho - \sigma\|_1 \log(\|\rho - \sigma\|_1) \leq \|\rho - \sigma\|_1 \cdot \log d + \frac{1}{e}.$$

¹⁰A density operator ρ is said to be in a *pure state* if $\text{rank}(\rho) = 1$, otherwise it is said to be in a *mixed state*.

Proof. Omitted. (See, *e.g.*, [NC11, Theorem 11.6] for details.) \square

Definition 1.36 (Conditional entropy, mutual information). Given a joint quantum system AB described by the density operator ρ_{AB} , the conditional entropy of A given B is defined as

$$\mathbf{H}(A|B) \triangleq \mathbf{H}(AB) - \mathbf{H}(B),$$

and the mutual information between the systems A and B is defined as

$$\mathbf{I}(A : B) \triangleq \mathbf{H}(A) + \mathbf{H}(B) - \mathbf{H}(AB),$$

where the reduced operators $\rho_A = \text{tr}_B(\rho_{AB})$ and $\rho_B = \text{tr}_A(\rho_{AB})$ are used for $\mathbf{H}(A)$ and $\mathbf{H}(B)$, respectively. \square

Remark 1.37. In the above definitions, the quantities $\mathbf{H}(A)$, $\mathbf{H}(A|B)$, and $\mathbf{I}(A : B)$ depend on the density operators of the involved system(s). If the density operators are not clear from the context, one may specify the density operators being considered by writing $\mathbf{H}(A)[\rho_A]$, $\mathbf{H}(A|B)[\rho_{AB}]$, and $\mathbf{I}(A : B)[\rho_{AB}]$, respectively.

Example 1.38 (Quantum Conditional Entropy can be Negative). Consider a joint quantum system AB with its density operator being $\rho_{AB} = |\psi_{AB}\rangle\langle\psi_{AB}|$, where $|\psi_{AB}\rangle = \frac{|00\rangle + |11\rangle}{\sqrt{2}}$ (see Example 1.28). In this case, $\mathbf{H}(AB) = 0$ (see Corollary 1.32), and $\mathbf{H}(A) = \mathbf{H}(B) = 1$ bit since $\rho_A = \rho_B = \frac{1}{2}I$. Moreover, one can verify that $\mathbf{H}(A|B) = \mathbf{H}(B|A) = -1$ bit and that $\mathbf{I}(A : B) = 2$ bits. (Note that we have used binary logarithm in this example.) \square

We omit the proof of the following two inequalities (see, *e.g.*, [NC11, Section 11.3.4, 11.4]).

Theorem 1.39 (Subadditivity). *Given a joint quantum system AB , it holds that*

$$\mathbf{H}(A, B) \leq \mathbf{H}(A) + \mathbf{H}(B), \quad (1.57)$$

$$\mathbf{H}(A, B) \geq |\mathbf{H}(A) - \mathbf{H}(B)|. \quad (1.58)$$

Theorem 1.40 (Strong subadditivity). *Given a joint quantum system ABC , it holds that*

$$\mathbf{H}(A, B, C) + \mathbf{H}(B) \leq \mathbf{H}(A, B) + \mathbf{H}(B, C). \quad (1.59)$$

1.2.3 Quantum Channels and Their Representations

Definition 1.41 (Quantum Channel). A quantum channel from system A to system B is a complete positive trace-preserving linear transformation from $\mathfrak{L}(\mathcal{H}_A)$ to $\mathfrak{L}(\mathcal{H}_B)$. Namely, $\mathcal{N} : \mathfrak{L}(\mathcal{H}_A) \rightarrow \mathfrak{L}(\mathcal{H}_B)$ is a quantum channel if

- \mathcal{N} is linear, namely $\mathcal{N}(a \cdot \rho + \sigma) = a \cdot \mathcal{N}(\rho) + \mathcal{N}(\sigma) \ \forall \rho, \sigma \in \mathfrak{L}(\mathcal{H}_A)$ and $a \in \mathbb{C}$;
- \mathcal{N} is completely positive, namely for any other system R,

$$(\mathcal{I}_R \otimes \mathcal{N})(\rho_{RA}) \in \mathfrak{L}_+(\mathcal{H}_{RB}) \quad \forall \rho_{RA} \in \mathfrak{L}_+(\mathcal{H}_{RA}),$$

where \mathcal{I}_R is the identity map on \mathcal{H}_R ;

- \mathcal{N} is trace-preserving, namely $\text{tr}(\mathcal{N}(\rho)) = \text{tr}(\rho)$ for any $\rho \in \mathfrak{L}(\mathcal{H}_A)$.

Additionally, \mathcal{N} is said to be finite-dimensional if both \mathcal{H}_A and \mathcal{H}_B are of finite dimension. \square

For the rest of this thesis, all quantum channels involved are assumed to be finite-dimensional, unless stated otherwise. In the following, we review two representations of quantum channels.

Theorem 1.42 (Operator-sum representation / Kraus representation). \mathcal{N} is a finite-dimensional quantum channel if and only if there exist M operators $\{E_k : \mathcal{H}_A \rightarrow \mathcal{H}_B\}_{k=1}^M$ such that

$$\mathcal{N} : \rho \mapsto \sum_{k=1}^M E_k \rho E_k^\dagger \tag{1.60}$$

and such that $1 \leq M \leq \dim(\mathcal{H}_A) \cdot \dim(\mathcal{H}_B)$ and $\sum_{k=1}^M E_k^\dagger E_k = I$. The set of operators $\{E_k\}_{k=1}^M$ is known as an operator-sum representation or a Kraus representation of the quantum channel \mathcal{N} .

Proof Outline (see, e.g., [NC11, Theorem 8.1] for details). It is relatively straightforward to show that the mapping $\rho \mapsto \sum_{k=1}^M E_k \rho E_k^\dagger$ is a quantum channel. To show any quantum channel can be represented in this way, we introduce an auxiliary system R with $\dim(\mathcal{H}_R) = \dim(\mathcal{H}_A)$, and define

$$\sigma \triangleq (\mathcal{I}_R \otimes \mathcal{N}) \left(\left(\sum_i |i_R\rangle \langle i_A| \right) \left(\sum_i |i_R\rangle \langle i_A| \right)^\dagger \right),$$

where $\{|i_R\rangle\}_i$ and $\{|i_A\rangle\}_i$ are some orthonormal bases for \mathcal{H}_R and \mathcal{H}_A , respectively. Decompose σ into $\sigma = \sum_k |k_{RB}\rangle\langle k_{RB}|$, where $|k_{RB}\rangle \in \mathcal{H}_{RB}$ need not be normalized. We claim that (1.60) can be satisfied by the operators $\{E_k\}_{k=1}^M$ defined as

$$E_k |\psi\rangle \triangleq \sum_i \langle i_A | \psi \rangle \langle i_R | k_{RB} \rangle \quad \forall |\psi\rangle \in \mathcal{H}_A$$

for each $k = 1, \dots, M$. (Please refer to the entry “ $\langle \phi_A | \psi_{AB} \rangle$ ” in the notation table.) Finally, $M \leq \dim(\mathcal{H}_A) \cdot \dim(\mathcal{H}_B)$, since the rank of σ is at most $\dim(\mathcal{H}_R \otimes \mathcal{H}_B) = \dim(\mathcal{H}_R) \cdot \dim(\mathcal{H}_B) = \dim(\mathcal{H}_A) \cdot \dim(\mathcal{H}_B)$. \square

Theorem 1.43 (Unitary representation/Stinespring representation). *\mathcal{N} is a finite-dimensional quantum channel if and only if there exists some environment system env with state space of dimension at most $\dim(\mathcal{H}_A) \cdot \dim(\mathcal{H}_B)$, and some unitary operator U such that*

$$\mathcal{N}(\rho) = \text{tr}_{\text{env}} \left(U(\rho \otimes |0\rangle\langle 0|)U^\dagger \right) \quad \forall \rho \in \mathfrak{L}(\mathcal{H}_A) \quad (1.61)$$

for some state vector $|0\rangle$ of env .

Proof Outline (see, e.g., [NC11, Box 8.1] for details). We use Theorem 1.42. Without loss of generality, assume $\dim(\mathcal{H}_A) = \dim(\mathcal{H}_B)$. Let $\{|i_{\text{env}}\rangle\}_i$ be an orthonormal basis for \mathcal{H}_{env} where $|0_{\text{env}}\rangle = |0\rangle$. In this case, by letting $E_k \triangleq \langle k_{\text{env}} | U | 0_{\text{env}} \rangle$, we have

$$\text{tr}_{\text{env}} \left(U(\rho \otimes |0\rangle\langle 0|)U^\dagger \right) = \sum_k E_k \rho E_k^\dagger.$$

By verifying $\sum_k E_k^\dagger E_k = I$, we have shown that the mapping \mathcal{N} in (1.61) is a quantum channel. On the other hand, to show that any quantum channel \mathcal{N} can be represented in this way, it suffices to, given any Kraus representation $\{E_k\}_k$ of some quantum channel, construct a unitary operator U such that $\langle k_{\text{env}} | U | 0_{\text{env}} \rangle = E_k$. This can be done by fixing the first column (of blocks) of $[U]$ to be $[E_k]$'s, and filling up the remaining columns of the matrix while ensuring all columns are orthonormal w.r.t. each other. Here, $[E_k]$ is the matrix representation of E_k under some orthonormal basis $\{|i_P\rangle\}_i$ (for both \mathcal{H}_A and \mathcal{H}_B); and $[U]$ is the matrix representation of U under the basis $\{|k_{\text{env}}\rangle \otimes |i_P\rangle\}_{k,i}$. \square

Corollary 1.44 (Choi–Jamiołkowski matrix). *Let $\mathcal{N} : \mathfrak{L}(\mathcal{H}_A) \rightarrow \mathfrak{L}(\mathcal{H}_B)$ be a quantum channel, and let $\{|\ell\rangle\}_{\ell=1}^d$ be an orthonormal basis for both \mathcal{H}_A and \mathcal{H}_B (where $d =$*

$\dim(\mathcal{H}_A) = \dim(\mathcal{H}_B)$). Let the matrix $W \in \mathbb{C}^{d^2 \times d^2}$ be defined as

$$W_{(i,j),(i',j')} \triangleq \langle j | \mathcal{N}(|i\rangle\langle i'|) | j' \rangle \quad \forall i, i', j, j' = 1, \dots, d. \quad (1.62)$$

Then the matrix W is PSD.

Proof. This is a direct result of Theorem 1.42. We omit the details. \square

The matrix W defined in Corollary 1.44 is often known as a *Choi–Jamiołkowski matrix* of the quantum channel \mathcal{N} (w.r.t. basis $\{|\ell\rangle\}_{\ell=1}^d$). In particular, it holds that

$$[\mathcal{N}(\rho)]_{j,j'} = \sum_{i,i'} W_{(i,j),(i',j')} \cdot [\rho]_{i,i'} \quad \forall \rho \in \mathfrak{D}(\mathcal{H}_A), \quad (1.63)$$

where $[\rho]$ and $[\mathcal{N}(\rho)]$ are the matrix representation of the corresponding operators under the basis $\{|\ell\rangle\}_{\ell=1}^d$.

Example 1.45. Below is a list of examples of quantum channels.

Bit flip channel $\rho \mapsto E_0 \rho E_0^\dagger + E_1 \rho E_1^\dagger$, $E_0 = \sqrt{p} \begin{bmatrix} 1 & 0 \\ 0 & 1 \end{bmatrix}$, $E_1 = \sqrt{1-p} \begin{bmatrix} 0 & 1 \\ 1 & 0 \end{bmatrix}$, $p \in (0, 1)$.

Phase flip channel $\rho \mapsto E_0 \rho E_0^\dagger + E_1 \rho E_1^\dagger$, $E_0 = \sqrt{p} \begin{bmatrix} 1 & 0 \\ 0 & 1 \end{bmatrix}$, $E_1 = \sqrt{1-p} \begin{bmatrix} 1 & 0 \\ 0 & -1 \end{bmatrix}$, $p \in (0, 1)$.

Amplitude damping $\rho \mapsto E_0 \rho E_0^\dagger + E_1 \rho E_1^\dagger$, $E_0 = \begin{bmatrix} 1 & 0 \\ 0 & \sqrt{1-\gamma} \end{bmatrix}$, $E_1 = \begin{bmatrix} 0 & \sqrt{\gamma} \\ 0 & 0 \end{bmatrix}$, $\gamma \in (0, 1)$.

Depolarizing channel $\rho \mapsto \frac{pI}{2} + (1-p)\rho$, $p \in (0, 1)$. \square

1.2.4 Communications over quantum channels

Quantum channels can be used to convey either classical or quantum information. In this section, we focus on classical communications. Though quantum communication is an important topic in quantum information theory, it is beyond our discussion scope.

Given (multiple copies of) a quantum channel from system A to system B , the task of classical communication over this channel is to transmit some classical information from Alice, who has *access* to the copies of system A , to Bob, who has *access* to the copies of system B , namely

- Alice is able to fully manipulate the (joint) state (*i.e.*, the density operator) of the copies of A ;
- Bob can perform any quantum measurement of his choice on the copies of B .

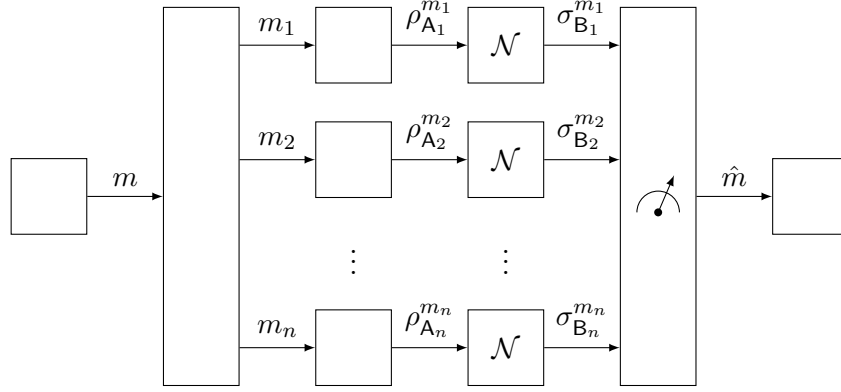


Figure 1.4: Product-state setup for classical communications over a quantum channel.

For example, to transmit a message $m \in \mathcal{M}_n$ using n copies of the channel (*i.e.*, $\mathcal{N}^{\otimes n}$ will be applied): Immediately before applying the channels, Alice prepares the states of the systems A_1^n such that its (joint) density operator becomes $\rho_{A_1}^{m_1} \otimes \rho_{A_2}^{m_2} \otimes \cdots \otimes \rho_{A_n}^{m_n}$, where (m_1, m_2, \dots, m_n) is some function of m .¹¹ Upon receiving the state of the systems B_1^n , Bob estimates the original message as a result of some physical operation on B_1^n , where, for each possible estimate \hat{m} , the corresponding effect is described by some POVM element $E_{\hat{m}}$. An error is said to have occurred if this estimate differs from m , and in this setup, this happens with probability $P_e^{(n)}(m) = 1 - \text{tr} \left(E_m \cdot \bigotimes_{\ell=1}^n \mathcal{N}(\rho_{A_\ell}^{m_\ell}) \right)$. If there exists a sequence (indexed by n) of encoders $m \mapsto \bigotimes_{\ell=1}^n \rho_{A_\ell}^{m_\ell}$ and POVMs $\{E_{\hat{m}}\}_{\hat{m} \in \mathcal{M}_n}$ such that $\lim_{n \rightarrow \infty} P_e^{(n)} = \mathbf{0}$, a communication rate of $R \triangleq \liminf_{n \rightarrow \infty} \frac{1}{n} \log |\mathcal{M}_n|$ is said to have been *achieved*. If the supremum of all achievable rates and the infimum of all unachievable rates are the same, this number is known as the capacity. The capacity of this particular setup exists and is often referred to as the *product-state capacity* of the quantum channel \mathcal{N} (see Theorem 1.47). The product-state capacity is denoted by C_1 .

Definition 1.46 (Holevo capacity). Given a quantum channel $\mathcal{N} : \mathfrak{L}(\mathcal{H}_A) \rightarrow \mathfrak{L}(\mathcal{H}_B)$, the non-negative real number

$$\chi(\mathcal{N}) \triangleq \sup_{\substack{p_i \geq 0, \sum_i p_i = 1 \\ \rho_i \in \mathfrak{D}(\mathcal{H}_A)}} \left\{ \mathbf{H} \left(\mathcal{N} \left(\sum_i p_i \rho_i \right) \right) - \sum_i p_i \mathbf{H}(\mathcal{N}(\rho_i)) \right\} \quad (1.64)$$

is called the the Holevo capacity of \mathcal{N} . □

¹¹Note that $A_1^n \triangleq A_1 \otimes \cdots \otimes A_n$, where A_i is the copy of A at the i -th channel use. Similar statement also applies to B_1^n .

Theorem 1.47 (HSW Theorem [Hol73; Hol98; SW97]). *The product-state capacity of a (memoryless) quantum channel coincides with its Holevo capacity. Namely, $C_1(\mathcal{N}) \equiv \chi(\mathcal{N})$.*

Proof. Omitted. (See, *e.g.*, [NC11, Section 12.3.2].) \square

As a result of Theorem 1.47, computing the product-state capacity is equivalent to maximizing the *Holevo quantity* $\chi(\{\varrho_i\}_i)$, where

$$\chi(\{\varrho_i\}_i) \triangleq \mathbf{H}\left(\mathcal{N}\left(\sum_i \varrho_i\right)\right) - \sum_i \mathbf{H}(\mathcal{N}(\varrho_i)) \quad (1.65)$$

and where $\{\varrho_i\}_i$ is an index set of operators such that¹² $\varrho_i > 0$ for each i , and $\text{tr}(\sum_i \varrho_i) = 1$. The complexity of solving this optimization problem *exactly* is NP-complete [BS07a]. Fortunately, given any positive tolerance (w.r.t. the distance from the exact maximizer), an estimated optimal $\{\varrho_i\}_i$ can be computed efficiently in an iterative manner [Nag98].

However, knowing C_1 is still steps away from finding the unrestricted capacity for transmitting classical information (a.k.a. classical capacity). If the channel is *additive* (see Definition 1.48), *i.e.*, joint manipulation of multiple input systems does not increase capacity, it holds that classical capacity $C = C_1$. Otherwise, the situation is more complicated. Namely, we need to consider a relaxed setup by allowing Alice to manipulate at most k input systems jointly, *i.e.*, Alice encodes each message m as $\rho_{\mathbf{A}_1^k}^{m_1} \otimes \rho_{\mathbf{A}_{k+1}^{2 \cdot k}}^{m_2} \otimes \cdots \otimes \rho_{\mathbf{A}_{(n-1) \cdot k}^{m_n}}^{m_n}$ for some $n \in \mathbb{Z}_{>0}$. The capacity of this relaxed setup is $C_k \triangleq \frac{1}{k} C_1(\mathcal{N}^{\otimes k})$. Finding the classical capacity is then equivalent to finding the supremum of $\{C_k\}_{k=1}^\infty$, *i.e.*, $C = \limsup_{k \rightarrow \infty} C_k(\mathcal{N})$.

Definition 1.48 (Additivity of classical capacity). The classical capacity of a quantum channel \mathcal{N} is said to be *additive* if

$$C_1(\mathcal{N}) = C_k(\mathcal{N}) \triangleq \frac{1}{k} C_1(\mathcal{N}^{\otimes k}) \quad (1.66)$$

for all positive integers k . \square

Unfortunately, classical capacities are *not* additive in general [Has09], despite the alternative speculations [AHW00; Fuk05] in the early years of the study. This makes the

¹²Such a set of positive operators is sometimes referred to as an *ensemble*; however, more often, an ensemble refers to an indexed set of pairs $\{(p_i, \rho_i)\}_i$ where $(p_i)_i$ is a PMF, and $\{\rho_i\}_i$'s are density operators. These two formalisms are equivalent.

computation of classical capacities particularly difficult, since evaluating the Holevo quantity alone would take an exponential amount of time (and storage) as the dimensions of the involved quantum systems grow. On the other hand, quite a number of additive channels exist, including quantum erasure channels [BDS97], unital qubit channels [Kin02], depolarizing channels [Kin03], and transpose depolarizing channels [DHS06].

Readers must be reminded that the setup presented in this section is not the only type of classical communication over quantum channels. Other important setups include entanglement-assist classical communications [BSST99; Hol02; Sho04] and private (classical) communications [Dev05]. These discussions are beyond the scope of this thesis, and we omit the details.

Chapter 2

Double-Edge Factor Graphs

In this chapter, we consider the problem of representing the dynamics of quantum systems using concepts of factor graphs. The result is a graphical model called double-edge factor graphs (DeFGs). The idea is based on the linear-algebraic descriptions of factor graphs [AMV11] and can be connected to the methods proposed by Loeliger and Vontobel for representing quantum systems [LV12; LV17]. Related studies also include [Mor15a], in which he proposed a generalized bipartite graphical model capable of representing quantum systems. For comparison, the global functions considered here are in the form of

$$g(\mathbf{x}, \tilde{\mathbf{x}}; \mathbf{y}) = \prod_{a \in \mathcal{F}} f_a(\mathbf{x}_{\partial a}, \tilde{\mathbf{x}}_{\partial a}; \mathbf{y}_{\delta a}), \quad (2.1)$$

where for any fixed $\mathbf{y}_{\delta a}$, the matrix $[f_a^{\mathbf{y}_{\delta a}}]_{\mathbf{x}_{\partial a}, \tilde{\mathbf{x}}_{\partial a}} \triangleq f_a^{\mathbf{y}_{\delta a}}(\mathbf{x}_{\partial a}, \tilde{\mathbf{x}}_{\partial a})$ is PSD. In contrast, in [LV12; LV17], the functions $\{f_a\}$'s are required to be decomposable, *i.e.*,

$$f_a(\mathbf{x}_{\partial a}, \tilde{\mathbf{x}}_{\partial a}; \mathbf{y}_{\delta a}) = \tilde{f}_a(\mathbf{x}_{\partial a}; \mathbf{y}_{\delta a}) \overline{\tilde{f}_a(\tilde{\mathbf{x}}_{\partial a}; \mathbf{y}_{\delta a})} \quad \exists \tilde{f}_a \quad \forall a. \quad (2.2)$$

Therefore, the scenario we consider here is more general. We also consider the problem of computing the partition sums of such global functions, *i.e.*,

$$Z(\mathcal{G}) \triangleq \sum_{\mathbf{y}} \sum_{\mathbf{x}, \tilde{\mathbf{x}}} g(\mathbf{x}, \tilde{\mathbf{x}}; \mathbf{y}). \quad (2.3)$$

This problem is directly related to inference problems on systems with quantum components. For solving this problem, we propose a generalized version of the BA algorithms for DeFGs. Some numerical results and (attempted) analysis of the algorithms are also included in this chapter.

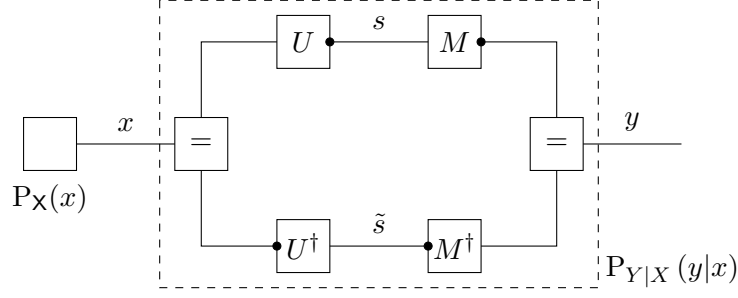


Figure 2.1: FG describing a simple quantum system.

2.1 From Factor Graphs for Quantum Probabilities to Double-Edge Factor Graphs

2.1.1 Factor Graphs for Quantum Probabilities

This section reviews the method proposed in [LV12; LV17], where a relaxed version of factor graphs is used to represent “quantum probabilities”. We start with the following example.

Example 2.1. Consider the factor graph in Figure 2.1. Here, some of the local functions are specified by matrices. The dots at the end of some of the edges specify which variable is the first index of the matrix. This setup depicts a cq-channel followed by a unitary evolution and then a measurement. In this case, the global function is

$$g(s, \tilde{s}; x, y) = P_X(x) \cdot U_{s,x} U_{x,\tilde{s}}^\dagger \cdot M_{y,s} M_{\tilde{s},y}^\dagger \quad (2.4)$$

$$= P_X(x) \cdot U(s, x) \overline{U(\tilde{s}, x)} \cdot M(y, s) \overline{M(y, \tilde{s})}, \quad (2.5)$$

where U and M are both complex unitary matrices. Note that the letters U and M denote matrices in (2.4), but functions in (2.5).

Though we have complex-valued functions as local functions in these cases, the marginals and the partition sum are still real and non-negative due to the symmetric structure. For example, by closing the dashed box in Figure 2.1, the resultant function can be expressed as

$$P_{Y|X}(y|x) = \sum_s U(s, x) M(y, s) \cdot \sum_{\tilde{s}} \overline{U(\tilde{s}, x) M(y, \tilde{s})} \quad (2.6)$$

$$= \left| \sum_s U(s, x) M(y, s) \right|^2, \quad (2.7)$$

which is the conditional probability of Y given X in this setup. \square

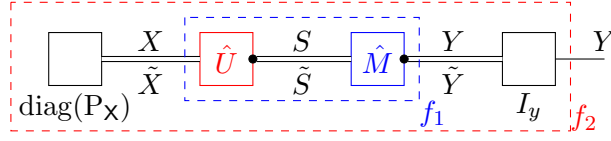


Figure 2.2: Quantum NFG for an elementary quantum system.

Consider the factor graphs constructed in a symmetric manner where complex functions always appear in conjugate pairs. In such cases, any factorization with local functions satisfying (2.2) can be represented by some factor graph as in Example 2.1. A variety of such representable quantum systems can be found in [LV12; LV17].

2.1.2 Double-Edge Factor Graphs (DeFGs)

Example 2.2 (Redrawing of Example 2.1). Consider the factor graph in Figure 2.2 as a redrawing of Figure 2.1, where each local function is specified by a matrix with the variables associated with upper edges composing the first index of the matrix. The dots in this graph are used to specify how the variables are *arranged* to compose the indices of the matrices. For example, the factors labeled by the matrices \hat{U} and \hat{M} are associated with the functions

$$\hat{U}(s, x; \tilde{s}, \tilde{x}) \triangleq \hat{U}_{(s,x),(\tilde{s},\tilde{x})} = U_{s,x} \cdot U_{\tilde{x},\tilde{s}}^\dagger = U(s, x) \overline{U(\tilde{s}, \tilde{x})}, \quad (2.8)$$

$$\hat{M}(y, s; \tilde{y}, \tilde{s}) \triangleq \hat{M}_{(y,s),(\tilde{y},\tilde{s})} = M_{y,s} \cdot M_{\tilde{s},\tilde{y}}^\dagger = M(y, s) \overline{M(\tilde{y}, \tilde{s})}, \quad (2.9)$$

respectively. Thus, the global function is

$$g(x, s, t, \tilde{x}, \tilde{s}, \tilde{y}) = P_X(x) \cdot \hat{U}(s, x; \tilde{s}, \tilde{x}) \cdot \hat{M}(y, s; \tilde{y}, \tilde{s}) \cdot \delta_{y,\tilde{y}}, \quad (2.10)$$

which is equivalent to (2.4). In addition, the exterior functions f_1 , f_2 corresponding to the inner and outer boxes in Figure 2.2 can be expressed as

$$f_1(x, y, \tilde{x}, \tilde{y}) = \sum_{s, \tilde{s}} U(s, x) \overline{U(\tilde{s}, \tilde{x})} \cdot M(y, s) \overline{M(\tilde{y}, \tilde{s})} \quad (2.11)$$

$$= \sum_s U(s, x) M(y, s) \cdot \overline{\sum_{\tilde{s}} U(\tilde{s}, \tilde{x}) M(\tilde{y}, \tilde{s})} \quad (2.12)$$

$$= [M \cdot U]_{y,x} \cdot [M \cdot U]_{\tilde{x},\tilde{y}}^\dagger, \quad (2.13)$$

$$f_2(y) = \sum_x P_X(x) \cdot f_1(x, y, x, \tilde{y}) = \sum_x [M \cdot U]_{y,x} \cdot P_X(x) \cdot [M \cdot U]_{x,\tilde{y}}^\dagger \quad (2.14)$$

$$= \left[M \cdot U \cdot \text{diag}(P_X) \cdot U^\dagger \cdot M^\dagger \right]_{y,y}, \quad (2.15)$$

respectively.¹ One can check that $f_2(y) = \sum_x P_X(x) \cdot P_{Y|X}(y|x)$, where $P_{Y|X}$ was defined earlier in (2.6), *i.e.*, $f_2(y)$ is the PMF of Y given the PMF of X being P_X . One can view f_1 as a matrix generalization of $P_{Y|X}$. In this example, $\text{diag}(f_1) = P_{Y|X}$. \square

In the above example, we have successfully described a quantum system using a simpler graph with compatible “closing-the-box” operations. Such techniques can be made generic, and we name such graphical models *double-edge factor graphs* (DeFGs).

Definition 2.3 (Double-Edge Factor Graph). A double-edge factor graph (DeFG) is a bipartite graph $\mathcal{G} = (\mathcal{V}_1 \sqcup \mathcal{V}_2, \mathcal{F}, \mathcal{E}_1 \sqcup \mathcal{E}_2)$ associated with variable sets $\mathfrak{V}_1, \mathfrak{V}_2$, and a factor set \mathfrak{F} , where

- $\mathcal{E}_1 \subseteq \mathcal{V}_1 \times \mathcal{F}, \mathcal{E}_2 \subseteq \mathcal{V}_2 \times \mathcal{F}$; and for each $a \in \mathcal{F}$, we denote the sets of its neighbors in \mathcal{V}_1 and \mathcal{V}_2 by δa and ∂a , respectively;
- $\mathfrak{V}_1 = \{\mathcal{X}_i\}_{i \in \mathcal{V}_1}$ and $\mathfrak{V}_2 = \{\mathcal{S}_j\}_{j \in \mathcal{V}_2}$ are indexed by \mathcal{V}_1 and \mathcal{V}_2 , respectively, and each element of \mathfrak{V}_1 and \mathfrak{V}_2 is a set (a.k.a. alphabets);
- $\mathfrak{F} = \{f_a\}_{a \in \mathcal{F}}$ is indexed by \mathcal{F} , where for each $a \in \mathcal{F}$ $f_a : \times_{i \in \partial a} \mathcal{S}_j^2 \times \times_{i \in \delta a} \mathcal{X}_i \rightarrow \mathbb{C}$ and where the matrix $[f_a(\mathbf{x}_{\delta a})]_{\mathbf{s}_{\partial a}, \tilde{\mathbf{s}}_{\partial a}} \triangleq f_a(\mathbf{s}_{\partial a}, \tilde{\mathbf{s}}_{\partial a}; \mathbf{x}_{\delta a})$ is PSD for each $\mathbf{x}_{\delta a}$.

The function $g(\mathbf{s}, \tilde{\mathbf{s}}; \mathbf{x}) \triangleq \prod_{a \in \mathcal{F}} f_a(\mathbf{s}_{\partial a}, \tilde{\mathbf{s}}_{\partial a}; \mathbf{x}_{\delta a})$ is called the *global function* of \mathcal{G} , and in this case, \mathcal{G} is also said to be representing the factorization $g(\mathbf{s}, \tilde{\mathbf{s}}; \mathbf{x}) \triangleq \prod_{a \in \mathcal{F}} f_a(\mathbf{s}_{\partial a}, \tilde{\mathbf{s}}_{\partial a}; \mathbf{x}_{\delta a})$. Like (classical) factor graphs, a DeFG is said to be *normal* if the degree of any vertex in $\mathcal{V}_1 \sqcup \mathcal{V}_2$ is at most 2. \square

Remark 2.4. Similar to factor graphs, in a normal DeFG, we redraw the vertices in \mathcal{V}_1 as edges and the vertices in \mathcal{V}_2 as double edges, as in Figure 2.2.

Remark 2.5. Any DeFG can be converted into a normal DeFG by properly introducing equality node(s) along with introducing suitable auxiliary variables.

In the previous example, we have converted a factor graph describing a quantum system into a DeFG. Such conversions can be done systematically, as described in Table 2.3.

¹Note that in (2.13), we take Hermitian of a matrix first, then extract the indices. Namely, for any complex matrix A , $A_{i,j}^\dagger = \overline{A_{j,i}}$.

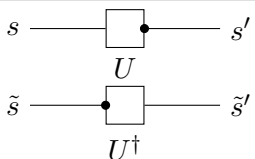
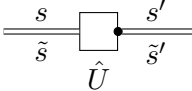
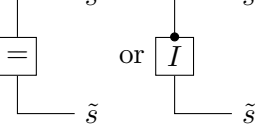
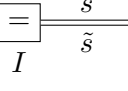
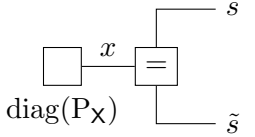
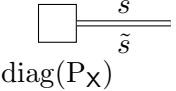
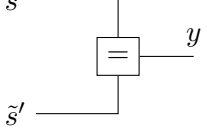
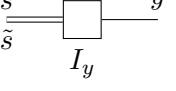
FG Description	DeFG Description	Remarks
		$\hat{U}((s', s), (\tilde{s}', \tilde{s})) = U_{s', s} U_{\tilde{s}', \tilde{s}}^\dagger$
		$I(s, \tilde{s}) = \delta_{s, \tilde{s}}$
		$\text{diag}(\mathbf{P}_\mathbf{X})(s, \tilde{s}) = \delta_{s, \tilde{s}} \cdot \mathbf{P}_\mathbf{X}(s)$
		$I_y(s, \tilde{s}) = \delta_{s, \tilde{s}} \cdot \delta_{s, y}$

Table 2.3: Conversions between factor graphs and DeFGs

2.1.3 “Closing-the-Box” Operations on DeFGs

We define the “closing-the-box” operations on DeFGs in the same manner as for factor graphs.

Definition 2.6 (“Closing-the-Box” Operations on DeFGs). Let $\mathcal{G} = (\mathcal{V}_1 \sqcup \mathcal{V}_2, \mathcal{F}, \mathcal{E}_1 \sqcup \mathcal{E}_2)$ be a DeFG as defined in Definition 2.3. Let $\mathcal{G}' = (\mathcal{V}'_1 \sqcup \mathcal{V}'_2, \mathcal{F}')$ be a subgraph of \mathcal{G} such that if a variable vertex is in \mathcal{G}' , then so do all of its neighbors (all of which are in \mathcal{F}). (We call such a subgraph a *box* of \mathcal{G} .) The “closing-the-box” operation (w.r.t. \mathcal{G}') is to replace \mathcal{G}' in \mathcal{G} by a factor vertex associated with the *exterior function* $f_{\mathcal{G}'}$ of \mathcal{G}' , where $f_{\mathcal{G}'}$ is the resultant function by summing the product of the local functions associated with \mathcal{F}' over the variables associated with $\mathcal{V}'_1 \sqcup \mathcal{V}'_2$. Namely, $f_{\mathcal{G}'}$ is defined as

$$f_{\mathcal{G}'}(s_{\cup_{a \in \mathcal{F}'} \partial a \setminus \mathcal{V}'_2}, \tilde{s}_{\cup_{a \in \mathcal{F}'} \partial a \setminus \mathcal{V}'_2}; \mathbf{x}_{\cup_{a \in \mathcal{F}'} \delta a \setminus \mathcal{V}'_1}) \triangleq \sum_{s_{\mathcal{V}'_2}, \tilde{s}_{\mathcal{V}'_2}, \mathbf{x}_{\mathcal{V}'_1}} \prod_{a \in \mathcal{F}'} f_a(s_{\partial a}, \tilde{s}_{\partial a}; \mathbf{x}_{\delta a}). \quad \square$$

An advantage of DeFGs over factor graphs for quantum probabilities is that a DeFG remains to be DeFG after any “closing-the-box” operations.

Theorem 2.7. *Given a DeFG, it remains a DeFG after a “closing-the-box” operation.*

Proof. Consider the setup in Definition 2.6. It suffices to show that the matrices associated with the exterior function $[f_{\mathcal{G}'}(\mathbf{x})]_{\mathbf{s}, \tilde{\mathbf{s}}} \triangleq f_{\mathcal{G}'}(\mathbf{s}, \tilde{\mathbf{s}}; \mathbf{x})$ are PSD. Using mathematical induction, it suffices to show that given any pair of functions $f_a(\mathbf{s}_{\partial a}, \tilde{\mathbf{s}}_{\partial a}; \mathbf{x}_{\delta a})$ and $f_b(\mathbf{s}_{\partial b}, \tilde{\mathbf{s}}_{\partial b}; \mathbf{x}_{\delta b})$ such that the matrices $[f_a(\mathbf{x}_{\delta a})]_{\mathbf{s}_{\partial a}, \tilde{\mathbf{s}}_{\partial a}} \triangleq f_a(\mathbf{s}_{\partial a}, \tilde{\mathbf{s}}_{\partial a}; \mathbf{x}_{\delta a})$ and $[f_b(\mathbf{x}_{\delta b})]_{\mathbf{s}_{\partial b}, \tilde{\mathbf{s}}_{\partial b}} \triangleq f_b(\mathbf{s}_{\partial b}, \tilde{\mathbf{s}}_{\partial b}; \mathbf{x}_{\delta b})$ are PSD, then, for each $i \in \delta a \cap \delta b$, $j \in \partial a \cap \partial b$, and $\mathbf{x}_{\delta a \cup \delta b \setminus i} \in \bigotimes_{\ell \in \delta a \cup \delta b \setminus i} \mathcal{X}_\ell$, the matrix $[f(\mathbf{x}_{\delta a \cup \delta b \setminus i})]$ with its $(\mathbf{s}_{\partial a \cup \partial b \setminus j}, \tilde{\mathbf{s}}_{\partial a \cup \partial b \setminus j})$ -th entry being $\sum_{s_j, \tilde{s}_j, x_i} f_a(\mathbf{s}_{\partial a}, \tilde{\mathbf{s}}_{\partial a}; \mathbf{x}_{\delta a}) \cdot f_b(\mathbf{s}_{\partial b}, \tilde{\mathbf{s}}_{\partial b}; \mathbf{x}_{\delta b})$ must also be PSD. However, notice that given any complex-valued function $h(\mathbf{s}_{\partial a \cup \partial b \setminus j})$, it holds that

$$\begin{aligned} & \sum_{\substack{\mathbf{s}_{\partial a \cup \partial b \setminus j}, \\ \tilde{\mathbf{s}}_{\partial a \cup \partial b \setminus j}}} h(\mathbf{s}_{\partial a \cup \partial b \setminus j}) \cdot \left[\sum_{s_j, \tilde{s}_j, x_i} f_a(\mathbf{s}_{\partial a}, \tilde{\mathbf{s}}_{\partial a}; \mathbf{x}_{\delta a}) \cdot f_b(\mathbf{s}_{\partial b}, \tilde{\mathbf{s}}_{\partial b}; \mathbf{x}_{\delta b}) \right] \cdot \overline{h(\tilde{\mathbf{s}}_{\partial a \cup \partial b \setminus j})} = \\ & \sum_{x_i} \sum_{\substack{\mathbf{s}_{\partial a \cup \partial b}, \\ \tilde{\mathbf{s}}_{\partial a \cup \partial b}}} h(\mathbf{s}_{\partial a \cup \partial b \setminus j}) \cdot \mathbf{1}(s_j) \cdot \left[f_a(\mathbf{s}_{\partial a}, \tilde{\mathbf{s}}_{\partial a}; \mathbf{x}_{\delta a}) \cdot f_b(\mathbf{s}_{\partial b}, \tilde{\mathbf{s}}_{\partial b}; \mathbf{x}_{\delta b}) \right] \cdot \overline{h(\tilde{\mathbf{s}}_{\partial a \cup \partial b \setminus j}) \cdot \mathbf{1}(\tilde{s}_j)} \geq 0, \end{aligned}$$

since the Hadamard product of two PSD matrices is PSD.² \square

Similar to factor graphs, we define the partition sum of a DeFG as the result of summing the global function over all of its variables. Namely, we have the definition

$$Z(\mathcal{G}) \triangleq \sum_{\mathbf{s}, \tilde{\mathbf{s}}, \mathbf{x}} g(\mathbf{s}, \tilde{\mathbf{s}}; \mathbf{x}). \quad (2.16)$$

Since the partition sum can be understood as the result of “closing-the-box” w.r.t. the graph itself, we have the following corollary as a direct result of Theorem 2.7.

Corollary 2.8. *The partition sum of a DeFG is real non-negative.*

2.2 DeFGs and Quantum Systems: Examples

In this section, we would like to present several examples of DeFGs, especially the DeFGs representing elementary quantum systems. Some of the examples presented here are related to the examples in [LV17; LV12]. In particular, we would like to illustrate the connection between the marginals of DeFGs and elements from quantum information theory.

Example 2.9. The DeFG in Figure 2.4 describes a quantum system with n steps of unitary evolutions followed by a projective measurement w.r.t. the computation basis.

²Here, $\mathbf{1}$ stands for the constant-1 function.

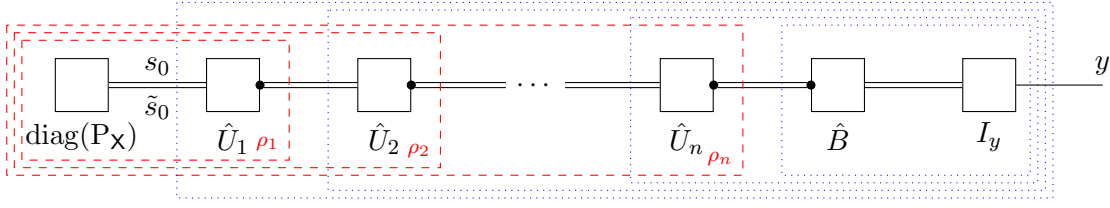


Figure 2.4: n steps of unitary evolution followed by a projective measurement w.r.t. the computation basis.

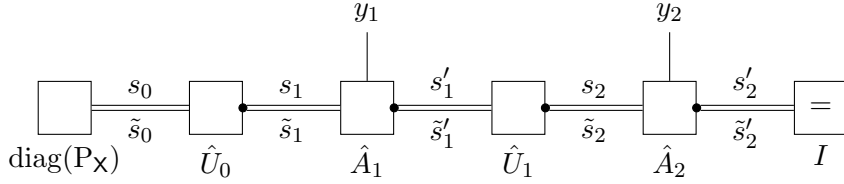


Figure 2.5: A factor graph describing a two-measurement quantum system.

For every $k \in \{1, 2, \dots, n\}$, the exterior function of the k -th dashed box can be expressed as³

$$\rho_k(s_k, \tilde{s}_k) = \sum_{s_{k-1}, \tilde{s}_{k-1}} \hat{U}_k((s_k, s_{k-1}), (\tilde{s}_k, \tilde{s}_{k-1})) \cdot \rho_{k-1}(s_{k-1}, \tilde{s}_{k-1}). \quad (2.17)$$

Here, note that $\hat{U}_k((s_k, s_{k-1}), (\tilde{s}_k, \tilde{s}_{k-1})) = U_{s_k, s_{k-1}} U_{\tilde{s}_{k-1}, \tilde{s}_k}^\dagger$ for some unitary matrix U . The functions $\{\rho_k\}_{k=1}^n$ are the Schrödinger representation of the system. Similarly, the exterior functions of the dotted boxes correspond to the Heisenberg representation. \square

Example 2.10. Figure 2.5 describes a DeFG for a quantum system with two measurements, where \hat{A}_1, \hat{A}_2 are functions such that $\sum_{y_k} \sum_{s'_k = \tilde{s}'_k} A_k(s'_k, s_k, \tilde{s}'_k, \tilde{s}_k; y_k) = \delta_{s_k, \tilde{s}_k}$ for each $k = 1, 2$. \square

Example 2.11. The DeFG in Figure 2.6 is a special case of Example 2.10, in which both measurements are projective measurements with one-dimensional eigenspaces. Here, $\hat{P}_k(y_k, s_k, \tilde{y}_k, \tilde{s}_k) = P_{y_k, s_k}^{(k)} P_{\tilde{s}_k, \tilde{y}_k}^{(k)\dagger}$ for some projective matrix $P^{(k)}$ for each $k = 1, 2$. \square

Example 2.12. The DeFG in Figure 2.7 depicts a quantum system with two partial measurements. Here, \hat{A}_1, \hat{A}_2 satisfy the same requirement as in Example 2.10, and $\hat{U}_1,$

³Note that we may sometimes group the arguments of some functions (e.g., \hat{U}_k in (2.17)) using parentheses for better readability.

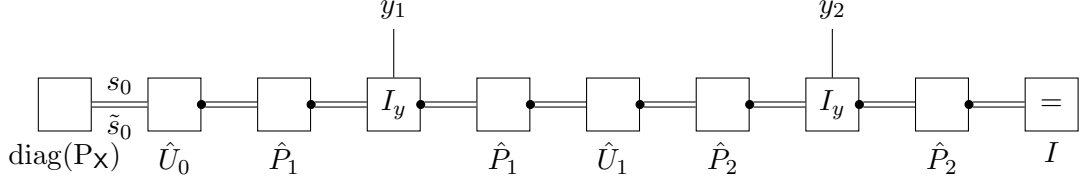


Figure 2.6: A factor graph describing a two-measurement quantum system with projective measure onto 1-dimension eigenspace.

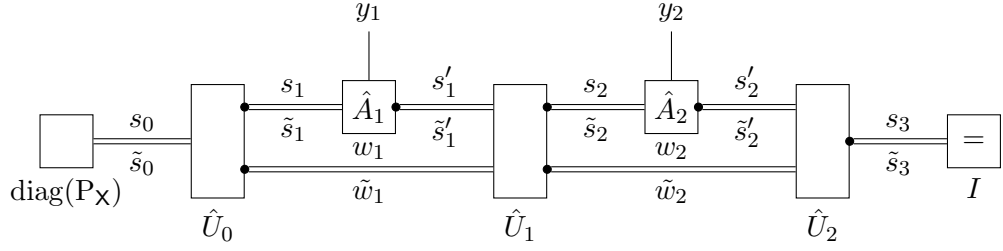


Figure 2.7: A quantum system with two partial measurements.

\hat{U}_2 , and \hat{U}_3 are functions such that

$$\begin{aligned}\hat{U}_1(s_1, w_1, s_0, \tilde{s}_1, \tilde{w}_1, \tilde{s}_0) &= U_{(s_1, w_1), s_0}^{(1)} U_{\tilde{s}_0, (\tilde{s}_1, \tilde{w}_1)}^{(1)\dagger} \\ \hat{U}_2(s_2, w_2, s'_1, w_1, \tilde{s}_2, \tilde{w}_2, \tilde{s}'_1, \tilde{w}_1) &= U_{(s_2, w_2), (s'_1, w_1)}^{(2)} U_{(\tilde{s}'_1, \tilde{w}_1), (\tilde{s}_2, \tilde{w}_2)}^{(2)\dagger} \\ \hat{U}_3(s_3, s'_2, w_2, \tilde{s}_3, \tilde{s}'_2, \tilde{w}_2) &= U_{s_3, (s'_2, w_2)}^{(3)} U_{(\tilde{s}'_2, \tilde{w}_2), \tilde{s}_3}^{(3)\dagger}\end{aligned}$$

for some unitary matrices $U^{(1)}$, $U^{(2)}$, $U^{(3)}$. Note that this DeFG contains cycles. \square

As illustrated by the above examples, the dynamics of a quantum system (see Section 1.2.1) can be described by DeFGs systematically, as summarized in Table 2.8.

2.3 Belief-Propagation Algorithms for DeFGs

In this section, we consider the problem of computing the partition sums of DeFGs. For acyclic cases, the problem is not so different from that on a factor graph and can be solved by a slightly modified version of the method in Section 1.1.3. For DeFGs with cycles, we propose and analyze a generalized version of the belief-propagation algorithms.

Without loss of generality, we assume all the DeFGs involved in the rest of this chapter do not have “single edges”. Namely, we only consider global functions in the

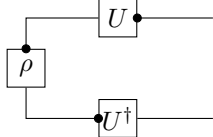
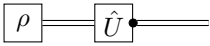
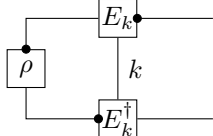
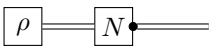
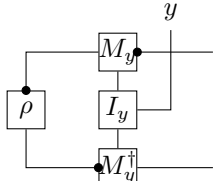
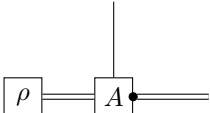
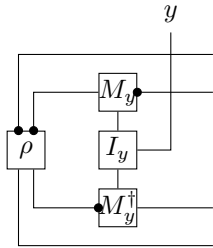
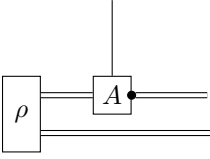


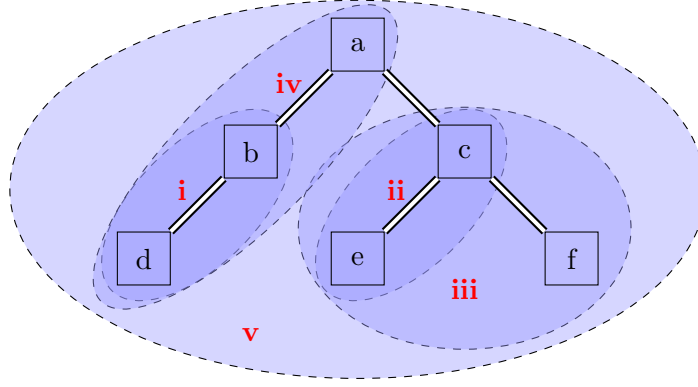
FG Description	DeFG Description	Remarks
		$\hat{U}(s', s, \tilde{s}', \tilde{s}) = U_{s', s} U_{\tilde{s}, \tilde{s}'}^\dagger$
		$N(s', s, \tilde{s}', \tilde{s}) = \sum_k E_{s', s} E_{\tilde{s}, \tilde{s}'}^\dagger$
		$A(s', s, \tilde{s}', \tilde{s}; y) = M_y(s', s) M_y^\dagger(\tilde{s}, \tilde{s}')$
		Same as above
		-

Table 2.8: Representing quantum systems using factor graphs and DeFGs.

Figure 2.9: Computing the partition sum of a normal *acyclic* DeFG.

form

$$g(s, \tilde{s}) = \prod_{a \in \mathcal{F}} f_a(s_{\partial a}, \tilde{s}_{\partial a}). \quad (2.18)$$

2.3.1 Computing the marginals/partition sum of an acyclic DeFG

Similar to the methods for acyclic factor graphs in Section 1.1.3, one can also “shrink” an acyclic DeFG to a root factor via a sequence of “closing-the-box” operations starting from the leaf nodes. The following example illustrates this idea.

Example 2.13. By taking a sequence of “closing-the-box” operations for each adjacent factor, the normal DeFG in Figure 2.9 can be “shrunk” to a null graph with a single local constant function. The roman numerals indicate the sequence of the “closing-the-box” operations. The constant obtained in the end is the partition sum. \square

We summarize the method above as Algorithm 2.1. Without loss of generality, we have assumed all the leaf vertices are from \mathcal{F} , since we can always append a constant-1 local function to a leaf vertex from \mathcal{V} without changing the partition sum.

In analogy to Theorem 1.8, we have the following theorem for acyclic DeFGs.

Theorem 2.14. *Given an acyclic DeFG $(\mathcal{G} = (\mathcal{V}, \mathcal{F}, \mathcal{E} \in \mathcal{V} \times \mathcal{F}), \{\mathcal{S}_j\}_{j \in \mathcal{V}}, \{f_a\}_{a \in \mathcal{F}})$, there exists a unique set of messages $\{m_{j \rightarrow a}, m_{a \rightarrow j} : \mathcal{S}_j^2 \rightarrow \mathbb{C}\}_{(j,a) \in \mathcal{E}}$ such that*

$$m_{j \rightarrow a}(s_j, \tilde{s}_j) = \prod_{c \in \partial j \setminus a} m_{c \rightarrow j}(s_j, \tilde{s}_j) \quad (2.19)$$

$$m_{a \rightarrow j}(s_j, \tilde{s}_j) = \sum_{s_{\partial a \setminus j}, \tilde{s}_{\partial a \setminus j}} f_a(s_{\partial a}, \tilde{s}_{\partial a}) \cdot \prod_{k \in \partial a \setminus j} m_{k \rightarrow a}(s_k, \tilde{s}_k). \quad (2.20)$$

Algorithm 2.1 Belief-Propagation Algorithm for Acyclic DeFGs

Input: An acyclic DeFG $(\mathcal{G} = (\mathcal{V}, \mathcal{F}, \mathcal{E} \in \mathcal{V} \times \mathcal{F}), \mathfrak{V} = \{\mathcal{S}_j\}_{j \in \mathcal{V}}, \mathfrak{F} = \{f_a\}_{a \in \mathcal{F}})$ with all leaf vertices belonging to \mathcal{F} , a root vertex $r \in \mathcal{F}$

Output: The partition sum $Z(\mathcal{G}) \triangleq \sum_{\mathbf{s}, \tilde{\mathbf{s}}} g(\mathbf{s}, \tilde{\mathbf{s}})$

```

1: Define the bipartite graph  $G' = (\mathcal{V}', \mathcal{F}', \mathcal{E}') \leftarrow \mathcal{G}$ ;
2: while  $\mathcal{F}' \neq \{r\}$  do
3:   for all  $a \in \mathcal{F}'$  being a leaf and  $j$  being its parent in  $\mathcal{G}'$  do
4:      $m_{a \rightarrow j}(s_j, \tilde{s}_j) \leftarrow \sum_{\mathbf{s}_{\partial a \setminus j}, \tilde{\mathbf{s}}_{\partial a \setminus j}} f_a(\mathbf{s}_{\partial a}, \tilde{\mathbf{s}}_{\partial a}) \cdot \prod_{k \in \partial a \setminus j} m_{k \rightarrow a}(s_k, \tilde{s}_k)$ ;
5:      $\mathcal{F}' \leftarrow \mathcal{F}' \setminus a$ ,  $\mathcal{E}' \leftarrow \mathcal{E}' \setminus (\partial a \times a)$ ; ▷ Remove  $a$  from  $\mathcal{G}'$ .
6:   end for
7:   for all  $j \in \mathcal{V}'$  being a leaf and  $a$  being its parent in  $\mathcal{G}'$  do
8:      $m_{j \rightarrow a}(s_j, \tilde{s}_j) \leftarrow \prod_{c \in \partial j \setminus a} m_{c \rightarrow j}(s_j, \tilde{s}_j)$ ;
9:      $\mathcal{V}' \leftarrow \mathcal{V}' \setminus j$ ,  $\mathcal{E}' \leftarrow \mathcal{E}' \setminus (j \times \partial j)$ ; ▷ Remove  $j$  from  $\mathcal{G}'$ .
10:  end for
11: end while
12:  $Z(\mathcal{G}) \leftarrow \sum_{\mathbf{s}_{\partial r}, \tilde{\mathbf{s}}_{\partial r}} f_r(\mathbf{s}_{\partial r}, \tilde{\mathbf{s}}_{\partial r}) \cdot \prod_{j \in \partial r} m_{j \rightarrow r}(s_j, \tilde{s}_j)$ ;

```

Moreover, in this case,

$$\sum_{\mathbf{s}_{\mathcal{V} \setminus j}, \tilde{\mathbf{s}}_{\mathcal{V} \setminus j}} \prod_{a \in \mathcal{F}} f_a(\mathbf{s}_{\partial a}, \tilde{\mathbf{s}}_{\partial a}) = \prod_{c \in \partial j} m_{c \rightarrow j}(s_j, \tilde{s}_j) \quad \forall j \in \mathcal{V}, \quad (2.21)$$

$$\sum_{\mathbf{s}_{\mathcal{V} \setminus \partial a}, \tilde{\mathbf{s}}_{\mathcal{V} \setminus \partial a}} \prod_{\hat{a} \in \mathcal{F}} f_{\hat{a}}(\mathbf{s}_{\partial \hat{a}}, \tilde{\mathbf{s}}_{\partial \hat{a}}) = f_a(\mathbf{s}_{\partial a}, \tilde{\mathbf{s}}_{\partial a}) \cdot \prod_{j \in \partial a} m_{j \rightarrow a}(s_j, \tilde{s}_j) \quad \forall a \in \mathcal{F}. \quad (2.22)$$

Proof. By treating (s_j, \tilde{s}_j) as a single variable for each j , the theorem is essentially the same as Theorem 1.8. We omit the details. \square

Remark 2.15. By Theorem 2.7, the matrices corresponding to the messages defined in (2.19) and (2.20) are PSD.

2.3.2 Belief-Propagation Algorithms for DeFG and BP Fixed Points

Similar to BP algorithms for factor graphs, we define BP algorithms as a heuristic generalization based on the messaging-passing rules (2.19) and (2.20). Namely, we

consider an iterative method with the updating rules

$$m_{j \rightarrow a}^{(t)}(s_j, \tilde{s}_j) \propto \prod_{c \in \partial j \setminus a} m_{c \rightarrow j}^{(t)}(s_j, \tilde{s}_j), \quad (2.23)$$

$$m_{a \rightarrow j}^{(t)}(s_j, \tilde{s}_j) \propto \sum_{\mathbf{s}_{\partial a \setminus j}, \tilde{\mathbf{s}}_{\partial a \setminus j}} f_a(\mathbf{s}_{\partial a}, \tilde{\mathbf{s}}_{\partial a}) \cdot \prod_{k \in \partial a \setminus j} m_{k \rightarrow a}^{(t-1)}(s_k, \tilde{s}_k), \quad (2.24)$$

where the initial messages $\{m_{j \rightarrow a}^{(0)}\}_{(j,a) \in \mathcal{E}}$ are some constant functions. Same as the BP algorithms for factor graphs, the updating sequence of the messages in (2.23) and (2.24) (a.k.a. schedule) can be cleverly designed to suit different scenarios. In this thesis, we choose to focus on the synchronous schedule (a.k.a. flooding schedule). Algorithm 2.2 lists BP algorithm for DeFGs with the flooding schedule.

BP fixed points of a DeFG, defined similarly below as those of a factor graph, are of great importance for investigating the properties of the BA algorithms for DeFGs.

Definition 2.16 (BP Fixed Points of a DeFG). Applying Algorithm 2.2 to a DeFG, a resulting set of messages $\{m_{j \rightarrow a}, m_{a \rightarrow j} : \mathcal{S}_j^2 \rightarrow \mathbb{C}\}_{(j,a) \in \mathcal{E}}$ is said to be a BP fixed point if

$$m_{j \rightarrow a}(s_j, \tilde{s}_j) \propto \prod_{c \in \partial j \setminus a} m_{c \rightarrow j}(s_j, \tilde{s}_j), \quad (2.25)$$

$$m_{a \rightarrow j}(s_j, \tilde{s}_j) \propto \sum_{\mathbf{s}_{\partial a \setminus j}, \tilde{\mathbf{s}}_{\partial a \setminus j}} f_a(\mathbf{s}_{\partial a}, \tilde{\mathbf{s}}_{\partial a}) \cdot \prod_{k \in \partial a \setminus j} m_{k \rightarrow a}(s_k, \tilde{s}_k). \quad (2.26)$$

In this case, the set $\{m_{j \rightarrow a}, m_{a \rightarrow j}\}_{(j,a) \in \mathcal{E}}$ is also called a set of fixed-point messages. \square

Definition 2.17. Given a set of normalized PSD messages $\{m_{j \rightarrow a}, m_{a \rightarrow j}\}_{(j,a) \in \mathcal{E}}$, not necessarily a BP fixed point, the *induced* partition sum (w.r.t. the messages) is defined as

$$Z_{\text{induced}}(\{m_{j \rightarrow a}, m_{a \rightarrow j}\}_{(j,a) \in \mathcal{E}}) = \frac{\prod_{a \in \mathcal{F}} Z_a(\{m_{j \rightarrow a}\}_{j \in \partial a}) \cdot \prod_{j \in \mathcal{V}} Z_j(\{m_{a \rightarrow j}\}_{a \in \partial j})}{\prod_{(j,a) \in \mathcal{E}} Z_{j,a}(m_{j \rightarrow a}, m_{a \rightarrow j})}, \quad (2.27)$$

where

$$\begin{aligned} Z_a(\{m_{j \rightarrow a}\}_{j \in \partial a}) &\triangleq \sum_{\mathbf{s}_{\partial a}, \tilde{\mathbf{s}}_{\partial a}} f_a(\mathbf{s}_{\partial a}, \tilde{\mathbf{s}}_{\partial a}) \cdot \prod_{j \in \partial a} m_{j \rightarrow a}(s_j, \tilde{s}_j) & \forall a \in \mathcal{F}, \\ Z_j(\{m_{a \rightarrow j}\}_{a \in \partial j}) &\triangleq \sum_{s_j, \tilde{s}_j} \prod_{a \in \partial j} m_{a \rightarrow j}(s_j, \tilde{s}_j) & \forall j \in \mathcal{V}, \\ Z_{j,a}(m_{j \rightarrow a}, m_{a \rightarrow j}) &\triangleq \sum_{s_j, \tilde{s}_j} m_{j \rightarrow a}(s_j, \tilde{s}_j) \cdot m_{a \rightarrow j}(s_j, \tilde{s}_j) & \forall (j, a) \in \mathcal{E}. \quad \square \end{aligned}$$

Algorithm 2.2 Belief-Propagation Algorithm for DeFGs (Flooding Schedule with Timeout)

Input: A DeFG $(\mathcal{G} = (\mathcal{V}, \mathcal{F}, \mathcal{E} \in \mathcal{V} \times \mathcal{F}), \mathfrak{V} = \{\mathcal{S}_j\}_{j \in \mathcal{V}}, \mathfrak{F} = \{f_a\}_{a \in \mathcal{F}}, \epsilon > 0$

Output: Messages $\{m_{j \rightarrow a}, m_{a \rightarrow j} : \mathcal{S}_j^2 \rightarrow \mathbb{C}\}_{(j,a) \in \mathcal{E}}, \text{FLAG} \in \{\text{completed}, \text{timeout}\}$.

```

1: for all  $(j, a) \in \mathcal{E}$  do
2:    $m_{j \rightarrow a}(s_j, \tilde{s}_j) \leftarrow 1/|\mathcal{S}|^2$  for each  $(s_j, \tilde{s}_j) \in \mathcal{S}_j^2$ ;
3: end for
4:  $t \leftarrow 0$ ;
5: do
6:    $t \leftarrow t + 1$ ;
7:   for all  $(j, a) \in \mathcal{E}$  do
8:      $m_{a \rightarrow j}^{(t)}(s_j, \tilde{s}_j) \propto \sum_{\mathbf{s}_{\partial a \setminus j}, \tilde{\mathbf{s}}_{\partial a \setminus j}} f_a(\mathbf{s}_{\partial a}, \tilde{\mathbf{s}}_{\partial a}) \cdot \prod_{k \in \partial a \setminus j} m_{k \rightarrow a}^{(t-1)}(s_k, \tilde{s}_k)$  for each
        $(s_j, \tilde{s}_j) \in \mathcal{S}_j^2$ ;
9:   end for
10:  for all  $(j, a) \in \mathcal{E}$  do
11:     $m_{j \rightarrow a}^{(t)}(s_j, \tilde{s}_j) \propto \prod_{c \in \partial j \setminus a} m_{c \rightarrow j}^{(t)}(s_j, \tilde{s}_j)$  for each  $(s_j, \tilde{s}_j) \in \mathcal{S}_j^2$ ;
12:  end for
13: while  $(\neg \text{timeout}) \wedge (\exists (j, a) \in \mathcal{E} \text{ s.t. } \|m_{j \rightarrow a}^{(t)} - m_{j \rightarrow a}^{(t-1)}\|_2 > \epsilon \text{ or } \|m_{a \rightarrow j}^{(t)} - m_{a \rightarrow j}^{(t-1)}\|_2 > \epsilon)$ 
    ▷ timeout = false unless the operating time exceeds a pre-selected waiting time.
14: if timeout then
15:   FLAG  $\leftarrow$  timeout;
16: else
17:   FLAG  $\leftarrow$  completed;
18:   for all  $(j, a) \in \mathcal{E}$  do
19:      $m_{j \rightarrow a} \leftarrow m_{j \rightarrow a}^{(t)}$ ;
20:      $m_{a \rightarrow j} \leftarrow m_{a \rightarrow j}^{(t)}$ ;
21:   end for
22: end if

```

Proposition 2.18. *The function Z_{induced} is real non-negative, and its stationary points correspond to BP fixed points.*

Proof. It suffice to show that the set of equations

$$\begin{aligned} \frac{d}{dh} \Big|_{h=0} Z_{\text{induced}}(m_{c \rightarrow k} + h \cdot \eta_{c \rightarrow k}) &= 0 \quad \forall \eta_{c \rightarrow k}(s_k, \tilde{s}_k) \text{ PSD} \\ \frac{d}{dh} \Big|_{h=0} Z_{\text{induced}}(m_{k \rightarrow c} + h \cdot \eta_{k \rightarrow c}) &= 0 \quad \forall \eta_{k \rightarrow c}(s_k, \tilde{s}_k) \text{ PSD} \end{aligned} \quad \forall (k, c) \in \mathcal{E} \quad (2.28)$$

is equivalent to the updating rules (2.25) and (2.26).

First, suppose $\{m_{j \rightarrow a}, m_{a \rightarrow j}\}_{(j,a) \in \mathcal{E}}$ is a stationary point of Z_{induced} , *i.e.*, (2.28) holds. By definition of Z_{induced} , one can rewrite the upper set of (2.28) as

$$\frac{d}{dh} \Big|_{h=0} Z_{k,c}(m_{c \rightarrow k} + h \cdot \eta_{c \rightarrow k}) / Z_{k,c} = \frac{d}{dh} \Big|_{h=0} Z_k(m_{c \rightarrow k} + h \cdot \eta_{c \rightarrow k}) / Z_k.$$

Substituting the definitions of Z_k and $Z_{k,c}$, the above is equivalent to

$$\sum_{s_k, \tilde{s}_k} m_{k \rightarrow c}(s_k, \tilde{s}_k) \cdot \eta_{c \rightarrow k}(s_k, \tilde{s}_k) = \frac{Z_{k,c}}{Z_k} \cdot \sum_{s_k, \tilde{s}_k} \tilde{m}_{k \rightarrow c}(s_k, \tilde{s}_k) \cdot \eta_{c \rightarrow k}(s_k, \tilde{s}_k), \quad (2.29)$$

where $\tilde{m}_{k \rightarrow c}(s_k, \tilde{s}_k) \triangleq \prod_{a \in \partial k \setminus c} m_{a \rightarrow k}(s_k, \tilde{s}_k)$. Since this holds for all PSD functions $\eta_{c \rightarrow k}$, linear algebra must hold that $m_{k \rightarrow c} \propto \tilde{m}_{k \rightarrow c}$, which recovers (2.25). Similarly, the lower set of equations of (2.28) can be rewritten as

$$\frac{d}{dh} \Big|_{h=0} Z_{k,c}(m_{k \rightarrow c} + h \cdot \eta_{k \rightarrow c}) / Z_{k,c} = \frac{d}{dh} \Big|_{h=0} Z_c(m_{k \rightarrow c} + h \cdot \eta_{k \rightarrow c}) / Z_c,$$

which is, in turn, equivalent to

$$\sum_{s_k, \tilde{s}_k} m_{c \rightarrow k}(s_k, \tilde{s}_k) \cdot \eta_{k \rightarrow c}(s_k, \tilde{s}_k) = \frac{Z_{k,c}}{Z_c} \cdot \sum_{s_k, \tilde{s}_k} \tilde{m}_{c \rightarrow k}(s_k, \tilde{s}_k) \cdot \eta_{k \rightarrow c}(s_k, \tilde{s}_k), \quad (2.30)$$

where $\tilde{m}_{c \rightarrow k}(s_k, \tilde{s}_k) \triangleq \sum_{\mathbf{s}_{\partial c \setminus k}, \tilde{\mathbf{s}}_{\partial c \setminus k}} f_c(\mathbf{s}_{\partial c}, \tilde{\mathbf{s}}_{\partial c}) \cdot \prod_{j \in \partial c \setminus k} m_{j \rightarrow c}(s_j, \tilde{s}_j)$. Again, since this also holds for all PSD functions $\eta_{k \rightarrow c}$, we have $m_{c \rightarrow k} \propto \tilde{m}_{c \rightarrow k}$, which recovers (2.26).

Second, suppose $\{m_{j \rightarrow a}, m_{a \rightarrow j}\}_{(j,a) \in \mathcal{E}}$ is a BP fixed point, *i.e.*, (2.25) and (2.26) hold. To show (2.28), it suffices to verify (2.29) and (2.30). The latter can be shown rather straightforwardly as soon as one notices that

$$\begin{aligned} \frac{Z_{k,c}}{Z_k} &= \frac{\sum_{s_k, \tilde{s}_k} m_{k \rightarrow c}(s_k, \tilde{s}_k) \cdot m_{c \rightarrow k}(s_k, \tilde{s}_k)}{\sum_{s_k, \tilde{s}_k} \left(\prod_{a \in \partial k \setminus c} m_{a \rightarrow k}(s_k, \tilde{s}_k) \right) \cdot m_{c \rightarrow k}(s_k, \tilde{s}_k)} = \frac{m_{k \rightarrow c}(s_k, \tilde{s}_k)}{\prod_{a \in \partial k \setminus c} m_{a \rightarrow k}(s_k, \tilde{s}_k)} \\ \frac{Z_{k,c}}{Z_c} &= \frac{\sum_{s_k, \tilde{s}_k} m_{c \rightarrow k}(s_k, \tilde{s}_k) \cdot m_{k \rightarrow c}(s_k, \tilde{s}_k)}{\sum_{s_k, \tilde{s}_k} \left(\sum_{\mathbf{s}_{\partial c \setminus k}, \tilde{\mathbf{s}}_{\partial c \setminus k}} f_c(\mathbf{s}_{\partial c}, \tilde{\mathbf{s}}_{\partial c}) \cdot \prod_{j \in \partial c \setminus k} m_{j \rightarrow c}(s_j, \tilde{s}_j) \right) \cdot m_{k \rightarrow c}(s_k, \tilde{s}_k)} \\ &= \frac{m_{c \rightarrow k}(s_k, \tilde{s}_k)}{\sum_{\mathbf{s}_{\partial c \setminus k}, \tilde{\mathbf{s}}_{\partial c \setminus k}} f_c(\mathbf{s}_{\partial c}, \tilde{\mathbf{s}}_{\partial c}) \cdot \prod_{j \in \partial c \setminus k} m_{j \rightarrow c}(s_j, \tilde{s}_j)} \end{aligned}$$

for all s_k, \tilde{s}_k since $m_{k \rightarrow c}$ is proportional to $\prod_{a \in \partial k \setminus c} m_{a \rightarrow k}$, and $m_{c \rightarrow k}$ is proportional to $\sum_{\mathbf{s}_{\partial c \setminus k}, \tilde{\mathbf{s}}_{\partial c \setminus k}} f_c \cdot \prod_{j \in \partial c \setminus k} m_{j \rightarrow c}$. \square

One *must* note that Z_{induced} is conceptually different from Z_B for factor graphs. In particular, Z_{induced} is a function of messages, instead of some local beliefs or marginals. More importantly, in the classical case, $Z_{\text{induced}} = Z_B$ for messages corresponding to the belief minimizing F_B . However, although F_B can be generalized to DeFGs by analytical continuation, it is not clear how to define a similar version of Z_B based on the minimum of F_B while maintaining the connections to BP algorithms. Thus, it is currently unclear how Z_{induced} is related to the partition sum Z (for general DeFGs). Nevertheless, for acyclic DeFGs, we still have the following corollary.

Corollary 2.19. *For an acyclic DeFG \mathcal{G} , its BP fixed point is unique. Also, in this case, Z_{induced} has only one stationary point, and at that point, $Z_{\text{induced}} = Z(\mathcal{G})$.*

Proof. This is a direct result of Theorem 2.14 and Proposition 2.18. \square

2.3.3 Holographic Transformations and Loop Calculus for DeFGs

In this section, we consider the generalization of the holographic transformation and the loop calculus expansion from factor graphs [Mor15b; CC07] to DeFGs.

The generalization of the holographic transformation for DeFG is rather straightforward. The following theorem is a direct generalization of Theorem 1.21.

Theorem 2.20 (Holant Theorem for DeFGs). *Let $\mathcal{G} = (\mathcal{V}, \mathcal{F}, \mathcal{E})$ be a DeFG representing the factorization $g(\mathbf{s}, \tilde{\mathbf{s}}) = \prod_{a \in \mathcal{F}} f_a(\mathbf{s}_{\partial a}, \tilde{\mathbf{s}}_{\partial a})$. Given the Hermitian functions⁴ $\{\hat{\phi}_{j,a} : \mathcal{T}_{j,a}^2 \times \mathcal{S}_j^2 \rightarrow \mathbb{C}\}_{(j,a) \in \mathcal{E}}$ and $\{\phi_{j,a} : \mathcal{S}_j^2 \times \mathcal{T}_{j,a}^2 \rightarrow \mathbb{C}\}_{(i,a) \in \mathcal{E}}$ such that (where the sets $\mathcal{T}_{j,a}$ and \mathcal{S}_j are finite)*

$$\sum_{\mathbf{t}, \tilde{\mathbf{t}}} \phi_{j,a}(\mathbf{s}, \tilde{\mathbf{s}}; \mathbf{t}, \tilde{\mathbf{t}}) \cdot \hat{\phi}_{j,a}(\mathbf{t}, \tilde{\mathbf{t}}; \mathbf{s}', \tilde{\mathbf{s}}') = \delta_{\mathbf{s}, \mathbf{s}'} \cdot \delta_{\tilde{\mathbf{s}}, \tilde{\mathbf{s}}'}, \quad (2.31)$$

the partition sum $Z(\mathcal{G})$ can be expressed as

$$Z(\mathcal{G}) \triangleq \sum_{\mathbf{s}, \tilde{\mathbf{s}}} \prod_{a \in \mathcal{F}} f_a(\mathbf{s}_{\partial a}, \tilde{\mathbf{s}}_{\partial a}) = \sum_{\mathbf{t}, \tilde{\mathbf{t}}} \prod_{a \in \mathcal{F}} \hat{f}_a(\mathbf{t}_{\partial a, a}, \tilde{\mathbf{t}}_{\partial a, a}) \prod_{j \in \mathcal{V}} \hat{h}_j(\mathbf{t}_{j, \partial j}, \tilde{\mathbf{t}}_{i, \partial j}), \quad (2.32)$$

⁴Here, a function $f : \times_k \mathcal{X}_k^2 \rightarrow \mathbb{C}$ is said to be Hermitian if $f(x_1, \dots, x_k; \tilde{x}_1, \dots, \tilde{x}_k) = \overline{f(\tilde{x}_1, \dots, \tilde{x}_k; x_1, \dots, x_k)}$ for all $x_1, \dots, x_k, \tilde{x}_1, \dots, \tilde{x}_k$.

where

$$\hat{f}_a(\mathbf{t}_{\partial a, a}, \tilde{\mathbf{t}}_{\partial a, a}) \triangleq \sum_{\mathbf{s}_{\partial a}, \tilde{\mathbf{s}}_{\partial a}} f_a(\mathbf{s}_{\partial a}, \tilde{\mathbf{s}}_{\partial a}) \cdot \prod_{j \in \partial a} \hat{\phi}_{j, a}(t_{j, a}, \tilde{t}_{j, a}; s_j, \tilde{s}_j), \quad (2.33)$$

$$\hat{h}_j(\mathbf{t}_{j, \partial j}, \tilde{\mathbf{t}}_{i, \partial j}) \triangleq \sum_{s_j, \tilde{s}_j} \prod_{a \in \partial j} \phi_{j, a}(s_j, \tilde{s}_j; t_{j, a}, \tilde{t}_{j, a}). \quad (2.34)$$

The idea behind the above theorem is the same as that of Theorem 1.21, and we omit the proof. Similar to the case of factor graphs, the holographic transform of \mathcal{G} (w.r.t. $\{\hat{\phi}_{j, a}, \phi_{j, a}\}_{(j, a)}$) is defined to be the DeFG $\hat{\mathcal{G}} = (\mathcal{E}, \mathcal{F} \cup \mathcal{V}, \{(e, e_1), (e, e_2) | e \in \mathcal{E}\})$ representing the factorization

$$\hat{g}(\mathbf{t}, \tilde{\mathbf{t}}) = \prod_{a \in \mathcal{F}} \hat{f}_a(\mathbf{t}_{\partial a, a}, \tilde{\mathbf{t}}_{\partial a, a}) \prod_{j \in \mathcal{V}} \hat{h}_j(\mathbf{t}_{j, \partial j}, \tilde{\mathbf{t}}_{i, \partial j}). \quad (2.35)$$

Following the idea of the method of loop calculus (recall Section 1.1.6), we consider a specific holographic transform such that

$$\hat{f}_a(\mathbf{t}_{\partial a, a}, \tilde{\mathbf{t}}_{\partial a, a}) = 0, \text{ if } \text{wt}(\mathbf{t}_{\partial a, a} \otimes \tilde{\mathbf{t}}_{\partial a, a}) = 1, \quad (2.36)$$

$$\hat{h}_j(\mathbf{t}_{j, \partial j}, \tilde{\mathbf{t}}_{i, \partial j}) = 0, \text{ if } \text{wt}(\mathbf{t}_{j, \partial j} \otimes \tilde{\mathbf{t}}_{i, \partial j}) = 1, \quad (2.37)$$

where we have assumed that each alphabet $\mathcal{T}_{j, a}$ contains an elements labeled as 0.⁵ In this case, the support of \hat{g} is limited to those $(t_{j, a}, \tilde{t}_{j, a})_{(j, a) \in \mathcal{E}}$ such that the edges (j, a) corresponding to $(t_{j, a}, \tilde{t}_{j, a}) \neq \mathbf{0}$ form a *generalized loop* (see (1.28)). Substituting (2.33) and (2.34) into (2.36) and (2.37), respectively, we can rewrite the latter as

$$\sum_{s_j, \tilde{s}_j} \left(\sum_{\mathbf{s}_{\partial a \setminus j}, \tilde{\mathbf{s}}_{\partial a \setminus j}} f_a(\mathbf{s}_{\partial a}, \tilde{\mathbf{s}}_{\partial a}) \cdot \prod_{k \in \partial a \setminus j} \hat{\phi}_{k, a}(0, 0; s_k, \tilde{s}_k) \right) \cdot \hat{\phi}_{j, a}(t_{j, a}, \tilde{t}_{j, a}; s_j, \tilde{s}_j) = 0 \quad (2.38)$$

$$\sum_{s_j, \tilde{s}_j} \left(\prod_{c \in \partial j \setminus a} \phi_{j, c}(s_j, \tilde{s}_j; 0, 0) \right) \cdot \phi_{j, a}(s_j, \tilde{s}_j; t_{j, a}, \tilde{t}_{j, a}) = 0 \quad (2.39)$$

for each $(j, a) \in \mathcal{E}$ and $(t_{j, a}, \tilde{t}_{j, a}) \neq \mathbf{0}$. Since all functions involved in (2.38) and (2.39) are Hermitian, the LHS of these equations are nothing more than the Frobenius inner product between matrices. In other words,

$$\left[\sum_{\mathbf{s}_{\partial a \setminus j}, \tilde{\mathbf{s}}_{\partial a \setminus j}} f_a(\mathbf{s}_{\partial a}, \tilde{\mathbf{s}}_{\partial a}) \cdot \prod_{k \in \partial a \setminus j} \hat{\phi}_{k, a}(0, 0; s_k, \tilde{s}_k) \right]_{s_j, \tilde{s}_j} \perp \left[\hat{\phi}_{j, a}(t_{j, a}, \tilde{t}_{j, a}; s_j, \tilde{s}_j) \right]_{s_j, \tilde{s}_j} \quad (2.40)$$

$$\left[\prod_{c \in \partial j \setminus a} \phi_{j, c}(s_j, \tilde{s}_j; 0, 0) \right]_{s_j, \tilde{s}_j} \perp \left[\phi_{j, a}(s_j, \tilde{s}_j; t_{j, a}, \tilde{t}_{j, a}) \right]_{s_j, \tilde{s}_j} \quad (2.41)$$

⁵Note that $\text{wt}(\mathbf{x}_1^n \otimes \tilde{\mathbf{x}}_1^n) \triangleq \sum_{i=1}^n 1_{(x_i, \tilde{x}_i) \neq (0, 0)}$, where $1_{\text{true}} = 1$ and $1_{\text{false}} = 0$.

for each $(j, a) \in \mathcal{E}$ and $(t_{j,a}, \tilde{t}_{j,a}) \neq \mathbf{0}$. Considering (2.31), we have

$$\phi_{j,a}(\cdot, \cdot; 0, 0) \propto \left[\sum_{\mathbf{s}_{\partial a \setminus j}, \tilde{\mathbf{s}}_{\partial a \setminus j}} f_a(\mathbf{s}_{\partial a}, \tilde{\mathbf{s}}_{\partial a}) \cdot \prod_{k \in \partial a \setminus j} \hat{\phi}_{k,a}(0, 0; s_k, \tilde{s}_k) \right]_{s_j, \tilde{s}_j}, \quad (2.42)$$

$$\hat{\phi}_{j,a}(0, 0; \cdot, \cdot) \propto \left[\prod_{c \in \partial j \setminus a} \phi_{j,c}(s_j, \tilde{s}_j; 0, 0) \right]_{s_j, \tilde{s}_j}. \quad (2.43)$$

Compare above with Definition 2.16. Eq (2.42) and (2.43) are equivalent to the existence of some fixed-point messages $\{m_{j \rightarrow a}, m_{a \rightarrow j}\}_{(j,a)}$ such that

$$\phi_{j,a}(s_j, \tilde{s}_j; 0, 0) = c_{j,a} \cdot m_{a \rightarrow j}(s_j, \tilde{s}_j) \quad (2.44)$$

$$\hat{\phi}_{j,a}(0, 0; s_j, \tilde{s}_j) = \hat{c}_{j,a} \cdot m_{j \rightarrow a}(s_j, \tilde{s}_j) \quad (2.45)$$

for some constants $c_{j,a}, \hat{c}_{j,a}$ such that $c_{j,a} \cdot \hat{c}_{j,a} = Z_{j,a}^{-1}(m_{j \rightarrow a}, m_{a \rightarrow j})$ for each $(j, a) \in \mathcal{E}$. Retracing the steps above, given any BP fixed point $\{m_{j \rightarrow a}, m_{a \rightarrow j}\}_{(j,a) \in \mathcal{E}}$ of the DeFG, one can construct a holographic transform satisfying (2.44) and (2.45); and thus satisfying (2.36) and (2.37). Additionally, in such a case, for each $a \in \mathcal{F}$ and $j \in \mathcal{V}$, we have

$$\hat{f}_a(\mathbf{0}, \mathbf{0}) = Z_a \prod_{j \in \partial a} \hat{c}_{j,a}, \quad \hat{h}_j(\mathbf{0}, \mathbf{0}) = Z_j \prod_{c \in \partial j} c_{j,c}, \quad (2.46)$$

and thus,

$$Z_{\text{induced}}(\{m_{j \rightarrow a}, m_{a \rightarrow j}\}_{(j,a) \in \mathcal{E}}) = \prod_{a \in \mathcal{F}} \hat{f}_a(\mathbf{0}, \mathbf{0}) \cdot \prod_{j \in \mathcal{V}} \hat{h}_j(\mathbf{0}, \mathbf{0}). \quad (2.47)$$

Theorem 2.21 (Loop Calculus Expansion for DeFGs). *Consider a DeFG representing the factorization $g(\mathbf{s}, \tilde{\mathbf{s}}) = \prod_{a \in \mathcal{F}} f_a(\mathbf{s}_{\partial a}, \tilde{\mathbf{s}}_{\partial a})$. Let $\{m_{j \rightarrow a}, m_{a \rightarrow j}\}_{(j,a)}$ be a set of fixed-point messages. Then, it holds that*

$$Z(\mathcal{G}) = Z_{\text{induced}}(\{m_{j \rightarrow a}, m_{a \rightarrow j}\}_{(j,a) \in \mathcal{E}}) \cdot \sum_{E \in \mathcal{L}(\mathcal{E})} \mathcal{K}(E), \quad (2.48)$$

where the set of generalized loops $\mathcal{L}(\mathcal{E})$ has been defined in (1.28) and where $\mathcal{K}(E)$ is some function of E such that $\mathcal{K}(\emptyset) = 1$.

Proof. Consider a holographic transform w.r.t. $\{\hat{\phi}_{j,a}, \phi_{j,a}\}_{(j,a)}$ as established throughout (2.36) to (2.45). Under such a setup,

$$Z(\mathcal{G}) = \sum_{(\mathbf{t}, \tilde{\mathbf{t}}) \in \text{Supp}(\hat{g})} \prod_{a \in \mathcal{F}} \hat{f}_a(\mathbf{t}_{\partial a, a}, \tilde{\mathbf{t}}_{\partial a, a}) \prod_{j \in \mathcal{V}} \hat{h}_j(\mathbf{t}_{j, \partial j}, \tilde{\mathbf{t}}_{i, \partial j}),$$

$$\begin{aligned}
&= Z_{\text{induced}} \cdot \sum_{(\mathbf{t}, \tilde{\mathbf{t}}) \in \text{Supp}(\hat{g})} \prod_{a \in \mathcal{F}} \frac{\hat{f}_a(\mathbf{t}_{\partial a, a}, \tilde{\mathbf{t}}_{\partial a, a})}{\hat{f}_a(\mathbf{0}, \mathbf{0})} \prod_{j \in \mathcal{V}} \frac{\hat{h}_j(\mathbf{t}_{j, \partial j}, \tilde{\mathbf{t}}_{j, \partial j})}{\hat{h}_j(\mathbf{0}, \mathbf{0})}, \\
&= Z_{\text{induced}} \cdot \sum_{(\mathbf{t}, \tilde{\mathbf{t}}) \in \text{Supp}(\hat{g})} \prod_{a \in \mathcal{F}} \left[\sum_{\mathbf{s}_{\partial a}, \tilde{\mathbf{s}}_{\partial a}} b_a(\mathbf{s}_{\partial a}, \tilde{\mathbf{s}}_{\partial a}) \cdot \prod_{j \in \partial a} \frac{\hat{\phi}_{j, a}(t_{j, a}, \tilde{t}_{j, a}; s_j, \tilde{s}_j)}{\hat{\phi}_{j, a}(0, 0; s_j, \tilde{s}_j)} \right] \\
&\quad \prod_{j \in \mathcal{V}} \left[\sum_{s_j, \tilde{s}_j} b_j(s_j, \tilde{s}_j) \cdot \prod_{a \in \partial j} \frac{\phi_{j, a}(s_j, \tilde{s}_j; t_{j, a}, \tilde{t}_{j, a})}{\phi_{j, a}(s_j, \tilde{s}_j; 0, 0)} \right], \\
&= Z_{\text{induced}} \cdot \sum_{E \in \mathcal{L}(\mathcal{E})} \sum_{(\mathbf{t}_E, \tilde{\mathbf{t}}_E) \neq \mathbf{0}} \prod_{a \in \mathcal{F}} \left[\sum_{\mathbf{s}_{\partial a}, \tilde{\mathbf{s}}_{\partial a}} b_a(\mathbf{s}_{\partial a}, \tilde{\mathbf{s}}_{\partial a}) \cdot \prod_{j \in \partial a: (j, a) \in E} \frac{\hat{\phi}_{j, a}(t_{j, a}, \tilde{t}_{j, a}; s_j, \tilde{s}_j)}{\hat{\phi}_{j, a}(0, 0; s_j, \tilde{s}_j)} \right] \\
&\quad \prod_{j \in \mathcal{V}} \left[\sum_{s_j, \tilde{s}_j} b_j(s_j, \tilde{s}_j) \cdot \prod_{a \in \partial j: (j, a) \in E} \frac{\phi_{j, a}(s_j, \tilde{s}_j; t_{j, a}, \tilde{t}_{j, a})}{\phi_{j, a}(s_j, \tilde{s}_j; 0, 0)} \right],
\end{aligned}$$

where

$$b_a(\mathbf{s}_{\partial a}, \tilde{\mathbf{s}}_{\partial a}) \triangleq \frac{1}{Z_a} \cdot f_a(\mathbf{s}_{\partial a}, \tilde{\mathbf{s}}_{\partial a}) \cdot \prod_{j \in \partial a} m_{j \rightarrow a}(s_j, \tilde{s}_j), \quad (2.49)$$

$$b_j(s_j, \tilde{s}_j) \triangleq \frac{1}{Z_j} \cdot \prod_{a \in \partial j} m_{a \rightarrow j}(s_j, \tilde{s}_j). \quad (2.50)$$

Finally, by letting

$$\begin{aligned}
\mathcal{K}(E) \triangleq & \sum_{(\mathbf{t}_E, \tilde{\mathbf{t}}_E) \neq \mathbf{0}} \prod_{a \in \mathcal{F}} \left[\sum_{\mathbf{s}_{\partial a}, \tilde{\mathbf{s}}_{\partial a}} b_a(\mathbf{s}_{\partial a}, \tilde{\mathbf{s}}_{\partial a}) \cdot \prod_{j \in \partial a: (j, a) \in E} \frac{\hat{\phi}_{j, a}(t_{j, a}, \tilde{t}_{j, a}; s_j, \tilde{s}_j)}{\hat{\phi}_{j, a}(0, 0; s_j, \tilde{s}_j)} \right] \\
& \prod_{j \in \mathcal{V}} \left[\sum_{s_j, \tilde{s}_j} b_j(s_j, \tilde{s}_j) \cdot \prod_{a \in \partial j: (j, a) \in E} \frac{\phi_{j, a}(s_j, \tilde{s}_j; t_{j, a}, \tilde{t}_{j, a})}{\phi_{j, a}(s_j, \tilde{s}_j; 0, 0)} \right],
\end{aligned} \quad (2.51)$$

Eq. (2.48) can be justified. \square

Unfortunately, even for the simplest case where $\mathcal{T}_{j, a}$ is binary for each $(j, a) \in \mathcal{E}$, (2.51) is pretty complicated. However, the theorem does *suggest* that Z_{induced} at a BP fixed point for DeFGs with a relatively smaller number of cycles tends to be closer to the partition sum.

2.4 Numerical Examples

In this section, we discuss various examples of DeFGs. In particular, we compare the induced partition sum Z_{induced} with the exact partition sum Z . (The DeFGs in this section have a modest size so that the exact partition sums are tractable.) Moreover, for the first example, we also make some analytical statements.

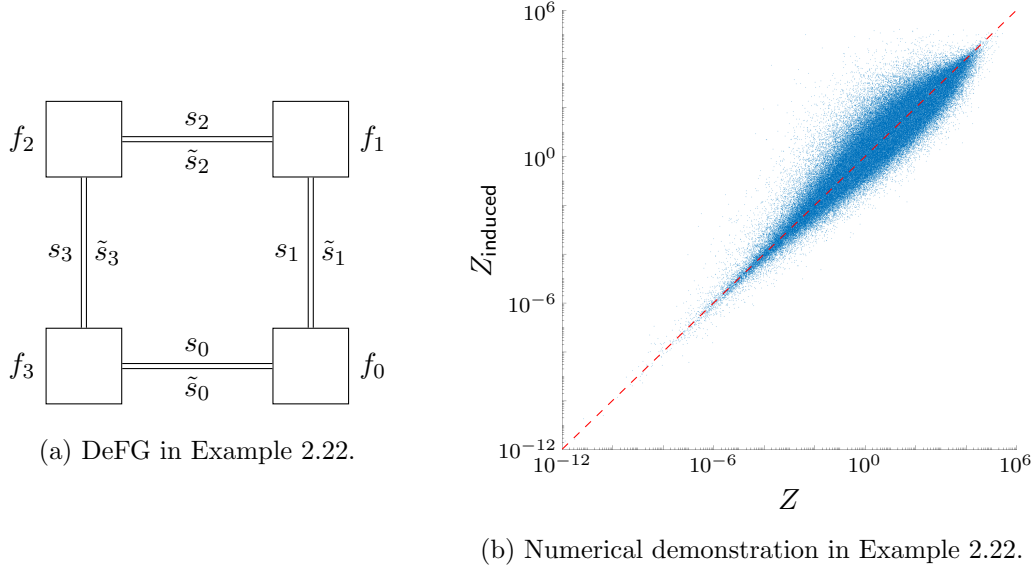


Figure 2.10: Plots for Example 2.22.

Example 2.22. Consider a normal DeFG whose topology is an n -cycle ($n > 1$) and where all variables take on values in the same finite alphabet \mathcal{S} . (Figure 2.10a shows such a DeFG for $n = 4$.) Let f be a complex-valued PD matrix of size $|\mathcal{S}|^2 \times |\mathcal{S}|^2$ with its $((s_0, s_1), (\tilde{s}_0, \tilde{s}_1))$ -th entries being $f(s_0, s_1; \tilde{s}_0, \tilde{s}_1)$. For $i \in \{0, 1, \dots, n-1\}$, we define the local function f_i to be $f_i(s_i, s_{i+1}; \tilde{s}_i, \tilde{s}_{i+1}) \triangleq f(s_i, s_{i+1}; \tilde{s}_i, \tilde{s}_{i+1})$. (All indices are modulo n .)

To proceed, it is convenient to define the complex-valued matrix F of size $|\mathcal{S}|^2 \times |\mathcal{S}|^2$ with its $((s_0, \tilde{s}_0), (s_1, \tilde{s}_1))$ -th entries being $f(s_0, s_1; \tilde{s}_0, \tilde{s}_1)$.

For $i \in \{0, 1, \dots, n-1\}$, let $m_{i \rightarrow i+1}^{(t)}(s_{i+1}, \tilde{s}_{i+1})$ and $m_{i \rightarrow i-1}^{(t)}(s_i, \tilde{s}_i)$ be the belief-propagation messages from f_i to f_{i+1} and f_{i-1} at time index t , respectively. Clearly,

$$m_{i \rightarrow i+1}^{(t)}(s_{i+1}, \tilde{s}_{i+1}) \propto \sum_{s_i, \tilde{s}_i} m_{i-1 \rightarrow i}^{(t-1)}(s_i, \tilde{s}_i) \cdot F_{(s_i, \tilde{s}_i), (s_{i+1}, \tilde{s}_{i+1})}, \quad (2.52)$$

$$m_{i \rightarrow i-1}^{(t)}(s_i, \tilde{s}_i) \propto \sum_{s_{i+1}, \tilde{s}_{i+1}} F_{(s_i, \tilde{s}_i), (s_{i+1}, \tilde{s}_{i+1})} \cdot m_{i+1 \rightarrow i}^{(t)}(s_{i+1}, \tilde{s}_{i+1}). \quad (2.53)$$

We assume $m_{i \rightarrow i+1}^{(0)}(s_{i+1}, \tilde{s}_{i+1}) \triangleq \delta_{s_{i+1}, \tilde{s}_{i+1}}$ and $m_{i \rightarrow i-1}^{(0)}(s_i, \tilde{s}_i) \triangleq \delta_{s_i, \tilde{s}_i}$ for each $i \in \{0, 1, \dots, n-1\}$.

Due to the properties of F (which are induced from that of f), the mappings specified in (2.52) and (2.53) are completely positive. Using generalizations of Perron–Frobenius theory (see [EH78; Sch00]), one can make the following statements:

- For each i , the messages $m_{i \rightarrow i+1}^{(t)}$ converge to a PD matrix as $t \rightarrow \infty$.

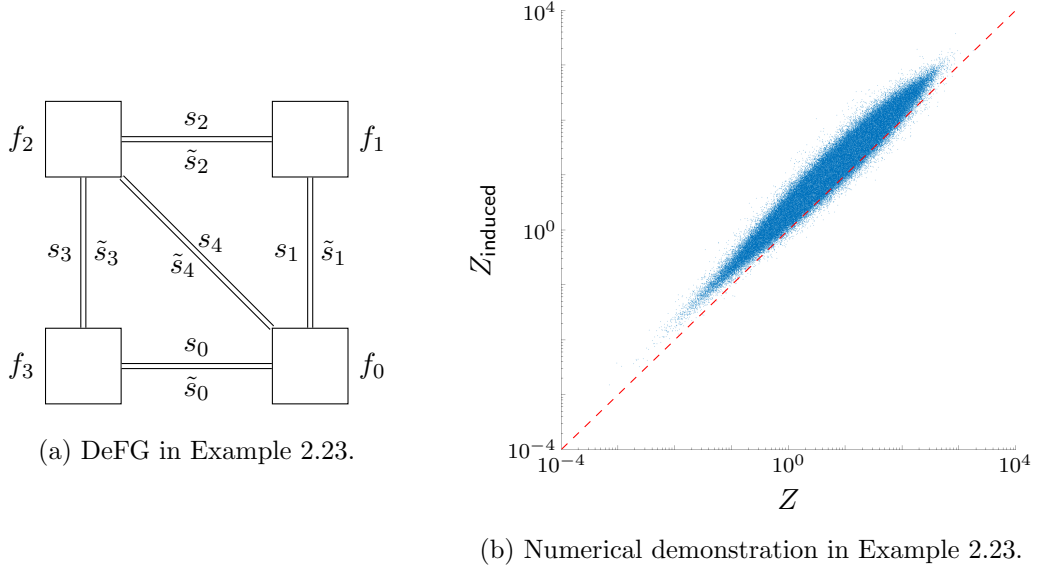


Figure 2.11: Plots for Example 2.23.

- For each i , the messages $m_{i \rightarrow i-1}^{(t)}$ converge to a PD matrix as $t \rightarrow \infty$.
- The eigenvalue of F with the largest absolute value is real and is unique. Denote it by λ_0 .
- When the messages converge, the induced partition sum $Z_{\text{induced}} = \lambda_0^n$.

Compare this result with the exact partition sum, which is

$$Z = \sum_{k=1}^{|\mathcal{S}|^2-1} \lambda_k^n = \lambda_0^n \cdot \left(1 + \sum_{k=1}^{|\mathcal{S}|^2-1} \left(\frac{\lambda_k}{\lambda_0} \right)^n \right), \quad (2.54)$$

where $\lambda_0, \dots, \lambda_{|\mathcal{S}|^2-1}$ are the eigenvalues of F . We see that the smaller the ratios $(\lambda_k/\lambda_0)^n$ for each k are, the better the approximation is.

For $n = 4$ and $|\mathcal{S}| = 2$, Figure 2.10b plots a million instances of the values of Z and Z_{induced} w.r.t. the randomly generated matrices $F = U \cdot D \cdot U^\dagger$, where the unitary matrix U is randomly generated according to the Haar measure and where D is a diagonal matrix with each of its diagonal entries drawn from the square of the standard normal distribution in an i.i.d. fashion. We see that, very often, the ratio Z_{induced}/Z is rather close to 1. \square

Example 2.23. Consider the DeFG in Figure 2.11a. For $|\mathcal{S}| = 2$, Figure 2.11b plots a million instances of the values of Z and Z_{induced} w.r.t. randomly generated local

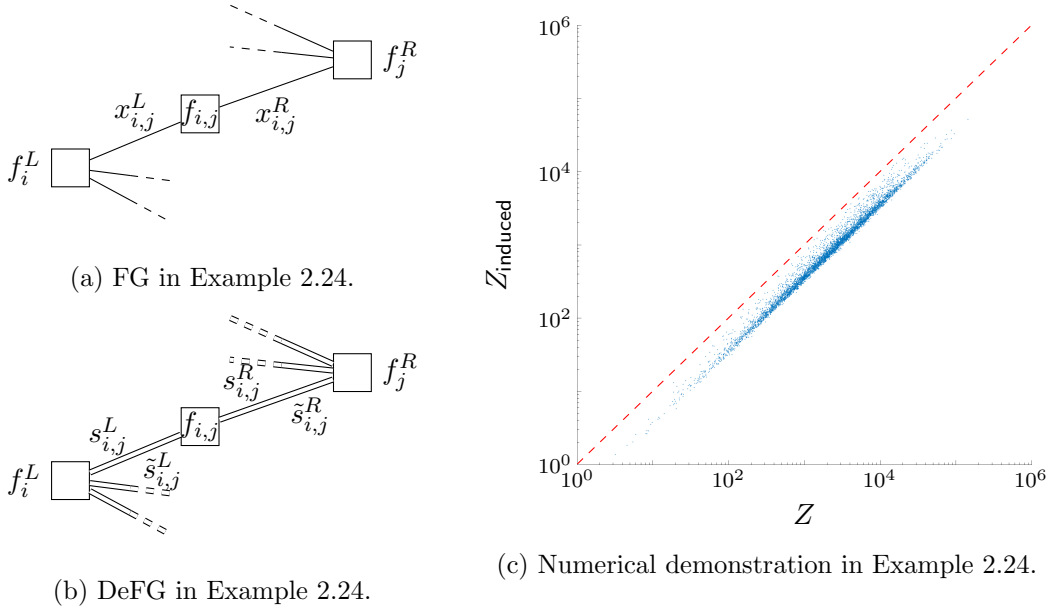


Figure 2.12: Plots for Example 2.24.

functions. In contrast to Example 2.22, where all local functions were the same for every instantiation, in this example, all local functions are generated independently. We observe that the ratio Z_{induced}/Z is reasonably close to 1 but typically larger than 1. \square

Example 2.24. Let θ be a complex-valued matrix of size $n \times n$ with its (i, j) -th entries being $\theta_{i,j}$. The permanent [Min84] of θ is defined to be $\text{perm}(\theta) \triangleq \sum_{\sigma} \prod_{i=1}^n \theta_{i,\sigma(i)}$, where the summation is over all $n!$ permutations of the set $\{1, \dots, n\}$. Ryser's algorithm, one of the most efficient algorithms for computing $\text{perm}(\theta)$ for general matrices θ exactly, requires $\Theta(n \cdot 2^n)$ arithmetic operations [Rys63], and so the exact computation of the permanent is intractable, even for moderate values of n . (Note that even the computation of the permanent of matrices containing only zeros and ones is #P-complete [Val79].)

One can formulate an NFG whose partition sum equals $\text{perm}(\theta)$ (see, *e.g.*, [Von13b, Figure 1]). That factor graph is a complete bipartite graph with n factor vertices on the left and n factor vertices on the right. Here, Figure 2.12a shows a slightly modified version of that NFG. All variables take values in the set $\mathcal{X} = \{0, 1\}$. Moreover, for each i , the function f_i^L is defined to be

$$f_i^L(\{x_{i,j}^L\}_{j=1}^n) \triangleq \begin{cases} 1 & \text{exactly one of } \{x_{i,j}^L\}_{j=1}^n \text{ equals 1} \\ 0 & \text{otherwise} \end{cases} \quad (2.55)$$

for each j , the function f_j^R is defined analogously; and for each (i, j) , the function $f_{i,j}$ is defined to be

$$f_{i,j}(x_{i,j}^L, x_{i,j}^R) \triangleq \delta_{x_{i,j}^L, x_{i,j}^R} \cdot \begin{cases} \theta_{i,j} & \text{if } x_{i,j}^L = 1 \\ 1 & \text{if } x_{i,j}^L = 0 \end{cases}. \quad (2.56)$$

In this example, we consider the following rather natural generalization to the DeFG in Figure 2.12b. Assume that for each (i, j) , $\tilde{\theta}_{i,j}$ is a PSD matrix of size 2×2 with its (k, ℓ) -th entries being $\tilde{\theta}_{i,j}(k, \ell)$. With this, for each i , the function \tilde{f}_i^L is defined to be

$$\tilde{f}_i^L(\{s_{i,j}^L, \tilde{s}_{i,j}^L\}_{j=1}^n) \triangleq f_i^L(\{s_{i,j}^L\}_{j=1}^n) \cdot f_i^L(\{\tilde{s}_{i,j}^L\}_{j=1}^n) \quad (2.57)$$

for each j , the function \tilde{f}_j^R is defined analogously; and for each (i, j) , the function $\tilde{f}_{i,j}$ is defined to be

$$\tilde{f}_{i,j}(s_{i,j}^L, s_{i,j}^R; \tilde{s}_{i,j}^L, \tilde{s}_{i,j}^R) \triangleq \delta_{s_{i,j}^L, s_{i,j}^R} \cdot \delta_{\tilde{s}_{i,j}^L, \tilde{s}_{i,j}^R} \cdot \tilde{\theta}_{i,j}(s_{i,j}^L, \tilde{s}_{i,j}^L). \quad (2.58)$$

(One can easily verify that these local functions satisfy the requirement of a DeFG.)

Finally, let \tilde{Z} be the partition sum of this DeFG.

This DeFG definition has the following two important special cases:

- If $\tilde{\theta}_{i,j} = \begin{pmatrix} 1 & 0 \\ 0 & \theta_{i,j} \end{pmatrix}$ for each (i, j) , then $\tilde{Z} = \text{perm}(\theta)$.
- If $\tilde{\theta}_{i,j} = \begin{pmatrix} 1 & \\ \theta_{i,j} & |\theta_{i,j}|^2 \end{pmatrix} \cdot \begin{pmatrix} 1 & \overline{\theta_{i,j}} \\ 0 & 1 \end{pmatrix}$ for each (i, j) , then $\tilde{Z} = \text{perm}(\theta) \cdot \text{perm}(\bar{\theta}) = |\text{perm}(\theta)|^2$, where $\bar{\theta}$ denotes the matrix whose entries are the complex-conjugate values of the entries of θ . (Note that such partition sums are of interest in quantum information processing [AA13], where θ are certain types of square matrices over the complex numbers. We refer to [AA13] for details.)

In our simulations, we considered the following setup. Namely, for every $(i, j) \in \{1, \dots, n\}^2$, we independently generate $\tilde{\theta}_{i,j}$ as follows: $\tilde{\theta}_{i,j}(0, 0) \triangleq 1$; $\tilde{\theta}_{i,j}(1, 0)$ is picked uniformly from the unit circle in the complex plane; $\tilde{\theta}_{i,j}(0, 1) \triangleq \overline{\tilde{\theta}_{i,j}(1, 0)}$; $\tilde{\theta}_{i,j}(1, 1)$ is picked uniformly (and independently of the other entries) from the real line interval $[1.10, 11.10]$. Figure 2.12c plots 5000 instances of the values of Z_{induced} and Z for the case when n is 5. We observe that the ratio Z_{induced}/Z is concentrated around a value smaller than 1. \square

Chapter 3

Quantum Factor Graphs

In this chapter, we consider a generalization of factor graphs known as quantum factor graphs (QFGs) [LP08]. This graphical model is a direct generalization of the bifactor networks proposed in the same paper, in which they considered generalized “factorizations” of positive operators like

$$\rho \triangleq \bigstar_{a \in \mathcal{F}} \rho_a = \exp \left(\sum_{a \in \mathcal{F}} \log \rho_a \right), \quad (3.1)$$

where, for each $a \in \mathcal{F}$, ρ_a is some positive operators and where \star is some associative and commutative binary operator on PSD matrices (see (3.3) and (3.4)). In this case, the generalized partition sum is defined to be

$$Z(\mathcal{G}) \triangleq \text{tr}(\rho) = \text{tr} \left(\exp \left(\sum_{a \in \mathcal{F}} \log \rho_a \right) \right). \quad (3.2)$$

Notice that the (classical) factor graphs are a special case of QFGs where all the involved local operators $\{\rho_a\}_{a \in \mathcal{F}}$ are diagonal. In [LP08], Leifer and Poulin also proposed and studied a generalized belief-propagation algorithm for bifactor networks.

In our study, we are interested in the scenarios without commutativity constraints as those in [LP08]. In such cases, many vital expressions that hold precisely for factor graphs only hold approximately for QFGs, provided the local operators are chosen randomly according to some distributions. We give some analytical and numerical characterizations of these approximations. In particular, we study how the “closing-the-box” operations and Bethe’s approximation can be generalized to QFGs in an approximate manner.

3.1 The \star -Product and Quantum Factor Graphs (QFGs)

This section reviews the definition of the \star -product and quantum factor graphs. We discuss various properties of the \star -product, particularly the (lack of) distributivity of \star over (partial) trace operations.

3.1.1 Definition of the \star -product and QFGs

As already mentioned in (3.1), for QFGs, we consider the factorization of some positive operator into the \star -product [War05],¹ of some local operators. Given (strictly) PD operators $\rho, \sigma \in \mathfrak{L}_{++}(\mathcal{H})$, their \star -product is defined to be

$$\rho \star \sigma \triangleq \exp(\log \rho + \log \sigma), \quad (3.3)$$

where \exp and \log stand for matrix exponential and logarithm, respectively. For PSD operators, we consider the Lie product formula [Bha13] and rewrite (3.3) as

$$\rho \star \sigma = \lim_{n \rightarrow \infty} \left(\rho^{\frac{1}{n}} \sigma^{\frac{1}{n}} \right)^n. \quad (3.4)$$

Using a continuity argument, one can generalize the \star -product to PSD operators $\rho, \sigma \in \mathfrak{L}_+(\mathcal{H})$. (For the proof of the convergence of the RHS of (3.4) for PSD operators ρ and σ , see, *e.g.*, [Bha13] and [Sim79, Theorem 1.2].) The \star -product is associative and commutative, *i.e.*,

$$\rho_1 \star \rho_2 = \rho_2 \star \rho_1 \quad \forall \rho_1, \rho_2 \in \mathfrak{L}_+(\mathcal{H}), \quad (3.5)$$

$$(\rho_1 \star \rho_2) \star \rho_3 = \rho_1 \star (\rho_2 \star \rho_3) \quad \forall \rho_1, \rho_2, \rho_3 \in \mathfrak{L}_+(\mathcal{H}). \quad (3.6)$$

As a convention, given ρ and σ acting on different Hilbert spaces, we treat the expression $\rho \star \sigma$ as the \star -product of the *embedded* operators of ρ and σ on some smallest *common* Hilbert space. For example, given $\rho_{AB} \in \mathfrak{L}_+(\mathcal{H}_A \otimes \mathcal{H}_B)$ and $\rho_{BC} \in \mathfrak{L}_+(\mathcal{H}_B \otimes \mathcal{H}_C)$, the convention

$$\rho_{AB} \star \rho_{BC} \triangleq (\rho_{AB} \otimes I_C) \star (I_A \otimes \rho_{BC}) \quad (3.7)$$

holds, where I_C and I_A are the identity operators on \mathcal{H}_A and \mathcal{H}_C , respectively; and $\rho_{AB} \star \rho_{BC}$ is an operator acting on $\mathcal{H}_A \otimes \mathcal{H}_B \otimes \mathcal{H}_C$. This convention also applies to the expression $\star_{a \in \mathcal{F}} \rho_a$, where some equations similar to (3.7) are applied recursively. As a reminder, note that $\log(\rho \otimes I) \equiv \log \rho \otimes I$.

¹Note that in [War05] this operation is denoted by \odot . However, in this thesis, \odot denotes the Hadamard product.



Figure 3.1: QFG in Example 3.3.

Definition 3.1 (Quantum Factor Graph [LP08]). A quantum factor graph (QFG) is a bipartite graph $\mathcal{G} = (\mathcal{V}, \mathcal{F}, \mathcal{E} \in \mathcal{V} \times \mathcal{F})$ associated with a variable set \mathfrak{V} and a factor set \mathfrak{F} , where

- $\mathfrak{V} = \{\mathcal{H}_i\}_{i \in \mathcal{V}}$ is indexed by \mathcal{V} , and each element of \mathfrak{V} is a Hilbert space;
- $\mathfrak{F} = \{\rho_a\}_{a \in \mathcal{F}}$ is indexed by \mathcal{F} , and $\rho_a \in \mathfrak{L}_+(\otimes_{i \in \partial a} \mathcal{H}_i)$ for each $a \in \mathcal{F}$.

The operator $\rho \triangleq \star_{a \in \mathcal{F}} \rho_a$ is called the *global operator* of \mathcal{G} , and in this case, \mathcal{G} is also said to be representing the factorization $\rho = \star_{a \in \mathcal{F}} \rho_a$. Similar to factor graphs, a QFG is said to be *normal* if the degree of any vertex in \mathcal{V} is at most 2. \square

Note that the global operator ρ is always a PSD operator on $\otimes_{i \in \mathcal{V}} \mathcal{H}_i$ (i.e., $\rho \in \mathfrak{L}_+(\otimes_{i \in \mathcal{V}} \mathcal{H}_i)$). Moreover, if all the local operators are *strictly* positive, i.e., $\rho_a \in \mathfrak{L}_{++}(\mathcal{H}_a)$ for each a , so is ρ .

Remark 3.2. Similar to NFGs, in a normal QFG, we redraw the vertices in \mathcal{V} as edges (see RHS of Figure 3.1 and Figure 3.2).

Example 3.3. The LHS of Figure 3.1 depicts a QFG with a single variable vertex and three factor vertices. Here, all local factors ρ_A , σ_A , and τ_A act on the same Hilbert space \mathcal{H}_A , and the global operator is given by $\rho_{\mathcal{G}} \triangleq \rho_A \star \sigma_A \star \tau_A$. On the RHS of Figure 3.1, we have a normal QFG, which is equivalent to the QFG on the left. Here, the new-introduced variable vertices B and C are associated with the Hilbert spaces \mathcal{H}_B and \mathcal{H}_C , each being of the same dimension as that of \mathcal{H}_A . The local operators σ_B and τ_C are the same as σ_A and τ_A , except that they act on \mathcal{H}_B and \mathcal{H}_C , respectively. The new-introduced operator π acts on $\mathcal{H}_A \otimes \mathcal{H}_B \otimes \mathcal{H}_C$ and is defined as

$$\pi \triangleq \exp(\log \sigma_A \otimes I_{BC} + \log \tau_A \otimes I_{BC} - I_A \otimes \log \sigma_B \otimes I_C - I_{AB} \otimes \log \tau_C). \quad (3.8)$$

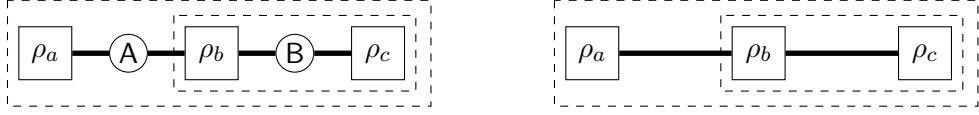


Figure 3.2: QFG in Example 3.5.

In this case, the global operator of the QFG on the RHS in Figure 3.1 can be expressed as

$$\begin{aligned}
 \tilde{\rho} &\triangleq \rho_A \star \sigma_B \star \tau_C \star \pi \\
 &= \exp(\log \rho_A \otimes I_{BC} + \log \sigma_A \otimes I_{BC} + \log \tau_A \otimes I_{BC}) \\
 &= \rho_{\mathcal{G}} \otimes I_{BC}.
 \end{aligned}$$

□

Remark 3.4. As illustrated in Example 3.3, any QFG can be converted into an equivalent normal QFG by introducing additional local operators. However, in contrast to factor graphs or DeFGs, the additional local operator introduced depends on the original local operators (see, *e.g.*, (3.8)). In the remaining part of this chapter, we will focus solely on normal QFGs.

3.1.2 Approximated Distributivity of the \star -Product over (Partial) Trace

For a factor graph or a DeFG, the “closing-the-box” operation is a handy visualization of the distributive law of addition over multiplication. However, for a QFG, the \star -product does not distribute over the partial trace operations in general, as illustrated in the example below.

Example 3.5. Consider the QFG in Figure 3.1 with the variable vertices $\mathcal{V} = \{A, B\}$, the factor vertices $\mathcal{F} = \{a, b, c\}$, and the local operators $\rho_a \in \mathfrak{L}_+(\mathcal{H}_A)$, $\rho_b \in \mathfrak{L}_+(\mathcal{H}_A \otimes \mathcal{H}_B)$, and $\rho_c \in \mathfrak{L}_+(\mathcal{H}_B)$. This QFG represents the factorization $\rho = \rho_a \star \rho_b \star \rho_c$, and the partition sum is $Z = \text{tr}(\rho_a \star \rho_b \star \rho_c)$. However, in general, we cannot compute Z in steps, *i.e.*,

$$\text{tr}(\rho_a \star \rho_b \star \rho_c) = \text{tr}_A(\text{tr}_B(\rho_a \star \rho_b \star \rho_c)) \neq \text{tr}_A(\rho_a \star \text{tr}_B(\rho_b \star \rho_c)). \quad (3.9)$$

In particular, let $\rho_a = \frac{1}{2} \begin{bmatrix} +1 & -1 \\ -1 & +1 \end{bmatrix}$, $\rho_b = \text{diag}([0, 1, 1, 0])$, and $\rho_c = \begin{bmatrix} 1 & 0 \\ 0 & 1 \end{bmatrix}$, then $\text{tr}_A(\text{tr}_B(\rho_a \star \rho_b \star \rho_c)) = 0$, but $\text{tr}_A(\rho_a \star \text{tr}_B(\rho_b \star \rho_c)) = 1$. (Here, we have used (3.4).) □

However, there do exist situations where $\text{tr}_A(\rho_a \star \text{tr}_B(\rho_b \star \rho_c))$ approximates $\text{tr}_A(\text{tr}_B(\rho_a \star \rho_b \star \rho_c))$ reasonably well. This subsection aims to understand when this happens so that an approximated notion of the “closing-the-box” operations can be salvaged.

Lemma 3.6. *Given $\rho_a \in \mathfrak{L}_{++}(\mathcal{H}_A)$, $\rho_b \in \mathfrak{L}_{++}(\mathcal{H}_A \otimes \mathcal{H}_B)$, and $\rho_c \in \mathfrak{L}_+(\mathcal{H}_B)$, we have*

$$S(\kappa(\rho_a))^{-1} \leq \frac{\text{tr}_A(\rho_a \star \text{tr}_B(\rho_b \star \rho_c))}{\text{tr}(\rho_a \star \rho_b \star \rho_c)} \leq S(\kappa(\rho_a)), \quad (3.10)$$

where $\kappa(\rho_a) \geq 1$ is the condition number of the operator ρ_a , and $S(\cdot)$ is the Specht ratio function defined as

$$S(r) \triangleq \frac{(r-1) \cdot r^{\frac{1}{r-1}}}{e \cdot \log r} \quad \forall r > 0. \quad (3.11)$$

Proof. Consider the Golden–Thompson inequality and its reverse [BS07b], i.e.,

$$\text{tr}(e^{V+W}) \leq \text{tr}(e^V \cdot e^W) \leq S(\alpha) \cdot \text{tr}(e^{V+W}), \quad (3.12)$$

where V and W are Hermitian operators, and α is the condition number of e^V . For arbitrary (strict) PD operators ρ and σ , since both $\log \rho$ and $\log \sigma$ are Hermitian, by substituting $V = \log \rho$ and $W = \log \sigma$ into (3.12), we have

$$\text{tr}(\rho \star \sigma) \leq \text{tr}(\rho \cdot \sigma) \leq S(\kappa(\rho)) \cdot \text{tr}(\rho \star \sigma) \quad \forall \rho, \sigma > 0. \quad (3.13)$$

To prove the first inequality in (3.10), we have

$$\begin{aligned} \text{tr}(\rho_a \star \rho_b \star \rho_c) &\stackrel{(a)}{\leq} \text{tr}(\rho_a \cdot (\rho_b \star \rho_c)) = \text{tr}_A(\rho_a \cdot \text{tr}_B(\rho_b \star \rho_c)) \\ &\stackrel{(b)}{\leq} S(\kappa(\rho_a)) \cdot \text{tr}_A(\rho_a \star \text{tr}_B(\rho_b \star \rho_c)) = S(\kappa(\rho_a)) \cdot \text{tr}(\rho_a \star \rho_b \star \rho_c), \end{aligned}$$

where we have applied the first and second inequalities in (3.13) to step (a) and step (b), respectively. Similarly, to show the second inequality in (3.10), we have

$$\begin{aligned} \text{tr}_A(\rho_a \star \text{tr}_B(\rho_b \star \rho_c)) &\stackrel{(a)}{\leq} \text{tr}_A(\rho_a \cdot \text{tr}_B(\rho_b \star \rho_c)) = \text{tr}(\rho_a \cdot (\rho_b \star \rho_c)) \\ &\stackrel{(b)}{\leq} S(\kappa(\rho_a)) \cdot \text{tr}(\rho_a \star (\rho_b \star \rho_c)) = S(\kappa(\rho_a)) \cdot \text{tr}(\rho_a \star \rho_b \star \rho_c), \end{aligned}$$

where, again, we have used (3.13) in step (a) and step (b). \square

Lemma 3.6 indicates that $\text{tr}_A(\rho_a \star \text{tr}_B(\rho_b \star \rho_c))$ is expected to approximate $\text{tr}(\rho_a \star \rho_b \star \rho_c)$ reasonably well when ρ_a or $\rho_b \star \rho_c$ is proportionally close to the identity matrix. This fact is further elaborated in the following theorem, where ρ_a and $\rho_b \star \rho_c$ are close

to the identity matrix in a linear fashion, *i.e.*, $\rho_a = I + tX$ and $\rho_b \star \rho_c = I + tY$ for some Hermitian matrices X and Y , and some real number t in a small neighborhood of zero. Another approach to study such approximations is to consider $\rho_a = e^{tX}$ and $\rho_b \star \rho_c = e^{tY}$, again, for some Hermitian matrices X and Y , and some real number t in a small neighborhood of zero. We present the second approach in Appendix A.

Theorem 3.7. *Consider finite-dimensional Hilbert spaces \mathcal{H}_A and \mathcal{H}_B . Given $X \in \mathfrak{L}_+(\mathcal{H}_A)$ and $Y \in \mathfrak{L}_+(\mathcal{H}_A \otimes \mathcal{H}_B)$, it holds that*

$$\mathrm{tr}((I + tX) \star (I + tY)) = \mathrm{tr}_A((I + tX) \star \mathrm{tr}_B(I + tY)) + O(t^4), \quad (3.14)$$

where the real number t is in a neighborhood of 0 such that $I + tX$ and $I + tY$ are always positive definite. In other words, $\mathrm{tr}_A((I + tX) \star \mathrm{tr}_B(I + tY))$ approximates $\mathrm{tr}((I + tX) \star (I + tY))$ when t is small, and the error is of fourth order in t .

Proof. The theorem is proven using the Taylor series expansion. Recall that, for a Hermitian matrix V and a positive definite matrix W with spectral radius less than 1, we have

$$\begin{aligned} \exp V &= I + V + \frac{1}{2}V^2 + \frac{1}{3!}V^3 + \cdots + \frac{1}{n!}V^n + \cdots, \\ \log(I + W) &= B - \frac{1}{2}W^2 + \frac{1}{3}W^3 - \cdots + \frac{(-1)^{n-1}}{n}W^n + \cdots. \end{aligned}$$

To simplify the proof, we introduce the *normalized* (partial) trace functions

$$\overline{\mathrm{tr}}(\rho) \triangleq \frac{\mathrm{tr}(\rho)}{\mathrm{tr}(I)}, \quad \overline{\mathrm{tr}}_A(\rho) \triangleq \frac{\mathrm{tr}_A(\rho)}{\mathrm{tr}_A(I)}.$$

Using the above notations, we rewrite (3.14) as

$$\overline{\mathrm{tr}}((I + tX) \star (I + tY)) = \overline{\mathrm{tr}}_A((I + tX) \star \overline{\mathrm{tr}}_B(I + tY)) + O(t^4).$$

Let $\tilde{X} \triangleq X \otimes I \in \mathfrak{L}_+(\mathcal{H}_A \otimes \mathcal{H}_B)$, and consider the Taylor series expansion of the terms (without $O(t^4)$) on both sides of the above equation:

$$\begin{aligned} \text{LHS} &= 1 + t \cdot \overline{\mathrm{tr}}(\tilde{X} + Y) + t^2 \cdot \frac{\overline{\mathrm{tr}}(\tilde{X}Y + Y\tilde{X})}{2} \\ &\quad + t^4 \cdot \frac{\overline{\mathrm{tr}}(\tilde{X}Y\tilde{X}Y - \tilde{X}^2Y^2)}{12} + O(t^5), \end{aligned} \quad (3.15)$$

$$\begin{aligned} \text{RHS} &= 1 + t \cdot \overline{\mathrm{tr}}_A(X + \overline{\mathrm{tr}}_B(Y)) + t^2 \cdot \frac{\overline{\mathrm{tr}}_A(X\overline{\mathrm{tr}}_B(Y) + \overline{\mathrm{tr}}_B(Y)X)}{2} \\ &\quad + t^4 \cdot \frac{\overline{\mathrm{tr}}_A(X\overline{\mathrm{tr}}_B(Y)X\overline{\mathrm{tr}}_B(Y) - X^2\overline{\mathrm{tr}}_B(Y)^2)}{12} + O(t^5). \end{aligned} \quad (3.16)$$

Note that $\overline{\text{tr}}_{\mathbf{B}}(\tilde{X} \cdot Z) = X \cdot \overline{\text{tr}}_{\mathbf{B}}(Z)$ for any operator $Z \in \mathfrak{L}_+(\mathcal{H}_{\mathbf{A}} \otimes \mathcal{H}_{\mathbf{B}})$. Thus, one can easily check that (3.15) and (3.16) agree up to t^3 . (Note that the coefficients of t^3 are both 0 for (3.15) and (3.16).) In particular, we have

$$\begin{aligned} \overline{\text{tr}}((I + tX) \star (I + tY)) &= \overline{\text{tr}}_{\mathbf{A}}((I + tX) \star \overline{\text{tr}}_{\mathbf{B}}(I + tY)) \\ &\quad + \frac{\overline{\text{tr}}_{\mathbf{A}}(X \cdot [\overline{\text{tr}}_{\mathbf{B}}(Y), X] \cdot \overline{\text{tr}}_{\mathbf{B}}(Y)) - \overline{\text{tr}}(\tilde{X} \cdot [\tilde{X}, Y] \cdot Y)}{12} \cdot t^4 + O(t^5), \end{aligned}$$

where $[V, W] \triangleq VW - WV$ for matrices V, W . \square

Using the same method, we have the following approximation as well.

Proposition 3.8. *Under the same setup as in Theorem 3.7, it holds that*

$$\text{tr}_{\mathbf{B}}((I + tX) \star (I + tY)) = (I + tX) \star \text{tr}_{\mathbf{B}}(I + tY) + O(t^3). \quad (3.17)$$

Proof. We use the same method as that in the proof of Theorem 3.7. In particular, we rewrite (3.17) as

$$\overline{\text{tr}}_{\mathbf{B}}((I + tX) \star (I + tY)) = (I + tX) \star \overline{\text{tr}}_{\mathbf{B}}(I + tY) + O(t^3)$$

and expand each side (without $O(t^3)$) of the above equation as

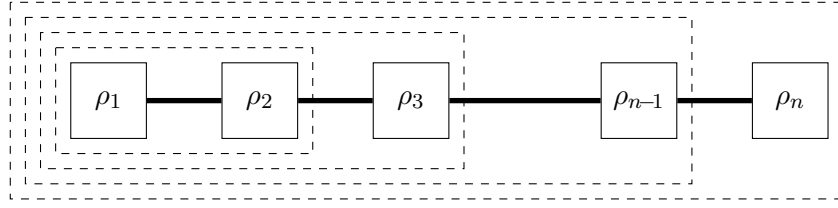
$$\begin{aligned} \text{LHS} &= I + t \cdot \overline{\text{tr}}_{\mathbf{B}}(\tilde{X} + Y) + t^2 \cdot \frac{\overline{\text{tr}}_{\mathbf{B}}(\tilde{X}Y + Y\tilde{X})}{2} \\ &\quad + t^3 \cdot \frac{\overline{\text{tr}}_{\mathbf{B}}(2\tilde{X}Y\tilde{X} + 2Y\tilde{X}Y - \tilde{X}^2Y - Y^2\tilde{X} - \tilde{X}Y^2 - Y\tilde{X}^2)}{12} + O(t^4), \end{aligned} \quad (3.18)$$

$$\begin{aligned} \text{RHS} &= I + t \cdot (X + \overline{\text{tr}}_{\mathbf{B}}(Y)) + t^2 \cdot \frac{X\overline{\text{tr}}_{\mathbf{B}}(Y) + \overline{\text{tr}}_{\mathbf{B}}(Y)X}{2} \\ &\quad + t^3 \cdot \left(\frac{2X\overline{\text{tr}}_{\mathbf{B}}(Y)X - X^2\overline{\text{tr}}_{\mathbf{B}}(Y) - X\overline{\text{tr}}_{\mathbf{B}}(Y)^2}{12} \right. \\ &\quad \left. + \frac{2\overline{\text{tr}}_{\mathbf{B}}(Y)X\overline{\text{tr}}_{\mathbf{B}}(Y) - \overline{\text{tr}}_{\mathbf{B}}(Y)^2X - \overline{\text{tr}}_{\mathbf{B}}(Y)X^2}{12} \right) + O(t^4). \end{aligned} \quad (3.19)$$

Comparing (3.18) with (3.19), we have

$$\begin{aligned} \overline{\text{tr}}_{\mathbf{B}}((I + tX) \star (I + tY)) &= (I + tX) \star \overline{\text{tr}}_{\mathbf{B}}(I + tY) + \\ &\quad t^3 \cdot \frac{2(\overline{\text{tr}}_{\mathbf{B}}(Y\tilde{X}Y) - \overline{\text{tr}}_{\mathbf{B}}(Y)X\overline{\text{tr}}_{\mathbf{B}}(Y)) + (\overline{\text{tr}}_{\mathbf{B}}(Y)^2 - \overline{\text{tr}}_{\mathbf{B}}(Y^2))X + X(\overline{\text{tr}}_{\mathbf{B}}(Y)^2 - \overline{\text{tr}}_{\mathbf{B}}(Y^2))}{12} \\ &\quad + O(t^4), \end{aligned}$$

which concludes the proof. \square

Figure 3.3: A chain QFG. ($n \geq 3$).

Remark 3.9. Theorem 3.7 and Proposition 3.8 also hold if the local operators are *proportionally* close to the identity matrix. Namely, it holds that

$$\mathrm{tr}(a(I + tX) \star b(I + tY)) = \mathrm{tr}_A(a(I + tX) \star \mathrm{tr}_B b(I + tY)) + O(t^4) \quad (3.20)$$

$$\mathrm{tr}_B(a(I + tX) \star b(I + tY)) = (a(I + tX) \star \mathrm{tr}_B b(I + tY)) + O(t^3) \quad (3.21)$$

for any real numbers a, b .

Corollary 3.10. *Let $n \geq 3$. Consider a chain QFG as in Figure 3.3, where $\rho_1 \in \mathfrak{L}_{++}(\mathcal{H}_1)$, $\rho_n \in \mathfrak{L}_{++}(\mathcal{H}_{n-1})$, and $\rho_k \in \mathfrak{L}_{++}(\mathcal{H}_{k-1} \otimes \mathcal{H}_k)$ for each $k = 2, \dots, n-1$. Suppose that for each k , $\rho_k \propto I + t \cdot H_k$ for some Hermitian operator H_k and some real number t close to 0, then Theorem 3.7 implies the estimate*

$$\mathrm{tr} \left(\bigstar_{k=1}^n \rho_k \right) = \mathrm{tr}_{n-1} (\mathrm{tr}_{n-2} (\cdots \mathrm{tr}_1 (\rho_1 \star \rho_2) \star \cdots \star \rho_{n-1}) \star \rho_n) + O(t^4). \quad (3.22)$$

Proof. We use mathematical induction to prove (3.22). For $n = 3$, (3.22) is the same as (3.14). Assume that (3.22) is true when $n = m$, for some arbitrary integer $m \geq 3$. Under this hypothesis, consider the case when $n = m + 1$, i.e.,

$$\begin{aligned} \mathrm{tr} \left(\bigstar_{k=1}^{m+1} \rho_k \right) &= \mathrm{tr} (\rho_1 \star \cdots \star \rho_{m-1} \star (\rho_m \star \rho_{m+1})) \\ &\stackrel{(a)}{=} \mathrm{tr}_{m,m-1} (\mathrm{tr}_{m-2} (\cdots \mathrm{tr}_1 (\rho_1 \star \rho_2) \cdots \star \rho_{m-1}) \star (\rho_m \star \rho_{m+1})) + O(t^4) \\ &\stackrel{(b)}{=} \mathrm{tr}_m (\mathrm{tr}_{m-1} (\mathrm{tr}_{m-2} (\cdots \mathrm{tr}_1 (\rho_1 \star \rho_2) \cdots \star \rho_{m-1}) \star \rho_m) \star \rho_{m+1}) + O(t^4), \end{aligned}$$

where we have used the induction hypothesis in step (a) and Theorem 3.7 in step (b). Thus, we have shown that (3.22) holds for $n = m + 1$ provided the same expression holding for $n = m$. By mathematical induction, the corollary is proven. \square

Via Theorem 3.7 and Proposition 3.8, we have established the following *approximate*

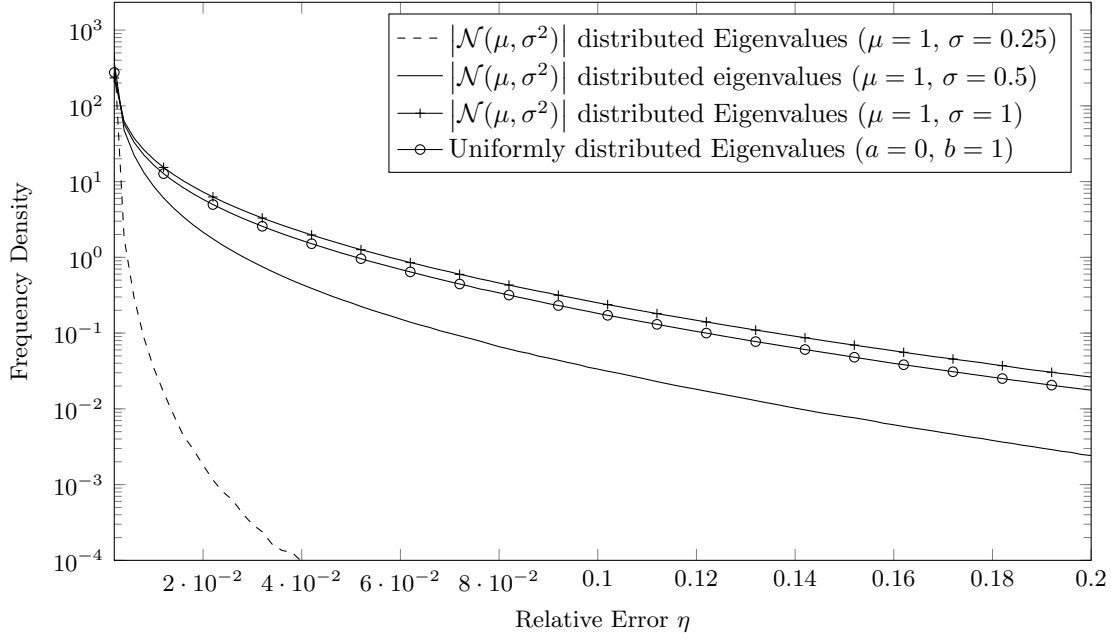


Figure 3.4: Distribution of η for random positive operators ρ_a and ρ_b under different randomization schemes.

distributive laws of the \star -product over the trace and the partial trace functions. Namely,

$$\text{tr}(\rho_a \star \rho_b) \approx \text{tr}_{\partial b \setminus \mathcal{I}}(\rho_a \star \text{tr}_{\mathcal{I}}(\rho_b)), \quad (3.23)$$

$$\text{tr}_{\mathcal{I}}(\rho_a \star \rho_b) \approx \rho_a \star \text{tr}_{\mathcal{I}}(\rho_b), \quad (3.24)$$

where $\partial a \subsetneq \partial b$ and where $\mathcal{I} \subseteq \partial b \setminus \partial a$ and where $\rho_a \in \mathfrak{L}_{++} \otimes_{i \in \partial a} \mathcal{H}_i$ and $\rho_b \in \mathfrak{L}_{++} \otimes_{i \in \partial b} \mathcal{H}_i$ are proportionally close to the identity matrix I .

It is worthwhile to make a brief numerical comparison between $\text{tr}_A(\rho_a \star \text{tr}_B(\rho_b))$ and $\text{tr}(\rho_a \star \rho_b)$. In Figure 3.4, we randomly generate $\rho_a \in \mathfrak{L}_{++}(\mathcal{H}_A)$ and $\rho_b \in \mathfrak{L}_{++}(\mathcal{H}_A \otimes \mathcal{H}_B)$, where $\mathcal{H}_A = \mathcal{H}_B = \mathbb{C}^2$, and plot statistical distribution of the relative error as in

$$\eta \triangleq \frac{|\text{tr}_A(\rho_a \star \text{tr}_B(\rho_b)) - \text{tr}(\rho_a \star \rho_b)|}{\text{tr}(\rho_a \star \rho_b)}. \quad (3.25)$$

Here, $\rho_a \triangleq U_A^\dagger \Lambda_A U_A$ and $\rho_b \triangleq U_{AB}^\dagger \Lambda_{AB} U_{AB}$, where the matrices U_A and U_{AB} are, respectively, random unitary matrices in \mathbb{C}^2 and \mathbb{C}^4 generated according to the Haar measures over unitary matrices of corresponding sizes and where Λ_A and Λ_{AB} are positive diagonal matrices with i.i.d. entries (these entries are eigenvalues of ρ_a and ρ_b). The distributions used to generate the eigenvalues are marked in the legend. For example, in the legend of Figure 3.4, $|\mathcal{N}(\mu, \sigma^2)|$ stands for the random variable distributed ac-

cording to the absolute value of a Gaussian random variable with mean μ and variance σ^2 .

3.2 Quantum Belief-Propagation Algorithms

In this section, we propose an approximated version of the “closing-the-box” operations for QFGs. The approximation is based on the approximated distributivity discussed in the previous section. The quantum belief-propagation algorithm, which was first proposed in [LP08], can then be understood as a natural extension of the approximated “closing-the-box” operations. At the end of this section, we discuss the holographic transformations of QFGs.

3.2.1 Approximated “Closing-the-Box” Operations on QFGs

Motivated by the approximated distributive law of the \star -product over partial trace operations (see (3.24)), we define the “closing-the-box” operations on QFGs as the process to replace the box with the result of the partial trace of the \star -product of the local operators *in* the box w.r.t. the Hilbert spaces *in* the box.

Definition 3.11 (“Closing-the-Box” Operations on QFGs). Let $\mathcal{G} = (\mathcal{V}, \mathcal{F}, \mathcal{E})$ be a QFG as defined in Definition 3.1. Let $\mathcal{G}' = (\mathcal{V}', \mathcal{F}')$ be a subgraph of \mathcal{G} such that if a variable vertex is in \mathcal{G}' , so do all of its neighbors (all of which are in \mathcal{F}). (We call such a subgraph a *box* of \mathcal{G} .) The “closing-the-box” operation (w.r.t. \mathcal{G}') is to replace \mathcal{G}' in \mathcal{G} by a factor vertex associated with the *exterior operator* $\rho_{\mathcal{G}'}$ of \mathcal{G}' , where $\rho_{\mathcal{G}'}$ is the resultant operator by taking the partial trace of the \star -product of the local operators associated with \mathcal{F}' over the Hilbert spaces associated with \mathcal{V}' . Namely,

$$\rho_{\mathcal{G}'} \triangleq \text{tr}_{i \in \mathcal{V}'} \left(\bigstar_{a \in \mathcal{F}'} \rho_a \right). \quad \square$$

Since the matrix exponential of Hermitian matrices is always PSD, a “closing-the-box” operation of a QFG always ends up with another QFG. As discussed in Corollary 3.10, for a chain QFG, its partition sum can be estimated via a sequence of “closing-the-box” operations. This can be further generalized to all acyclic QFGs (see Theorem 3.12 below).

Theorem 3.12. *Given an acyclic QFG $(\mathcal{G} = (\mathcal{V}, \mathcal{F}, \mathcal{E} \in \mathcal{V} \times \mathcal{F}), \mathfrak{V} = \{\mathcal{H}_i\}_{i \in \mathcal{V}}, \mathfrak{F} = \{\rho_a\}_{a \in \mathcal{F}})$, there exists a sequence of “closing-the-box” operations, tracing out one Hilbert space at each step, that shrinks the QFG to a constant² \hat{Z} . If all local operators are proportionally close to I , i.e., for each a , $\rho_a \propto I + t \cdot H_a$ for some Hermitian operator H_a and some small number t , we have*

$$\hat{Z} = Z(\mathcal{G}) + O(t^4). \quad (3.26)$$

Proof. The first part of the theorem is a direct result of acyclicity: Pick a vertex from \mathcal{V} as a root of \mathcal{G} . Since \mathcal{G} is a tree, there must exist another vertex $v \in \mathcal{V}$ with no descendent from \mathcal{V} (note that \mathcal{G} is bipartite). Closing the box encompassing v and all of its neighbors will result in a tree with one less vertex from \mathcal{V} . The process can be repeated until there is only one vertex from \mathcal{V} left in the resultant graph, which can be then “closed” into a trivial QFG.

The second part of the theorem is a direct generalization of Corollary 3.10 and can be justified using mathematical induction similar to that in the corollary’s proof. We omit the details. \square

However, due to the approximating nature of the “closing-the-box” operations for QFGs, we do not have similar results as in Theorem 2.14 or Theorem 1.8 for QFGs. The process to estimate the partition sum, as mentioned in Theorem 3.12, is summarized in Algorithm 3.1. Here, without loss of generality, we have assumed all the leaf vertices are from \mathcal{F} , since we can always append an identity factor vertex to a leaf vertex from \mathcal{V} without changing the partition sum. Note that, in Algorithm 3.1, we describe the “closing-the-box” operations as some message-passing rules, i.e.,

$$m_{i \rightarrow a} \triangleq \bigstar_{c \in \partial i \setminus a} m_{c \rightarrow i}, \quad (3.27)$$

$$m_{a \rightarrow i} \triangleq \text{tr}_{\partial a \setminus i} \left(\rho_a \star \bigotimes_{k \in \partial a \setminus i} m_{k \rightarrow a} \right), \quad (3.28)$$

where for each $(i, a) \in \mathcal{E}$, $m_{a \rightarrow i}$, $m_{i \rightarrow a}$ are some PSD operators acting on \mathcal{H}_i .

²More precisely, the word “constant” here refers to a trivial QFG representing a constant operator on a 1-dimensional Hilbert space.

Algorithm 3.1 Belief-Propagation Algorithm for Acyclic QFGs

Input: An acyclic QFG $(\mathcal{G} = (\mathcal{V}, \mathcal{F}, \mathcal{E} \in \mathcal{V} \times \mathcal{F}), \mathfrak{V} = \{\mathcal{H}_i\}_{i \in \mathcal{V}}, \mathfrak{F} = \{\rho_a\}_{a \in \mathcal{F}})$ with all leaf vertices belonging to \mathcal{F} , a root vertex $r \in \mathcal{F}$; and for each $a \in \mathcal{F}$, $\rho_a \propto I + t \cdot H_a$ for some Hermitian operator H_a and some small number t

Output: An estimated partition sum $\hat{Z} = Z(\mathcal{G}) + O(t^4)$

- 1: Define the bipartite graph $G' = (\mathcal{V}', \mathcal{F}', \mathcal{E}') \leftarrow \mathcal{G}$;
 - 2: **while** $\mathcal{F}' \neq \{r\}$ **do**
 - 3: **for all** $a \in \mathcal{F}'$ being a leaf and i being its parent in \mathcal{G}' **do**
 - 4: $m_{a \rightarrow i} \leftarrow \text{tr}_{\partial a \setminus i} \left(\rho_a \star \bigotimes_{k \in \partial a \setminus i} m_{k \rightarrow a} \right)$;
 - 5: $\mathcal{F}' \leftarrow \mathcal{F}' \setminus a$, $\mathcal{E}' \leftarrow \mathcal{E}' \setminus (\partial a \times a)$; ▷ Remove a from \mathcal{G}' .
 - 6: **end for**
 - 7: **for all** $i \in \mathcal{V}'$ being a leaf and a being its parent in \mathcal{G}' **do**
 - 8: $m_{i \rightarrow a} \leftarrow \bigstar_{c \in \partial i \setminus a} m_{c \rightarrow i}$;
 - 9: $\mathcal{V}' \leftarrow \mathcal{V}' \setminus i$, $\mathcal{E}' \leftarrow \mathcal{E}' \setminus (i \times \partial j)$; ▷ Remove i from \mathcal{G}' .
 - 10: **end for**
 - 11: **end while**
 - 12: $\hat{Z} \leftarrow \text{tr} \left(\rho_r \star \bigotimes_{i \in \partial r} m_{i \rightarrow r} \right)$;
-

3.2.2 Belief-Propagation Algorithms for QFGs

Similar to factor graphs and DeFGs, for generic QFGs, we define BP algorithms as a heuristic generalization of the message-passing rules (3.28) and (3.27). Namely, we consider an iterative method with the updating rules

$$m_{i \rightarrow a}^{(t)} \propto \bigstar_{c \in \partial i \setminus a} m_{c \rightarrow i}^{(t)}, \quad (3.29)$$

$$m_{a \rightarrow i}^{(t)} \propto \text{tr}_{\partial a \setminus i} \left(\rho_a \star \bigotimes_{k \in \partial a \setminus i} m_{k \rightarrow a}^{(t-1)} \right), \quad (3.30)$$

where the initial messages $\{m_{i \rightarrow a}^{(0)}\}_{(i,a) \in \mathcal{E}}$ are proportional to identity operators. The resultant BP algorithms for QFGs share a similar idea as that of the quantum belief-propagation (QBP) algorithm [LP08]. However, the latter was derived via a different approach and required the target QFG to be *bifactor*, *i.e.*, each vertex in \mathcal{F} has a degree at most 2. Similar to BP algorithms for factor graphs and DeFGs, different updating sequences of the messages in (3.29) and (3.30) (a.k.a. schedules) exist. However, as usual, we will focus on the synchronous schedule (a.k.a. flooding schedule) in this thesis. Algorithm 3.2 lists BP algorithm for QFGs with the flooding schedule.

We define the BP fixed points of a QFG similarly to those of a factor graph or a DeFG.

Definition 3.13 (BP Fixed Points of a QFG). Given a QFG as provided to Algorithm 3.2, a set of messages $\{m_{i \rightarrow a}, m_{a \rightarrow i} \in \mathfrak{L}_+(\mathcal{H}_i)\}_{(i,a) \in \mathcal{E}}$ is said to be a BP fixed point if

$$m_{i \rightarrow a} \propto \bigstar_{c \in \partial i \setminus a} m_{c \rightarrow i}, \quad (3.31)$$

$$m_{a \rightarrow i} \propto \text{tr}_{\partial a \setminus i} \left(\rho_a \star \bigotimes_{k \in \partial a \setminus i} m_{k \rightarrow a} \right). \quad (3.32)$$

In this case, the set $\{m_{i \rightarrow a}, m_{a \rightarrow i}\}_{(i,a) \in \mathcal{E}}$ is also called a set of fixed-point messages. \square

At a BP fixed point, we estimate the partition sum using the induced partition sum (see definition below). We will discuss an interpretation of the BP fixed points and the corresponding induced partition sums in Section 3.3.

Definition 3.14. Given a set of normalized PSD messages $\{m_{i \rightarrow a}, m_{a \rightarrow i}\}_{(i,a) \in \mathcal{E}}$, not necessarily a BP fixed point, the *induced* partition sum (w.r.t. the messages) is defined

Algorithm 3.2 Belief-Propagation Algorithm for QFGs (Flooding Schedule with Timeout)

Input: A QFG $(\mathcal{G} = (\mathcal{V}, \mathcal{F}, \mathcal{E} \in \mathcal{V} \times \mathcal{F}), \mathfrak{V} = \{\mathcal{H}_i\}_{i \in \mathcal{V}}, \mathfrak{F} = \{\rho_a\}_{a \in \mathcal{F}})$ with all leaf vertices belonging to \mathcal{F} , a root vertex $r \in \mathcal{F}$; and for each $a \in \mathcal{F}$, $\rho_a \propto I + t \cdot H_a$ for some Hermitian operator H_a and some small number t ; $\epsilon > 0$

Output: Messages $\{m_{i \rightarrow a}, m_{a \rightarrow i} \in \mathfrak{L}_+(\mathcal{H}_i)\}_{(i,a) \in \mathcal{E}}$, FLAG $\in \{\text{completed}, \text{timeout}\}$.

```

1: for all  $(i, a) \in \mathcal{E}$  do
2:    $m_{i \rightarrow a} \leftarrow I$ ;  $\triangleright I$  is the identity operator on  $\mathcal{H}_i$ .
3: end for
4:  $t \leftarrow 0$ ;
5: do
6:    $t \leftarrow t + 1$ ;
7:   for all  $(i, a) \in \mathcal{E}$  do
8:      $m_{a \rightarrow i}^{(t)} \propto \text{tr}_{\partial a \setminus i} \left( \rho_a \star \bigotimes_{k \in \partial a \setminus i} m_{k \rightarrow a}^{(t-1)} \right)$ ;
9:   end for
10:  for all  $(i, a) \in \mathcal{E}$  do
11:     $m_{i \rightarrow a}^{(t)} \propto \star_{c \in \partial i \setminus a} m_{c \rightarrow i}^{(t)} \equiv \bigotimes_{c \in \partial i \setminus a} m_{c \rightarrow i}^{(t)}$ ;
12:  end for
13:  while  $(\neg \text{timeout}) \wedge \left( \exists (i, a) \in \mathcal{E} \text{ s.t. } \left\| m_{i \rightarrow a}^{(t)} - m_{i \rightarrow a}^{(t-1)} \right\|_2 > \epsilon \text{ or } \left\| m_{a \rightarrow i}^{(t)} - m_{a \rightarrow i}^{(t-1)} \right\|_2 > \epsilon \right)$ 
     $\triangleright \text{timeout} = \text{false}$  unless the operating time exceeds a pre-selected waiting time.
14:  if timeout then
15:    FLAG  $\leftarrow$  timeout;
16:  else
17:    FLAG  $\leftarrow$  completed;
18:    for all  $(i, a) \in \mathcal{E}$  do
19:       $m_{i \rightarrow a} \leftarrow m_{i \rightarrow a}^{(t)}$ ;
20:       $m_{a \rightarrow i} \leftarrow m_{a \rightarrow i}^{(t)}$ ;
21:    end for
22:  end if

```

as

$$Z_{\text{induced}}(\{m_{i \rightarrow a}, m_{a \rightarrow i}\}_{(i,a) \in \mathcal{E}}) = \frac{\prod_{a \in \mathcal{F}} Z_a(\{m_{i \rightarrow a}\}_{i \in \partial a}) \cdot \prod_{i \in \mathcal{V}} Z_i(\{m_{a \rightarrow i}\}_{a \in \partial i})}{\prod_{(j,a) \in \mathcal{E}} Z_{i,a}(m_{i \rightarrow a}, m_{a \rightarrow i})}, \quad (3.33)$$

where

$$\begin{aligned} Z_a(\{m_{i \rightarrow a}\}_{i \in \partial a}) &\triangleq \text{tr} \left(\rho_a \star \bigotimes_{i \in \partial a} m_{i \rightarrow a} \right) & \forall a \in \mathcal{F}, \\ Z_i(\{m_{a \rightarrow i}\}_{a \in \partial i}) &\triangleq \text{tr} \left(\bigstar_{a \in \partial i} m_{a \rightarrow i} \right) & \forall i \in \mathcal{V}, \\ Z_{i,a}(m_{i \rightarrow a}, m_{a \rightarrow i}) &\triangleq \text{tr} (m_{i \rightarrow a} \star m_{a \rightarrow i}) & \forall (i, a) \in \mathcal{E}. \end{aligned} \quad \square$$

3.2.3 Holographic Transformations of QFGs

The following theorem is a generalization of Theorem 1.21 for QFGs. The holographic transformations of QFGs is a direct result of this theorem.

Theorem 3.15 (Holant Theorem for QFGs). *Let $\mathcal{G} = (\mathcal{V}, \mathcal{F}, \mathcal{E})$ be a QFG representing the factorization $\rho = \bigstar_{a \in \mathcal{F}} \rho_a$. Given Hermitian operators $\{\hat{\phi}_{i,a} \in \mathfrak{L}_\dagger(\mathcal{H}_{i,a} \otimes \mathcal{H}_i)\}_{i,a \in \mathcal{E}}$ and $\{\phi_{i,a} \in \mathfrak{L}_\dagger(\mathcal{H}_i \otimes \mathcal{H}_{i,a})\}_{i,a \in \mathcal{E}}$ such that*

$$\text{tr}_{\mathcal{H}_{i,a}} (\phi_{i,a} \star \hat{\phi}_{i,a}) = I_{\mathcal{H}_i} \quad (3.34)$$

for each $(i, a) \in \mathcal{E}$, and supposing $\{\rho_a\}_{a \in \mathcal{F}}$, $\{\hat{\phi}_{i,a}, \phi_{i,a}\}_{(i,a) \in \mathcal{E}}$ are proportionally close to the identity operator, the partition sum $Z(\mathcal{G})$ can be approximated as

$$Z(\mathcal{G}) \triangleq \text{tr} \left(\bigstar_{a \in \mathcal{F}} \rho_a \right) \approx \text{tr} \left(\bigotimes_{a \in \mathcal{F}} \hat{\rho}_a \star \bigotimes_{i \in \mathcal{V}} \hat{\tau}_i \right), \quad (3.35)$$

where

$$\hat{\rho}_a \triangleq \text{tr}_{\partial a} \left(\rho_a \star \bigstar_{i \in \partial a} \hat{\phi}_{i,a} \right) \in \mathfrak{L}_\dagger \left(\bigotimes_{i \in \partial a} \mathcal{H}_{i,a} \right) = \mathfrak{L}_\dagger(\mathcal{H}_{\partial a, a}), \quad (3.36)$$

$$\hat{\tau}_i = \text{tr}_i \left(\bigstar_{a \in \partial i} \phi_{i,a} \right) \in \mathfrak{L}_\dagger \left(\bigotimes_{a \in \partial i} \mathcal{H}_{i,a} \right) = \mathfrak{L}_\dagger(\mathcal{H}_{i, \partial i}). \quad (3.37)$$

Proof. The proof is based on the approximated distributivity of \star over trace operation (3.23). Namely,

$$\text{tr} \left(\bigotimes_{a \in \mathcal{F}} \hat{\rho}_a \star \bigotimes_{i \in \mathcal{V}} \hat{\tau}_i \right) \stackrel{(a)}{=} \text{tr} \left(\bigstar_{a \in \mathcal{F}} \hat{\rho}_a \star \bigstar_{i \in \mathcal{V}} \hat{\tau}_i \right)$$

$$\begin{aligned}
&= \text{tr} \left(\bigstar_{a \in \mathcal{F}} \text{tr}_{\partial a} \left(\rho_a \star \bigstar_{i \in \partial a} \hat{\phi}_{i,a} \right) \star \bigstar_{i \in \mathcal{V}} \text{tr}_i \left(\bigstar_{a \in \partial i} \phi_{i,a} \right) \right) \\
&\stackrel{(b)}{\approx} \text{tr} \left(\bigstar_{(i,a) \in \mathcal{E}} \left(\hat{\phi}_{i,a} \star \phi_{i,a} \right) \star \bigstar_{a \in \mathcal{F}} \rho_a \right) \\
&\stackrel{(c)}{\approx} \text{tr} \left(\bigstar_{(i,a) \in \mathcal{E}} \text{tr}_{\mathcal{H}_{i,a}} \left(\hat{\phi}_{i,a} \star \phi_{i,a} \right) \star \bigstar_{a \in \mathcal{F}} \rho_a \right) \\
&= \text{tr} \left(\bigstar_{(i,a) \in \mathcal{E}} I_{\mathcal{H}_i} \star \bigstar_{a \in \mathcal{F}} \rho_a \right) \\
&= \text{tr} \left(I_{\mathcal{H}_{\mathcal{V}}} \star \bigstar_{a \in \mathcal{F}} \rho_a \right) = \text{tr} \left(\bigstar_{a \in \mathcal{F}} \rho_a \right) = Z(\mathcal{G}),
\end{aligned}$$

where step (a) is due to the convention that $\rho_A \star \rho_B \equiv \rho_A \otimes \rho_B$ given ρ_A and τ_B acting on isolated Hilbert spaces and where we have used (3.23) in step (b) and (c). \square

We define the holographic transform of \mathcal{G} (w.r.t. $\{\hat{\phi}_{i,a}, \phi_{i,a}\}_{(i,a) \in \mathcal{E}}$) to be the QFG $\hat{\mathcal{G}} = (\mathcal{E}, \mathcal{F} \cup \mathcal{V}, \{(e, e_1), (e, e_2) | e \in \mathcal{E}\})$ representing the factorization

$$\hat{\rho} = \bigotimes_{a \in \mathcal{F}} \hat{\rho}_a \star \bigotimes_{i \in \mathcal{V}} \hat{\tau}_i = \bigstar_{a \in \mathcal{F}} \hat{\rho}_a \star \bigstar_{i \in \mathcal{V}} \hat{\tau}_i. \quad (3.38)$$

3.3 Generalization of Bethe's approximation for QFGs

Bethe's approximation (see Section 1.1.5) is a successful approach to interpret BP algorithms for factor graphs. In this section, we generalize the method to QFGs. In particular, we prove a generalized version of Theorem 1.17 (*i.e.*, [YFW05, Theorem 2]).

3.3.1 From Local Density Operators to Global Density Operators

An important result following from Theorem 3.7 and Proposition 3.8 is the ability to construct the global density operators from the local operators under suitable conditions. This is stated in the following lemma. Notice that this lemma serves as a quantum analog of Lemma 2 in [Mor15b].

Lemma 3.16. *Consider an acyclic QFG $(\mathcal{V}, \mathcal{F}, \mathcal{E})$. Given the density operators $\{\sigma_a \in \mathfrak{D}(\bigotimes_{i \in \partial a} \mathcal{H}_i)\}_{a \in \mathcal{F}}$ and $\{\sigma_i \in \mathfrak{D}(\mathcal{H}_i)\}_{i \in \mathcal{V}}$, all of which are proportionally close to the identity operator, such that*

$$\sigma_i = \text{tr}_{\partial a \setminus i}(\sigma_a) \quad \forall (i, a) \in \mathcal{E}, \quad (3.39)$$

there exists a global density operator $\sigma \in \mathfrak{D}(\otimes_{i \in \mathcal{V}} \mathcal{H}_i)$ such that

$$\mathrm{tr}_{\mathcal{V} \setminus \partial a}(\sigma) \approx \sigma_a \quad \forall a \in \mathcal{F}, \quad (3.40)$$

$$\mathrm{tr}_{\mathcal{V} \setminus i}(\sigma) \approx \sigma_i \quad \forall i \in \mathcal{V}, \quad (3.41)$$

where the approximations “ \approx ” in the above equations are based on (3.23).

Proof. Let σ be a density operator acting on $\otimes_{i \in \mathcal{V}} \mathcal{H}_i$ such that

$$\sigma \propto \exp \left(\sum_{a \in \mathcal{F}} \log \sigma_a - \sum_{i \in \mathcal{V}} (d_i - 1) \log \sigma_i \right), \quad (3.42)$$

where $d_i = \deg(i)$ for each $i \in \mathcal{V}$. We claim that both (3.40) and (3.41) hold for this σ .

To verify (3.40), we have

$$\begin{aligned} \mathrm{tr}_{\mathcal{V} \setminus \partial a}(\sigma) &\propto \mathrm{tr}_{\mathcal{V} \setminus \partial a} \left(\exp \left(\sum_{a \in \mathcal{F}} \log \sigma_a - \sum_{i \in \mathcal{V}} (d_i - 1) \log \sigma_i \right) \right) \\ &\stackrel{(a)}{=} \mathrm{tr}_{\mathcal{V} \setminus \partial a} \left(\exp \left(\log \sigma_a + \sum_{n=0}^N \sum_{\substack{i \in \partial^n a, \\ c \in \partial_a^* i}} (\log \sigma_c - \log \sigma_i) \right) \right) \\ &= \mathrm{tr}_{\mathcal{V} \setminus \partial a} \left(\exp \left(\log \sigma_a + \sum_{n=0}^{N-1} \sum_{\substack{i \in \partial^n a, \\ c \in \partial_a^* i}} (\log \sigma_c - \log \sigma_i) \right) \star \bigstar_{\substack{i \in \partial^N a, \\ c \in \partial_a^* i}} (\sigma_c \star \sigma_i^{-1}) \right) \\ &\stackrel{(b)}{\approx} \mathrm{tr}_{\mathcal{V} \setminus \partial a} \left(\exp \left(\log \sigma_a + \sum_{n=0}^{N-1} \sum_{\substack{i \in \partial^n a, \\ c \in \partial_a^* i}} (\log \sigma_c - \log \sigma_i) \right) \star \bigstar_{\substack{i \in \partial^N a, \\ c \in \partial_a^* i}} (\mathrm{tr}_{\partial c \setminus i}(\sigma_c) \star \sigma_i^{-1}) \right) \\ &= \mathrm{tr}_{\mathcal{V} \setminus \partial a} \left(\exp \left(\log \sigma_a + \sum_{n=0}^{N-1} \sum_{\substack{i \in \partial^n a, \\ c \in \partial_a^* i}} (\log \sigma_c - \log \sigma_i) \right) \right) \\ &\approx \cdots \approx \mathrm{tr}_{\mathcal{V} \setminus \partial a} (\exp (\log \sigma_a)) = \sigma_a, \end{aligned}$$

where $\partial^n a$ denotes the set of vertices in \mathcal{V} reachable from $a \in \mathcal{F}$ after walking through n vertices in \mathcal{F} (without backtracking), where $\partial_a^* i$ denotes the set of the neighbors of i excluding the vertex through which a reaches i , and where N is the largest integer such that $\partial^N a$ is nonempty. Step (a) is due to the tree structure. Step (b) and the “ \approx ” on the last line follow directly from Proposition 3.8.

We omit the verification of (3.40) since the process is very similar. \square

It is worth noting that if we had defined the global density operator $\tilde{\sigma}$ as

$$\tilde{\sigma} \triangleq \exp \left(\sum_{a \in \mathcal{F}} \log \sigma_a - \sum_{i \in \mathcal{V}} (d_i - 1) \log \sigma_i \right), \quad (3.43)$$

we would have encountered the problem that $\text{tr}(\tilde{\sigma}) \neq 1$, despite that a similar result holds for acyclic (classical) factor graphs, *i.e.*,

$$\sum_{\mathbf{x}} \prod_{a \in \mathcal{F}} \frac{b_a(\mathbf{x}_{\partial a})}{\prod_{i \in \partial a} b_i(x_i)} \prod_{i \in \mathcal{V}} b_i(x_i) = 1, \quad (3.44)$$

given the PMFs $\{b_a\}_{a \in \mathcal{F}}$, $\{b_i\}_{i \in \mathcal{V}}$ such that $\sum_{\mathbf{x}_{\partial a \setminus i}} b_a(\mathbf{x}_{\partial a}) = b_i(x_i)$ for all $(i, a) \in \mathcal{E}$. However, approximately speaking (using (3.23)), we have

$$\text{tr}(\tilde{\sigma}) = \text{tr}_{\partial a} \left(\text{tr}_{\mathcal{V} \setminus \partial a} \left(\exp \left(\sum_{a \in \mathcal{F}} \log \sigma_a - \sum_{i \in \mathcal{V}} (d_i - 1) \log \sigma_i \right) \right) \right) \approx \text{tr}_{\partial a}(\sigma_a) = 1. \quad (3.45)$$

Thus, we can treat $\tilde{\sigma}$ as an approximate global density operator.

3.3.2 Free Energies of QFGs

We define quantum analogies of the Helmholtz free energy and the Gibbs free energy function as follows.

Definition 3.17. Given a QFG \mathcal{G} representing the factorization $\rho = \star_{a \in \mathcal{F}} \rho_a$, we define the *quantum Helmholtz free energy* and the *quantum Gibbs free energy function* w.r.t. the density operator $\sigma \in \mathfrak{D}(\mathcal{H}_{\mathcal{V}})$ as

$$F_{\text{H}} \triangleq -\log Z(\mathcal{G}), \quad (3.46)$$

$$F_{\text{G}}(\sigma) \triangleq -\sum_{a \in \mathcal{F}} \text{tr} \left(\sigma \cdot (\log \rho_a \otimes I_{\mathcal{H}_{\mathcal{V} \setminus \partial a}}) \right) - \mathbf{H}(\sigma), \quad (3.47)$$

where $\mathbf{H}(\sigma)$ is the von Neumann entropy of σ . □

Theorem 3.18. $F_{\text{G}}(\sigma)$ is lower bounded by F_{H} . In particular,

$$F_{\text{G}}(\sigma) = F_{\text{H}} + \text{D}(\sigma \| \tilde{\rho}), \quad (3.48)$$

where $\tilde{\rho} \triangleq \rho / Z(\mathcal{G}) \propto \star_{a \in \mathcal{F}} \rho_a$ is a density operator.

Proof. This is a result of the direct computation, *i.e.*,

$$F_{\text{G}}(\sigma) - F_{\text{H}} = -\sum_{a \in \mathcal{F}} \text{tr} \left(\sigma \cdot (\log \rho_a \otimes I_{\mathcal{H}_{\mathcal{V} \setminus \partial a}}) \right) - \mathbf{H}(\sigma) + \log(Z(\mathcal{G}))$$

$$\begin{aligned}
&= -\operatorname{tr} \left(\sigma \cdot \left(\sum_{a \in \mathcal{F}} \log \rho_a - \log Z(\mathcal{G}) \cdot I \right) \right) + \operatorname{tr} (\sigma \cdot \log \sigma) \\
&= -\operatorname{tr} \left(\sigma \cdot \log \left(\exp \left(\sum_{a \in \mathcal{F}} \log \rho_a - \log Z(\mathcal{G}) \cdot I \right) \right) \right) + \operatorname{tr} (\sigma \cdot \log \sigma) \\
&= -\operatorname{tr} (\sigma \cdot \log \tilde{\rho}) + \operatorname{tr} (\sigma \cdot \log \sigma) = D(\sigma \| \tilde{\rho}).
\end{aligned}$$

By the Klein's inequality, we have $F_G(\sigma) \geq F_H$, with equality if and only if $\sigma = \tilde{\rho}$. \square

Theorem 3.18 allows us to compute F_H via minimizing $F_G(\sigma)$ over all possible $\sigma \in \mathfrak{D}(\mathcal{H}_V)$. However, such an optimization problem is, in general, not tractable due to the enormous dimension of the density operator σ . In analogy to the Bethe free energy (see Definition 1.13), we propose the following quantum Bethe free energy as an approximation to F_G .

Definition 3.19 (Quantum Bethe Free Energy). Given a QFG \mathcal{G} representing the factorization $\rho = \star_{a \in \mathcal{F}} \rho_a$, the *quantum Bethe free energy function* is the function

$$\begin{aligned}
F_B(\{\sigma_a\}_{a \in \mathcal{F}}, \{\sigma_i\}_{i \in \mathcal{V}}) &\triangleq - \sum_{a \in \mathcal{F}} \operatorname{tr} (\sigma_a \cdot \log \rho_a) + \sum_{a \in \mathcal{F}} \operatorname{tr} (\sigma_a \cdot \log \sigma_a) \\
&\quad - \sum_{i \in \mathcal{V}} (d_i - 1) \cdot \operatorname{tr} (\sigma_i \cdot \log \sigma_i),
\end{aligned} \tag{3.49}$$

where the domain of F_B is

$$\mathcal{L}(\mathcal{G}) \triangleq \left\{ (\{\sigma_a\}_{a \in \mathcal{F}}, \{\sigma_i\}_{i \in \mathcal{V}}) \left| \begin{array}{ll} \sigma_a \in \mathfrak{D}(\otimes_{i \in \partial a} \mathcal{H}_i) & \forall a \in \mathcal{F} \\ \sigma_i \in \mathfrak{D}(\mathcal{H}_i) & \forall i \in \mathcal{V} \\ \operatorname{tr}_{\partial a \setminus i} \sigma_a = \sigma_i & \forall (i, a) \in \mathcal{E} \end{array} \right. \right\}. \quad \square$$

For acyclic QFGs, the quantum Bethe free energy approximates the Gibbs free energy, as shown in the following theorem.

Theorem 3.20. Consider an acyclic QFG $(\mathcal{V}, \mathcal{F}, \mathcal{E})$ representing the factorization $\rho = \star_{a \in \mathcal{F}} \rho_a$. Let σ be a global density operator, and for each $a \in \mathcal{F}$, let $\sigma_a \triangleq \operatorname{tr}_{V \setminus \partial a}(\sigma)$, and for each $i \in \mathcal{V}$, let $\sigma_i \triangleq \operatorname{tr}_{V \setminus i}(\sigma)$. Supposing $\{\rho_a\}_{a \in \mathcal{F}}$ and σ are proportionally close to the identity operators, i.e., $\rho_a \propto I + t \cdot H_a$ and $\sigma \propto I + t \cdot H$ for some Hermitian operators H_a and H and some small number t , then

$$F_G(\sigma) = F_B(\{\sigma_a\}_{a \in \mathcal{F}}, \{\sigma_i\}_{i \in \mathcal{V}}) + O(t^3). \tag{3.50}$$

Proof. By definition of partial trace, it holds that

$$\mathrm{tr} \left(\sigma \cdot (\log \rho_a \otimes I_{\mathcal{H}_{\mathcal{V} \setminus \partial a}}) \right) = \mathrm{tr} (\sigma_a \cdot \log \rho_a).$$

Considering the definitions of $F_{\mathcal{G}}$ and $F_{\mathcal{B}}$, it suffices to show

$$\sum_{a \in \mathcal{F}} \mathrm{tr} (\sigma_a \cdot \log \sigma_a) - \sum_{i \in \mathcal{V}} (d_i - 1) \cdot \mathrm{tr} (\sigma_i \cdot \log \sigma_i) - \mathrm{tr} (\sigma \cdot \log \sigma) = O(t^3).$$

By letting $\tilde{\sigma} \triangleq \exp \left(\sum_{a \in \mathcal{F}} \log \sigma_a - \sum_{i \in \mathcal{V}} (d_i - 1) \log \sigma_i \right)$, the LHS of above can be rewritten as

$$\begin{aligned} \mathrm{tr} (\sigma \cdot \log \tilde{\sigma}) - \mathrm{tr} (\sigma \cdot \log \sigma) &= \mathrm{tr} \left(\sigma \cdot \log \frac{\tilde{\sigma}}{\mathrm{tr}(\tilde{\sigma})} \right) - \mathrm{tr} (\sigma \cdot \log \sigma) + \mathrm{tr} (\tilde{\sigma}), \\ &= \mathrm{tr} \left(\sigma \cdot \log \frac{\tilde{\sigma}}{\mathrm{tr}(\tilde{\sigma})} \right) - \mathrm{tr} (\sigma \cdot \log \sigma) + O(t^4), \end{aligned}$$

where we have used (3.45) and Theorem 3.7 in the very last step.

Now, consider the quantum exponential family as in Example B.2 in Appendix B.

By Lemma 3.16, we know that

$$\begin{aligned} \mathrm{tr}_{\mathcal{V} \setminus \partial a}(\sigma) - \mathrm{tr}_{\mathcal{V} \setminus \partial a} \left(\frac{\tilde{\sigma}}{\mathrm{tr}(\tilde{\sigma})} \right) &= \sigma_a - \mathrm{tr}_{\mathcal{V} \setminus \partial a} \left(\frac{\tilde{\sigma}}{\mathrm{tr}(\tilde{\sigma})} \right) = O(t^3), \\ \mathrm{tr}_{\mathcal{V} \setminus i}(\sigma) - \mathrm{tr}_{\mathcal{V} \setminus i} \left(\frac{\tilde{\sigma}}{\mathrm{tr}(\tilde{\sigma})} \right) &= \sigma_i - \mathrm{tr}_{\mathcal{V} \setminus i} \left(\frac{\tilde{\sigma}}{\mathrm{tr}(\tilde{\sigma})} \right) = O(t^3). \end{aligned}$$

In terms of their dual parameters, this can be written as $\boldsymbol{\eta}(\sigma) = \boldsymbol{\eta}(\frac{\tilde{\sigma}}{\mathrm{tr}(\tilde{\sigma})}) + t^3 \cdot \Delta \boldsymbol{\eta} + O(t^4)$ for some real vector $\Delta \boldsymbol{\eta}$ (see Appendix B). Define the function $f(\boldsymbol{\eta}) : \boldsymbol{\eta} \mapsto -\mathrm{tr} (\sigma \cdot \log \sigma(\boldsymbol{\eta}))$. In this case, we have

$$\begin{aligned} \lim_{t \rightarrow 0} \frac{\mathrm{tr} \left(\sigma \cdot \log \frac{\tilde{\sigma}}{\mathrm{tr}(\tilde{\sigma})} \right) - \mathrm{tr} (\sigma \cdot \log \sigma)}{t^3} &= \lim_{t \rightarrow 0} \frac{f(\boldsymbol{\eta}(\frac{\tilde{\sigma}}{\mathrm{tr}(\tilde{\sigma})})) - f(\boldsymbol{\eta}(\sigma))}{t^3} \\ &= \lim_{t \rightarrow 0} \frac{f(\boldsymbol{\eta}(\frac{\tilde{\sigma}}{\mathrm{tr}(\tilde{\sigma})})) - f(\boldsymbol{\eta}(\frac{\tilde{\sigma}}{\mathrm{tr}(\tilde{\sigma})}) + t^3 \cdot \Delta \boldsymbol{\eta} + O(t^4))}{t^3} \\ &= \nabla f^{\top} \cdot \Delta \boldsymbol{\eta}, \end{aligned}$$

where the differentiability of f is justified in Appendix C. Since $\nabla f^{\top} \cdot \Delta \boldsymbol{\eta}$ is a finite number, we conclude that $\mathrm{tr} \left(\sigma \cdot \log \frac{\tilde{\sigma}}{\mathrm{tr}(\tilde{\sigma})} \right) - \mathrm{tr} (\sigma \cdot \log \sigma) = O(t^3)$. Thus, we have $\mathrm{tr} (\sigma \cdot \log \tilde{\sigma}) - \mathrm{tr} (\sigma \cdot \log \sigma) = O(t^3)$, which finishes the proof. \square

3.3.3 Correspondence between the Stationary Points of $F_{\mathcal{B}}$ and the BP Fixed Points

Motivated by Theorem 3.20, which allows us to treat the Bethe free energy $F_{\mathcal{B}}$ as an approximation to the Gibbs free energy $F_{\mathcal{G}}$, we define the following optimization problem as an approximated version of the Gibbs minimization problem.

Definition 3.21 (Constrained Quantum Bethe Minimization Problem). Given a QFG $(\mathcal{V}, \mathcal{F}, \mathcal{E})$ representing the factorization $\rho = \star_{a \in \mathcal{F}} \rho_a$, the optimization problem

$$\begin{aligned}
\min \quad & F_{\mathbf{B}}(\{\sigma_a\}_{a \in \mathcal{F}}, \{\sigma_i\}_{i \in \mathcal{V}}) \\
\text{s. t.} \quad & \sigma_a \in \mathfrak{D}(\bigotimes_{i \in \partial a} \mathcal{H}_i) \quad \forall a \in \mathcal{F} \\
& \sigma_i \in \mathfrak{D}(\mathcal{H}_i) \quad \forall i \in \mathcal{V} \\
& \text{tr}_{\partial a \setminus i} \sigma_a = \sigma_i \quad \forall (i, a) \in \mathcal{E}
\end{aligned} \tag{3.51}$$

is called the *constrained Bethe minimization problem*. \square

One must note that even for acyclic QFGs, $F_{\mathbf{B}}$ is merely an approximation to $F_{\mathbf{G}}$ under suitable conditions. Thus, the constrained Bethe minimization problem does not guarantee the recovery of the quantum Helmholtz free energy $F_{\mathbf{H}}$, even for acyclic cases. In contrast, for acyclic factor graphs, $F_{\mathbf{B}}$ and $F_{\mathbf{G}}$ share the same minimum, which equals the Helmholtz free energy $F_{\mathbf{H}}$. In other words, the BP algorithm for acyclic factor graphs is exact, but BP algorithms for acyclic QFGs are not.

In the remainder of this section, we show how the quantum BP algorithms, particularly the BP fixed points, are connected to the constrained Bethe minimization problem.

Theorem 3.22. *Given a QFG $((\mathcal{V}, \mathcal{F}, \mathcal{E}), \{\mathcal{H}_i\}_{i \in \mathcal{V}}, \{\rho_a\}_{a \in \mathcal{F}})$ with (straightly) PD local operators, $(\{\sigma_a\}_{a \in \mathcal{F}}, \{\sigma_i\}_{i \in \mathcal{V}}) \in \mathcal{L}(\mathcal{G})$ is an interior stationary point of $F_{\mathbf{B}}$ if*

$$\sigma_a \propto \rho_a \star \bigstar_{i \in \partial a} m_{i \rightarrow a}, \tag{3.52}$$

$$\sigma_i \propto \bigstar_{a \in \partial i} m_{a \rightarrow i}, \tag{3.53}$$

where $\{m_{i \rightarrow a}, m_{a \rightarrow i} \in \mathfrak{D}(\mathcal{H}_i)\}_{(i,a) \in \mathcal{E}}$ are (straightly) PD messages such that

$$m_{i \rightarrow a} \propto \bigstar_{c \in \partial i \setminus a} m_{c \rightarrow i}, \tag{3.54}$$

$$m_{a \rightarrow i} \propto \text{tr}_{\partial a \setminus i} \left(\rho_a \star \bigotimes_{k \in \partial a} m_{k \rightarrow a} \right) \star m_{i \rightarrow a}^{-1}. \tag{3.55}$$

Conversely, (3.54) and (3.55) hold if $(\{\sigma_a\}_{a \in \mathcal{F}}, \{\sigma_i\}_{i \in \mathcal{V}})$ defined according to (3.52) and (3.53) form an internal stationary point of $F_{\mathbf{B}}$.

Proof. This theorem is a quantum analogy of Theorem 1.17. Part of the ideas of this proof originated from [YFW05].

Suppose $(\{\sigma_a\}_{a \in \mathcal{F}}, \{\sigma_i\}_{i \in \mathcal{V}}) \in \mathcal{L}(\mathcal{G})$ is an *interior* stationary point of the constrained Bethe minimization problem. In this case, the Lagrangian of this problem can be expressed as

$$L \triangleq F_B + \sum_{a \in \mathcal{F}} \gamma_a \cdot (\text{tr}(\sigma_a) - 1) + \sum_{i \in \mathcal{V}} \gamma_i \cdot (\text{tr}(\sigma_i) - 1) + \sum_{(i,a) \in \mathcal{E}} \text{tr}(\lambda_{i,a} \cdot (\sigma_i - \text{tr}_{\partial a \setminus i}(\sigma_a))),$$

where $\{\gamma_a \in \mathbb{R}\}_{a \in \mathcal{F}}$, $\{\gamma_i \in \mathbb{R}\}_{i \in \mathcal{V}}$, and $\{\lambda_{i,a} \in \mathfrak{L}(\mathcal{H}_i)\}_{(i,a) \in \mathcal{E}}$ are Lagrangian dual variables. At the stationary point, it must hold that

$$\frac{\partial L}{\partial \gamma_a} = 0 \quad \forall a \in \mathcal{F}, \quad (3.56)$$

$$\frac{\partial L}{\partial \gamma_i} = 0 \quad \forall i \in \mathcal{V}, \quad (3.57)$$

$$\left. \frac{d}{dt} \right|_{t=0} L(\lambda_{i,a} + t \cdot H_{i,a}) = 0 \quad \forall H_{i,a} \in \mathfrak{L}_+(\mathcal{H}_i), \forall (i,a) \in \mathcal{E}, \quad (3.58)$$

$$\left. \frac{d}{dt} \right|_{t=0} L(\sigma_a + t \cdot H_a) = 0 \quad \forall H_a \in \mathfrak{L}_+(\mathcal{H}_{\partial a}), \forall a \in \mathcal{F}, \quad (3.59)$$

$$\left. \frac{d}{dt} \right|_{t=0} L(\sigma_i + t \cdot H_i) = 0, \quad \forall H_i \in \mathfrak{L}_+(\mathcal{H}_i), \forall i \in \mathcal{V}. \quad (3.60)$$

Eqs. (3.56), (3.57), (3.58) are equivalent to the constraints of the problem. By Spectral theorem and the first-order perturbation theory [Kat95], (3.59) and (3.60) can be expanded as

$$\begin{aligned} -\text{tr}(H_a \cdot \log \rho_a) + \text{tr}(H_a \cdot (I + \log \sigma_a)) + \text{tr}(H_a) \cdot \gamma_a - \sum_{i \in \partial a} \text{tr}(\lambda_{i,a} \cdot \text{tr}_{\partial a \setminus i} H_a) &= 0, \\ (1 - d_i) \cdot \text{tr}(H_i \cdot (I + \log \sigma_i)) + \text{tr}(H_i) \cdot \gamma_i + \sum_{a \in \partial i} \text{tr}(H_i \cdot \lambda_{i,a}) &= 0. \end{aligned}$$

Solving the above equations for $\{\sigma_a\}_{a \in \mathcal{F}}$ and $\{\sigma_i\}_{i \in \mathcal{V}}$, respectively, we have

$$\sigma_a = \exp \left(\log \rho_a + \sum_{i \in \partial a} \lambda_{i,a} - (1 + \gamma_a) \cdot I \right) \quad \forall a \in \mathcal{F}, \quad (3.61)$$

$$\sigma_i = \exp \left(\frac{1}{d_i - 1} \cdot \left(\sum_{a \in \partial i} \lambda_{i,a} + (1 + \gamma_i) \cdot I \right) \right) \quad \forall i \in \mathcal{V}. \quad (3.62)$$

Eqs. (3.52) and (3.53) can be shown by making the identification that

$$\lambda_{i,a} = \log m_{i \rightarrow a} = \sum_{c \in \partial i \setminus a} \log m_{c \rightarrow i} \quad \forall (i,a) \in \mathcal{E}. \quad (3.63)$$

In this case, (3.55) can be derived from the constraints that $\text{tr}_{\partial a \setminus i} \sigma_a = \sigma_i$ for each $(i,a) \in \mathcal{E}$.

Conversely, suppose there exist some PD messages $\{m_{i \rightarrow a}, m_{a \rightarrow i} \in \mathfrak{D}(\mathcal{H}_i)\}_{(i,a) \in \mathcal{E}}$ satisfying (3.54) and (3.55). Let $(\{\sigma_a\}_{a \in \mathcal{F}}, \{\sigma_i\}_{i \in \mathcal{V}}) \in \mathcal{L}(\mathcal{G})$ be defined according to (3.52) and (3.53). By choosing $\{\gamma_a\}_{a \in \mathcal{F}}$, $\{\gamma_i\}_{i \in \mathcal{V}}$, and $\{\lambda_{i,a}\}_{(i,a) \in \mathcal{E}}$ by such that (3.61), (3.62), and (3.63) hold simultaneously, we have satisfied (3.59) and (3.60). Eqs. (3.56) and (3.57) also hold since $\{\sigma_a\}_{a \in \mathcal{F}}$ and $\{\sigma_i\}_{i \in \mathcal{V}}$ are density operators. Finally, (3.58) holds since $\text{tr}_{\partial a \setminus i} \sigma_a = \sigma_i$ for each $(i, a) \in \mathcal{E}$, which in turn can be derived from (3.55). Thus, we have verified $(\{\sigma_a\}_{a \in \mathcal{F}}, \{\sigma_i\}_{i \in \mathcal{V}})$ to be a stationary point. \square

Under suitable conditions, by Proposition 3.8, (3.55) can be approximated as

$$m_{a \rightarrow i} \propto \text{tr}_{\partial a \setminus i} \left(\rho_a \star \bigotimes_{k \in \partial a} m_{k \rightarrow a} \right) \star m_{i \rightarrow a}^{-1} \approx \text{tr}_{\partial a \setminus i} \left(\rho_a \star \bigotimes_{k \in \partial a \setminus i} m_{k \rightarrow a} \right), \quad (3.64)$$

which is exactly the second half of the BP fixed point condition (recall Definition 3.13). Therefore, Theorem 3.22 provides an interpretation of the quantum BP algorithm as an iterative method for finding a stationary point of the constrained Bethe minimization problem. Unfortunately, there is no guarantee of convergence of such an iterative method. Moreover, even for acyclic QFGs, we have made multiple approximations to link the BP fixed points to the partition sum (including Theorem 3.20 and Eq. (3.64)). Despite such concerns, as illustrated in the next section, the quantum BP algorithm still shows a rather promising performance in some numerical applications.

The following corollary generalizes Corollary 1.22 and is a direct result of Theorem 3.22.

Corollary 3.23. *Consider a QFG \mathcal{G} representing the factorization $\rho = \star_{a \in \mathcal{F}} \rho_a$. For a collection of positive messages $\{m_{i \rightarrow a}, m_{a \rightarrow i}\}_{i,a}$ satisfying (3.54) and (3.55), we have*

$$Z_B(\{\sigma_a\}_{a \in \mathcal{F}}, \{\sigma_i\}_{i \in \mathcal{V}}) \triangleq \exp(-F_B(\{\sigma_a\}_{a \in \mathcal{F}}, \{\sigma_i\}_{i \in \mathcal{V}})) \quad (3.65)$$

$$= Z_{\text{induced}}(\{m_{i \rightarrow a}, m_{a \rightarrow i}\}_{(i,a) \in \mathcal{E}}), \quad (3.66)$$

where the density operators $\{\sigma_a\}_{a \in \mathcal{F}}$ and $\{\sigma_i\}_{i \in \mathcal{V}}$ are defined according to (3.52) and (3.53).

3.4 Numerical Example

In this section, we consider the QFG as in Figure. 3.5, where each local operator $\{\rho_a\}_{a=1,\dots,6}$ is generated in the same fashion as ρ_a and ρ_b for Figure 3.4. We are interested in comparing the induced partition sum Z_{induced} at BP fixed points with the

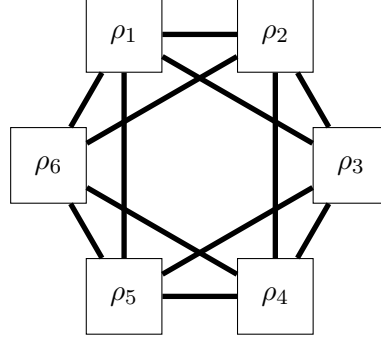


Figure 3.5: QFG in Section 3.4.

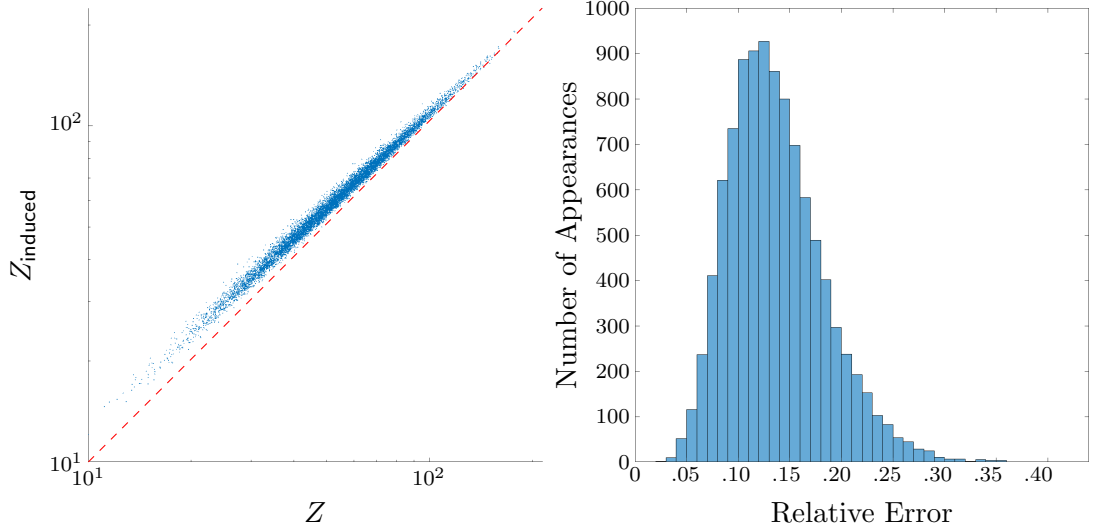


Figure 3.6: The partition sum Z and the induced partition sum Z_{induced} produced by Algorithm 3.2. The plot consists of 10,000 instances based on the QFG in Figure 3.5, where each local factors $\{\rho_i\}_{i=1}^6$ are generated independently as $\rho_i \leftarrow U \cdot \text{diag}(\lambda_1^{16}) \cdot U$, and where (for each ρ_i) U is some 16-by-16 unitary matrix (independently) randomly generated according to Haar measure, and where each $\{\lambda_k\}_{k=1}^{16}$ are independently uniformly distributed on $[0, 1]$.

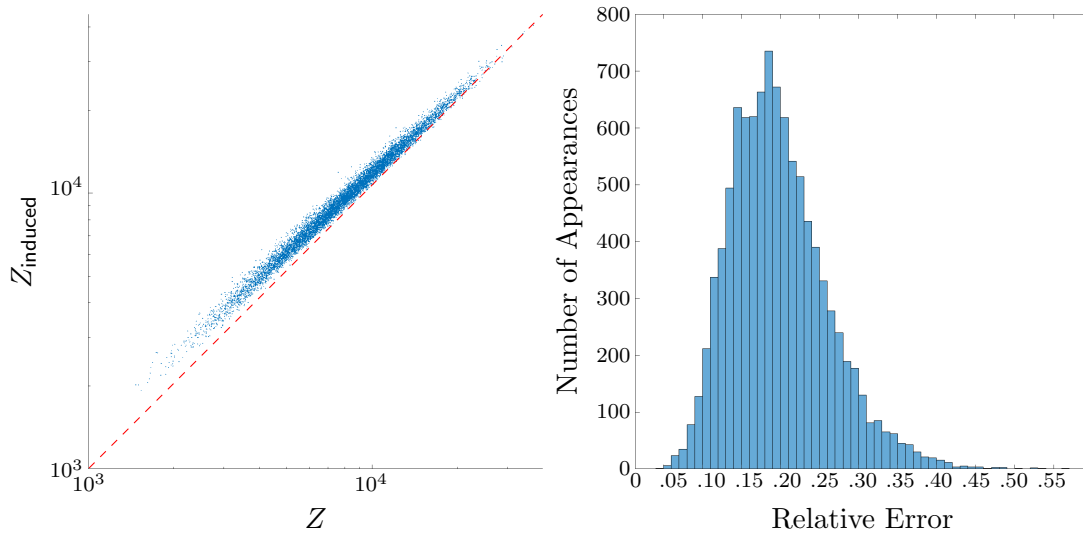


Figure 3.7: The partition sum Z and the induced partition sum Z_{induced} produced by Algorithm 3.2. The plot consists of 10,000 instances based on the QFG in Figure 3.5, where each local factors $\{\rho_i\}_{i=1}^6$ are generated independently as $\rho_i \leftarrow U \cdot \text{diag}(\lambda_1^{16}) \cdot U$, and where (for each ρ_i) U is some 16-by-16 unitary matrix (independently) randomly generated according to Haar measure, and where each $\{\lambda_k\}_{k=1}^{16}$ are independently distributed according to $|\mathcal{N}(1, 1)|$. ($\mathcal{N}(\mu, \sigma)$ denotes the Gaussian distribution with mean μ and standard variation σ .)

actual partition sum $Z(\mathcal{G})$. In particular, in Figure 3.6 and 3.7, we have plotted the statistics of the relative error $\eta \triangleq |(Z_{\text{induced}} - Z)/Z|$ w.r.t. different distributions of the eigenvalues. The plots are based on 10,000 simulations.

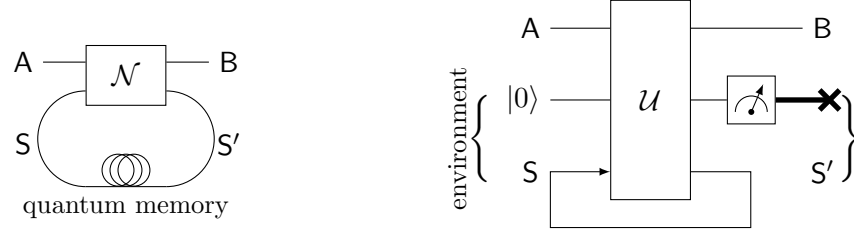
Chapter 4

Bounding and Estimating the Classical Information Rate of Quantum Channels with Memory

In this chapter, we consider the transmission rate of classical information over a finite-dimensional quantum channel with memory. A *quantum channel with memory* [BM04; KW05; CGLM14] is a quantum channel (from input system A to output system B) equipped with a memory system S ; namely it is a CPTP map from the set of density operators on $\mathcal{H}_A \otimes \mathcal{H}_S$ to the set of density operators on $\mathcal{H}_B \otimes \mathcal{H}_{S'}$. The system S can be understood either as a state of the channel (as illustrated in Figure 4.1a), or as a part of the environment that does not decay between consecutive channel uses (as illustrated in Figure 4.1b). Interesting examples of quantum channels with memory include spin chains [Bos03] and fiber optic links [BDB04].

Classical communication over such channels is accomplished by encoding classical data into some density operators before the transmission and applying measurements to the outputs of the channel. In the most generic case, an ensemble and a measurement on the *joint* input and output systems of multiple channels uses can be used for encoding and decoding, respectively. The scenario involving a k -channel joint ensemble and a k -channel joint measurement is depicted in Figure 4.2b, where

- the encoding process \mathcal{E} is described by some ensemble $\{P_X(x), \rho_{A_1^k}^{(x)}\}_{x \in \mathcal{X}}$ on the joint input system (A_1, \dots, A_k) , with \mathcal{X} being the input alphabet, $P_X(x)$ being



(a) Memory as the state of the channel. (b) Memory as undecayed partial environment.

Figure 4.1: Interpretations of quantum channels with memory.

the input distribution, and $\rho_{A_1^k}^{(x)}$ being the density operator on the input systems A_1^k corresponding to the classical input x ;

- the decoding process \mathcal{D} is described by some positive-operator valued measurement (POVM) $\{\Lambda_{B_1^k}^{(y)}\}_{y \in \mathcal{Y}}$ on the joint output system (B_1, \dots, B_k) , with \mathcal{Y} being the output alphabet;
- the classical input and output are represented by some random variables X and Y , respectively.

For comparison, Figure 4.2a shows the corresponding memoryless setup. The above arrangement results in a (classical) channel from X to Y , whose rate of transmission is given by

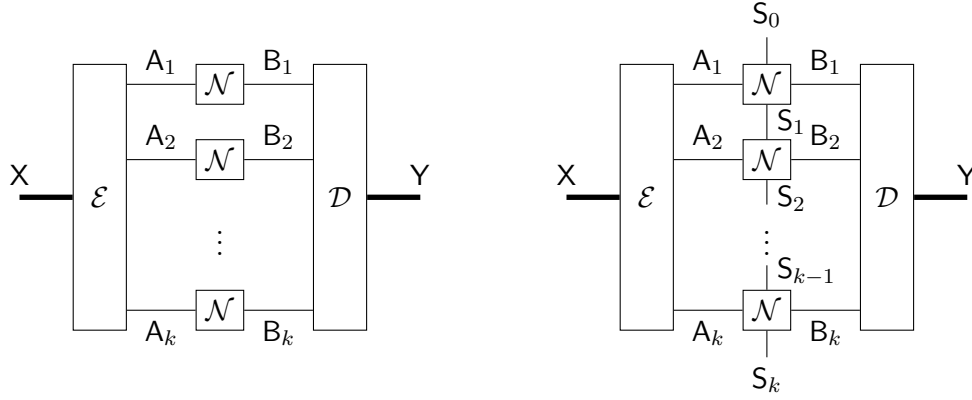
$$I(\mathcal{E}, \mathcal{N}^{\boxtimes k}, \mathcal{D}) = \limsup_{n \rightarrow \infty} \frac{1}{n} I(X_1^n; Y_1^n), \quad (4.1)$$

where we use the above transmission scheme n times consecutively (as depicted in Figure 4.2c) and where

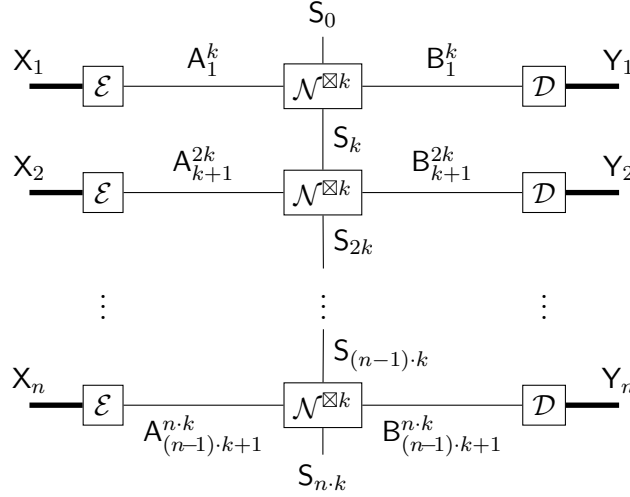
$$\begin{aligned} \mathcal{N}^{\boxtimes k} \triangleq & \left(\mathcal{N}_{A_k S_{k-1} \rightarrow B_k S_k} \otimes \mathcal{I}_{B_1^{k-1} \rightarrow B_1^{k-1}} \right) \circ \left(\mathcal{I}_{A_k \rightarrow A_k} \otimes \mathcal{N}_{A_{k-1} S_{k-2} \rightarrow B_{k-1} S_{k-1}} \otimes \mathcal{I}_{B_1^{k-2} \rightarrow B_1^{k-2}} \right) \\ & \circ \dots \circ \left(\mathcal{I}_{A_2^k \rightarrow A_2^k} \otimes \mathcal{N}_{A_1 S_0 \rightarrow B_1 S_1} \right). \end{aligned}$$

Here, I stands for the mutual information. As a fundamental result, this quantity can be simplified to $I(X; Y)$ for the memoryless case [Sha48; CT06]. Optimizing $I(\mathcal{E}, \mathcal{N}^{\boxtimes k}, \mathcal{D})$ over \mathcal{E} and \mathcal{D} (with $k \rightarrow \infty$) yields the classical capacity of the quantum channel \mathcal{N} , namely

$$C(\mathcal{N}) = \limsup_k \frac{1}{k} \sup_{\mathcal{E}, \mathcal{D}} I(\mathcal{E}, \mathcal{N}^{\boxtimes k}, \mathcal{D}). \quad (4.2)$$



(a) Using the memoryless quantum channel \mathcal{N} consecutively. (b) Using the quantum channel with memory \mathcal{N} consecutively.



(c) Generic classical communication corresponding to (4.1).

Figure 4.2: Classical communications over quantum channels.

In this chapter, we are interested in computing and bounding the information rate as in (4.1) for finite-dimensional quantum channels with memory using only separable input ensembles and local output measurements, *i.e.*, the case $k = 1$, which is depicted in Figure 4.3. This restriction is equivalent to the scenario where no quantum computing device is present at the sending or receiving end or where our manipulation of the channel is limited to a single-channel use. The difficulty of the problem lies with the presence of the quantum memory. In the simplest situation, the memory system exhibits classical properties under certain ensembles and measurements. In this case, the resulting classical communication setup is equivalent to a finite-state-machine channel (FSMC) [Gal68]. Though the evaluation of the information rate of an FSMC

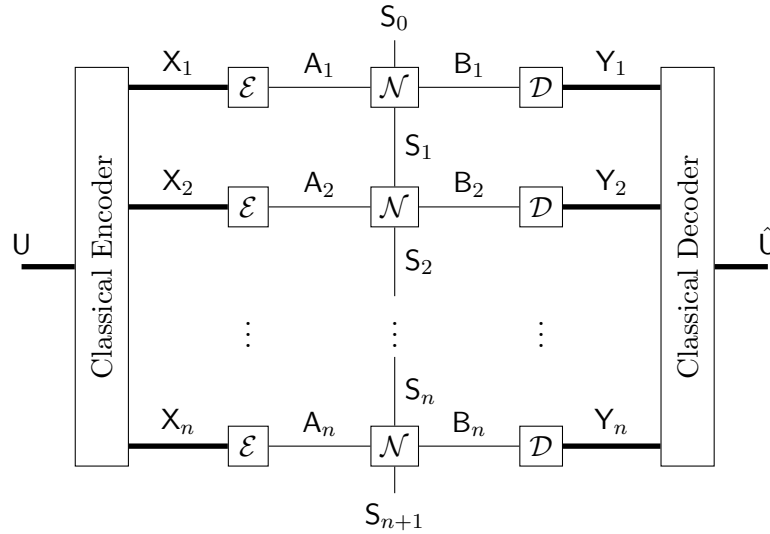


Figure 4.3: Classical communication over a quantum channel with memory using a separable ensemble and local measurements.

is nontrivial in general, efficient stochastic methods for estimating and bounding this quantity have been developed [ALV+06; SVS09].

Our work is highly inspired by [ALV+06], where the authors considered the information rate of FSMCs. In particular, for an indecomposable FSMC [Gal68] with its channel law described by PMF W , its information rate, which is independent of the initial channel state, is given by

$$I_W(Q) = \lim_{n \rightarrow \infty} \frac{1}{n} \mathbf{I}(X_1^n; Y_1^n), \quad (4.3)$$

where $X_1^n = (X_1, \dots, X_n)$ is the channel input process characterized by some sequence of distributions $\{Q^{(n)}\}_n$ and where $Y_1^n = (Y_1, \dots, Y_n)$ is the channel output process. Although, except for very special cases, there are no single-letter or other simple expressions for information rate available, efficient stochastic techniques have been developed for estimating the information rate for *stationary* and *ergodic* input processes $\{Q^{(n)}\}_n$ [ALV+06; SS01; PSS01]. (For these techniques, under mild conditions, the numerical estimate of the information rate converges with probability one to the true value when the length of the channel input sequence goes to infinity.) In this chapter, we extend such techniques to quantum channels with memory; in particular, we use *factor graphs* for quantum probabilities [LV17] (see Section 2.1.1) for estimating quantities of interest. These graphical models are useful for visualizing the relevant

computations and for providing a clear comparison between the setup considered in this chapter and its classical counterparts in [ALV+06] and [SVS09].¹

Our work is also partially inspired by [SVS09], where the authors proposed upper and lower bounds based on some so-called auxiliary FSMCs, which are often lower-complexity approximations of the original FSMC. They also provided efficient methods for optimizing these bounds. Such techniques have been proven useful for FSMCs with large state spaces, when the above-mentioned information rate estimation techniques can be overly time-consuming. Interestingly enough, the lower bounds represent achievable rates under mismatched decoding, where the decoder bases its computations not on the original FSMC but on the auxiliary FSMC [GLT00]. (See [SVS09] for a more detailed discussion of this topic and for further references.) In this chapter, we also consider auxiliary channels and their induced bounds. However, the auxiliary channels of our interest are chosen from a larger set of channels called *quantum-state channels*, which will be defined in Section 4.2. We also propose a method for optimizing these bounds. In particular, our method for optimizing the lower bound is “data-driven” in the sense that only the input/output sequences of the original channel are needed, but not the mathematical model of the original channel.

One must note that even if we can efficiently compute or bound the information rate, it is still a long way to go to compute the classical capacity of a quantum channel with memory. On the one hand, maximizing $I(\mathcal{E}, \mathcal{N}, \mathcal{D})$ is a difficult problem. (The analogous classical problems have been addressed in [Ari72], [Bla72], and [VKAL08].) On the other hand, due to the superadditivity property [Has09] of quantum channels, which happens to be more common for quantum channels with memory [MPV04; KM06; LM10] (compared with memoryless quantum channels), it is inevitable to consider joint ensembles on input systems and joint measurements on output systems across multiple channel uses.

The rest of this chapter is organized as follows. Section 4.1 reviews the method of estimating the information rate of an FSMC. Section 4.2 models the classical communication scheme over a quantum channel with memory, and defines the notion of

¹Clearly, the graphical models that we use are very similar to tensor networks (see, for example, the discussion in Appendix D A of [LV17]). A benefit of the graphical models that we use (including the corresponding terminology), is that they are compatible with the graphical models that are being used in classical information processing.

quantum-state channels as an equivalent description. A graphical notation for representing such channels is also presented in this section. Section 4.3 estimates the information rate of such channels. Section 4.4 considers the upper and lower bounds induced by auxiliary quantum-state channels, and presents methods for optimizing them. Section 4.5 contains numerical examples.

4.1 Review of (Classical) Finite-State Machine Channels: Information Rate, its Estimation, and Bounds

In this section, we review the methods developed in [ALV+06] for estimating the information rate of a (classical) FSMC, and the auxiliary-channel-induced upper and lower bounds studied in [SVS09]. As we will see, the development in later sections about quantum channels will have many similarities, but also some important differences. We emphasize that this section is a *brief review* of [ALV+06] and [SVS09] for the purpose of introducing necessary tools and ideas for later sections.

4.1.1 Finite-State Machine Channels (FSMCs) and their Graphical Representation

A (time-invariant) finite-state machine channel (FSMC) consists of an input alphabet \mathcal{X} , an output alphabet \mathcal{Y} , a state alphabet \mathcal{S} , all of which are finite, and a channel law $W(y, s'|x, s)$, where the latter equals the probability of receiving $y \in \mathcal{Y}$ and ending up in state $s' \in \mathcal{S}$ given the channel input $x \in \mathcal{X}$ and the previous channel state $s \in \mathcal{S}$. The relationship among the input, output, and state processes X_1^n, Y_1^n, S_0^n of n -channel uses can be described by the conditional PMF

$$W(\mathbf{y}_1^n, \mathbf{s}_1^n | \mathbf{x}_1^n, s_0) \triangleq P_{Y_1^n, S_1^n | X_1^n, S_0}(\mathbf{y}_1^n, \mathbf{s}_1^n | \mathbf{x}_1^n, s_0) = \prod_{\ell=1}^n W(y_\ell, s_\ell | x_\ell, s_{\ell-1}), \quad (4.4)$$

where $x_\ell \in \mathcal{X}$, $y_\ell \in \mathcal{Y}$, and $s_\ell \in \mathcal{S}$ for each ℓ .

Example 4.1 (Gilbert–Elliott channels). A notable class of examples of FSMCs are the Gilbert–Elliott channels [MB89], which behave like a binary symmetric channel (BSC) with cross-over probability p_s controlled by the channel state $s \in \{\text{“b”}, \text{“g”}\}$, where usually $|p_b - \frac{1}{2}| < |p_g - \frac{1}{2}|$. The state process itself is a first-order stationary

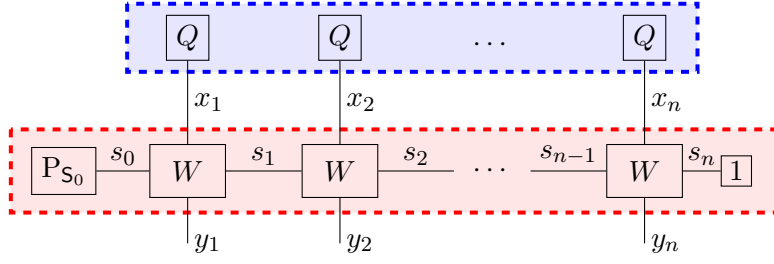


Figure 4.4: Channel with a classical state: closing the **top** box yields the input process $Q^{(n)}$, closing the **bottom** box yields the joint channel law $W(\mathbf{y}_1^n | \mathbf{x}_1^n)$.

ergodic Markov process that is independent of the input process.² (For more details, see, *e.g.*, the discussions in [SVS09].) \square

Given an input process $\{Q^{(n)}\}_n$ and an initial state PMF $P_{S_0}(s_0)$, we can write down the joint PMF of $(\mathbf{X}_1^n, \mathbf{Y}_1^n, \mathbf{S}_0^n)$ as

$$g(\mathbf{x}_1^n, \mathbf{y}_1^n, \mathbf{s}_0^n) \triangleq P_{\mathbf{X}_1^n, \mathbf{Y}_1^n, \mathbf{S}_0^n}(\mathbf{x}_1^n, \mathbf{y}_1^n, \mathbf{s}_0^n) = P_{S_0}(s_0) \cdot Q^{(n)}(\mathbf{x}_1^n) \cdot \prod_{\ell=1}^n W(y_\ell, s_\ell | x_\ell, s_{\ell-1}). \quad (4.5)$$

The factorization of $g(\mathbf{x}_1^n, \mathbf{y}_1^n, \mathbf{s}_0^n)$ as shown in (4.5) can be visualized with the help of an NFG as in Figure 4.4. In particular:

- a) The part of the factor graph inside the **bottom** box represents $W(\mathbf{y}_1^n, \mathbf{s}_1^n | \mathbf{x}_1^n, s_0)$, *i.e.*, the probability of obtaining \mathbf{y}_1^n and \mathbf{s}_1^n given \mathbf{x}_1^n and s_0 . After applying the “closing-the-box” operation (see Section 1.1.3) w.r.t. the **bottom** box, we obtain the joint channel law $W(\mathbf{y}_1^n | \mathbf{x}_1^n) \triangleq \sum_{\mathbf{s}_0^n} P_{S_0}(s_0) \cdot W(\mathbf{y}_1^n, \mathbf{s}_1^n | \mathbf{x}_1^n, s_0)$.
- b) The part of the factor graph inside the **top** box represents the input process $Q^{(n)}(\mathbf{x}_1^n)$. Here, for simplicity, the input process is an i.i.d. process characterized by the PMF Q , *i.e.*, $Q^{(n)}(\mathbf{x}_1^n) = \prod_{\ell=1}^n Q(x_\ell)$.
- c) The marginal function $g(\mathbf{x}_1^n, \mathbf{y}_1^n) \triangleq \sum_{\mathbf{s}_0^n} g(\mathbf{x}_1^n, \mathbf{y}_1^n, \mathbf{s}_0^n)$ is the marginal PMF of \mathbf{x}_1^n and \mathbf{y}_1^n . The marginal function $g(\mathbf{s}_0^n) \triangleq \sum_{\mathbf{x}_1^n, \mathbf{y}_1^n} g(\mathbf{x}_1^n, \mathbf{y}_1^n, \mathbf{s}_0^n)$ is the marginal PMF of \mathbf{s}_0^n . Other marginal PMFs can be obtained similarly.

Using the “closing-the-box” operations, such factor graph representations can be useful in computing a number of quantities of interests. For example, to prove that (4.4) is

²The independence of the state process on the input process is a particular feature of the Gilbert–Elliott channel. In general, the state process of a finite-state channel can depend on the input process.

indeed a valid conditional PMF, it suffices to show that

$$\sum_{\mathbf{s}_1^n, \mathbf{y}_1^n} W(\mathbf{y}_1^n, \mathbf{s}_1^n | \check{\mathbf{x}}_1^n, \check{s}_0) = 1 \quad \forall \check{\mathbf{x}}_1^n \in \mathcal{X}^n, \check{s}_0 \in \mathcal{S}, \quad (4.6)$$

which can be verified via a sequence of “closing-the-box” operations as shown in Figure D.1 in the Appendix D. Such techniques are at the heart of the information-rate-estimation methods as in [ALV+06]. The details are reviewed in the next subsection.

4.1.2 Information Rate Estimation

The approach of [ALV+06] for estimating information rate of FSMCs, as reviewed in this section, is based on the Shannon–McMillan–Breiman theorem (see *e.g.*, [CT06]) and suitable generalizations. We make the following assumptions.

- As already mentioned, the derivations in this chapter are for the case where the input process $\mathbf{X} = (\mathbf{X}_1, \mathbf{X}_2, \dots)$ is an i.i.d. process. The results can be generalized to other stationary ergodic input processes that can be represented by a finite-state-machine source (FSMS). Technically, this is done by defining a new state that combines the source state and the channel state.
- We assume that the FSMC is indecomposable, which roughly means that in the long term the behavior of the channel is independent of the initial channel state distribution P_{S_0} (see [Gal68, Section 4.6] for the exact definition). For such channels and stationary ergodic input processes, the information rate I_W in (4.3) is well defined.

Let $W(\mathbf{y}_1^n | \mathbf{x}_1^n)$ be the joint channel law of an FSMC satisfying the assumptions above. As aforementioned, the information rate of such a channel using the i.i.d. input distribution $\{Q^{(n)} \triangleq Q^{\otimes n}\}_n$ is given by (4.3), where the input process \mathbf{X}_1^n and the output process \mathbf{Y}_1^n are jointly distributed according to

$$P_{\mathbf{X}_1^n, \mathbf{Y}_1^n}(\mathbf{x}_1^n, \mathbf{y}_1^n) = \prod_{\ell=1}^n Q(x_\ell) \cdot W(\mathbf{y}_1^n | \mathbf{x}_1^n). \quad (4.7)$$

One can rewrite (4.3) as

$$I_W(Q) = H(\mathbf{X}) + H(\mathbf{Y}) - H(\mathbf{X}, \mathbf{Y}), \quad (4.8)$$

where the *entropic rates* $H(X)$, $H(Y)$ and $H(X, Y)$ are defined as

$$H(X) \triangleq \lim_{n \rightarrow \infty} \frac{1}{n} H(X_1^n), \quad (4.9)$$

$$H(Y) \triangleq \lim_{n \rightarrow \infty} \frac{1}{n} H(Y_1^n), \quad (4.10)$$

$$H(X, Y) \triangleq \lim_{n \rightarrow \infty} \frac{1}{n} H(X_1^n, Y_1^n). \quad (4.11)$$

We proceed as in [ALV+06]. (For more background information, see the references in [ALV+06], in particular [EM02].) Namely, because of (4.8) and

$$-\frac{1}{n} \log P_{X_1^n}(X_1^n) \xrightarrow{n \rightarrow \infty} H(X) \quad \text{in probability,} \quad (4.12)$$

$$-\frac{1}{n} \log P_{Y_1^n}(Y_1^n) \xrightarrow{n \rightarrow \infty} H(Y) \quad \text{in probability,} \quad (4.13)$$

$$-\frac{1}{n} \log P_{X_1^n, Y_1^n}(X_1^n, Y_1^n) \xrightarrow{n \rightarrow \infty} H(X, Y) \quad \text{in probability,} \quad (4.14)$$

by choosing some large number n , we have the approximation

$$I_W(Q) \approx -\frac{1}{n} \log P_{X_1^n}(\tilde{x}_1^n) - \frac{1}{n} \log P_{Y_1^n}(\tilde{y}_1^n) + \frac{1}{n} \log P_{X_1^n, Y_1^n}(\tilde{x}_1^n, \tilde{y}_1^n) \quad (4.15)$$

where \tilde{x}_1^n and \tilde{y}_1^n are some input and output sequences, respectively, randomly generated according to

$$P_{X_1^n, Y_1^n}(\tilde{x}_1^n, \tilde{y}_1^n) = \sum_{s_0^n} P_{S_0}(s_0) \cdot Q^{(n)}(\tilde{x}_1^n) \cdot W(\tilde{y}_1^n, s_1^n | \tilde{x}_1^n, s_0), \quad (4.16)$$

where $W(\tilde{y}_1^n, s_1^n | \tilde{x}_1^n, s_0)$ is defined in (4.4). Note that \tilde{x}_1^n can be obtained by simulating the input process, and \tilde{y}_1^n can be obtained by simulating the channel for the given input string \tilde{x}_1^n . The latter can be done by keeping track of $P_{Y_\ell | X_1^\ell, Y_1^{\ell-1}}(y_\ell | \tilde{x}_1^\ell, \tilde{y}_1^{\ell-1})$, which is proportional to $P_{Y_\ell, Y_1^{\ell-1} | X_1^\ell}(y_\ell, \tilde{y}_1^{\ell-1} | \tilde{x}_1^\ell)$, and can be efficiently calculated by applying suitable “closing-the-box” operations as in Figure D.3 in the Appendix D.

We continue by showing how the three terms appearing on the right-hand side of (4.15) can be computed efficiently. We show it explicitly for the second term, and then outline it for the first and the third term.

In order to efficiently compute the second term on the right-hand side of (4.15), *i.e.*, $-\frac{1}{n} \log P_{Y_1^n}(\tilde{y}_1^n)$, we consider the *state metric* defined in [ALV+06] as

$$\mu_\ell^Y(s_\ell) \triangleq \sum_{x_1^\ell} \sum_{s_0^{\ell-1}} P_{S_0}(s_0) \cdot Q^{(\ell)}(x_1^\ell) \cdot W(\tilde{y}_1^\ell, s_1^\ell | x_1^\ell, s_0). \quad (4.17)$$

In this case,

$$P_{Y_1^n}(\tilde{y}_1^n) = \sum_{s_n} \mu_n^Y(s_n), \quad (4.18)$$

and the calculation of $\mu_\ell^Y(s_\ell)$ can be done iteratively as

$$\mu_\ell^Y(s_\ell) = \sum_{x_\ell} \sum_{s_{\ell-1}} \mu_{\ell-1}^Y(s_{\ell-1}) \cdot Q(x_\ell | \mathbf{x}_1^{\ell-1}) \cdot W(\check{y}_\ell, s_\ell | x_\ell, s_{\ell-1}) \quad (4.19)$$

$$= \sum_{x_\ell} \sum_{s_{\ell-1}} \mu_{\ell-1}^Y(s_{\ell-1}) \cdot Q(x_\ell) \cdot W(\check{y}_\ell, s_\ell | x_\ell, s_{\ell-1}). \quad (4.20)$$

Eq. (4.20) is visualized in Figure D.5 as applying suitable “closing-the-box” operations to the NFG in Figure 4.4.

However, since the value of $\mu_\ell^Y(s_\ell)$ tends to zero as ℓ grows, such recursive calculations are numerically inconvenient. A solution is to *normalize* $\mu_\ell^Y(s_\ell)$ after each use of (4.20) and to keep track of the scaling coefficients. Namely,

$$\bar{\mu}_\ell^Y(s_\ell) \triangleq \frac{1}{\lambda_\ell^Y} \sum_{x_\ell} \sum_{s_{\ell-1}} \bar{\mu}_{\ell-1}^Y(s_{\ell-1}) \cdot Q(x_\ell) \cdot W(\check{y}_\ell, s_\ell | x_\ell, s_{\ell-1}), \quad (4.21)$$

where the scaling factor $\lambda_\ell^Y > 0$ is chosen such that $\sum_{s_\ell} \bar{\mu}_\ell^Y(s_\ell) = 1$. With this, Eq. (4.18) can be rewritten as

$$P_{Y_1^n}(\check{\mathbf{y}}_1^n) = \prod_{\ell=1}^n \lambda_\ell^Y. \quad (4.22)$$

Finally, we arrive at the following efficient procedure for computing $-\frac{1}{n} \log P_{Y_1^n}(\check{\mathbf{y}}_1^n)$:

- For $\ell = 1, \dots, n$, iteratively compute the normalized state metric and with that the scaling factors λ_ℓ^Y .
- Conclude with the result

$$-\frac{1}{n} \log P_{Y_1^n}(\check{\mathbf{y}}_1^n) = \frac{1}{n} \sum_{\ell=1}^n \log(\lambda_\ell^Y). \quad (4.23)$$

The third term on the right-hand side of (4.15) can be evaluated by an analogous procedure, where the state metric $\mu_\ell^Y(s_\ell)$ is replaced by the state metric

$$\mu_\ell^{XY}(s_\ell) \triangleq \sum_{\mathbf{s}_0^{\ell-1}} P_{S_0}(s_0) \cdot Q^{(\ell)}(\check{\mathbf{x}}_1^\ell) \cdot W(\check{\mathbf{y}}_1^\ell, \mathbf{s}_1^\ell | \check{\mathbf{x}}_1^\ell). \quad (4.24)$$

The iterative calculation of $\mu_\ell^{XY}(s_\ell)$ is visualized in Figure D.7.

Finally, the first term on the right-hand side of (4.15) can be trivially evaluated if \mathbf{X} is an i.i.d. process, and with a similar approach as above if it is described by an FSMS.

The above discussion is summarized as Algorithm 4.1. On the side, note that for each $\ell = 2, \dots, n$, the quantities λ_ℓ^Y and λ_ℓ^{XY} in the algorithm are the conditional probabilities $P_{Y_\ell | Y_1^{\ell-1}}(\check{y}_\ell | \check{\mathbf{y}}_1^{\ell-1})$ and $P_{X_\ell Y_\ell | X_1^{\ell-1} Y_1^{\ell-1}}(\check{x}_\ell, \check{y}_\ell | \check{\mathbf{x}}_1^{\ell-1}, \check{\mathbf{y}}_1^{\ell-1})$, respectively.

Algorithm 4.1 Estimating the Information Rate of an FSMC

Input: An indecomposable FSMC channel law W , a input distribution Q , a positive integer n large enough.

Output: $I_W(Q) \approx \mathbf{H}(\mathbf{X}) + \hat{\mathbf{H}}(\mathbf{Y}) - \hat{\mathbf{H}}(\mathbf{X}, \mathbf{Y})$.

- 1: Initialize the channel state distribution P_{S_0} as a uniform distribution over \mathcal{S}
 - 2: Generate an input sequence $\tilde{\mathbf{x}}_1^n \sim Q^{\otimes n}$
 - 3: Generate a corresponding output sequence $\tilde{\mathbf{y}}_1^n$
 - 4: $\bar{\mu}_0^Y \leftarrow P_{S_0}$
 - 5: **for each** $\ell = 1, \dots, n$ **do**
 - 6: $\mu_\ell^Y(s_\ell) \leftarrow \sum_{x_\ell, s_{\ell-1}} \bar{\mu}_{\ell-1}^Y(s_{\ell-1}) \cdot Q(x_\ell) \cdot W(\tilde{y}_\ell, s_\ell | x_\ell, s_{\ell-1})$
 - 7: $\lambda_\ell^Y \leftarrow \sum_{s_\ell} \mu_\ell^Y(s_\ell)$;
 - 8: $\bar{\mu}_\ell^Y \leftarrow \mu_\ell^Y / \lambda_\ell^Y$
 - 9: **end for**
 - 10: $\hat{\mathbf{H}}(\mathbf{Y}) \leftarrow -\frac{1}{n} \sum_{\ell=1}^n \log(\lambda_\ell^Y)$
 - 11: $\bar{\mu}_0^{XY} \leftarrow P_{S_0}$
 - 12: **for each** $\ell = 1, \dots, n$ **do**
 - 13: $\mu_\ell^{XY}(s_\ell) \leftarrow \sum_{s_{\ell-1}} \bar{\mu}_{\ell-1}^{XY}(s_{\ell-1}) \cdot Q(\tilde{x}_\ell) \cdot W(\tilde{y}_\ell, s_\ell | \tilde{x}_\ell, s_{\ell-1})$
 - 14: $\lambda_\ell^{XY} \leftarrow \sum_{s_\ell} \mu_\ell^{XY}(s_\ell)$
 - 15: $\bar{\mu}_\ell^{XY} \leftarrow \mu_\ell^{XY} / \lambda_\ell^{XY}$
 - 16: **end for**
 - 17: $\hat{\mathbf{H}}(\mathbf{X}, \mathbf{Y}) \leftarrow -\frac{1}{n} \sum_{\ell=1}^n \log(\lambda_\ell^{XY})$
 - 18: $\mathbf{H}(\mathbf{X}) \leftarrow -\sum_x Q(x) \log Q(x)$
 - 19: Estimate $I_W(Q)$ as $\mathbf{H}(\mathbf{X}) + \hat{\mathbf{H}}(\mathbf{Y}) - \hat{\mathbf{H}}(\mathbf{X}, \mathbf{Y})$.
-

4.1.3 Auxiliary Channels and Bounds on the Information Rate

As mentioned earlier in this chapter, auxiliary channels³ are introduced when the state space of the FSMC is too large, making the calculation in Algorithm 4.1 (practically) intractable. More precisely, given an auxiliary forward FSMC (AF-FSMC) $\hat{W}(y_\ell, \hat{s}_\ell | x_\ell, \hat{s}_{\ell-1})$ and an auxiliary backward FSMC (AB-FSMC) $\hat{V}(x_\ell, \hat{s}_\ell | y_\ell, \hat{s}_{\ell-1})$, a pair of upper and lower bounds of the information rate is given in [ALV+06; SVS09] as

$$\bar{I}_W^{(n)}(\hat{W}) \triangleq \frac{1}{n} \sum_{\mathbf{x}_1^n, \mathbf{y}_1^n} Q(\mathbf{x}_1^n) W(\mathbf{y}_1^n | \mathbf{x}_1^n) \log \frac{W(\mathbf{y}_1^n | \mathbf{x}_1^n)}{(Q\hat{W})(\mathbf{y}_1^n)}, \quad (4.25)$$

$$I_W^{(n)}(\hat{V}) \triangleq \frac{1}{n} \sum_{\mathbf{x}_1^n, \mathbf{y}_1^n} Q(\mathbf{x}_1^n) W(\mathbf{y}_1^n | \mathbf{x}_1^n) \log \frac{\hat{V}(\mathbf{x}_1^n | \mathbf{y}_1^n)}{Q(\mathbf{x}_1^n)}, \quad (4.26)$$

where $(Q\hat{W})(\mathbf{y}_1^n) \triangleq \sum_{\mathbf{x}_1^n} Q(\mathbf{x}_1^n) \cdot \hat{W}(\mathbf{y}_1^n | \mathbf{x}_1^n)$. To see that (4.25) and (4.26) are, respectively, upper and lower bounds, one can verify that

$$\bar{I}_W(\hat{W}) - I_W = \frac{1}{n} D\left((QW)(\mathbf{Y}_1^n) \parallel (Q\hat{W})(\mathbf{Y}_1^n)\right), \quad (4.27)$$

$$I_W - I_W(\hat{V}) = \frac{1}{n} \sum_{\mathbf{y}_1^n} (QW)(\mathbf{y}_1^n) \cdot D\left(V(\mathbf{X}_1^n | \mathbf{y}_1^n) \parallel \hat{V}(\mathbf{X}_1^n | \mathbf{y}_1^n)\right), \quad (4.28)$$

where the backward channel $V(\mathbf{x} | \mathbf{y})$ is defined as $V(\mathbf{x} | \mathbf{y}) \triangleq Q(\mathbf{x}) W(\mathbf{y} | \mathbf{x}) / (QW)(\mathbf{y})$. In particular, given an AF-FSMC \hat{W} , [SVS09] considered the induced AB-FSMC $\hat{V}(\mathbf{x} | \mathbf{y}) \triangleq Q(\mathbf{x}) \hat{W}(\mathbf{y} | \mathbf{x}) / (Q\hat{W})(\mathbf{y})$. In this case,

$$I_W^{(n)}(\hat{V}) = \frac{1}{n} \sum_{\mathbf{x}_1^n, \mathbf{y}_1^n} Q(\mathbf{x}_1^n) W(\mathbf{y}_1^n | \mathbf{x}_1^n) \log \frac{\hat{W}(\mathbf{y}_1^n | \mathbf{x}_1^n)}{(Q\hat{W})(\mathbf{y}_1^n)}. \quad (4.29)$$

The difference function $\Delta_W^{(n)}(\hat{W})$ is defined as

$$\begin{aligned} \Delta_W^{(n)}(\hat{W}) &\triangleq \bar{I}_W^{(n)}(\hat{W}) - I_W^{(n)}(\hat{V}) \\ &= \frac{1}{n} \sum_{\mathbf{x}_1^n, \mathbf{y}_1^n} Q(\mathbf{x}_1^n) W(\mathbf{y}_1^n | \mathbf{x}_1^n) \log \frac{W(\mathbf{y}_1^n | \mathbf{x}_1^n)}{\hat{W}(\mathbf{y}_1^n | \mathbf{x}_1^n)} \\ &= \frac{1}{n} D\left(Q(\mathbf{X}_1^n) W(\mathbf{Y}_1^n | \mathbf{X}_1^n) \parallel Q(\mathbf{X}_1^n) \hat{W}(\mathbf{Y}_1^n | \mathbf{X}_1^n)\right). \end{aligned} \quad (4.30)$$

Apparently, $\Delta_W^{(n)}(\hat{W}) \geq 0$, and equality holds if and only if $\hat{W}(\mathbf{y}_1^n | \mathbf{x}_1^n) = W(\mathbf{y}_1^n | \mathbf{x}_1^n)$ for all \mathbf{x}_1^n and \mathbf{y}_1^n with positive support w.r.t. $P_{\mathbf{X}_1^n, \mathbf{Y}_1^n}$ as in (4.7). An efficient algorithm for

³Technically speaking, an auxiliary channel can be defined as *any* channel with the same input/output alphabet. For example, an auxiliary channel for an FSMC can be just another FSMC with smaller state space; in contrast, in Section 4.4, an auxiliary channel can also be a quantum-state channel.

finding a local minimum of the difference function was proposed in [SVS09]; we refer to [SVS09] for further details.

4.2 Quantum Channel with Memory and their Graphical Representation

In this section, we formalize our notations and modeling of quantum channels with memory [BM04; KW05; CGLM14] and of classical communications over such channels. In particular, we will define a class of channels named *quantum-state channels*, which is an alternative description of the classical communications over quantum channels with memory. In addition, we will introduce several NFGs for representing these channels and processes.

4.2.1 Classical Communication over a Quantum Channel with Memory

As mentioned earlier in this chapter, we define a quantum channel with memory as follows.

Definition 4.2. A *quantum channel with memory* is a CPTP map:

$$\mathcal{N} : \mathfrak{D}(\mathcal{H}_A \otimes \mathcal{H}_S) \rightarrow \mathfrak{D}(\mathcal{H}_B \otimes \mathcal{H}_{S'}), \quad (4.31)$$

where A is the input system, B is the output system, S and S' are, respectively, the memory systems before and after the channel use. The Hilbert spaces \mathcal{H}_A , \mathcal{H}_B , and $\mathcal{H}_S = \mathcal{H}_{S'}$ are the state spaces corresponding to those systems. \square

We consider classical communication over such channels using some separable input ensemble and local output measurements; namely, the encoder and decoder are, respectively, some classical-to-quantum and quantum-to-classical channels involving a single input or output system. In particular, given an ensemble $\{\rho_A^{(x)}\}_{x \in \mathcal{X}}$ and a measurement $\{\Lambda_B^{(y)}\}_{y \in \mathcal{Y}}$, we define the encoding and decoding function, respectively, as

$$\text{Encoding } \mathcal{E} : P_X \mapsto \sum_{x \in \mathcal{X}} P_X(x) \rho_A^{(x)} \quad \forall P_X \text{ PMF over } \mathcal{X}, \quad (4.32)$$

$$\text{Decoding } \mathcal{D} : \sigma_B \mapsto \left\{ \text{tr}(\Lambda_B^{(y)} \cdot \sigma_B) \right\}_{y \in \mathcal{Y}} \quad \forall \sigma_B \in \mathfrak{L}_+(\mathcal{H}_B). \quad (4.33)$$

We emphasize that in our setup, the ensemble $\{\rho_A^{(x)}\}_{x \in \mathcal{X}}$ and measurements $\{\Lambda_B^{(y)}\}_{y \in \mathcal{Y}}$ are given and fixed. Furthermore, we assume that one does not have access to the memory systems of the channel. For the case of i.i.d. inputs, the memory system S before each channel use shall be independent of the input system A , namely, the joint memory-input operator shall take the form of $\rho_A \otimes \rho_S$ at each channel input.⁴

With this, the probability of receiving $y \in \mathcal{Y}$, given that $x \in \mathcal{X}$ was sent and given that the density operator of the memory system *before* the usage of the channel was ρ_S , equals

$$P_{Y|X;S}(y|x; \rho_S) = \text{tr} \left(\Lambda_B^{(y)} \cdot \text{tr}_{S'} \left(\mathcal{N}(\rho_A^{(x)} \otimes \rho_S) \right) \right), \quad (4.34)$$

which can also be written as

$$P_{Y|X;S}(y|x; \rho_S) = \text{tr} \left((\Lambda_B^{(y)} \otimes I_S) \cdot \mathcal{N}(\rho_A^{(x)} \otimes \rho_S) \right). \quad (4.35)$$

Moreover, assuming that y was observed, the density operator of the memory system *after* the channel use is given by

$$\rho_{S'} = \frac{\text{tr}_B \left((\Lambda_B^{(y)} \otimes I_S) \cdot \mathcal{N}(\rho_A^{(x)} \otimes \rho_S) \right)}{\text{tr} \left((\Lambda_B^{(y)} \otimes I_S) \cdot \mathcal{N}(\rho_A^{(x)} \otimes \rho_S) \right)}. \quad (4.36)$$

Notice that the denominator in (4.36) equals the expressions in (4.34) and (4.35). One should note that, though the input and the memory systems are independent before each channel use (given i.i.d. inputs), the output and the memory systems after each channel use can be correlated or even entangled. In particular, this translates to the fact that the measurement outcome y can have an influence on the memory system as indicated in (4.36).

Consider using the channel n times consecutively with the above scheme. The joint channel law, namely the conditional PMF of the channel outputs Y_1^n given the channel inputs X_1^n and the initial channel state ρ_{S_0} , can be computed iteratively using (4.35) and (4.36). In particular, the joint conditional PMF can be computed as

$$P_{Y_1^n | X_1^n; S_0}(y_1^n | x_1^n; \rho_{S_0}) = \prod_{\ell=1}^n P_{Y_\ell | X_\ell; S_{\ell-1}}(y_\ell | x_\ell; \rho_{S_{\ell-1}}), \quad (4.37)$$

where we compute the density operators $\{\rho_{S_\ell}\}_{\ell=1}^n$ iteratively using (4.36) as

$$\rho_{S_\ell} = \frac{\text{tr}_B \left((\Lambda_B^{(y_\ell)} \otimes I_S) \cdot \mathcal{N}(\rho_A^{(x_\ell)} \otimes \rho_{S_{\ell-1}}) \right)}{\text{tr} \left((\Lambda_B^{(y_\ell)} \otimes I_S) \cdot \mathcal{N}(\rho_A^{(x_\ell)} \otimes \rho_{S_{\ell-1}}) \right)}. \quad (4.38)$$

⁴More generally, for FSMSSs, this statement also holds by conditioning on all previous inputs.

4.2.2 Quantum-State Channels

For each channel-ensemble-measurement configuration $(\mathcal{N}, \{\rho_A^{(x)}\}_{x \in \mathcal{X}}, \{\Lambda_B^{(y)}\}_{y \in \mathcal{Y}})$ as introduced above, one ends up with a joint conditional PMF, as in (4.37). However, this relationship is not bijective. In particular, consider some unitary operators U_A and U_B acting on \mathcal{H}_A and \mathcal{H}_B , respectively. The following setup induces exactly the same joint conditional PMF:

$$\begin{aligned} \tilde{\mathcal{N}} : \tilde{\rho}_{AS} &\mapsto (U_B \otimes I_S) \cdot \mathcal{N} \left((U_A \otimes I_S) \tilde{\rho}_{AS} (U_A^\dagger \otimes I_S) \right) \cdot (U_B^\dagger \otimes I_S), \\ \tilde{\rho}_A^{(x)} &\triangleq U_A^\dagger \cdot \rho_A^{(x)} \cdot U_A & \forall x \in \mathcal{X}, \\ \tilde{\Lambda}_B^{(y)} &\triangleq U_B^\dagger \cdot \Lambda_B^{(y)} \cdot U_B & \forall y \in \mathcal{Y}. \end{aligned}$$

Such redundancy is not only tedious, but also detrimental when we try to compare different channels; in particular, when we try to introduce proper auxiliary channels to approximate the original communication scheme.

In this subsection, we introduce a class of channels called *quantum-state channels* to eliminate such redundancies. In particular, notice that the statistical behavior of the aforementioned communication scheme is fully specified via (4.35) and (4.36); which are in turn determined by the set of completely positive mappings $\{\mathcal{N}^{y|x}\}_{x \in \mathcal{X}, y \in \mathcal{Y}}$ defined as

$$\mathcal{N}^{y|x} : \rho_S \mapsto \text{tr}_B \left((\Lambda_B^{(y)} \otimes I_S) \cdot \mathcal{N}(\rho_A^{(x)} \otimes \rho_S) \right). \quad (4.39)$$

In this case, (4.35), (4.36), and (4.37) can be rewritten, respectively, as

$$P_{Y|X,S}(y|x; \rho_S) = \text{tr} \left(\mathcal{N}^{y|x}(\rho_S) \right), \quad (4.40)$$

$$\rho_{S'} = \mathcal{N}^{y|x}(\rho_S) / \text{tr} \left(\mathcal{N}^{y|x}(\rho_S) \right), \quad (4.41)$$

$$P_{Y_1^n | X_1^n; S_0}(\mathbf{y}_1^n | \mathbf{x}_1^n; \rho_{S_0}) = \text{tr} \left(\mathcal{N}^{y_n|x_n} \circ \dots \circ \mathcal{N}^{y_1|x_1}(\rho_{S_0}) \right). \quad (4.42)$$

Thus, the operators $\{\mathcal{N}^{y|x}\}_{x \in \mathcal{X}, y \in \mathcal{Y}}$ fully specify the joint conditional PMF as in (4.42). Moreover, such specification is also *unique*; namely, any two sets of channel-ensemble-measurement configuration shall end up with the same joint channel law if and only if the mappings defined in (4.39) are identical. This inspires us to make the following definition.

Definition 4.3 (Quantum-State Channel). A (finite indexed) set of completely positive operators $\{\mathcal{N}^{y|x}\}_{x \in \mathcal{X}, y \in \mathcal{Y}}$ (acting on the same Hilbert space) is said to be a

(classical-input classical-output) quantum-state channel (CC-QSC) if $\sum_{y \in \mathcal{Y}} \mathcal{N}^{y|x}$ is trace-preserving for each $x \in \mathcal{X}$. \square

Given any channel-ensemble-measurement configuration as described in Section 4.2.1, one can always define a corresponding CC-QSC by (4.39). On the other hand, as stated in the proposition below, the converse is also true.

Proposition 4.4. *For any CC-QSC $\{\mathcal{N}^{y|x}\}_{x \in \mathcal{X}, y \in \mathcal{Y}}$, there exists some quantum channel with memory \mathcal{N} as in (4.31) such that (4.39) holds with the ensemble $\{\rho_{\mathbf{A}}^{(x)} = |x\rangle\langle x|\}_{x \in \mathcal{X}}$ and the measurement $\{\Lambda_{\mathbf{B}}^{(y)} = |y\rangle\langle y|\}_{y \in \mathcal{Y}}$. Here, $\mathcal{H}_{\mathbf{A}}$ and $\mathcal{H}_{\mathbf{B}}$ are defined such that $\{|x\rangle\}_x$ and $\{|y\rangle\}_y$ are orthonormal bases of $\mathcal{H}_{\mathbf{A}}$ and $\mathcal{H}_{\mathbf{B}}$, respectively.*

Proof. It suffices to show that there exists a CPTP map $\mathcal{N} : \mathfrak{D}(\mathcal{H}_{\mathbf{A}} \otimes \mathcal{H}_{\mathbf{S}}) \rightarrow \mathfrak{D}(\mathcal{H}_{\mathbf{B}} \otimes \mathcal{H}_{\mathbf{S}})$ such that for all $\rho_{\mathbf{S}} \in \mathfrak{D}(\mathcal{H}_{\mathbf{S}})$, and $x \in \mathcal{X}$,

$$\mathcal{N} : |x\rangle\langle x| \otimes \rho_{\mathbf{S}} \mapsto \sum_{y \in \mathcal{Y}} |y\rangle\langle y| \otimes \mathcal{N}^{y|x}(\rho_{\mathbf{S}}).$$

Such an \mathcal{N} can be constructed as

$$\mathcal{N} : \rho \mapsto \sum_{x, y, k} \left(|y\rangle\langle x| \otimes E_k^{y|x} \right) \cdot \rho \cdot \left(|y\rangle\langle x| \otimes E_k^{y|x} \right)^{\dagger},$$

where $\{E_k^{y|x}\}_k$ is a Kraus representation of $\mathcal{N}^{y|x}$. It remains to check if \mathcal{N} is a CPTP, which is indeed the case:

$$\begin{aligned} \sum_{x, y, k} \left(|y\rangle\langle x| \otimes E_k^{y|x} \right)^{\dagger} \cdot \left(|y\rangle\langle x| \otimes E_k^{y|x} \right) &= \sum_x \sum_{y, k} |x\rangle\langle x| \otimes (E_k^{y|x})^{\dagger} E_k^{y|x} \\ &= \sum_x |x\rangle\langle x| \otimes I = I. \end{aligned} \quad \square$$

4.2.3 Visualization using Normal Factor Graphs

In this subsection, we focus on the computations of (4.40), (4.41), and (4.42) for the situation where the involved channel \mathcal{N} is of finite dimension. In analogy to the FSMCs, we demonstrate how to use NFGs to facilitate and visualize the relevant computations (see Section 2.1.1 and [LV17]).

By Proposition 4.4, let us consider a CC-QSC $\{\mathcal{N}^{y|x}\}_{x \in \mathcal{X}, y \in \mathcal{Y}}$ acting on $\mathcal{H}_{\mathbf{S}}$, where $d = \dim(\mathcal{H}_{\mathbf{S}})$ is finite, and $\{|s\rangle\}_{s \in \mathcal{S}}$ is an orthonormal basis of $\mathcal{H}_{\mathbf{S}}$. (Apparently,

$|\mathcal{S}| = d$.) Since for each x and y , $\mathcal{N}^{y|x}$ is a completely positive map, there must exist finitely many (not necessarily unique) matrices $\{F_k^{y|x} \in \mathbb{C}^{\mathcal{S} \times \mathcal{S}}\}_k$ such that

$$[\mathcal{N}^{y|x}(\rho_{\mathcal{S}})] = \sum_k F_k^{y|x} \cdot [\rho_{\mathcal{S}}] \cdot (F_k^{y|x})^\dagger \quad \forall \rho_{\mathcal{S}} \in \mathfrak{D}(\mathcal{H}_{\mathcal{S}}), \quad (4.43)$$

where $[\mathcal{N}^{y|x}(\rho_{\mathcal{S}})]$ and $[\rho_{\mathcal{S}}]$ are, respectively, the matrix representation of the operator $\mathcal{N}^{y|x}(\rho_{\mathcal{S}})$ and $\rho_{\mathcal{S}}$ under $\{|s\rangle\}_{s \in \mathcal{S}}$. The reason for such matrices $\{F_k^{y|x}\}_k$ to exist is the same as for the Kraus operators of CPTP maps (see Theorem 1.42). Also note that $\sum_{y \in \mathcal{Y}} \mathcal{E}^{y|x}$ is trace-preserving, thus it must hold that

$$\sum_{y \in \mathcal{Y}} \sum_k (F_k^{y|x})^\dagger F_k^{y|x} = I \quad \forall x \in \mathcal{X}. \quad (4.44)$$

Now, define a set of functions $\{W^{y|x}\}_{x \in \mathcal{X}, y \in \mathcal{Y}}$ as

$$W^{y|x} : (s', s, \tilde{s}', \tilde{s}) \mapsto \sum_k F_k^{y|x}(s', s) \overline{F_k^{y|x}(\tilde{s}', \tilde{s})}, \quad (4.45)$$

where $s', s, \tilde{s}', \tilde{s} \in \mathcal{S}$ are indices of the corresponding matrices, namely, $F_k^{y|x}(s', s)$ is the (s', s) -th entry of the matrix $F_k^{y|x}$. In this case, one can rewrite (4.40), (4.41) and (4.42), respectively, into

$$P_{Y|X;S}(y|x; \rho_{\mathcal{S}}) = \sum_{\substack{s', \tilde{s}': \\ s' = \tilde{s}'}} \sum_{s, \tilde{s}} W^{y|x}(s', s, \tilde{s}', \tilde{s}) \cdot [\rho_{\mathcal{S}}]_{s, \tilde{s}}, \quad (4.46)$$

$$[\rho_{\mathcal{S}'}]_{s', \tilde{s}'} = \frac{\sum_{s, \tilde{s}} W^{y|x}(s', s, \tilde{s}', \tilde{s}) \cdot [\rho_{\mathcal{S}}]_{s, \tilde{s}}}{\sum_{\substack{s', \tilde{s}': \\ s' = \tilde{s}'}} \sum_{s, \tilde{s}} W^{y|x}(s', s, \tilde{s}', \tilde{s}) \cdot [\rho_{\mathcal{S}}]_{s, \tilde{s}}}, \quad (4.47)$$

$$P_{Y_1^n | X_1^n; S_0}(\mathbf{y}_1^n | \mathbf{x}_1^n; \rho_{S_0}) = \sum_{\substack{s_n, \tilde{s}_n: \\ s_n = \tilde{s}_n}} \sum_{\substack{s_0^{n-1}, \tilde{s}_0^{n-1}}} [\rho_{S_0}]_{s_0, \tilde{s}_0} \cdot \prod_{\ell=1}^n W^{y_\ell | x_\ell}(s_\ell, s_{\ell-1}, \tilde{s}_\ell, \tilde{s}_{\ell-1}). \quad (4.48)$$

By rearranging the entries of $W^{y|x}$ (for each x, y) into a matrix $[W^{y|x}] \in \mathbb{C}^{\mathcal{S}^2 \times \mathcal{S}^2}$ as

$$[W^{y|x}]_{(s', \tilde{s}'), (s, \tilde{s})} \triangleq W^{y|x}(s', s, \tilde{s}', \tilde{s}), \quad (4.49)$$

where $(s', \tilde{s}') \in \mathcal{S}^2$ is the first index, and $(s, \tilde{s}) \in \mathcal{S}^2$ is the second index of $[W^{y|x}]$, we can simplify (4.46), (4.47), and (4.48) as

$$P_{Y|X;S}(y|x; \rho_{\mathcal{S}}) = \text{tr}([W^{y|x}] \cdot [\rho_{\mathcal{S}}]), \quad (4.50)$$

$$[\rho_{\mathcal{S}'}] = \frac{[W^{y|x}] \cdot [\rho_{\mathcal{S}}]}{\text{tr}([W^{y|x}] \cdot [\rho_{\mathcal{S}}])}, \quad (4.51)$$

$$P_{Y_1^n | X_1^n; S_0}(\mathbf{y}_1^n | \mathbf{x}_1^n; \rho_{S_0}) = \text{tr}([W^{y_n | x_n}] \cdots [W^{y_1 | x_1}] \cdot [\rho_{S_0}]), \quad (4.52)$$

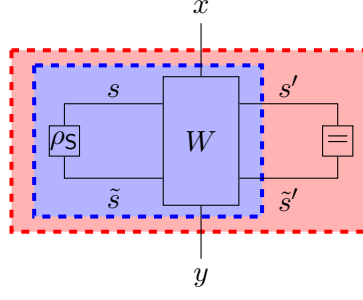
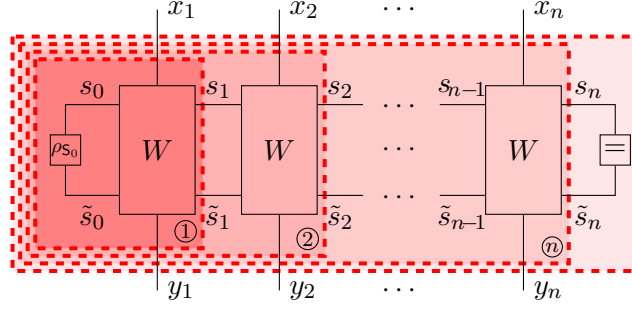
Figure 4.5: Representation of $\{W^{y|x}\}_{x,y}$ using an NFG.

Figure 4.6: The joint channel law (4.48) and (4.52) can be visualized as the result of the “closing of the **outermost** box” above, which can in turn be carried out by a sequence of “closing-the-box” operations as indicated.

respectively. Here we treat $[\rho_S]$ as a length- d^2 vector indexed by $(s, \tilde{s}) \in \mathcal{S}^2$ in the above equations.

By considering $\{W^{y|x}\}_{x,y}$ as a function of six variables, we can represent it using a factor vertex of degree six in an NFG as in Figure 4.5. In this case, Eqs. (4.46) and (4.50) can be visualized as “closing the **outer** box” in the factor graph. Similarly, (4.47) and (4.51) can be visualized as “closing the **inner** box”. The factor graph corresponding to using the channel n times consecutively is depicted in Figure 4.6, where (4.48) and (4.52) are visualized as closing the **outermost** box. Interestingly, this “closing-the-box” operation can be carried out by a sequence of simpler “closing-the-box” operations as shown in the figure.

A number of statistical quantities and density operators of interest can be computed and visualized as “closing-the-box” operations on suitable NFGs similar to that of Figure 4.6. The following example highlights how quantities of this kind can be computed in such a manner.

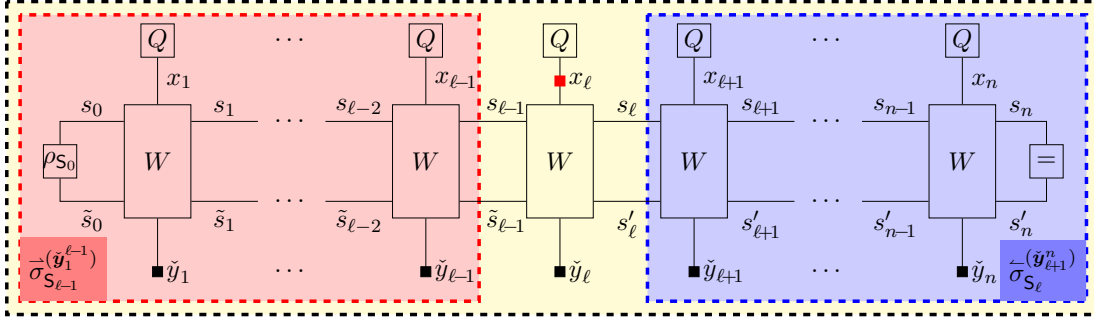


Figure 4.7: Computation of the marginal PMF $P_{X_\ell|Y_1^n; S_0}$ using a sequence of “closing-the-box” operations.

Example 4.5 (BCJR [BCJR74] decoding for CC-QSCs). For fixed $\tilde{y}_1^n \in \mathcal{Y}^n$ and a given initial density operator ρ_{S_0} , the conditional probability $P_{X_\ell|Y_1^n; S_0}(x_\ell|\tilde{y}_1^n; \rho_{S_0})$ can be computed via

$$P_{X_\ell|Y_1^n; S_0}(\cdot|\tilde{y}_1^n; \rho_{S_0}) \propto P_{X_\ell, Y_1^n|S_0}(\cdot, \tilde{y}_1^n|\rho_{S_0}), \quad (4.53)$$

where the right-hand side of (4.53) is a marginal PMF defined as

$$P_{X_\ell, Y_1^n|S_0}(x_\ell, \tilde{y}_1^n|\rho_{S_0}) = \sum_{\mathbf{x}_1^{\ell-1}, \mathbf{x}_{\ell+1}^n} \sum_{\mathbf{s}_0^n, \tilde{\mathbf{s}}_0^n} [\rho_{S_0}]_{s_0, \tilde{s}_0} \cdot \prod_{i=1}^n Q(x_i) \cdot \prod_{j=1}^n W^{\tilde{y}_j|x_j}(s_j, s_{j-1}, \tilde{s}_j, \tilde{s}_{j-1}), \quad (4.54)$$

where we have assumed that the input process X_1^n is i.i.d. characterized by some PMF Q . The evaluation of (4.54) can be carried out efficiently using a sequence of “closing-the-box” operations as visualized in Figure 4.7. These operations can be roughly divided into the following three steps:

1. Closing the **left inner** box: this results in an operator $\bar{\sigma}_{S_{\ell-1}}^{(\tilde{y}_1^{\ell-1})}$ on $\mathcal{H}_{S_{\ell-1}}$.
2. Closing the **right inner** box: this results in another operator $\bar{\sigma}_{S_\ell}^{(\tilde{y}_{\ell+1}^n)}$ on \mathcal{H}_{S_ℓ} .
3. Applying the “closing-the-box” operation to the yellow box: the result is the marginal PMF $P_{X_\ell, Y_1^n|S_0}(x_\ell, \tilde{y}_1^n|\rho_{S_0})$, from which the desired conditional probability $P_{X_\ell|Y_1^n; S_0}(x_\ell|\tilde{y}_1^n; \rho_{S_0})$ can be easily obtained by normalization.

The operators mentioned in 1) and 2) can be computed recursively, using a sequence of “closing-the-box” operations. Namely, one can carry out the computations in 1) consecutively with $\ell = 1, 2, \dots, n$; and the computations in 2) consecutively with $\ell = n, n-1, \dots, 1$. This provides an efficient way to evaluate $P_{X_\ell|Y_1^n; S_0}(x_\ell|\tilde{y}_1^n; \rho_{S_0})$ for each

$\ell = 1, \dots, n$; and thus provides an efficient symbol-wise decoding algorithm. The idea in this example is conceptually identical to that of the BCJR decoding algorithm for an FSMC. \square

As shown in the above example, very often the desired functions or quantities are based on the same partial results. The NFG framework is very helpful to visualize these partial results and to show how they can be combined to obtain the desired functions and quantities.

We emphasize that the functions $\{W^{y|x}\}_{x,y}$ defined in (4.45) are unique for a given finite-dimensional CC-QSC $\{\mathcal{N}^{y|x}\}_{x,y}$; even though such uniqueness does not apply to the Kraus operators $\{F^{y|x}\}_k$ being used to define $\{W^{y|x}\}_{x,y}$. This can be proven by making the identification that

$$[\mathcal{N}^{y|x}(\rho_S)] = [W^{y|x}] \cdot [\rho_S] \quad \forall \rho_S \in \mathfrak{D}(\mathcal{H}_S) \quad (4.55)$$

for all x and y . Moreover, we argue that the functions $\{W^{y|x}\}_{x,y}$, are an *equivalent* way to specify a CC-QSC, or classical communication over a quantum channel with memory as described at the beginning of this section. Namely, for any set of complex-valued functions $\{W^{y|x}\}_{x,y}$ on \mathcal{S}^4 satisfying some constraints to be clarified later, there must exist a unique CC-QSC $\{\mathcal{N}^{y|x}\}_{x,y}$ such that (4.55) holds; and thus, there must exist some corresponding channel-ensemble-measurement configuration, unique up to its channel law. As for such constraints, we rearrange the entries of $W^{y|x}$ (for each x, y) into another matrix $\llbracket W^{y|x} \rrbracket \in \mathbb{C}^{\mathcal{S}^2 \times \mathcal{S}^2}$ (a.k.a. Choi–Jamiołkowski matrix [Jam72]), whose entries are defined as

$$\llbracket W^{y|x} \rrbracket_{(s',s),(\tilde{s}',\tilde{s})} \triangleq W^{y|x}(s',s,\tilde{s}',\tilde{s}), \quad (4.56)$$

where $(s',s) \in \mathcal{S}^2$ is the first index, and $(\tilde{s}',\tilde{s}) \in \mathcal{S}^2$ is the second index of $\llbracket W^{y|x} \rrbracket$. Notice that, $\llbracket W^{y|x} \rrbracket$ is a PSD matrix, and satisfies the equation

$$\sum_{y \in \mathcal{Y}} \sum_{s', \tilde{s}': s' = \tilde{s}'} \llbracket W^{y|x} \rrbracket_{(s',s),(\tilde{s}',\tilde{s})} = \delta_{s,\tilde{s}} \quad \forall x \in \mathcal{X}. \quad (4.57)$$

In this case, the “equivalence” can be shown by the following proposition.

Proposition 4.6. *Let \mathcal{X}, \mathcal{Y} be finite sets, and \mathcal{H}_S be a finite-dimensional Hilbert space with an orthonormal basis $\{|s\rangle\}_{s \in \mathcal{S}}$. For any set of functions*

$$\{W^{y|x} : \mathcal{S} \times \mathcal{S} \times \mathcal{S} \times \mathcal{S} \rightarrow \mathbb{C}\}_{x \in \mathcal{X}, y \in \mathcal{Y}}$$

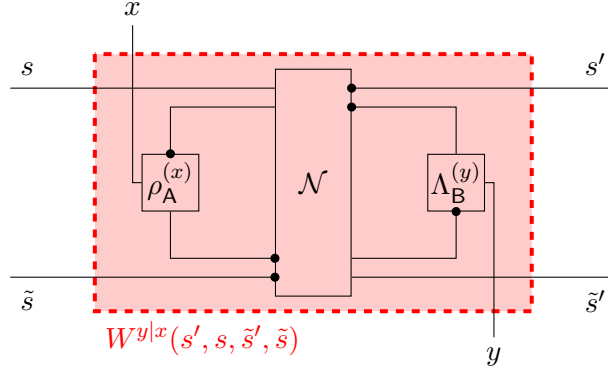


Figure 4.8: NFG representation of the channel-ensemble-measurement configuration $(\mathcal{N}, \{\rho_A^{(x)}\}_{x \in \mathcal{X}}, \{\Lambda_B^{(y)}\}_{y \in \mathcal{Y}})$.

such that their matrix form $\{\llbracket W^{y|x} \rrbracket\}_{x,y}$ consists of PSD matrices and satisfies (4.57), there must exist a unique CC-QSC $\{\mathcal{N}^{y|x}\}_{x,y}$ acting on \mathcal{H}_S such that (4.55) holds.

Proof. The idea of the proof is to consider the eigenvalue decomposition of $\llbracket W^{y|x} \rrbracket$, and reconstruct $\mathcal{N}^{y|x}$ by following the equations (4.45) and (4.43) backwardly. We omit the details here. \square

Let us conclude this section by pointing out that the functions $\{W^{y|x}\}_{x,y}$, particularly the corresponding NFG, can be constructed from the channel-ensemble-measurement configuration $(\mathcal{N}, \{\rho_A^{(x)}\}_{x \in \mathcal{X}}, \{\Lambda_B^{(y)}\}_{y \in \mathcal{Y}})$ as in Figure 4.8. This can be justified by checking (4.39) and (4.55).

4.3 Information Rate and its Estimation

In this section, we focus on the information rate of the communication scheme described in Section 4.2. As defined in (4.1), the information rate is the limit superior of the average mutual information $\frac{1}{n} \mathbf{I}(\mathbf{X}_1^n; \mathbf{Y}_1^n)$ between the input and output processes \mathbf{X}_1^n and \mathbf{Y}_1^n as n tends to infinity. We assume that \mathbf{X}_1^n is distributed according to some i.i.d. process⁵ characterized by the PMF Q , i.e., $Q^{(n)}(\mathbf{x}_1^n) = \prod_{\ell=1}^n Q(x_\ell)$. In this case,

⁵For more general type of sources, like a finite-state-machine source (FSMS), one can consider “merging” the memory of the source into that of the channel, and thus obtaining an equivalent memoryless input process.

the joint distribution of $(\mathbf{X}_1^n, \mathbf{Y}_1^n)$ is given by

$$P_{\mathbf{X}_1^n, \mathbf{Y}_1^n | \mathbf{S}_0}(\mathbf{x}_1^n, \mathbf{y}_1^n | \rho_{\mathbf{S}_0}) = \prod_{\ell=1}^n Q(x_\ell) \cdot P_{\mathbf{Y}_1^n | \mathbf{X}_1^n; \mathbf{S}_0}(\mathbf{y}_1^n | \mathbf{x}_1^n; \rho_{\mathbf{S}_0}), \quad (4.58)$$

where $P_{\mathbf{Y}_1^n | \mathbf{X}_1^n; \mathbf{S}_0}$ is specified in (4.37), (4.42), (4.48) or (4.52), depending on which notation we use to specify the channel (see Propositions 4.4 and 4.6). It is obvious that the value of (4.58), and thus the information rate, depends on the initial density operator $\rho_{\mathbf{S}_0}$. In this sense, we denote the information rate as a function of the input PMF Q , the CC-QSC $\{\mathcal{N}^{y|x}\}_{x,y}$ describing the channel, and the initial density operator $\rho_{\mathbf{S}_0}$, namely

$$\mathbf{I}(Q, \{\mathcal{N}^{y|x}\}_{x,y}, \rho_{\mathbf{S}_0}) \triangleq \limsup_{n \rightarrow \infty} \mathbf{I}^{(n)}(Q, \{\mathcal{N}^{y|x}\}_{x,y}, \rho_{\mathbf{S}_0}), \quad (4.59)$$

$$\mathbf{I}^{(n)}(Q, \{\mathcal{N}^{y|x}\}_{x,y}, \rho_{\mathbf{S}_0}) \triangleq \frac{1}{n} \mathbf{I}(\mathbf{X}_1^n; \mathbf{Y}_1^n)(\rho_{\mathbf{S}_0}). \quad (4.60)$$

Here, $\mathbf{I}(\mathbf{X}_1^n; \mathbf{Y}_1^n)(\rho_{\mathbf{S}_0})$ is the mutual information between \mathbf{X}_1^n and \mathbf{Y}_1^n ; and the latter are jointly distributed according to (4.58). The argument $\rho_{\mathbf{S}_0}$ emphasizes the dependency of $\frac{1}{n} \mathbf{I}(\mathbf{X}_1^n; \mathbf{Y}_1^n)$ on $\rho_{\mathbf{S}_0}$.

Similar to the case of an FSMC, the dependency of the information rate on the initial density operator usually cannot be ignored. However, as already mentioned in Section 4.1.2, for a class of FSMCs, namely the indecomposable FSMCs, it is known that the information rate is independent of the initial channel state [Gal68]. An indecomposable FSMC, intuitively speaking, is an FSMC whose state distribution, given different initial states, tends to be indistinguishable as $n \rightarrow \infty$, independently of the input sequence realized. A quantum analogy was proposed by Bowen, Devetak, and Mancini [BDM05], where they defined the indecomposable quantum channels with memory, and proved that the quantum entropic bound for such channels is independent of the initial density operator.

In the remainder of this section we firstly define the indecomposability of CC-QSCs, and prove the independence of the information rate as in (4.59) from the initial density operator. Secondly, we generalize the methods in Algorithm 4.1 for estimating such information rate efficiently.

The definition of an indecomposable CC-QSC in this chapter is similar (but different) and closely related to that of an indecomposable (quantum) channel with memory in [BDM05]. Namely, an indecomposable channel with memory equipped with separable input ensemble and local output measurement will always induce an indecomposable

CC-QSC, but not necessarily vice versa. Moreover, in [BDM05] the classical capacity of quantum channels with finite memory was considered, where the capacity is essentially the Holevo bound and where the latter was proven to be achievable [BM04]. However, in our work, we focus on the situation where the ensemble and the measurement are fixed.

4.3.1 Indecomposable Quantum-State Channel

Definition 4.7. A CC-QSC $\{\mathcal{N}^{y|x}\}_{x,y}$ is said to be *indecomposable* if for any initial density operators α_{S_0} and β_{S_0} , the following statement holds: for any $\epsilon > 0$, there exists some positive integer N s.t.

$$\left\| \alpha_{S_n}^{(\mathbf{x}_1^n)} - \beta_{S_n}^{(\mathbf{x}_1^n)} \right\|_1 < \epsilon \quad \forall n \geq N, \quad \forall \mathbf{x}_1^n \in \mathcal{X}^n, \quad (4.61)$$

where

$$\alpha_{S_n}^{(\mathbf{x}_1^n)} \triangleq \sum_{\mathbf{y}_1^n} \mathcal{N}^{y_n|x_n} \circ \dots \circ \mathcal{N}^{y_1|x_1}(\alpha_{S_0}), \quad (4.62)$$

$$\beta_{S_n}^{(\mathbf{x}_1^n)} \triangleq \sum_{\mathbf{y}_1^n} \mathcal{N}^{y_n|x_n} \circ \dots \circ \mathcal{N}^{y_1|x_1}(\beta_{S_0}), \quad (4.63)$$

and where $\|A\|_1$ is the trace distance for an operator A on \mathcal{H}_S , i.e., $\|A\|_1 \triangleq \frac{1}{2} \text{tr} \sqrt{A^\dagger A}$.

□

Theorem 4.8.⁶ *The information rate of an indecomposable CC-QSC with an i.i.d. input process is independent of the initial density operator. Namely, if $\{\mathcal{N}^{y|x}\}_{x,y}$ is indecomposable, then*

$$I^{(n)}(Q, \{\mathcal{N}^{y|x}\}_{x,y}, \alpha_{S_0}) - I^{(n)}(Q, \{\mathcal{N}^{y|x}\}_{x,y}, \beta_{S_0}) \xrightarrow{n \rightarrow \infty} 0 \quad (4.64)$$

for any initial density operators $\alpha_{S_0}, \beta_{S_0} \in \mathfrak{D}(\mathcal{H}_{S_0})$.

In the proof below, we follow a similar idea as in [Gal68] for indecomposable FSMCs, and as that in [BDM05] for indecomposable quantum channels with memory.

Proof. Let A and B be quantum systems described by Hilbert spaces \mathcal{H}_A and \mathcal{H}_B , respectively, where $\{|x\rangle\}_{x \in \mathcal{X}}$ and $\{|y\rangle\}_{y \in \mathcal{Y}}$ are orthonormal bases of \mathcal{H}_A and \mathcal{H}_B , respectively. Let A_1^n and B_1^n be n copies of A and B, respectively. Let ρ_{S_0} be some initial

⁶A similar result regarding indecomposable/forgetful quantum channel with memory can be found in [KW05] and [BDM05].

density operator; and let the joint density operator on the system $A_1^n B_1^n$ be

$$\rho_{A_1^n B_1^n} \triangleq \sum_{\mathbf{x}_1^n} Q(\mathbf{x}_1^n) \cdot |\mathbf{x}_1^n\rangle\langle\mathbf{x}_1^n| \otimes \sum_{\mathbf{y}_1^n} \text{tr} \left(\mathcal{N}^{\mathbf{y}_1^n | \mathbf{x}_1^n}(\rho_{S_0}) \right) \cdot |\mathbf{y}_1^n\rangle\langle\mathbf{y}_1^n|,$$

where $\mathcal{N}^{\mathbf{y}_1^n | \mathbf{x}_1^n} \triangleq \mathcal{N}^{y_n | x_n} \circ \dots \circ \mathcal{N}^{y_1 | x_1}$. In this case, it is not hard to see that

$$\mathbf{I}(\mathbf{X}_1^n; \mathbf{Y}_1^n)[\rho_{S_0}] = \mathbf{I}(A_1^n; B_1^n)[\rho_{S_0}].$$

In fact, one can easily check that

$$\mathbf{H}(A_1^n) = \mathbf{H}(\mathbf{X}_1^n),$$

$$\mathbf{H}(B_1^n) = \mathbf{H}(\mathbf{Y}_1^n),$$

$$\mathbf{H}(A_1^n, B_1^n) = \mathbf{H}(\mathbf{X}_1^n, \mathbf{Y}_1^n).$$

In particular, $\mathbf{H}(A_1^n)$ is independent of the initial density operator ρ_{S_0} . We also claim that, for each $\rho_{S_0} \in \mathfrak{D}(\mathcal{H}_{S_0})$ and a positive integer $N < n$,

$$\mathbf{I}(A_1^N B_1^N; A_{N+1}^n B_{N+1}^n) \leq 2\mathbf{H}(S_N), \quad (4.65)$$

$$\mathbf{I}(B_1^N; B_{N+1}^n) \leq 2\mathbf{H}(S_N), \quad (4.66)$$

where the density operator for S_N is defined as (depending on ρ_{S_0})

$$\rho_{S_N} \triangleq \sum_{\mathbf{x}_1^N} Q(\mathbf{x}_1^N) \cdot \sum_{\mathbf{y}_1^N} \mathcal{N}^{\mathbf{y}_1^N | \mathbf{x}_1^N}(\rho_{S_0}).$$

Proof of (4.65): We define a class of CPTP maps $\{\Phi_a^b : \mathfrak{D}(\mathcal{H}_{S_a}) \rightarrow \mathfrak{D}(\mathcal{H}_{A_a^b B_a^b})\}_{a,b \in \mathbb{N}}$ as

$$\Phi_a^b : \rho_{S_a} \mapsto \sum_{\mathbf{x}_a^b} Q(\mathbf{x}_a^b) \cdot |\mathbf{x}_a^b\rangle\langle\mathbf{x}_a^b| \otimes \sum_{\mathbf{y}_a^b} \text{tr} \left(\mathcal{N}^{\mathbf{y}_a^b | \mathbf{x}_a^b}(\rho_{S_a}) \right) \cdot |\mathbf{y}_a^b\rangle\langle\mathbf{y}_a^b|.$$

Since the input process Q is i.i.d., we can rewrite $\rho_{A_1^n B_1^n}$ for each positive integer $N < n$, as

$$\rho_{A_1^n B_1^n} = \left(I_{A_1^N B_1^N} \otimes \Phi_{N+1}^n \right) \left(\rho_{A_1^N B_1^N S_N} \right),$$

where

$$\rho_{A_1^N B_1^N S_N} \triangleq \sum_{\mathbf{x}_1^N} Q(\mathbf{x}_1^N) |\mathbf{x}_1^N\rangle\langle\mathbf{x}_1^N| \otimes \sum_{\mathbf{y}_1^N} \mathcal{N}^{\mathbf{y}_1^N | \mathbf{x}_1^N}(\rho_{S_0}) |\mathbf{y}_1^N\rangle\langle\mathbf{y}_1^N|.$$

Hence, by data processing inequality for quantum mutual information (see *e.g.*, [Wil17, Theorem 11.9.4]), one must have

$$\mathbf{I}(A_1^N B_1^N; A_{N+1}^n B_{N+1}^n) \leq \mathbf{I}(A_1^N B_1^N; S_N).$$

Additionally, by subadditivity of joint entropy, we have

$$\begin{aligned} \mathbf{I}(\mathbf{A}_1^N \mathbf{B}_1^N; \mathbf{S}_N) &\triangleq \mathbf{H}(\mathbf{A}_1^N \mathbf{B}_1^N) + \mathbf{H}(\mathbf{S}_N) - \mathbf{H}(\mathbf{A}_1^N \mathbf{B}_1^N \mathbf{S}_N) \\ &\leq \mathbf{H}(\mathbf{A}_1^N \mathbf{B}_1^N) + \mathbf{H}(\mathbf{S}_N) - |\mathbf{H}(\mathbf{A}_1^N \mathbf{B}_1^N) - \mathbf{H}(\mathbf{S}_N)| \\ &\leq 2\mathbf{H}(\mathbf{S}_N). \end{aligned}$$

Combining the above two inequalities, we have proven (4.65).

Proof of (4.66): (4.66) can be shown via the same approach above by considering another class of CPTP maps $\{\Psi_a^b : \mathcal{D}(\mathcal{H}_{\mathbf{S}_a}) \rightarrow \mathcal{D}(\mathcal{H}_{\mathbf{B}_a^b})\}_{a < b \in \mathbb{N}}$ as

$$\Psi_a^b : \rho_{\mathbf{S}_a} \mapsto \sum_{\mathbf{x}_a^b} Q(\mathbf{x}_a^b) \cdot \sum_{\mathbf{y}_a^b} \text{tr} \left(\mathcal{N}^{\mathbf{y}_a^b | \mathbf{x}_a^b}(\rho_{\mathbf{S}_a}) \right) \cdot |\mathbf{y}_a^b\rangle \langle \mathbf{y}_a^b|.$$

We omit the details.

Now return to the main proof. Given the initial density operators $\alpha_{\mathbf{S}_0}$, and $\beta_{\mathbf{S}_0}$, we define $\alpha_{\mathbf{A}_1^n \mathbf{B}_1^n}$, $\beta_{\mathbf{A}_1^n \mathbf{B}_1^n}$ and $\alpha_{\mathbf{S}_N}$, $\beta_{\mathbf{S}_N}$ in a similar fashion as we have defined $\rho_{\mathbf{A}_1^n \mathbf{B}_1^n}$ and $\rho_{\mathbf{S}_N}$ based on $\rho_{\mathbf{S}_0}$. In this case, one obtains

$$\begin{aligned} &|\mathbf{H}(\alpha_{\mathbf{A}_1^n \mathbf{B}_1^n}) - \mathbf{H}(\beta_{\mathbf{A}_1^n \mathbf{B}_1^n})| - |\mathbf{H}(\alpha_{\mathbf{A}_{N+1}^n \mathbf{B}_{N+1}^n}) - \mathbf{H}(\beta_{\mathbf{A}_{N+1}^n \mathbf{B}_{N+1}^n})| \\ &\stackrel{(a)}{\leq} \left| \mathbf{H}(\alpha_{\mathbf{A}_1^N \mathbf{B}_1^N}) - \mathbf{H}(\beta_{\mathbf{A}_1^N \mathbf{B}_1^N}) \right| + \left| \mathbf{I}(\mathbf{A}_1^N \mathbf{B}_1^N; \mathbf{A}_{N+1}^n \mathbf{B}_{N+1}^n)[\alpha_{\mathbf{A}_1^n \mathbf{B}_1^n}] - \mathbf{I}(\mathbf{A}_1^N \mathbf{B}_1^N; \mathbf{A}_{N+1}^n \mathbf{B}_{N+1}^n)[\beta_{\mathbf{A}_1^n \mathbf{B}_1^n}] \right| \\ &\stackrel{(b)}{\leq} N \cdot \log(\dim \mathcal{H}_{\mathbf{AB}}) + 2 \cdot \max \{ \mathbf{H}(\alpha_{\mathbf{S}_N}), \mathbf{H}(\beta_{\mathbf{S}_N}) \}, \end{aligned} \quad (4.67)$$

where we have used the triangle inequality in step (a), and Corollary 1.32 and (4.65) in step (b). Similarly, using (4.66), one can prove

$$|\mathbf{H}(\alpha_{\mathbf{B}_1^n}) - \mathbf{H}(\beta_{\mathbf{B}_1^n})| - |\mathbf{H}(\alpha_{\mathbf{B}_{N+1}^n}) - \mathbf{H}(\beta_{\mathbf{B}_{N+1}^n})| \leq N \cdot \log(\dim \mathcal{H}_{\mathbf{B}}) + 2 \cdot \max \{ \mathbf{H}(\alpha_{\mathbf{S}_N}), \mathbf{H}(\beta_{\mathbf{S}_N}) \}. \quad (4.68)$$

By assumption, there exists some positive integer d such that $\max \{ \dim \mathcal{H}_{\mathbf{A}}, \dim \mathcal{H}_{\mathbf{B}}, \dim \mathcal{H}_{\mathbf{S}} \} \leq d$. Thus, we have

$$\begin{aligned} &\frac{1}{n} |\mathbf{I}(\mathbf{X}_1^n; \mathbf{Y}_1^n)[\alpha_{\mathbf{S}_0}] - \mathbf{I}(\mathbf{X}_1^n; \mathbf{Y}_1^n)[\beta_{\mathbf{S}_0}]| \\ &= \frac{1}{n} |\mathbf{I}(\mathbf{A}_1^n; \mathbf{B}_1^n)[\alpha_{\mathbf{S}_0}] - \mathbf{I}(\mathbf{A}_1^n; \mathbf{B}_1^n)[\beta_{\mathbf{S}_0}]| \\ &= \frac{1}{n} |(\mathbf{H}(\alpha_{\mathbf{B}_1^n}) - \mathbf{H}(\alpha_{\mathbf{A}_1^n \mathbf{B}_1^n})) - (\mathbf{H}(\beta_{\mathbf{B}_1^n}) - \mathbf{H}(\beta_{\mathbf{A}_1^n \mathbf{B}_1^n}))| \\ &\stackrel{(c)}{\leq} \frac{1}{n} |\mathbf{H}(\alpha_{\mathbf{B}_1^n}) - \mathbf{H}(\beta_{\mathbf{B}_1^n})| + \frac{1}{n} |\mathbf{H}(\alpha_{\mathbf{A}_1^n \mathbf{B}_1^n}) - \mathbf{H}(\beta_{\mathbf{A}_1^n \mathbf{B}_1^n})| \end{aligned}$$

$$\begin{aligned}
&\stackrel{(d)}{\leq} \frac{3N+4}{n} \cdot \log d + \frac{1}{n} |\mathbf{H}(\alpha_{\mathbf{B}_{N+1}^n}) - \mathbf{H}(\beta_{\mathbf{B}_{N+1}^n})| + \frac{1}{n} |\mathbf{H}(\alpha_{\mathbf{A}_{N+1}^n \mathbf{B}_{N+1}^n}) - \mathbf{H}(\beta_{\mathbf{A}_{N+1}^n \mathbf{B}_{N+1}^n})| \\
&= \frac{3N+4}{n} \cdot \log d + \frac{1}{n} |\mathbf{H}(\Psi_{N+1}^n(\alpha_{\mathbf{S}_N})) - \mathbf{H}(\Psi_{N+1}^n(\beta_{\mathbf{S}_N}))| + \frac{1}{n} |\mathbf{H}(\Phi_{N+1}^n(\alpha_{\mathbf{S}_N})) - \mathbf{H}(\Phi_{N+1}^n(\beta_{\mathbf{S}_N}))|,
\end{aligned}$$

where we have used the triangle inequality in step (c), and [NC11, Theorem 11.8], (4.67), (4.68) in step (d). Using a loose variant of Fannes' inequality [Fan73]⁷, we have

$$\begin{aligned}
|\mathbf{H}(\Psi_{N+1}^n(\alpha_{\mathbf{S}_N})) - \mathbf{H}(\Psi_{N+1}^n(\beta_{\mathbf{S}_N}))| &\leq (n-N) \cdot \log d \cdot \|\Psi_{N+1}^n(\alpha_{\mathbf{S}_N}) - \Psi_{N+1}^n(\beta_{\mathbf{S}_N})\|_1 + e^{-1}, \\
|\mathbf{H}(\Phi_{N+1}^n(\alpha_{\mathbf{S}_N})) - \mathbf{H}(\Phi_{N+1}^n(\beta_{\mathbf{S}_N}))| &\leq 2 \cdot (n-N) \cdot \log d \cdot \|\Phi_{N+1}^n(\alpha_{\mathbf{S}_N}) - \Phi_{N+1}^n(\beta_{\mathbf{S}_N})\|_1 + e^{-1}.
\end{aligned}$$

Moreover, by the contractivity of the trace distance, we have,

$$\begin{aligned}
\|\Psi_{N+1}^n(\alpha_{\mathbf{S}_N}) - \Psi_{N+1}^n(\beta_{\mathbf{S}_N})\|_1 &\leq \|\alpha_{\mathbf{S}_N} - \beta_{\mathbf{S}_N}\|_1, \\
\|\Phi_{N+1}^n(\alpha_{\mathbf{S}_N}) - \Phi_{N+1}^n(\beta_{\mathbf{S}_N})\|_1 &\leq \|\alpha_{\mathbf{S}_N} - \beta_{\mathbf{S}_N}\|_1.
\end{aligned}$$

This allows us to bound the difference of the information rate by

$$\frac{1}{n} |\mathbf{I}(\mathbf{X}_1^n; \mathbf{Y}_1^n)[\alpha_{\mathbf{S}_0}] - \mathbf{I}(\mathbf{X}_1^n; \mathbf{Y}_1^n)[\beta_{\mathbf{S}_0}]| \leq \frac{3N+4}{n} \cdot \log d + \frac{3(n-N)}{n} \cdot \log d \cdot \|\alpha_{\mathbf{S}_N} - \beta_{\mathbf{S}_N}\|_1 + \frac{2}{n \cdot e}.$$

Finally, because the CC-QSC is indecomposable, for any $\varepsilon > 0$, we can choose N large enough such that

$$\|\alpha_{\mathbf{S}_N} - \beta_{\mathbf{S}_N}\|_1 < \frac{\varepsilon}{6 \cdot \log d}$$

and then choose an integer $M > N$ such that

$$\frac{3N+4}{M} \cdot \log d + \frac{2}{M \cdot e} < \frac{\varepsilon}{2}.$$

This will ensure that for any $n > M$, we have

$$\frac{3N+4}{n} \cdot \log d + \frac{3(n-N)}{n} \cdot \log d \cdot \|\alpha_{\mathbf{S}_N} - \beta_{\mathbf{S}_N}\|_1 + \frac{2}{n \cdot e} < \varepsilon,$$

which concludes the proof. \square

4.3.2 Estimation of the Information Rate

The development in this section is very similar to the development in Subsection 4.1.2. In particular, we follow the same approach as in (4.8)–(4.15). This similarity stems from the similarity of the factor graphs in Figures 4.4 and 4.7, and highlights

⁷Namely, we used the inequality $|\mathbf{H}(\rho) - \mathbf{H}(\sigma)| \leq \log \dim \cdot \|\rho - \sigma\|_1 + e^{-1}$. Note that tighter variants of Fannes' inequality exist, but the above inequality is good enough to prove the desired result.

one of the benefits of the factor-graph approach that we take to estimate information rate of quantum channels with memory.

We make the following assumptions.

- As already mentioned, the derivations in this chapter are for the case where the input process $\mathbf{X}_1^n = (X_1, \dots, X_n)$ is an i.i.d. process. The results can be generalized to other stationary ergodic input processes that can be represented by a finite-state-machine source (FSMS). Technically, this is done by defining a new state that combines the FSMS state and the channel state.
- We assume that the corresponding quantum-state channel $\{\mathcal{N}^{y|x}\}_{x \in \mathcal{X}, y \in \mathcal{Y}}$ is finite-dimensional and indecomposable. We also assume it can be represented by some functions $\{W^{y|x}\}_{x,y}$ as defined in (4.45).

The major difference compared with Section 4.1.2 is the conditional PMF $P_{Y_1^n | X_1^n; S_0}$, and thus the joint PMF $P_{Y_1^n, X_1^n | S_0}$ as specified in (4.52) and (4.58), respectively. In this case, in order to compute $-\frac{1}{n} \log P_{Y_1^n}(\tilde{\mathbf{y}}_1^n)$ and $-\frac{1}{n} \log P_{X_1^n Y_1^n}(\tilde{\mathbf{x}}_1^n, \tilde{\mathbf{y}}_1^n)$ using a similar method as in Section 4.1.2, we consider the state metrics $\{\sigma_\ell^Y\}_{\ell=1}^n$ and $\{\sigma_\ell^{XY}\}_{\ell=1}^n$ (which are operators on \mathcal{H}_{S_ℓ} for each ℓ) defined w.r.t. $\tilde{\mathbf{y}}_1^n$ and w.r.t. $\tilde{\mathbf{x}}_1^n$ and $\tilde{\mathbf{y}}_1^n$, respectively, as

$$\sigma_\ell^Y \triangleq \sum_{\mathbf{x}_1^\ell} Q^{(\ell)}(\mathbf{x}_1^\ell) \cdot \mathcal{N}^{\tilde{y}_n | x_n} \circ \dots \circ \mathcal{N}^{\tilde{y}_1 | x_1}(\rho_{S_0}), \quad (4.69)$$

$$\sigma_\ell^{XY} \triangleq \mathcal{N}^{\tilde{y}_n | \tilde{x}_n} \circ \dots \circ \mathcal{N}^{\tilde{y}_1 | \tilde{x}_1}(\rho_{S_0}). \quad (4.70)$$

In this case, we have $P_{Y_1^n}(\tilde{\mathbf{y}}_1^n) = \text{tr}(\sigma_n^Y)$, and $P_{X_1^n Y_1^n}(\tilde{\mathbf{x}}_1^n, \tilde{\mathbf{y}}_1^n) = \text{tr}(\sigma_n^{XY})$. Notice that $\{\sigma_\ell^Y\}_\ell$ and $\{\sigma_\ell^{XY}\}_\ell$ can be computed iteratively as

$$[\sigma_\ell^Y] = \sum_{x_\ell} Q(x_\ell) \cdot [W^{y|x}] \cdot [\sigma_{\ell-1}^Y], \quad (4.71)$$

$$[\sigma_\ell^{XY}] = [W^{y|x}] \cdot [\sigma_{\ell-1}^{XY}], \quad (4.72)$$

where we treat $[\sigma_\ell^Y]$ and $[\sigma_\ell^{XY}]$ as length- d^2 vectors indexed by $(s, \tilde{s}) \in \mathcal{S}^2$ in the above two equations. (See (4.49) and (4.52) for notations.) Moreover, we can also introduce normalizing coefficients $\{\lambda_\ell^Y\}_\ell$ and $\{\lambda_\ell^{XY}\}_\ell$, similar to (4.21), for the sake of numerical

stability. In the latter case, we have iterative updating rules

$$[\bar{\sigma}_\ell^Y] = \frac{1}{\lambda_\ell^Y} \cdot \sum_{x_\ell} Q(x_\ell) \cdot [W^{y|x}] \cdot [\bar{\sigma}_{\ell-1}^Y], \quad (4.73)$$

$$[\bar{\sigma}_\ell^{XY}] = \frac{1}{\lambda_\ell^{XY}} \cdot [W^{y|x}] \cdot [\bar{\sigma}_{\ell-1}^{XY}], \quad (4.74)$$

where the scaling factors $\lambda_\ell^Y > 0$ and $\lambda_\ell^{XY} > 0$ are chosen such that $\text{tr}(\bar{\sigma}_\ell^Y) = 1$ and $\text{tr}(\bar{\sigma}_\ell^{XY}) = 1$, respectively. In addition, one can verify that $P_{Y_1^n}(\check{y}_1^n) = \prod_{\ell=1}^n \lambda_\ell^Y$, and $P_{X_1^n Y_1^n}(\check{x}_1^n, \check{y}_1^n) = \prod_{\ell=1}^n \lambda_\ell^{XY}$.

The above discussion is summarized as Algorithm 4.2. The computations corresponding to Line 3, 5–9 and 12–16 are visualized in Figures D.4, D.6, and D.8 in the Appendix D, respectively.

4.4 Information rate upper/lower bounds and their Optimization

In this section, we consider auxiliary channels and their induced upper and lower bounds on the information rate. As mentioned in the beginning of this chapter auxiliary channels are often introduced as a low-complexity approximation of the original channel, which are useful in mismatch decoding. The techniques developed in this section only require the channel input/output data, but not the channel model itself. This is particularly useful when the channel is only made physically, but not mathematically, available. In this case, the task of minimizing the difference between the upper and lower bound is equivalent to finding the channel model (within a specified class of channel models) best fitting the *empirical* channel law. Similarly, minimizing the upper bound corresponds to finding the channel model best fitting the *empirical* channel output distribution, and maximizing the lower bound corresponds to finding the channel model best fitting the *empirical* reverse channel law. Motivated by the above scenarios, we particularly consider the auxiliary channels chosen from the domain of all CC-QSCs with the same input and output alphabet as the original channel, and acting on a memory system of a certain dimension (which can be different from the memory dimension of the original channel). Throughout this section, we assume the original channel as described in Section 4.2 is indecomposable, and that all the involved Hilbert spaces are of finite dimension, and that the alphabets \mathcal{X} and \mathcal{Y} are finite.

Algorithm 4.2 Estimating the Information Rate of a CC-QSC

Input: An indecomposable CC-QSC $\{\mathcal{N}^{y|x}\}_{x \in \mathcal{X}, y \in \mathcal{Y}}$, which can be represented by functions $\{W^{y|x}\}_{x,y}$, a input distribution Q , a positive integer n large enough.

Output: $I^{(n)}(Q, \{\mathcal{N}^{y|x}\}_{x,y}) \approx \mathbf{H}(\mathbf{X}) + \hat{\mathbf{H}}(\mathbf{Y}) - \hat{\mathbf{H}}(\mathbf{X}, \mathbf{Y})$.

- 1: Initialize the memory density operator $\rho_{\mathbf{S}_0} \leftarrow |0_{\mathbf{S}}\rangle\langle 0_{\mathbf{S}}|$
 - 2: Generate an input sequence $\tilde{\mathbf{x}}_1^n \sim Q^{\otimes n}$
 - 3: Generate a corresponding output sequence $\tilde{\mathbf{y}}_1^n$
 - 4: $\bar{\sigma}_0^{\mathbf{Y}} \leftarrow \rho_{\mathbf{S}_0}$
 - 5: **for each** $\ell = 1, \dots, n$ **do**
 - 6: $[\sigma_\ell^{\mathbf{Y}}] \leftarrow \sum_{x_\ell} Q(x_\ell) \cdot [W^{\tilde{y}_\ell|x_\ell}] \cdot [\bar{\sigma}_{\ell-1}^{\mathbf{Y}}]$
 - 7: $\lambda_\ell^{\mathbf{Y}} \leftarrow \text{tr}(\sigma_\ell^{\mathbf{Y}})$
 - 8: $\bar{\sigma}_\ell^{\mathbf{Y}} \leftarrow \sigma_\ell^{\mathbf{Y}} / \lambda_\ell^{\mathbf{Y}}$
 - 9: **end for**
 - 10: $\hat{\mathbf{H}}(\mathbf{Y}) \leftarrow -\frac{1}{n} \sum_{\ell=1}^n \log(\lambda_\ell^{\mathbf{Y}})$
 - 11: $\bar{\sigma}_0^{\mathbf{XY}} \leftarrow \rho_{\mathbf{S}_0}$
 - 12: **for each** $\ell = 1, \dots, n$ **do**
 - 13: $[\sigma_\ell^{\mathbf{XY}}] \leftarrow [W^{\tilde{y}_\ell|\tilde{x}_\ell}] \cdot [\bar{\sigma}_{\ell-1}^{\mathbf{XY}}]$
 - 14: $\lambda_\ell^{\mathbf{XY}} \leftarrow \text{tr}(\sigma_\ell^{\mathbf{XY}})$
 - 15: $\bar{\sigma}_\ell^{\mathbf{XY}} \leftarrow \sigma_\ell^{\mathbf{XY}} / \lambda_\ell^{\mathbf{XY}}$
 - 16: **end for**
 - 17: $\hat{\mathbf{H}}(\mathbf{X}, \mathbf{Y}) \leftarrow -\frac{1}{n} \sum_{\ell=1}^n \log(\lambda_\ell^{\mathbf{XY}})$
 - 18: $\mathbf{H}(\mathbf{X}) \leftarrow -\sum_x Q(x) \log Q(x)$
 - 19: Estimate $I^{(n)}(Q, \{\mathcal{N}^{y|x}\}_{x,y})$ as $\mathbf{H}(\mathbf{X}) + \hat{\mathbf{H}}(\mathbf{Y}) - \hat{\mathbf{H}}(\mathbf{X}, \mathbf{Y})$.
-

Suppose we have some auxiliary CC-QSC $\{\hat{\mathcal{N}}^{y|x}\}_{x,y}$, describable by some functions $\{\hat{W}^{y|x}\}_{x,y}$ as in (4.45). Let $\hat{P}_{Y_1^n|X_1^n, \hat{S}_0}$ denote its joint channel law, similar to (4.42), (4.48), or (4.52). Namely,

$$\hat{P}_{Y_1^n|X_1^n, \hat{S}_0}(\mathbf{y}_1^n|\mathbf{x}_1^n; \hat{\rho}_{S_0}) \triangleq \text{tr} \left([\hat{W}^{y_n|x_n}] \cdots [\hat{W}^{y_1|x_1}] \cdot [\hat{\rho}_{S_0}] \right). \quad (4.75)$$

We follow a similar approach as in [ALV+06; SVS09], and define the quantities

$$\begin{aligned} \bar{I}_W^{(n)}(\hat{W}) &\triangleq \frac{1}{n} \sum_{\mathbf{x}_1^n, \mathbf{y}_1^n} Q^{(n)}(\mathbf{x}_1^n) \cdot P_{Y_1^n|X_1^n, S_0}(\mathbf{y}_1^n|\mathbf{x}_1^n; \rho_{S_0}) \\ &\quad \cdot \log \frac{P_{Y_1^n|X_1^n, S_0}(\mathbf{y}_1^n|\mathbf{x}_1^n; \rho_{S_0})}{\sum_{\tilde{\mathbf{x}}_1^n} Q^{(n)}(\tilde{\mathbf{x}}_1^n) \hat{P}_{Y_1^n|X_1^n, \hat{S}_0}(\mathbf{y}_1^n|\tilde{\mathbf{x}}_1^n; \rho_{\hat{S}_0})}, \end{aligned} \quad (4.76)$$

$$\begin{aligned} \underline{I}_W^{(n)}(\hat{W}) &\triangleq \frac{1}{n} \sum_{\mathbf{x}_1^n, \mathbf{y}_1^n} Q^{(n)}(\mathbf{x}_1^n) \cdot P_{Y_1^n|X_1^n, S_0}(\mathbf{y}_1^n|\mathbf{x}_1^n; \rho_{S_0}) \\ &\quad \cdot \log \frac{\hat{P}_{Y_1^n|X_1^n, S_0}(\mathbf{y}_1^n|\mathbf{x}_1^n; \rho_{S_0})}{\sum_{\tilde{\mathbf{x}}_1^n} Q^{(n)}(\tilde{\mathbf{x}}_1^n) \hat{P}_{Y_1^n|X_1^n, \hat{S}_0}(\mathbf{y}_1^n|\tilde{\mathbf{x}}_1^n; \rho_{\hat{S}_0})}, \end{aligned} \quad (4.77)$$

where $P_{Y_1^n|X_1^n, S_0}$ is defined in (4.42), (4.48) or (4.52). By following similar arguments like those in (4.27) and (4.28), one can verify that

$$\underline{I}_W^{(n)}(\hat{W}) \leq I_W^{(n)} \leq \bar{I}_W^{(n)}(\hat{W}), \quad (4.78)$$

where the first inequality holds with equality if and only if $\hat{P}_{Y_1^n|X_1^n, \hat{S}_0}(\mathbf{y}_1^n|\mathbf{x}_1^n; \rho_{\hat{S}_0})$ and $P_{Y_1^n|X_1^n, S_0}(\mathbf{y}_1^n|\mathbf{x}_1^n; \rho_{S_0})$ coincide for all \mathbf{x}_1^n and \mathbf{y}_1^n with positive support of $P_{Y_1^n|X_1^n, S_0}$ and where the second inequalities holds with equality if and only if $\hat{P}_{Y_1^n|\hat{S}_0}(\mathbf{y}_1^n|\rho_{\hat{S}_0})$ and $P_{Y_1^n|S_0}(\mathbf{y}_1^n|\rho_{S_0})$ coincide for all \mathbf{y}_1^n with positive support of $P_{Y_1^n|S_0}$. Another quantity of interest is the *difference function* defined as

$$\Delta_W^{(n)}(\hat{W}) \triangleq \bar{I}_W^{(n)}(\hat{W}) - \underline{I}_W^{(n)}(\hat{W}). \quad (4.79)$$

Explicit expressions of (4.76), (4.77), and (4.79) are given by

$$\bar{I}_W^{(n)}(\hat{W}) = \frac{1}{n} \left\langle \log \frac{\text{tr}([W^{Y_n|X_n}] \cdots [W^{Y_1|X_1}] \cdot [\rho_{S_0}])}{\sum_{\mathbf{x}_1^n} Q^{(n)}(\mathbf{x}_1^n) \cdot \text{tr}([\hat{W}^{Y_n|x_n}] \cdots [\hat{W}^{Y_1|x_1}] \cdot [\rho_{\hat{S}_0}])} \right\rangle_{\mathbf{x}_1^n, \mathbf{y}_1^n}, \quad (4.80)$$

$$\underline{I}_W^{(n)}(\hat{W}) = \frac{1}{n} \left\langle \log \frac{\text{tr}([\hat{W}^{Y_n|X_n}] \cdots [\hat{W}^{Y_1|X_1}] \cdot [\rho_{\hat{S}_0}])}{\sum_{\mathbf{x}_1^n} Q^{(n)}(\mathbf{x}_1^n) \cdot \text{tr}([\hat{W}^{Y_n|x_n}] \cdots [\hat{W}^{Y_1|x_1}] \cdot [\rho_{\hat{S}_0}])} \right\rangle_{\mathbf{x}_1^n, \mathbf{y}_1^n}, \quad (4.81)$$

$$\Delta_W^{(n)}(\hat{W}) = \frac{1}{n} \left\langle \log \frac{\text{tr}([W^{Y_n|X_n}] \cdots [W^{Y_1|X_1}] \cdot [\rho_{S_0}])}{\text{tr}([\hat{W}^{Y_n|x_n}] \cdots [\hat{W}^{Y_1|x_1}] \cdot [\rho_{\hat{S}_0}])} \right\rangle_{\mathbf{x}_1^n, \mathbf{y}_1^n}, \quad (4.82)$$

respectively, where \mathbf{X}_1^n and \mathbf{Y}_1^n are random variables distributed according to the joint distribution $Q^{(n)}(\mathbf{x}_1^n) \cdot P_{\mathbf{Y}_1^n|\mathbf{X}_1^n, \mathbf{S}_0}(\mathbf{y}_1^n|\mathbf{x}_1^n; \rho_{\mathbf{S}_0})$ and where $\langle \cdot \rangle$ stands for the expectation function.

In the remainder of this section, we propose an algorithm based on the gradient-descent method and the techniques described in Section 4.2.3 and 4.3 for optimizing the quantities in (4.76), (4.77), and (4.79). In particular, we consider $\{\hat{W}^{y|x}\}_{x,y}$ to be an *interior* point in the domain of CC-QSCs, namely

- The Choi–Jamiołkowski matrices $\llbracket \hat{W}^{y|x} \rrbracket$, defined similarly as (4.56), are strictly positive definite for each x and y ,
- Eq. (4.57) holds by replacing $W^{y|x}$ with $\hat{W}^{y|x}$, namely $\sum_{y \in \mathcal{Y}} \sum_{s', \tilde{s}': s' = \tilde{s}'} \llbracket \hat{W}^{y|x} \rrbracket_{(s', s), (\tilde{s}', \tilde{s})} = \delta_{s, \tilde{s}}$ for all $x \in \mathcal{X}$.

For any set of functions $\{H^{y|x} : \mathcal{S}^4 \rightarrow \mathbb{C}\}_{x,y}$ such that $\llbracket H^{y|x} \rrbracket$ (again, defined similarly as (4.56)) is Hermitian for each x and y and such that

$$\sum_{y \in \mathcal{Y}} \sum_{s', \tilde{s}': s' = \tilde{s}'} \llbracket H^{y|x} \rrbracket_{(s', s), (\tilde{s}', \tilde{s})} = 0 \quad \forall x \in \mathcal{X}, \quad (4.83)$$

the functions $\{\hat{W}^{y|x} + t \cdot H^{y|x}\}_{x,y}$ describe a valid CC-QSC, for all t in some neighborhood of 0. In this case, the directional derivatives of the functions $\mathbb{I}_W^{(n)}$, $\bar{\mathbb{I}}_W^{(n)}$, and $\Delta_W^{(n)}$ at $\{\hat{W}^{y|x}\}_{x,y}$ along $\{H^{y|x}\}_{x,y}$ is well defined, and can be expressed as (4.84), (4.85), and (4.86) on next page, where we define the messages $\{\bar{\varrho}_{\mathbf{S}_\ell}^{(\tilde{\mathbf{y}}_1^\ell)}\}_\ell$, $\{\bar{\varrho}_{\mathbf{S}_\ell}^{(\tilde{\mathbf{y}}_{\ell+1}^n)}\}_\ell$, $\{\bar{\varrho}_{\mathbf{S}_\ell}^{(\tilde{\mathbf{x}}_1^\ell, \tilde{\mathbf{y}}_1^\ell)}\}_\ell$, and $\{\bar{\varrho}_{\mathbf{S}_\ell}^{(\tilde{\mathbf{x}}_{\ell+1}^n, \tilde{\mathbf{y}}_{\ell+1}^n)}\}_\ell$ in a recursive manner as

$$[\bar{\varrho}_{\mathbf{S}_\ell}^{(\tilde{\mathbf{y}}_1^\ell)}] \triangleq \sum_{\mathbf{x}_1^\ell} Q(\mathbf{x}_1^\ell) \cdot [\hat{W}^{\tilde{\mathbf{y}}_\ell|x_\ell}] \cdots [\hat{W}^{\tilde{\mathbf{y}}_1|x_1}] \cdot [\rho_{\mathbf{S}_0}], \quad (4.87)$$

$$[\bar{\varrho}_{\mathbf{S}_\ell}^{(\tilde{\mathbf{y}}_{\ell+1}^n)}] \triangleq \sum_{\mathbf{x}_{\ell+1}^n} Q(\mathbf{x}_{\ell+1}^n) \cdot [I_{\mathbf{S}_n}] \cdot [\hat{W}^{\tilde{\mathbf{y}}_n|x_n}] \cdots [\hat{W}^{\tilde{\mathbf{y}}_{\ell+1}|x_{\ell+1}}], \quad (4.88)$$

$$[\bar{\varrho}_{\mathbf{S}_\ell}^{(\tilde{\mathbf{x}}_1^\ell, \tilde{\mathbf{y}}_1^\ell)}] \triangleq [\hat{W}^{\tilde{\mathbf{y}}_\ell|\tilde{\mathbf{x}}_\ell}] \cdots [\hat{W}^{\tilde{\mathbf{y}}_1|\tilde{\mathbf{x}}_1}] \cdot [\rho_{\mathbf{S}_0}], \quad (4.89)$$

$$[\bar{\varrho}_{\mathbf{S}_\ell}^{(\tilde{\mathbf{x}}_{\ell+1}^n, \tilde{\mathbf{y}}_{\ell+1}^n)}] \triangleq [I_{\mathbf{S}_n}] \cdot [\hat{W}^{\tilde{\mathbf{y}}_n|\tilde{\mathbf{x}}_n}] \cdots [\hat{W}^{\tilde{\mathbf{y}}_{\ell+1}|\tilde{\mathbf{x}}_{\ell+1}}]. \quad (4.90)$$

Recall that, in above equations, $[I_{\mathbf{S}_n}]$ is a row vector, and $[\rho_{\mathbf{S}_0}]$ is a column vector.

By extending the domain of the functions $\mathbb{I}_W^{(n)}$, $\bar{\mathbb{I}}_W^{(n)}$, and $\Delta_W^{(n)}$ to include *all* PSD matrices $\llbracket \hat{W}^{y|x} \rrbracket$, one can omit the linear constraint (4.83). Namely, the “direction” $\{\llbracket H^{y|x} \rrbracket\}_{x,y}$ can take any Hermitian matrices. Using some linear algebra, the gradient

$$\begin{aligned}
\left. \frac{d}{dt} \right|_{t=0} \bar{\mathbf{I}}_W^{(n)} (\hat{W} + tH) &\propto -\frac{1}{n} \left\langle \sum_{k=1}^n \sum_{\mathbf{x}_1^n} Q^{(n)}(\mathbf{x}_1^n) \cdot \text{tr} \left([\hat{W}^{\gamma_n | x_n}] \dots [\hat{W}^{\gamma_{k+1} | x_{k+1}}] [H^{\gamma_k | x_k}] [\hat{W}^{\gamma_{k-1} | x_{k-1}}] \dots [\hat{W}^{\gamma_1 | x_1}] \cdot [\rho_{\mathbf{S}_0}] \right) \right\rangle_{Y_1^n} \\
&= -\frac{1}{n} \sum_{\mathbf{x}_1^n, \mathbf{y}_1^n} P_{X_1^n, Y_1^n | S_0}(\mathbf{x}_1^n, \mathbf{y}_1^n | \rho_{S_0}) \cdot \sum_k \sum_{s', s, \tilde{s}, \tilde{s}} \bar{\rho}_{\tilde{S}_{k-1}}^{(\mathbf{y}_1^n)}(s, \tilde{s}) \cdot H^{y_k | x_k}(s', s, \tilde{s}, \tilde{s}) \cdot \bar{\rho}_{\tilde{S}_k}^{(\mathbf{y}_{k+1}^n)}(s', \tilde{s}') \quad (4.84)
\end{aligned}$$

$$\begin{aligned}
\left. \frac{d}{dt} \right|_{t=0} \underline{\mathbf{I}}_W^{(n)} (\hat{W} + tH) &\propto -\frac{1}{n} \left\langle \sum_{k=1}^n \sum_{\mathbf{x}_1^n} Q^{(n)}(\mathbf{x}_1^n) \cdot \text{tr} \left([\hat{W}^{\gamma_n | x_n}] \dots [\hat{W}^{\gamma_{k+1} | x_{k+1}}] [H^{\gamma_k | x_k}] [\hat{W}^{\gamma_{k-1} | x_{k-1}}] \dots [\hat{W}^{\gamma_1 | x_1}] \cdot [\rho_{\mathbf{S}_0}] \right) \right\rangle_{Y_1^n} \\
&\quad + \frac{1}{n} \left\langle \sum_{k=1}^n \text{tr} \left([\hat{W}^{\gamma_n | X_n}] \dots [\hat{W}^{\gamma_{k+1} | X_{k+1}}] [H^{\gamma_k | X_k}] [\hat{W}^{\gamma_{k-1} | X_{k-1}}] \dots [\hat{W}^{\gamma_1 | X_1}] \cdot [\rho_{\mathbf{S}_0}] \right) \right\rangle_{X_1^n Y_1^n} \\
&= -\frac{1}{n} \sum_{\mathbf{x}_1^n, \mathbf{y}_1^n} P_{X_1^n, Y_1^n | S_0}(\mathbf{x}_1^n, \mathbf{y}_1^n | \rho_{S_0}) \cdot \sum_k \sum_{s', s, \tilde{s}, \tilde{s}} \bar{\rho}_{\tilde{S}_{k-1}}^{(\mathbf{y}_1^{k-1})}(s, \tilde{s}) \cdot H^{y_k | x_k}(s', s, \tilde{s}, \tilde{s}) \cdot \bar{\rho}_{\tilde{S}_k}^{(\mathbf{y}_{k+1}^n)}(s', \tilde{s}') \quad (4.85) \\
&\quad + \frac{1}{n} \sum_{\mathbf{x}_1^n, \mathbf{y}_1^n} P_{X_1^n, Y_1^n | S_0}(\mathbf{x}_1^n, \mathbf{y}_1^n | \rho_{S_0}) \cdot \sum_k \sum_{s', s, \tilde{s}, \tilde{s}} \bar{\rho}_{\tilde{S}_{k-1}}^{(\mathbf{x}_1^{k-1}, \mathbf{y}_1^{k-1})}(s, \tilde{s}) \cdot H^{y_k | x_k}(s', s, \tilde{s}, \tilde{s}) \cdot \bar{\rho}_{\tilde{S}_k}^{(\mathbf{x}_{k+1}^n, \mathbf{y}_{k+1}^n)}(s', \tilde{s}')
\end{aligned}$$

$$\begin{aligned}
\left. \frac{d}{dt} \right|_{t=0} \Delta_W^{(n)} (\hat{W} + tH) &\propto -\frac{1}{n} \left\langle \sum_{k=1}^n \text{tr} \left([\hat{W}^{\gamma_n | X_n}] \dots [\hat{W}^{\gamma_{k+1} | X_{k+1}}] [H^{\gamma_k | X_k}] [\hat{W}^{\gamma_{k-1} | X_{k-1}}] \dots [\hat{W}^{\gamma_1 | X_1}] \cdot [\rho_{\mathbf{S}_0}] \right) \right\rangle_{X_1^n Y_1^n} \\
&= -\frac{1}{n} \sum_{\mathbf{x}_1^n, \mathbf{y}_1^n} P_{X_1^n, Y_1^n | S_0}(\mathbf{x}_1^n, \mathbf{y}_1^n | \rho_{S_0}) \cdot \sum_k \sum_{s', s, \tilde{s}, \tilde{s}} \bar{\rho}_{\tilde{S}_{k-1}}^{(\mathbf{x}_1^{k-1}, \mathbf{y}_1^{k-1})}(s, \tilde{s}) \cdot H^{y_k | x_k}(s', s, \tilde{s}, \tilde{s}) \cdot \bar{\rho}_{\tilde{S}_k}^{(\mathbf{x}_{k+1}^n, \mathbf{y}_{k+1}^n)}(s', \tilde{s}') \quad (4.86)
\end{aligned}$$

w.r.t. \hat{W} of these functions on this *extended* domain can be expressed as

$$\left(\nabla \bar{I}_{W,\text{ext}}^{(n)}(\hat{W})\right)^{y|x} \propto -\frac{1}{n} \left\langle \sum_{k=1}^n \delta_{X_k,x} \cdot \delta_{Y_k,y} \cdot \bar{\varrho}_{\hat{S}_{k-1}}^{(Y_1^{k-1})} \otimes \bar{\varrho}_{\hat{S}_k}^{(Y_{k+1}^n)} \right\rangle_{X_1^n Y_1^n}, \quad (4.91)$$

$$\left(\nabla I_{W,\text{ext}}^{(n)}(\hat{W})\right)^{y|x} \propto -\frac{1}{n} \left\langle \sum_{k=1}^n \delta_{X_k,x} \cdot \delta_{Y_k,y} \cdot \left(\bar{\varrho}_{\hat{S}_{k-1}}^{(Y_1^{k-1})} \otimes \bar{\varrho}_{\hat{S}_k}^{(Y_{k+1}^n)} - \bar{\varrho}_{\hat{S}_{k-1}}^{(X_1^{k-1}, Y_1^{k-1})} \otimes \bar{\varrho}_{\hat{S}_k}^{(X_{k+1}^n, Y_{k+1}^n)} \right) \right\rangle_{X_1^n Y_1^n}, \quad (4.92)$$

$$\left(\nabla \Delta_{W,\text{ext}}^{(n)}(\hat{W})\right)^{y|x} \propto -\frac{1}{n} \left\langle \sum_{k=1}^n \delta_{X_k,x} \cdot \delta_{Y_k,y} \cdot \bar{\varrho}_{\hat{S}_{k-1}}^{(X_1^{k-1}, Y_1^{k-1})} \otimes \bar{\varrho}_{\hat{S}_k}^{(X_{k+1}^n, Y_{k+1}^n)} \right\rangle_{X_1^n Y_1^n}, \quad (4.93)$$

respectively. For stationary and ergodic input and output processes (X_1^n, Y_1^n) , we can *estimate* (4.91) and (4.93), respectively, as

$$\left(\nabla \bar{I}_{W,\text{ext}}^{(n)}(\hat{W})\right)^{y|x} \dot{\propto} -\frac{1}{n} \sum_{k: \substack{\tilde{x}_k=x \\ \tilde{y}_k=y}} \bar{\varrho}_{\hat{S}_{k-1}}^{(\tilde{y}_1^{k-1})} \otimes \bar{\varrho}_{\hat{S}_k}^{(\tilde{y}_{k+1}^n)}, \quad (4.94)$$

$$\left(\nabla \Delta_{W,\text{ext}}^{(n)}(\hat{W})\right)^{y|x} \dot{\propto} -\frac{1}{n} \sum_{k: \substack{\tilde{x}_k=x \\ \tilde{y}_k=y}} \bar{\varrho}_{\hat{S}_{k-1}}^{(\tilde{x}_1^{k-1}, \tilde{y}_1^{k-1})} \otimes \bar{\varrho}_{\hat{S}_k}^{(\tilde{x}_{k+1}^n, \tilde{y}_{k+1}^n)}, \quad (4.95)$$

where $(\tilde{x}_1^n, \tilde{y}_1^n)$ is a realization of the channel input/output processes generated by the original channel model. The dot in (4.94) and (4.95) stands for “approximation”. Notice that the messages $\bar{\varrho}_{\hat{S}_{k-1}}^{(\tilde{y}_1^{k-1})}$, $\bar{\varrho}_{\hat{S}_k}^{(\tilde{y}_{k+1}^n)}$, $\bar{\varrho}_{\hat{S}_{k-1}}^{(\tilde{x}_1^{k-1}, \tilde{y}_1^{k-1})}$, and $\bar{\varrho}_{\hat{S}_k}^{(\tilde{x}_{k+1}^n, \tilde{y}_{k+1}^n)}$ can be computed iteratively. Thus, (4.94) and (4.95) provide efficient means to estimate the gradient. However, due to the extension of the domain, the gradients computed above may not satisfy constraint (4.83). This can be compensated using a projection w.r.t. the linear constraint, which can be solved using linear programming. On the other hand, the above gradient method may lead to a violation of the PSD condition required by CC-QSCs. However, since the feasible domain of CC-QSCs is convex and bounded, this can be corrected using convex programming at each step.

We summarize the above discussion as Algorithm 4.3, which is an iterative gradient-descent method for minimizing $\Delta_W^{(n)}$. Notice that the quantity λ_ℓ in this case is the conditional probability $P_{X_\ell Y_\ell | X_1^{\ell-1} Y_1^{\ell-1}}(\tilde{x}_\ell, \tilde{y}_\ell | \tilde{x}_1^{\ell-1}, \tilde{y}_1^{\ell-1})$. The algorithm for minimizing the upper and lower bounds are similar, and we omit the details.

Algorithm 4.3 Optimizing the Difference Function $\Delta_W^{(n)}(\hat{W})$ **Input:** An indecomposable CC-QSC, an input distribution Q , a positive integer n large enough, an initial auxiliary CC-QSC $\{\hat{W}^{y|x}\}_{x,y}$, step size $\gamma > 0$.**Output:** $\{\hat{W}^{y|x}\}_{x,y}$, an estimated local minimum point of $\Delta_W^{(n)}$.

- 1: Initialize the memory density operator $\rho_{\hat{S}_0} \leftarrow |0\rangle\langle 0|$
- 2: Generate an input sequence $\tilde{\mathbf{x}}_1^n \sim Q^{\otimes n}$
- 3: Generate a corresponding output sequence $\tilde{\mathbf{y}}_1^n$
- 4: **repeat**
- 5: $\vec{\varrho}_{\hat{S}_0} \leftarrow \rho_{\hat{S}_0}$
- 6: **for each** $\ell = 1, \dots, n$ **do**
- 7: $[\vec{\varrho}_{\hat{S}_\ell}] \leftarrow [\hat{W}^{\tilde{y}_\ell|\tilde{x}_\ell}] \cdot [\vec{\varrho}_{\hat{S}_{\ell-1}}]$
- 8: $\lambda_\ell \leftarrow \text{tr}(\vec{\varrho}_{\hat{S}_\ell})$
- 9: $\vec{\varrho}_{\hat{S}_\ell} \leftarrow \lambda_\ell^{-1} \cdot \vec{\varrho}_{\hat{S}_\ell}$
- 10: **end for**
- 11: $\vec{\varrho}_{\hat{S}_n} \leftarrow I_{\hat{S}_n}$
- 12: **for each** $\ell = n, \dots, 1$ **do**
- 13: $[\vec{\varrho}_{\hat{S}_{\ell-1}}] \leftarrow [\vec{\varrho}_{\hat{S}_\ell}] \cdot [\hat{W}^{\tilde{y}_\ell|\tilde{x}_\ell}]$
- 14: $\vec{\varrho}_{\hat{S}_{\ell-1}} \leftarrow \left(\text{tr}(\vec{\varrho}_{\hat{S}_{\ell-1}}) \right)^{-1} \cdot \vec{\varrho}_{\hat{S}_{\ell-1}}$
- 15: **end for**
- 16: for each x, y , let $\left(\nabla \Delta_{W, \text{ext}}^{(n)}(\hat{W}) \right)^{y|x} \leftarrow \mathbf{0}$
- 17: **for each** $k = 1, \dots, n$ **do**
- 18: $\left(\nabla \Delta_{W, \text{ext}}^{(n)}(\hat{W}) \right)^{\tilde{y}_k|\tilde{x}_k} += \frac{1}{n} \cdot \frac{\vec{\varrho}_{\hat{S}_{k-1}} \otimes \vec{\varrho}_{\hat{S}_k}}{\lambda_k \cdot \text{tr}(\vec{\varrho}_{\hat{S}_k} \cdot \vec{\varrho}_{\hat{S}_k})}$
- 19: **end for**
- 20: Project $\left\{ \left(\nabla \Delta_{W, \text{ext}}^{(n)}(\hat{W}) \right)^{y|x} \right\}_{x,y}$ onto the subspace satisfying (4.83); denoting the result by $\left\{ \left(\nabla \Delta_W^{(n)}(\hat{W}) \right)^{y|x} \right\}_{x,y}$
- 21: $\{\hat{W}^{y|x}\}_{x,y} \leftarrow \{\hat{W}^{y|x}\}_{x,y} - \gamma \cdot \left\{ \left(\nabla \Delta_W^{(n)}(\hat{W}) \right)^{y|x} \right\}_{x,y}$
- 22: Solve the following convex program w.r.t. $\{\tilde{W}^{y|x}\}_{x,y}$:

$$\begin{aligned}
& \min \quad \sum_{x,y} \text{tr} \left(([\tilde{W}^{y|x}] - [\hat{W}^{y|x}]) \cdot ([\tilde{W}^{y|x}] - [\hat{W}^{y|x}])^\dagger \right) \\
& \text{s. t.} \quad [\tilde{W}^{y|x}] \in \mathbb{C}^{\mathcal{S}^2 \times \mathcal{S}^2} \text{ being PSD} \quad \forall x, y \\
& \quad \sum_{y \in \mathcal{Y}} \sum_{s', \tilde{s}': s' = \tilde{s}'} [\tilde{W}^{y|x}]_{(s', s), (\tilde{s}', \tilde{s})} = \delta_{s, \tilde{s}} \quad \forall x
\end{aligned}$$

- 23: $\{\hat{W}^{y|x}\} \leftarrow \{\tilde{W}^{y|x}\}$
- 24: **until** $\{\hat{W}^{y|x}\}_{x,y}$ has converged.

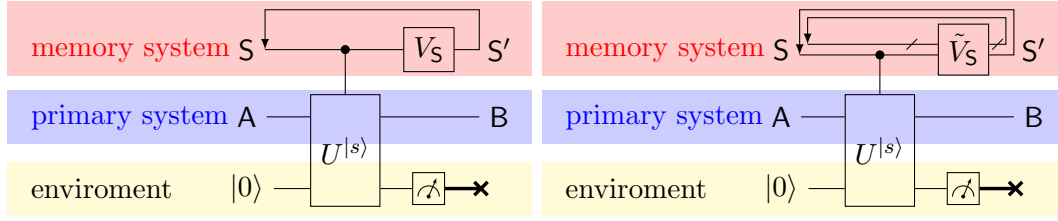


Figure 4.9: A quantum Gilbert–Elliott channel (LHS), and a variant where the memory system consists of multiple qubits with only one of them controlling $U^{|s\rangle}$ (RHS).

4.5 Example: Quantum Gilbert–Elliott Channels

In this section we present some numerical results as a demonstration of the algorithms introduced in this chapter. In particular, as a generalization of Example 4.1, we consider a class of quantum channels with memory named the quantum Gilbert–Elliott channels (QGECs), which were introduced in [CV17b], and consider their information rate using some separable input ensemble and local output measurement. Note that the numerical results in this section are based on binary logarithm, and thus the information rate is measured in bits.

A QGEC is a quantum channel with memory defined by⁸

$$\begin{aligned} \mathcal{N} : \mathfrak{D}(\mathcal{H}_S \otimes \mathcal{H}_A) &\rightarrow \mathfrak{D}(\mathcal{H}_{S'} \otimes \mathcal{H}_B) \\ \rho_{SA} &\mapsto (V_S \otimes I_B) \cdot \Phi^{\text{CBF}}(\rho_{SA}) \cdot (V_S^\dagger \otimes I_B), \end{aligned}$$

where \mathcal{H}_A , \mathcal{H}_B , and $\mathcal{H}_S = \mathcal{H}_{S'}$ are of dimension 2, namely each of them is made up of one qubit, and where Φ^{CBF} is the *controlled bit-flip channel* defined by $\Phi^{\text{CBF}}(\rho_{SA}) \triangleq E_0 \rho^{\text{SA}} E_0^\dagger + E_1 \rho^{\text{SA}} E_1^\dagger$ with

$$E_0 \triangleq \begin{bmatrix} \sqrt{1-p_g} & 0 & 0 & 0 \\ 0 & \sqrt{1-p_g} & 0 & 0 \\ 0 & 0 & \sqrt{1-p_b} & 0 \\ 0 & 0 & 0 & \sqrt{1-p_b} \end{bmatrix}, \quad E_1 \triangleq \begin{bmatrix} 0 & \sqrt{p_g} & 0 & 0 \\ \sqrt{p_g} & 0 & 0 & 0 \\ 0 & 0 & 0 & \sqrt{p_b} \\ 0 & 0 & \sqrt{p_b} & 0 \end{bmatrix},$$

and where V_S is some unitary operator on \mathcal{H}_S to be specified later. The controlled bit-flip channel Φ^{CBF} applies a quantum bit-flip channel to the system A with flipping probability p_g when the system S is in the state of $|0\rangle$, and with flipping probability p_b when the system S is in the state of $|1\rangle$. The action of a QGEC is the combined effect of a controlled bit-flip channel and a unitary evolution on S; as depicted in the

⁸We put the system S ahead of A and B in this example to emphasize the role of S as a *control* qubit, and also for simplicity reasons.

following circuit diagram in Figure 4.9, where $U^{(s)}$ is a Stinespring representation of Φ^{CBF} :

$$U^{(0)} \triangleq \begin{bmatrix} \sqrt{1-p_g} & 0 & 0 & -\sqrt{p_g} \\ 0 & \sqrt{1-p_g} & \sqrt{p_g} & 0 \\ 0 & -\sqrt{p_g} & \sqrt{1-p_g} & 0 \\ \sqrt{p_g} & 0 & 0 & \sqrt{1-p_g} \end{bmatrix}, \quad U^{(1)} \triangleq \begin{bmatrix} \sqrt{1-p_b} & 0 & 0 & -\sqrt{p_b} \\ 0 & \sqrt{1-p_b} & \sqrt{p_b} & 0 \\ 0 & -\sqrt{p_b} & \sqrt{1-p_b} & 0 \\ \sqrt{p_b} & 0 & 0 & \sqrt{1-p_b} \end{bmatrix}.$$

In Figure 4.10–4.13, we present some numerical information rate lower bounds estimated for a QGEC and a variant of a QGEC (as depicted in Figure 4.9), equipped with “trivial” orthonormal ensemble and projective measurements. Namely, the original channel in Figure 4.10 and 4.12 can be described by the CC-QSC

$$\mathcal{N}^{y|x}(\rho_S) = \text{tr}_B \left((V_S^\dagger V_S \otimes |y\rangle\langle y|) \cdot \Phi^{\text{CBF}}(\rho_S \otimes |x\rangle\langle x|) \right), \quad (4.96)$$

whereas Figure 4.11 and 4.13 is described by

$$\mathcal{N}^{y|x}(\rho_S) = \text{tr}_B \left((\tilde{V}_S^\dagger \tilde{V}_S \otimes |y\rangle\langle y|) \cdot (\mathcal{I} \otimes \Phi^{\text{CBF}})(\rho_S \otimes |x\rangle\langle x|) \right), \quad (4.97)$$

where $\{|x\rangle\}_{x \in \mathcal{X}}$ and $\{|y\rangle\}_{y \in \mathcal{Y}}$ are some orthonormal basis of \mathcal{H}_A and \mathcal{H}_B , respectively. In the latter case, the memory system S is extended as $\mathcal{H}_S = \mathcal{H}_{S_1} \otimes \mathcal{H}_{S_0}$. More specifically, in (4.97), ρ_S and \tilde{V}_S are operators on \mathcal{H}_S , and Φ^{CBF} acts on $\mathfrak{D}(\mathcal{H}_{S_0} \otimes \mathcal{H}_A)$, and \mathcal{I} is the identity map on S_1 . For both scenarios, the input processes are binary symmetric i.i.d. processes, *i.e.*, $Q^{(n)}(\mathbf{x}_1^n) \triangleq 2^{-n}$ for all $\mathbf{x}_1^n \in \{0, 1\}^n$. The lower bounds in those figures were obtained by minimizing the difference function $\Delta_W^{(n)}$ defined in (4.30) w.r.t. different classes of auxiliary channels (subject to certain time and threshold constraints). For the case where the auxiliary channels are CC-QSCs, Algorithm 4.3 was applied. For FSMC auxiliary channels, we implemented the expectation-maximization type algorithm in [SVS09] for comparison. As already emphasized beforehand, these lower bounds represent rates that are achievable with the help of a mismatched decoder [GLT00]. Figure 4.14 is an example illustrating the typical convergence time of different methods (including our own) for minimizing the difference function. In all of the above figures, $n = 10,000$, and we have used Algorithm 4.2 to *estimate* the information rate. According to our experience, the error of the estimation in this case lies within the line-width in the figures.

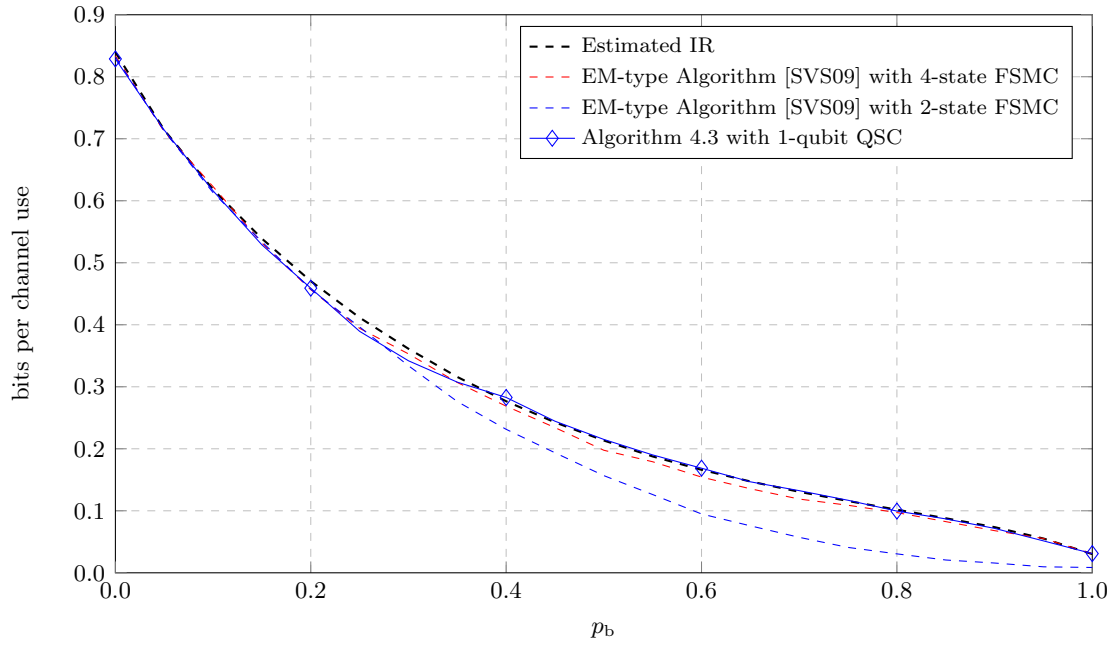


Figure 4.10: Quantum Gilbert–Elliott channel: $p_g = 0.05$ is fixed; p_b varies from 0 to 1; $V_S = \exp(-j\alpha H)$, where H is some fixed 2-by-2 Hermitian matrix and where $\alpha = 1$ is fixed; $n = 10^5$.

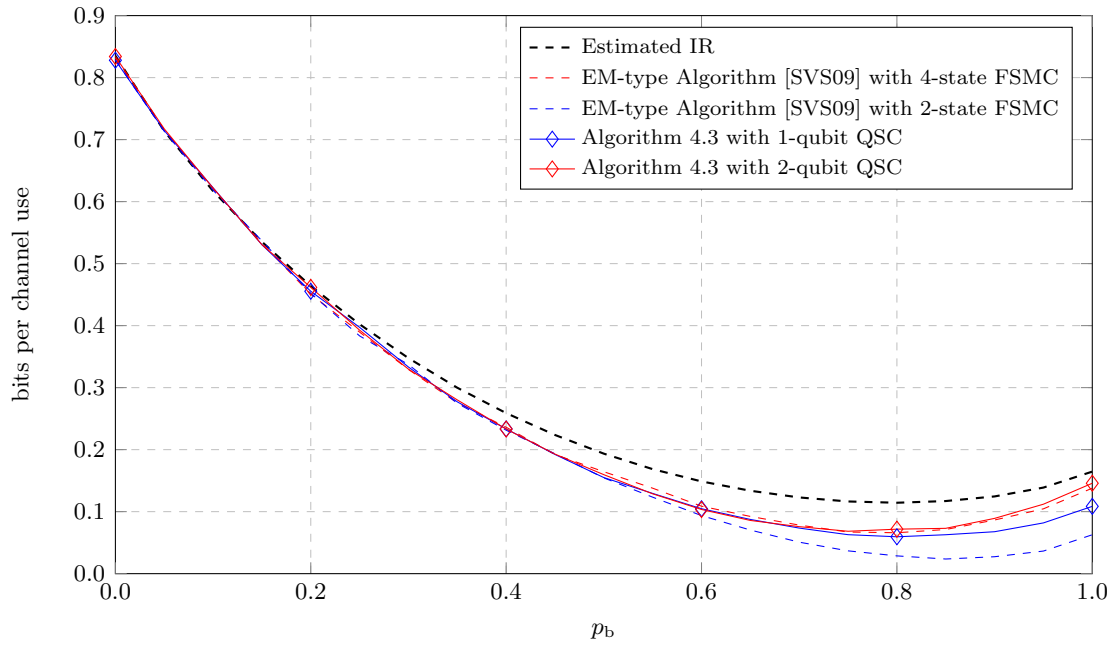


Figure 4.11: Variant of the quantum Gilbert–Elliott channel described in the RHS of Figure 4.9. Parameters: $p_g = 0.05$; $p_b \in [0, 1]$; $\tilde{V}_S = \exp(-j\alpha H)$, where H is some fixed 4-by-4 Hermitian matrix and where $\alpha = 1$ is fixed; $n = 10^5$.

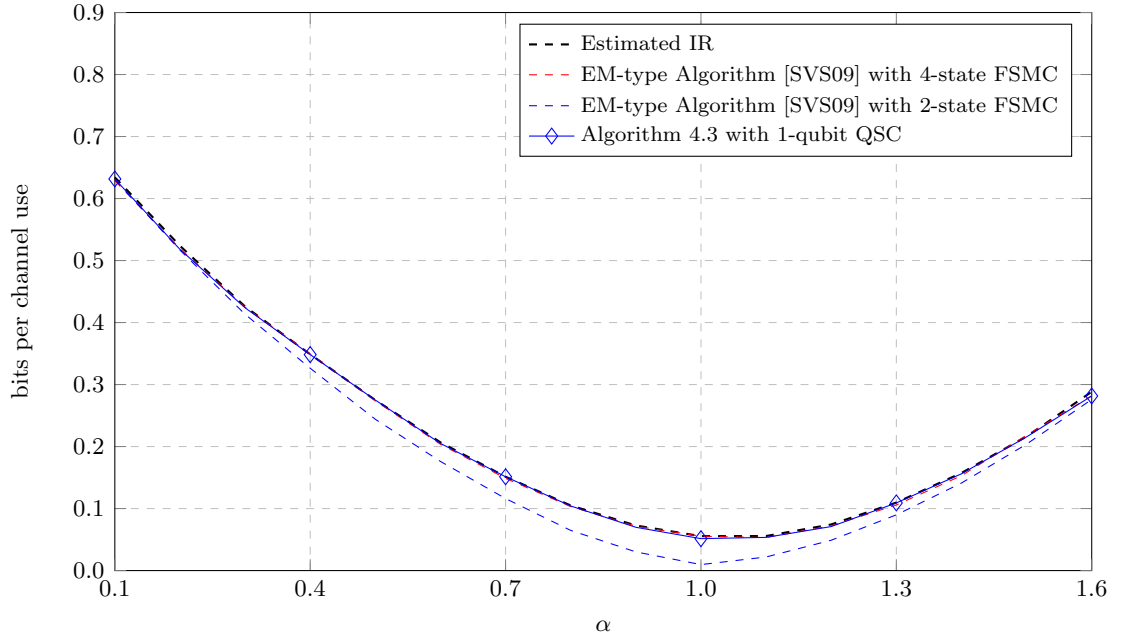


Figure 4.12: Quantum Gilbert–Elliott channel: $p_g = 0.05$ is fixed; $p_b = 0.95$ is fixed; $V_S = \exp(-j\alpha H)$, where H is the same 2-by-2 Hermitian matrix as in Figure 4.10 and where α varies from 0.1 to +1.5; $n = 10^5$.

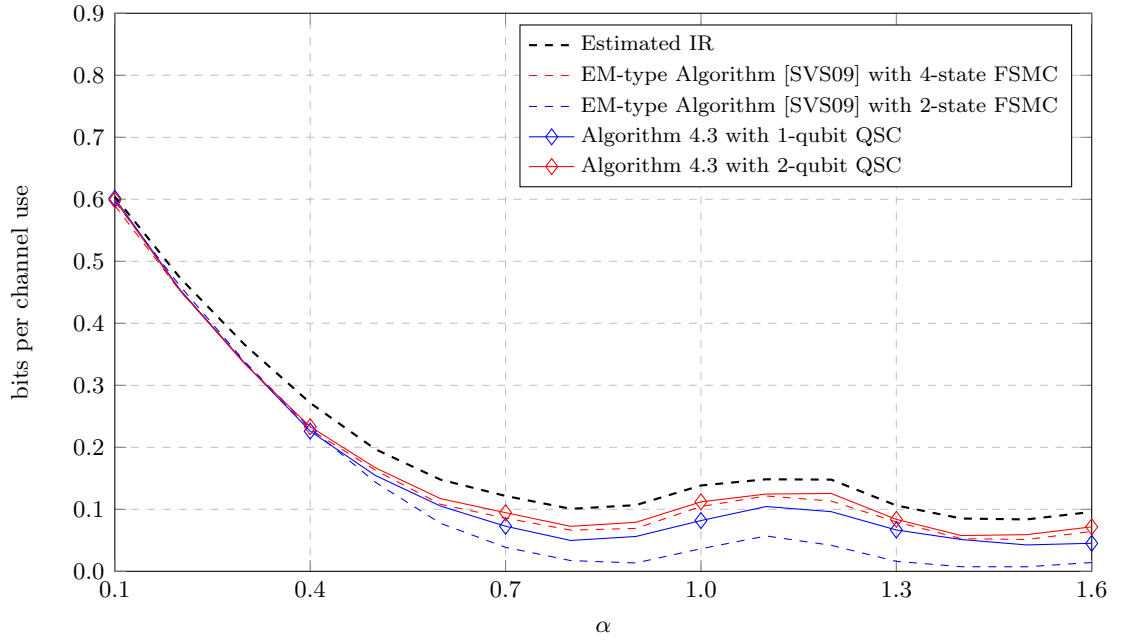


Figure 4.13: Same variant of the quantum Gilbert–Elliott channel as in Figure 4.11 with different parameters: $p_g = 0.05$; $p_b = 0.95$; $V_S = \exp(-j\alpha H)$, where H is the same 4-by-4 Hermitian matrix as in Figure 4.11 and where α varies from 0.1 to +1.5; $n = 10^5$.

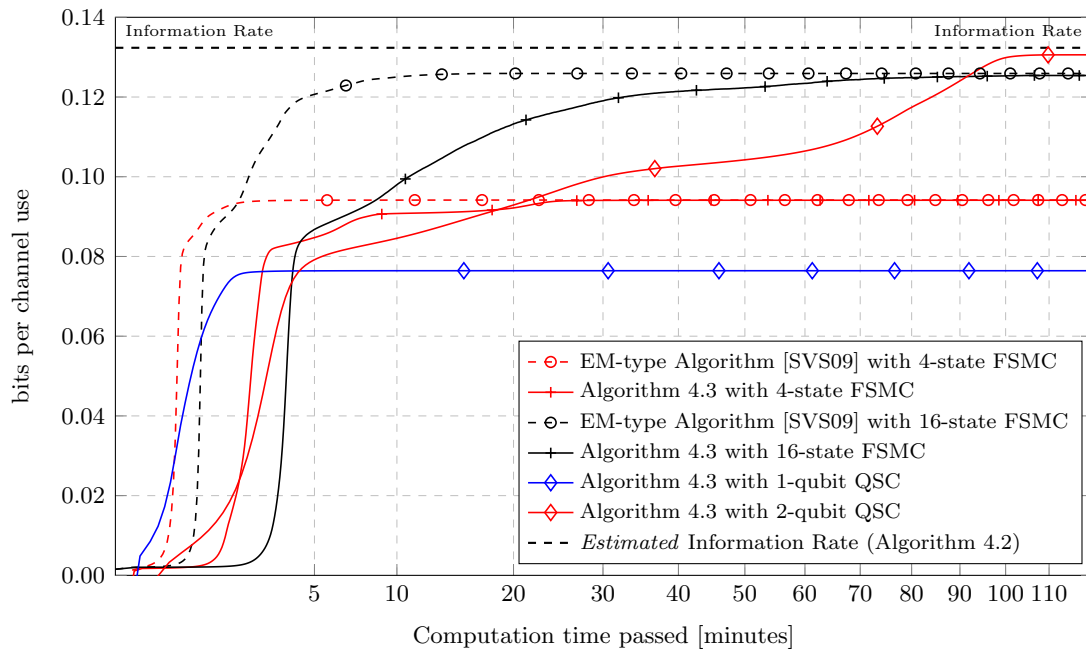


Figure 4.14: Minimizing the difference function $\Delta_W^{(n)}$ using different methods. The markers appear after every 400 updates.

Summary and Outlook

Chapter 2 proposed a generalized factor graph model called double-edge factor graphs (DeFGs) for representing quantum systems. Compared with the factor graph for quantum probabilities [LV12; LV17], DeFGs provide a neat generalization of the “closing-the-box” operations and is also more generic. We also proposed generalized versions of the belief-propagation (BP) algorithms for DeFGs and derived the loop calculus expansion for DeFGs (see (2.48)) at BP fixed points. However, it is still unclear how the induced partition sum $Z_{\text{induced}}(\{m_{j \rightarrow a}, m_{a \rightarrow j}\}_{(j,a) \in \mathcal{E}})$ at BP fixed points can be related to the actual partition sum $Z(\mathcal{G})$. In comparison, for factor graphs, it was shown that the induced partition sum Z_{induced} coincides with the Bethe partition sum Z_{B} at BP fixed points (see Corollary 1.22), and how well the latter estimates $Z(\mathcal{G})$ depends on how F_{B} estimates F_{G} . Nevertheless, we studied several numerical examples. We observed a promising performance of BP algorithms for DeFGs.

Chapter 3 studied a graphical model called quantum factor graphs. In particular, we investigated how “closing-the-box” operations behave when all the local operators are proportionally close to identity operators. Under such a setup, the “closing-the-box” operations provide an *approximation* to the partition sum of a QFG, as we found that the distributivity of the \star -product over the (partial) trace operations holds approximately. We also introduced BP algorithms for QFGs as a natural generalization of the “closing-the-box” operations. The algorithm coincided with the quantum belief-propagation algorithm for bifactor networks [LP08]. We were able to generalize Bethe’s approximation to QFGs and show that the positive BP fixed points *approximately* correspond to the quantum Bethe free energy’s interior stationary points.

Chapter 4 considered the scenario of transmitting classical information over a quantum channel with finite memory using separable-state ensembles and local measurements. We defined the classical-input classical-output quantum-state channel (CC-

QSC) as an equivalent way to describe such communication setups and demonstrated how normal factor graphs could be used to visualize such channels. We showed that a CC-QSC's information rate is independent of the initial density operator under suitable conditions and proposed algorithms for estimating and bounding such information rate. The computations in such algorithms can be carried out using the corresponding factor graphs of the CC-QSC. We emphasize that our approach for optimizing the lower bound is data-driven and does not require the knowledge of the actual channel model.

Despite the obstacles we have encountered in analyzing the corresponding generalized versions of BP algorithms in Chapter 2 and Chapter 3, we have observed promising numerical results in a number of examples. This suggests potential connections between the generalized BP-fixed points and the corresponding generalized partition sums of DeFGs and QFGs, respectively, yet to be discovered. One of the directions is to generalize the method of graph covers to these new factor graphs. (For some initial results, see [HV20].) Another is to consider the regional method as in [YFW05]. In some earlier studies of (classical) factor graphs [Mor15b], some methods from information geometry have been proven useful in analyzing the loop calculus expansion at the fixed points. Though it is currently unclear whether (or how much) quantum information geometry can be helpful in analyzing the loop calculus expansion for DeFGs, it is still an interesting direction to look into.

Appendix A

Alternative Approximated Distributivity of \star over (Partial) Trace

In this appendix, we discuss how $\text{tr}(\rho_A \star \sigma_{AB})$ and $\text{tr}_B(\rho_A \star \sigma_{AB})$ can be approximated by $\text{tr}_A(\rho_A \star \text{tr}_B(\sigma_{AB}))$ and $\rho_A \star \text{tr}_B(\sigma_{AB})$, respectively, when the operators ρ_A and σ_{AB} are proportionally close to identity operator in a nonlinear manner, *i.e.*,

$$\rho_A \propto \exp(t \cdot X) \tag{A.1}$$

$$\sigma_{AB} \propto \exp(t \cdot Y) \tag{A.2}$$

for some Hermitian matrices X and Y (each of proper size) and some small $t > 0$. We present some results similar to Theorem 3.7 and Proposition 3.8.

Theorem A.1. *Consider finite-dimensional Hilbert spaces \mathcal{H}_A and \mathcal{H}_B . Given $X \in \mathfrak{L}_+(\mathcal{H}_A)$, and $Y \in \mathfrak{L}_+(\mathcal{H}_A \otimes \mathcal{H}_B)$, it holds that*

$$\text{tr}(e^{tX} \star e^{tY}) = \text{tr}_A(e^{tX} \star \text{tr}_B(e^{tY})) + O(t^4), \tag{A.3}$$

where the real number $t > 0$ is in some neighborhood of 0.

Proof. We use similar techniques in the proof of Theorem 3.7 in proving this theorem. Using the notation of normalized trace functions, we rewrite (A.3) as

$$\overline{\text{tr}}(e^{tX} \star e^{tY}) = \overline{\text{tr}}_A(e^{tX} \star \overline{\text{tr}}_B(e^{tY})) + O(t^4). \tag{A.4}$$

Let $\tilde{X} \triangleq X \otimes I_{\mathbf{B}}$. The Taylor series expansion of each side of (A.4) (without $O(t^4)$) can be expressed as

$$\begin{aligned} \text{LHS} &= 1 + t \cdot \overline{\text{tr}}(\tilde{X} + Y) + \frac{1}{2}t^2 \cdot \overline{\text{tr}}(\tilde{X} + Y)^2 \\ &\quad + \frac{1}{3!}t^3 \cdot \overline{\text{tr}}(\tilde{X} + Y)^3 + \frac{1}{4!}t^4 \cdot \overline{\text{tr}}(\tilde{X} + Y)^4 + O(t^5), \end{aligned} \quad (\text{A.5})$$

$$\begin{aligned} \text{RHS} &= 1 + t \cdot \overline{\text{tr}}_{\mathbf{A}}(X + \overline{\text{tr}}_{\mathbf{B}}(Y)) + \frac{t^2}{2} \cdot \overline{\text{tr}}_{\mathbf{A}}(X^2 + X\overline{\text{tr}}_{\mathbf{B}}(Y) + \overline{\text{tr}}_{\mathbf{B}}(Y)X + \overline{\text{tr}}_{\mathbf{B}}(Y^2)) \\ &\quad + \frac{t^3}{6} \cdot \overline{\text{tr}}_{\mathbf{A}}(X^3 + 3 \cdot X^2 \cdot \overline{\text{tr}}_{\mathbf{B}}(Y) + 3 \cdot X \cdot \overline{\text{tr}}_{\mathbf{B}}(Y^2) + \overline{\text{tr}}_{\mathbf{B}}(Y^3)) + O(t^4). \end{aligned} \quad (\text{A.6})$$

Note that (A.5) and (A.6) agree up to t^3 , which concludes the proof. \square

We can also show the following proposition in a similar way.

Proposition A.2. *Under the same setup as in Theorem A.1, it holds that*

$$\text{tr}_{\mathbf{B}}(e^{tX} \star e^{tY}) = e^{tX} \star \text{tr}_{\mathbf{B}}(e^{tY}) + O(t^3). \quad (\text{A.7})$$

Proof. Rewrite (A.7) as

$$\overline{\text{tr}}_{\mathbf{B}}(e^{tX} \star e^{tY}) = e^{tX} \star \overline{\text{tr}}_{\mathbf{B}}(e^{tY}) + O(t^3), \quad (\text{A.8})$$

and note that each side of the above equation (without $O(t^3)$) can be expressed as

$$\text{LHS} = I + t \cdot \overline{\text{tr}}_{\mathbf{B}}(\tilde{X} + Y) + \frac{1}{2}t^2 \cdot \overline{\text{tr}}_{\mathbf{B}}(\tilde{X} + Y)^2 + \frac{1}{3!}t^3 \cdot \overline{\text{tr}}_{\mathbf{B}}(\tilde{X} + Y)^3 + O(t^4), \quad (\text{A.9})$$

$$\begin{aligned} \text{RHS} &= I + t \cdot (X + \overline{\text{tr}}_{\mathbf{B}}(Y)) + \frac{1}{2}t^2 \cdot (X^2 + X\overline{\text{tr}}_{\mathbf{B}}(Y) + \overline{\text{tr}}_{\mathbf{B}}(Y)X + \overline{\text{tr}}_{\mathbf{B}}(Y^2)) + O(t^3), \\ &\quad (\text{A.10}) \end{aligned}$$

respectively. The proposition can be justified since the above two expressions agree up to t^2 . \square

Appendix B

Quantum Exponential Family

Definition B.1 (Quantum Exponential Family [Mor15b]). Similar to classical exponential families, a *quantum exponential family* (of degree d) is a parametric family of quantum operators in the form of

$$\rho_{\boldsymbol{\theta}} \triangleq \exp \left(\sum_{k=1}^d \theta_k \cdot \mathbf{T}_k - \Psi(\boldsymbol{\theta}) \right) \quad (\text{B.1})$$

for *natural parameter* $\boldsymbol{\theta}$ in some open subset $\Theta \in \mathbb{R}^d$, where $\mathbf{T}_k \in \mathfrak{L}_{\dagger}(\mathcal{H}_{\partial k}) = \mathfrak{L}_{\dagger}(\otimes_{i \in \partial k} \mathcal{H}_i)$ are some given Hermitian operators ($\partial k \subseteq \{1, \dots, N\}$), and conventions as in (3.7) are applied in the summation in (B.1). Moreover, the scalar $\Psi(\boldsymbol{\theta})$ is defined as

$$\Psi(\boldsymbol{\theta}) \triangleq \log \left(\text{tr} \left(\exp \left(\sum_{k=1}^d \theta_k \cdot \mathbf{T}_k \right) \right) \right). \quad (\text{B.2})$$

Thus, $\rho_{\boldsymbol{\theta}}$ is a density operator. □

Note that if $\{\mathbf{T}_k\}_{k=1}^d$ are linearly independent, then the mapping $\boldsymbol{\theta} \mapsto \rho_{\boldsymbol{\theta}}$ is injective. In this appendix, we assume $\{\mathbf{T}_k\}_{k=1}^d$ to be linearly independent. In this case, the (strict) convexity of the function Ψ follows naturally from the (strict) convexity of the exponential function (see, *e.g.*, [Car10]).

Example B.2. Consider the quantum exponential family

$$\sigma_{\boldsymbol{\theta}} = \exp \left(\sum_{a \in \mathcal{F}} \sum_k \theta_k^{(a)} \cdot \mathbf{T}_k^{(a)} - \Psi(\boldsymbol{\theta}) \right), \quad (\text{B.3})$$

where $\boldsymbol{\theta} \in \mathbb{R}^d$ and where $\{\mathbf{T}_k^{(a)}\}_k$ form a basis of $\mathfrak{L}_{\dagger}(\mathcal{H}_{\partial a})$. The parametrization of $\sigma_{\boldsymbol{\theta}}$ corresponds to all the density operators σ that can be decomposed as

$$\sigma \propto \bigstar_{a \in \mathcal{F}} \sigma_a = \exp \left(\sum_{a \in \mathcal{F}} \log \sigma_a \right), \quad (\text{B.4})$$

where $\sigma_a \in \mathfrak{D}(\mathcal{H}_{\partial a})$ for each $a \in \mathcal{F}$. \square

Definition B.3 (Dual Parameters). Given a quantum exponential family as in (B.3).

We define the *dual parameter* (w.r.t. $\boldsymbol{\theta}$) to be $\boldsymbol{\eta} = (\eta_l)_{l=1}^d$ where

$$\eta_l \triangleq \frac{\partial}{\partial \theta_l} \Psi(\boldsymbol{\theta}) \quad (\text{B.5})$$

for each $l = 1, \dots, d$. \square

We can re-express $\boldsymbol{\eta}$ as a function of $\rho_{\boldsymbol{\theta}}$, *i.e.*,

$$\begin{aligned} \eta_l &= \frac{\partial}{\partial \theta_l} \Psi(\boldsymbol{\theta}) = \frac{\partial}{\partial \theta_l} \log \left(\text{tr} \left(\exp \left(\sum_{k=1}^d \theta_k \cdot \mathbf{T}_k \right) \right) \right), \\ &= \text{tr} \left(\exp \left(\sum_{k=1}^d \theta_k \mathbf{T}_k \right) \right)^{-1} \frac{\partial}{\partial \theta_l} \text{tr} \left(\exp \left(\sum_{k=1}^d \theta_k \mathbf{T}_k \right) \right), \\ &\stackrel{(a)}{=} \text{tr} \left(\exp \left(\sum_{k=1}^d \theta_k \mathbf{T}_k \right) \right)^{-1} \text{tr} \left(\exp \left(\sum_{k=1}^d \theta_k \mathbf{T}_k \right) \cdot \mathbf{T}_l \right), \\ &= \text{tr} (\rho_{\boldsymbol{\theta}} \cdot \mathbf{T}_l), \end{aligned} \quad (\text{B.6})$$

where step (a) was obtained by applying the first-order perturbation theory [Kat95].

Due to the strict convexity of Ψ , the mapping $\boldsymbol{\eta}(\boldsymbol{\theta}) : \boldsymbol{\theta} \mapsto (\text{tr} (\rho_{\boldsymbol{\theta}} \cdot \mathbf{T}_l))_{l=1}^d$ is injective. On the other hand, by considering the conjugate function of Ψ defined as (which is also strictly convex)

$$\Phi(\boldsymbol{\eta}) \triangleq \sup_{\boldsymbol{\theta}} \left\{ \sum_{k=1}^d \theta_k \cdot \eta_k - \Psi(\boldsymbol{\theta}) \right\}, \quad (\text{B.7})$$

the inverse mapping can be expressed as

$$\boldsymbol{\theta}(\boldsymbol{\eta}) : \boldsymbol{\eta} \mapsto \left(\frac{\partial}{\partial \eta_k} \Phi(\boldsymbol{\eta}) \right)_k. \quad (\text{B.8})$$

Thus, the correspondence between the natural parameters and the dual parameters is bijective.

Example B.4. We continue Example B.2. The dual parameters can be expressed as

$$\eta_k^{(a)} = \text{tr} (\sigma_{\boldsymbol{\theta}} \cdot \mathbf{T}_k^{(a)}) = \text{tr}_{\partial a} \left(\text{tr}_{\mathcal{V} \setminus \partial a} (\sigma_{\boldsymbol{\theta}} \cdot \mathbf{T}_k^{(a)}) \right) = \text{tr} (\sigma_a \cdot \mathbf{T}_k^{(a)}), \quad (\text{B.9})$$

where $\sigma_a \triangleq \text{tr}_{\mathcal{V} \setminus \partial a} (\sigma_{\boldsymbol{\theta}})$. Since $\{\mathbf{T}_k^{(a)}\}_k$ is a basis of $\mathfrak{L}_{\dagger}(\mathcal{H}_{\partial a})$, (B.9) has established an injection from σ_a to $\boldsymbol{\eta}^{(a)}$. In other words, given some local densities operators, there exists at most one global density operator in the quantum exponential family such that its partial traces match these local densities operators. \square

Appendix C

Differentiability of $-\text{tr}(\sigma \cdot \log \rho(\boldsymbol{\eta}))$

First, we verify the differentiability of the bijective mapping $\boldsymbol{\eta} : \boldsymbol{\theta} \mapsto (\text{tr}(\rho_{\boldsymbol{\theta}} \cdot \mathbf{T}_i))_i$.

Note that,

$$\frac{\partial \eta_i}{\partial \theta_j} = \frac{\partial \text{tr}(\rho_{\boldsymbol{\theta}} \cdot \mathbf{T}_i)}{\partial \theta_j} = \frac{d}{dt} \Big|_{t=0} \text{tr} \left(\exp \left(\sum_{k=1}^d \theta_k \cdot \mathbf{T}_k + t \cdot \mathbf{T}_i - \Psi(\boldsymbol{\theta} + t \cdot \mathbf{e}_i) \right) \cdot \mathbf{T}_i \right) \quad (\text{C.1})$$

$$= \frac{d}{dt} \Big|_{t=0} \frac{\text{tr} \left(\exp \left(\sum_{k=1}^d \theta_k \cdot \mathbf{T}_k + t \cdot \mathbf{T}_i \right) \cdot \mathbf{T}_i \right)}{\exp(\Psi(\boldsymbol{\theta} + t \cdot \mathbf{e}_i))}. \quad (\text{C.2})$$

Since the denominator $\exp(\Psi(\boldsymbol{\theta} + t \cdot \mathbf{e}_i))$ is clearly differentiable, it suffice to show the differentiability of $t \mapsto \text{tr} \left(\exp \left(\sum_{k=1}^d \theta_k \cdot \mathbf{T}_k + t \cdot \mathbf{T}_i \right) \cdot \mathbf{T}_i \right)$ at $t = 0$. By the Taylor series expansion, we can write

$$\text{tr} \left(\exp \left(\sum_{k=1}^d \theta_k \cdot \mathbf{T}_k + t \cdot \mathbf{T}_i \right) \cdot \mathbf{T}_i \right) - \text{tr} \left(\exp \left(\sum_{k=1}^d \theta_k \cdot \mathbf{T}_k \right) \cdot \mathbf{T}_i \right) \quad (\text{C.3})$$

$$= \text{tr} \left(\sum_{n=0}^{\infty} \frac{\left(\sum_{k=1}^d \theta_k \cdot \mathbf{T}_k + t \cdot \mathbf{T}_i \right)^n}{n!} \cdot \mathbf{T}_i \right) - \text{tr} \left(\sum_{n=0}^{\infty} \frac{\left(\sum_{k=1}^d \theta_k \cdot \mathbf{T}_k \right)^n}{n!} \cdot \mathbf{T}_i \right) \quad (\text{C.4})$$

$$= \text{tr} \left(\sum_{n=0}^{\infty} \frac{\left(\sum_{k=1}^d \theta_k \cdot \mathbf{T}_k + t \cdot \mathbf{T}_i \right)^n - \left(\sum_{k=1}^d \theta_k \cdot \mathbf{T}_k \right)^n}{n!} \cdot \mathbf{T}_i \right) \quad (\text{C.5})$$

$$= \text{tr} \left(\sum_{n=1}^{\infty} \frac{t \cdot \left(\sum_{\ell=0}^{n-1} \left(\sum_{k=1}^d \theta_k \cdot \mathbf{T}_k \right)^{n-1-\ell} \cdot \mathbf{T}_i \cdot \left(\sum_{k=1}^d \theta_k \cdot \mathbf{T}_k \right)^{\ell} \right) + O(t^2)}{n!} \cdot \mathbf{T}_i \right) \quad (\text{C.6})$$

$$= t \cdot \sum_{n=1}^{\infty} \frac{\text{tr} \left(\left(\sum_{k=1}^d \theta_k \cdot \mathbf{T}_k \right)^{n-1} \cdot \mathbf{T}_i \right)}{(n-1)!} + O(t^2). \quad (\text{C.7})$$

Notice that

$$\sum_{n=1}^{\infty} \left| \frac{\text{tr} \left(\left(\sum_{k=1}^d \theta_k \cdot \mathbf{T}_k \right)^{n-1} \cdot \mathbf{T}_i \right)}{(n-1)!} \right| \leq \sum_{n=1}^{\infty} \frac{\left\| \sum_{k=1}^d \theta_k \cdot \mathbf{T}_k \right\|^{n-1} \cdot |\text{tr}(\mathbf{T}_i)|}{(n-1)!} \quad (\text{C.8})$$

$$= \exp \left(\left\| \sum_{k=1}^d \theta_k \cdot \mathbf{T}_k \right\| \right) \cdot |\text{tr}(\mathbf{T}_i)|, \quad (\text{C.9})$$

where, for a matrix A , $\|A\|$ stands for the absolute value of the largest-in-absolute-value eigenvalue of A and where we have applied the inequalities

$$|\text{tr}(A \cdot B)| \leq \|A\| \cdot |\text{tr}(B)| \quad (\text{C.10})$$

$$\|A \cdot B\| \leq \|A\| \cdot \|B\| \quad (\text{C.11})$$

in deriving (C.8). Equation (C.9) implies that the series

$$\sum_{n=1}^{\infty} \frac{\text{tr} \left(\left(\sum_{k=1}^d \theta_k \cdot \mathbf{T}_k \right)^{n-1} \cdot \mathbf{T}_i \right)}{(n-1)!}$$

is absolute convergent and thus is convergent. Therefore, the limit

$$\lim_{t \rightarrow 0} \frac{1}{t} \cdot \left(\text{tr} \left(\exp \left(\sum_{k=1}^d \theta_k \cdot \mathbf{T}_k + t \cdot \mathbf{T}_i \right) \cdot \mathbf{T}_i \right) - \text{tr} \left(\exp \left(\sum_{k=1}^d \theta_k \cdot \mathbf{T}_k \right) \cdot \mathbf{T}_i \right) \right) \quad (\text{C.12})$$

exists, which justifies the differentiability of $t \mapsto \text{tr} \left(\exp \left(\sum_{k=1}^d \theta_k \cdot \mathbf{T}_k + t \cdot \mathbf{T}_i \right) \cdot \mathbf{T}_i \right)$ at $t = 0$, and of $\boldsymbol{\eta} : \boldsymbol{\theta} \mapsto (\text{tr}(\rho_{\boldsymbol{\theta}} \cdot \mathbf{T}_i))_i$ as well.

Second, we consider the function $\hat{f}(\boldsymbol{\theta}) \triangleq -\text{tr}(\sigma \cdot \log \rho_{\boldsymbol{\theta}})$. Consider a small change in $\boldsymbol{\theta}$ along its i -th component. The change in \hat{f} can be expressed as

$$\hat{f}(\boldsymbol{\theta} + h \cdot \mathbf{e}_i) - \hat{f}(\boldsymbol{\theta}) = h \cdot \text{tr}(\sigma \cdot \mathbf{T}_i) - (\Psi(\boldsymbol{\theta} + h \cdot \mathbf{e}_i) - \Psi(\boldsymbol{\theta})). \quad (\text{C.13})$$

Clearly, \hat{f} is differentiable.

Finally, note that $f(\boldsymbol{\eta}) = \hat{f}(\boldsymbol{\theta}(\boldsymbol{\eta}))$. Since the bijective mapping $\boldsymbol{\theta} \mapsto \boldsymbol{\eta}$ is differentiable, then so is its inverse mapping $\boldsymbol{\eta} \mapsto \boldsymbol{\theta}$. Therefore, the differentiability of f follows directly from the differentiability of \hat{f} .

Appendix D

Additional Figures for Chapter 4

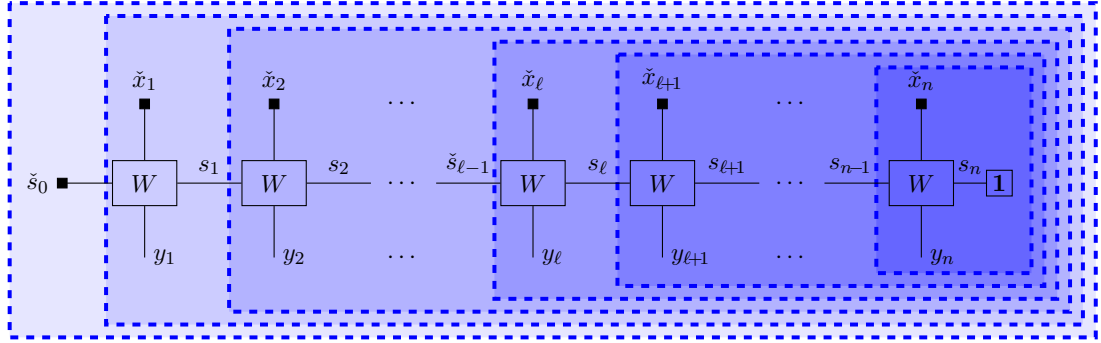


Figure D.1: Verification of (4.6). Note that every “closing-the-box” operation yields a function node representing the constant function 1.

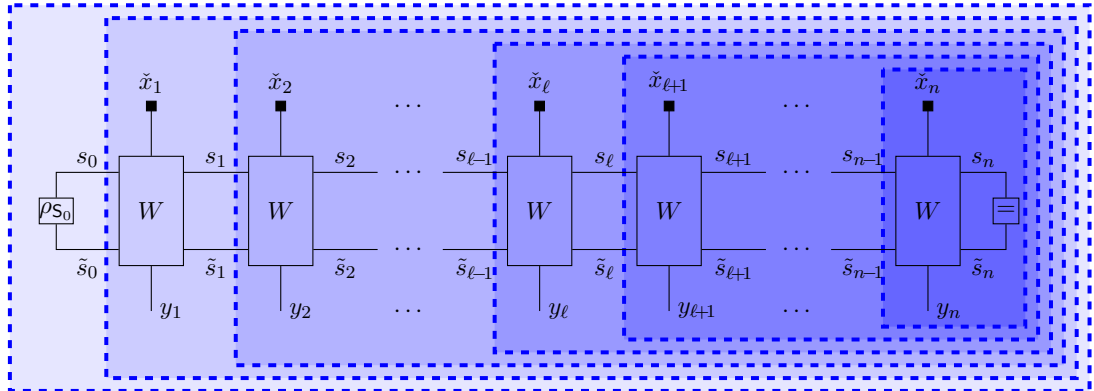


Figure D.2: Counterpart of Figure D.1 for QSCs. Note that every “closing-the-box” operation yields a function node representing a Kronecker-delta function node, *i.e.*, a degree-two equality function node.

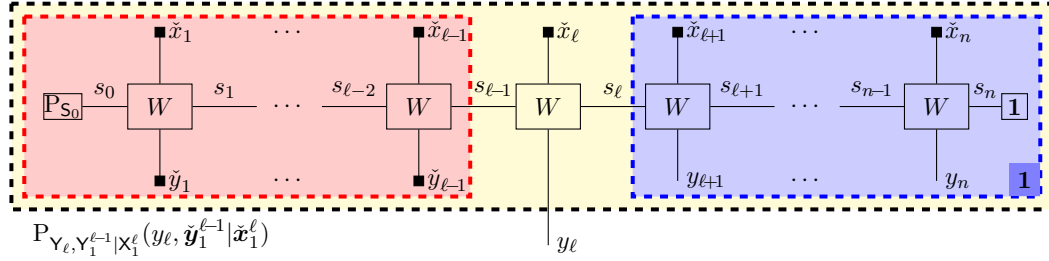


Figure D.3: Efficient simulation of the channel output at step ℓ given the channel input \tilde{x}_1^n and the channel output $\tilde{y}_1^{\ell-1}$ for an FSMC.

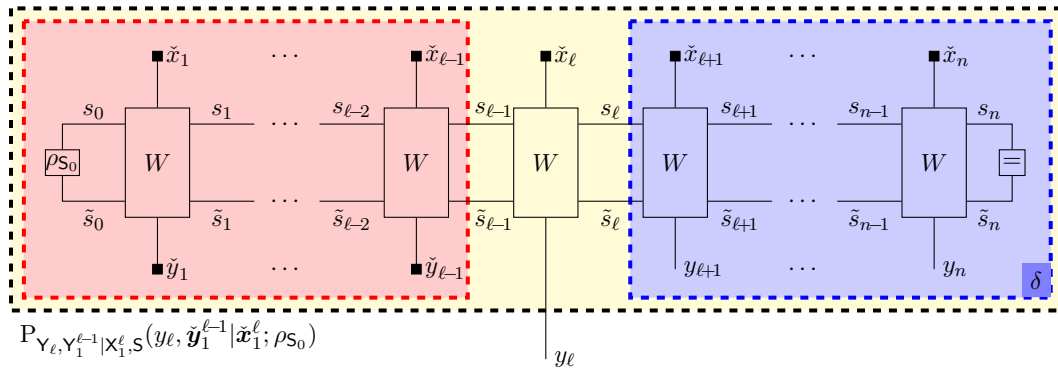


Figure D.4: Efficient simulation of the channel output at step ℓ given the channel input \tilde{x}_1^n and the channel output $\tilde{y}_1^{\ell-1}$ for a QSC.

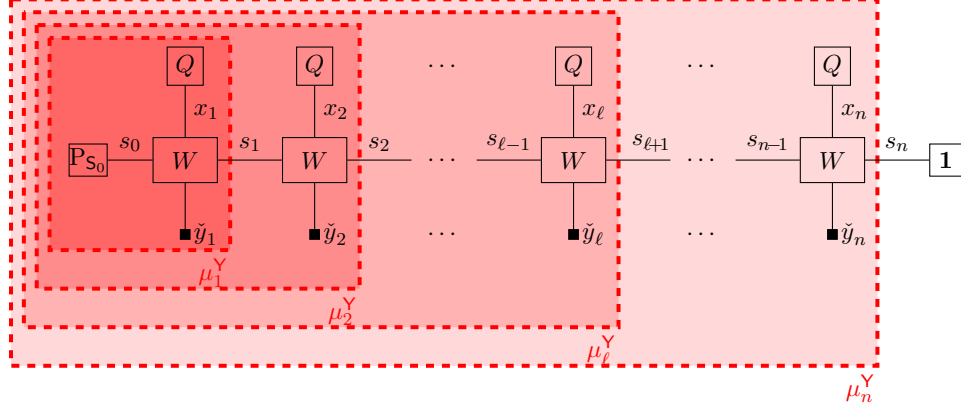


Figure D.5: The iterative computation of μ_ℓ^Y as in (4.20) can be understood as a sequence of “closing-the-box” operations as shown above.

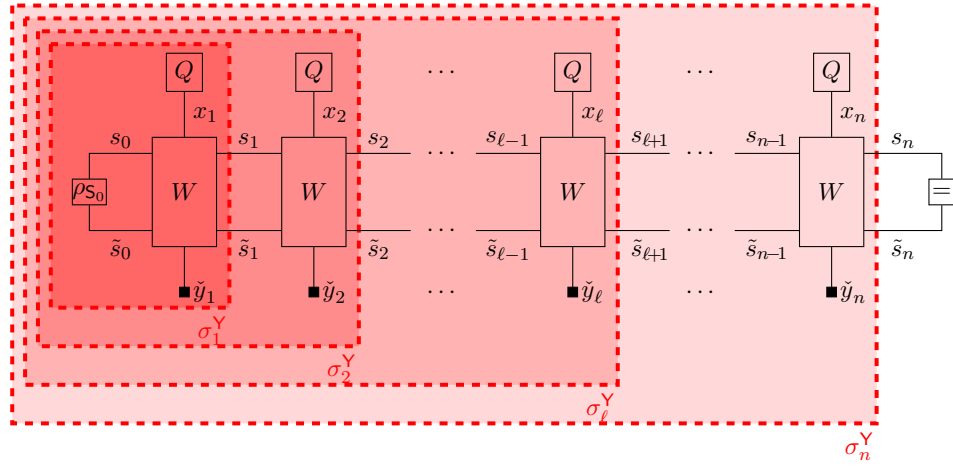


Figure D.6: The iterative computation of σ_ℓ^Y as in (4.71) can be understood as a sequence of “closing-the-box” operations as shown above.

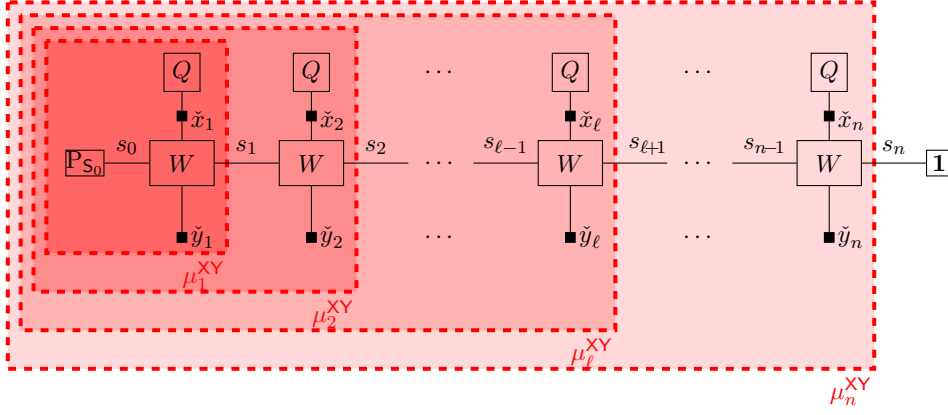


Figure D.7: The iterative computation of μ_ℓ^{XY} can be understood as a sequence of “closing-the-box” operations as shown above.

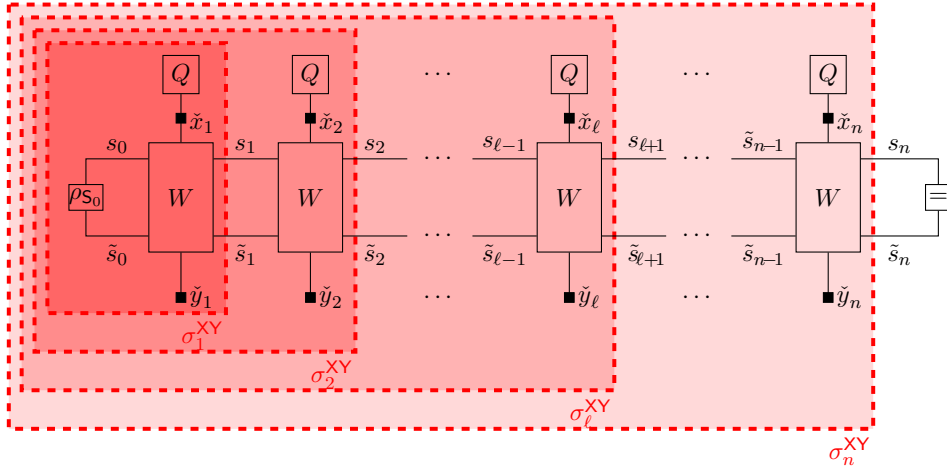


Figure D.8: The iterative computation of σ_ℓ^{XY} as in (4.72) can be understood as a sequence of “closing-the-box” operations as shown above.

Bibliography

- [AA13] S. Aaronson and A. Arkhipov, “The computational complexity of linear optics,” *Theory of Computing*, vol. 9, no. 4, pp. 143–252, 2013.
- [AHW00] G. G. Amosov, A. S. Holevo, and R. F. Werner, “On some additivity problems in quantum information theory,” 2000. arXiv: [math-ph/0003002](#).
- [ALV+06] D. M. Arnold, H.-A. Loeliger, P. O. Vontobel, A. Kavčić, and W. Zeng, “Simulation-based computation of information rates for channels with memory,” *IEEE Transactions on Information Theory*, vol. 52, no. 8, pp. 3498–3508, 2006.
- [AM11] A. Al-Bashabsheh and Y. Mao, “Normal factor graphs and holographic transformations,” *IEEE Transactions on Information Theory*, vol. 57, no. 2, pp. 752–763, 2011.
- [AMV11] A. Al-Bashabsheh, Y. Mao, and P. O. Vontobel, “Normal factor graphs: A diagrammatic approach to linear algebra,” in *Proceedings IEEE International Symposium on Information Theory (ISIT)*, St. Petersburg, Russia, 2011, pp. 2178–2182.
- [AN00] S. Amari and H. Nagaoka, *Methods of Information Geometry*, ser. Translations of Mathematical Monographs. Oxford, UK: Oxford University Press, 2000, vol. 191, ISBN: 9780821843024.
- [Ari72] S. Arimoto, “An algorithm for computing the capacity of arbitrary discrete memoryless channels,” *IEEE Transactions on Information Theory*, vol. 18, no. 1, pp. 14–20, 1972.
- [BCJR74] L. Bahl, J. Cocke, F. Jelinek, and J. Raviv, “Optimal decoding of linear codes for minimizing symbol error rate,” *IEEE Transactions on Information Theory*, vol. 20, no. 2, pp. 284–287, 1974.

- [BDB04] J. Ball, A. Dragan, and K. Banaszek, “Exploiting entanglement in communication channels with correlated noise,” *Physical Review A*, vol. 69, no. 4, p. 042324, 2004.
- [BDM05] G. Bowen, I. Devetak, and S. Mancini, “Bounds on classical information capacities for a class of quantum memory channels,” *Physical Review A*, vol. 71, no. 3, p. 034310, 2005.
- [BDS97] C. H. Bennett, D. P. DiVincenzo, and J. A. Smolin, “Capacities of quantum erasure channels,” *Physical Review Letters*, vol. 78, no. 16, p. 3217, 1997.
- [Bet35] H. A. Bethe, “Statistical theory of superlattices,” *Proceedings of the Royal Society of London. Series A, Containing Papers of a Mathematical and Physical Character*, vol. 150, no. 871, pp. 552–575, 1935.
- [Bha13] R. Bhatia, *Matrix Analysis*, ser. Graduate Texts in Mathematics. New York, NY, USA: Springer, 2013, vol. 169, ISBN: 9781461268574.
- [Bla72] R. Blahut, “Computation of channel capacity and rate-distortion functions,” *IEEE Transactions on Information Theory*, vol. 18, no. 4, pp. 460–473, 1972.
- [BM04] G. Bowen and S. Mancini, “Quantum channels with a finite memory,” *Physical Review A*, vol. 69, no. 1, p. 012306, 2004.
- [Bos03] S. Bose, “Quantum communication through an unmodulated spin chain,” *Physical Review Letters*, vol. 91, no. 20, p. 207901, 2003.
- [BS07a] S. Beigi and P. W. Shor, “On the complexity of computing zero-error and Holevo capacity of quantum channels,” 2007. arXiv: 0709.2090 [quant-ph].
- [BS07b] J.-C. Bourin and Y. Seo, “Reverse inequality to Golden–Thompson type inequalities: Comparison of e^{A+B} and $e^A e^B$,” *Linear Algebra and its Applications*, vol. 426, no. 2-3, pp. 312–316, 2007.
- [BSST99] C. H. Bennett, P. W. Shor, J. A. Smolin, and A. V. Thapliyal, “Entanglement-assisted classical capacity of noisy quantum channels,” *Physical Review Letters*, vol. 83, no. 15, p. 3081, 1999.

- [Car10] E. Carlen, “Trace inequalities and quantum entropy: An introductory course,” in *Entropy and the quantum: Arizona School of Analysis with Applications*, ser. Contemporary Mathematics, vol. 529, Tucson, AZ, USA, 2010, pp. 73–140.
- [CC06] M. Chertkov and V. Y. Chernyak, “Loop calculus in statistical physics and information science,” *Physical Review E*, vol. 73, no. 6, p. 065 102, 2006.
- [CC07] V. Y. Chernyak and M. Chertkov, “Loop calculus and belief propagation for q-ary alphabet: Loop tower,” in *Proceedings IEEE International Symposium on Information Theory (ISIT)*, Nice, France, 2007, pp. 316–320.
- [CGLM14] F. Caruso, V. Giovannetti, C. Lupo, and S. Mancini, “Quantum channels and memory effects,” *Reviews of Modern Physics*, vol. 86, no. 4, p. 1203, 2014.
- [CT06] T. M. Cover and J. A. Thomas, *Elements of Information Theory*, 2nd ed. Hoboken, NJ, USA: John Wiley & Sons, 2006, ISBN: 0471241954.
- [CV16] M. X. Cao and P. O. Vontobel, “Quantum factor graphs: Closing-the-box operation and variational approaches,” in *Proceedings International Symposium on Information Theory and Its Applications (ISITA)*, Monterey, CA, USA, 2016, pp. 651–655.
- [CV17a] —, “Double-edge factor graphs: Definition, properties, and examples,” in *Proceedings IEEE Information Theory Workshop (ITW)*, Kaohsiung, Taiwan, 2017, pp. 136–140.
- [CV17b] —, “Estimating the information rate of a channel with classical input and output and a quantum state,” in *Proceedings IEEE International Symposium on Information Theory (ISIT)*, Aachen, Germany, 2017, pp. 3205–3209.
- [CV19] —, “Optimizing bounds on the classical information rate of quantum channels with memory,” in *Proceedings IEEE International Symposium on Information Theory (ISIT)*, Paris, France, 2019, pp. 265–269.
- [CV20] —, “Bounding and estimating the classical information rate of quantum channels with memory,” *IEEE Transactions on Information Theory*, vol. 66, no. 9, pp. 5601–5619, 2020.

- [Dev05] I. Devetak, “The private classical capacity and quantum capacity of a quantum channel,” *IEEE Transactions on Information Theory*, vol. 51, no. 1, pp. 44–55, 2005.
- [DHS06] N. Datta, A. S. Holevo, and Y. Suhov, “Additivity for transpose depolarizing channels,” *International Journal of Quantum Information*, vol. 4, no. 01, pp. 85–98, 2006.
- [EH78] D. E. Evans and R. Høegh-Krohn, “Spectral properties of positive maps on C^* -algebras,” *Journal of the London Mathematical Society*, vol. s2-17, no. 2, pp. 345–355, 1978.
- [EM02] Y. Ephraim and N. Merhav, “Hidden Markov processes,” *IEEE Transactions on Information Theory*, vol. 48, no. 6, pp. 1518–1569, 2002.
- [Fan73] M. Fannes, “A continuity property of the entropy density for spin lattice systems,” *Communications in Mathematical Physics*, vol. 31, no. 4, pp. 291–294, 1973.
- [For01] G. D. Forney, “Codes on graphs: Normal realizations,” *IEEE Transactions on Information Theory*, vol. 47, no. 2, pp. 520–548, 2001.
- [Fuk05] M. Fukuda, “Extending additivity from symmetric to asymmetric channels,” *Journal of Physics A: Mathematical and General*, vol. 38, no. 45, p. L753, 2005.
- [FYZ17] C. Fan, X. Yuan, and Y. Zhang, “Scalable uplink signal detection in crans via randomized gaussian message passing,” *IEEE Transactions on Wireless Communications*, vol. 16, no. 8, pp. 5187–5200, 2017.
- [Gal62] R. G. Gallager, “Low-density parity-check codes,” *IRE Transactions on Information Theory*, vol. 8, no. 1, pp. 21–28, 1962.
- [Gal68] ———, *Information Theory and Reliable Communication*, 1st ed. 1968, ISBN: 9780471290483.
- [GLT00] A. Ganti, A. Lapidoth, and I. E. Telatar, “Mismatched decoding revisited: General alphabets, channels with memory, and the wide-band limit,” *IEEE Transactions on Information Theory*, vol. 46, no. 7, pp. 2315–2328, 2000.

- [Has09] M. B. Hastings, “Superadditivity of communication capacity using entangled inputs,” *Nature Physics*, vol. 5, no. 4, p. 255, 2009.
- [Hol02] A. S. Holevo, “On entanglement-assisted classical capacity,” *Journal of Mathematical Physics*, vol. 43, no. 9, pp. 4326–4333, 2002.
- [Hol73] —, “Bounds for the quantity of information transmitted by a quantum communication channel,” *Problemy Peredachi Informatsii*, vol. 9, no. 3, pp. 3–11, 1973.
- [Hol98] —, “The capacity of the quantum channel with general signal states,” *IEEE Transactions on Information Theory*, vol. 44, no. 1, pp. 269–273, 1998.
- [HV20] Y. Huang and P. O. Vontobel, “Characterizing the Bethe partition function of double-edge factor graphs via graph covers,” in *Proceedings International Symposium on Information Theory and Its Applications (ISITA)*, Los Angeles, CA, USA, 2020, pp. 1331–1336.
- [Jam72] A. Jamiolkowski, “Linear transformations which preserve trace and positive semidefiniteness of operators,” *Reports on Mathematical Physics*, vol. 3, no. 4, pp. 275–278, 1972.
- [Kat95] T. Kato, *Perturbation Theory for Linear Operators*, 2, Corrected, ser. Classic in Mathematics. Berlin Heidelberg, Germany: Springer, 1995, ISBN: 9783642662829.
- [KFL01] F. R. Kschischang, B. J. Frey, and H.-A. Loeliger, “Factor graphs and the sum-product algorithm,” *IEEE Transactions on Information Theory*, vol. 47, no. 2, pp. 498–519, 2001.
- [Kin02] C. King, “Additivity for unital qubit channels,” *Journal of Mathematical Physics*, vol. 43, no. 10, pp. 4641–4653, 2002.
- [Kin03] —, “The capacity of the quantum depolarizing channel,” *IEEE Transactions on Information Theory*, vol. 49, no. 1, pp. 221–229, 2003.
- [Kle31] O. Klein, “Zur quantenmechanischen begründung des zweiten hauptsatzes der wärmelehre,” *Zeitschrift für Physik*, vol. 72, no. 11-12, pp. 767–775, 1931.

- [KM06] V. Karimipour and L. Memarzadeh, “Entanglement and optimal strings of qubits for memory channels,” *Physical Review A*, vol. 74, no. 6, p. 062 311, 2006.
- [KW05] D. Kretschmann and R. F. Werner, “Quantum channels with memory,” *Physical Review A*, vol. 72, no. 6, p. 062 323, 2005.
- [LM10] C. Lupo and S. Mancini, “Transitional behavior of quantum Gaussian memory channels,” *Physical Review A*, vol. 81, no. 5, p. 052 314, 2010.
- [Loe04] H.-A. Loeliger, “An introduction to factor graphs,” *IEEE Signal Processing Magazine*, vol. 21, no. 1, pp. 28–41, 2004.
- [LP08] M. S. Leifer and D. Poulin, “Quantum graphical models and belief propagation,” *Annals of Physics*, vol. 323, no. 8, pp. 1899–1946, 2008.
- [LV12] H.-A. Loeliger and P. O. Vontobel, “A factor-graph representation of probabilities in quantum mechanics,” in *Proceedings IEEE International Symposium on Information Theory (ISIT)*, Cambridge, MA, USA, 2012, pp. 656–660.
- [LV17] ———, “Factor graphs for quantum probabilities,” *IEEE Transactions on Information Theory*, vol. 63, no. 9, pp. 5642–5665, 2017.
- [MB89] M. Mushkin and I. Bar-David, “Capacity and coding for the Gilbert–Elliott channels,” *IEEE Transactions on Information Theory*, vol. 35, no. 6, pp. 1277–1290, 1989.
- [Min84] H. Minc, *Permanents*, ser. Encyclopedia of Mathematics and its Applications. Cambridge, UK: Cambridge University Press, 1984, vol. 6, ISBN: 0201135051.
- [MJW06] D. M. Malioutov, J. K. Johnson, and A. S. Willsky, “Walk-sums and belief propagation in gaussian graphical models,” *Journal of Machine Learning Research*, vol. 7, no. Oct, pp. 2031–2064, 2006.
- [ML13] M. Molkaiaie and H.-A. Loeliger, “Partition function of the Ising model via factor graph duality,” in *Proceedings IEEE International Symposium on Information Theory (ISIT)*, Istanbul, Turkey, 2013, pp. 2304–2308.

- [Mor15a] R. Mori, “Holographic transformation, belief propagation and loop calculus for quantum information science,” in *Proceedings IEEE International Symposium on Information Theory (ISIT)*, Hong Kong, China, 2015, pp. 1099–1103.
- [Mor15b] —, “Loop calculus for nonbinary alphabets using concepts from information geometry,” *IEEE Transactions on Information Theory*, vol. 61, no. 4, pp. 1887–1904, 2015.
- [MPV04] C. Macchiavello, G. M. Palma, and S. Virmani, “Transition behavior in the channel capacity of two-qubit channels with memory,” *Physical Review A*, vol. 69, no. 1, p. 010 303, 2004.
- [Nag98] H. Nagaoka, “Algorithms of arimoto-blahut type for computing quantum channel capacity,” in *Proceedings IEEE International Symposium on Information Theory (ISIT)*, IEEE, Cambridge, MA, USA, 1998, p. 354.
- [NC11] M. A. Nielsen and I. L. Chuang, *Quantum Computation and Quantum Information*, 10th Anniversary. Cambridge, UK: Cambridge University Press, 2011, ISBN: 9781107002173.
- [PSS01] H. D. Pfister, J. B. Soriaga, and P. H. Siegel, “On the achievable information rates of finite state ISI channels,” in *Proceedings IEEE Global Telecommunications Conference*, vol. 5, San Antonio, TX, USA, 2001, pp. 2992–2996.
- [Ruo12] N. Ruozzi, “The Bethe partition function of log-supermodular graphical models,” in *Advances in Neural Information Processing Systems*, Lake Tahoe, NV, USA, 2012, pp. 117–125.
- [Rys63] H. J. Ryser, *Combinatorial mathematics*, ser. The Carus Mathematical Monographs. Buffalo, NY, USA: The Mathematical Association of America, 1963, vol. 14, ISBN: 9780883850145.
- [Sch00] R. Schrader, “Perron–Frobenius theory for positive maps on trace ideals,” 2000. arXiv: math-ph/0007020.
- [Sha48] C. E. Shannon, “A mathematical theory of communication,” *Bell System Technical Journal*, vol. 27, no. 3, pp. 379–423, 1948.

- [Sho04] P. W. Shor, “The classical capacity achievable by a quantum channel assisted by a limited entanglement,” *Quantum Information & Computation*, vol. 4, no. 6, pp. 537–545, 2004.
- [Sim79] B. Simon, *Functional Integration and Quantum Physics*, ser. Pure and Applied Mathematics. New York, NY, USA: Academic Press Inc., 1979, vol. 86, ISBN: 0126442509.
- [SLG07] E. Sharon, S. Litsyn, and J. Goldberger, “Efficient serial message-passing schedules for ldpc decoding,” *IEEE Transactions on Information Theory*, vol. 53, no. 11, pp. 4076–4091, 2007.
- [SS01] V. Sharma and S. K. Singh, “Entropy and channel capacity in the regenerative setup with applications to Markov channels,” in *Proceedings IEEE International Symposium on Information Theory*, Washington, DC, USA, 2001, p. 283.
- [SVS09] P. Sadeghi, P. O. Vontobel, and R. Shams, “Optimization of information rate upper and lower bounds for channels with memory,” *IEEE Transactions on Information Theory*, vol. 55, no. 2, pp. 663–688, 2009.
- [SW08] E. B. Sudderth and M. J. Wainwright, “Loop series and Bethe variational bounds in attractive graphical models,” in *Advances in Neural Information Processing Systems*, Vancouver, BC, Canada, 2008, pp. 1425–1432.
- [SW97] B. Schumacher and M. D. Westmoreland, “Sending classical information via noisy quantum channels,” *Physical Review A*, vol. 56, no. 1, p. 131, 1997.
- [Val79] L. G. Valiant, “The complexity of computing the permanent,” *Theoretical computer science*, vol. 8, no. 2, pp. 189–201, 1979.
- [VKAL08] P. O. Vontobel, A. Kavčić, D. M. Arnold, and H.-A. Loeliger, “A generalization of the Blahut–Arimoto algorithm to finite-state channels,” *IEEE Transactions on Information Theory*, vol. 54, no. 5, pp. 1887–1918, 2008.
- [Von13a] P. O. Vontobel, “Counting in graph covers: A combinatorial characterization of the Bethe entropy function,” *IEEE Transactions on Information Theory*, vol. 59, no. 9, pp. 6018–6048, 2013.

- [Von13b] ———, “The Bethe permanent of a nonnegative matrix,” *IEEE Transactions on Information Theory*, vol. 59, no. 3, pp. 1866–1901, 2013.
- [War05] M. K. Warmuth, “A Bayes rule for density matrices,” in *Advances in Neural Information Processing Systems*, vol. 18, Vancouver, BC, Canada, 2005, pp. 1457–1464.
- [Wil17] M. M. Wilde, *Quantum Information Theory*, 2nd ed. Cambridge, UK: Cambridge University Press, 2017, ISBN: 9781107176164.
- [WJ08] M. J. Wainwright and M. I. Jordan, “Graphical models, exponential families, and variational inference,” *Foundations and Trends[®] in Machine Learning*, vol. 1, no. 1-2, pp. 1–305, 2008.
- [YFW05] J. S. Yedidia, W. T. Freeman, and Y. Weiss, “Constructing free-energy approximations and generalized belief propagation algorithms,” *IEEE Transactions on Information Theory*, vol. 51, no. 7, pp. 2282–2312, 2005.